

Kharkiv National Medical University

DENTAL RADIOLOGY

(Text-book for students of dental faculties)

Kharkiv 2018

01 Technical support of radiological diagnostics of pathology of teeth and jaws

Optimum interpretable radiographs can only be achieved with a carefully performed radiographic technique. Only a profound knowledge of the technical possibilities and limitations will permit the creation of acceptable radiographs. An unsystematic “search” according to one’s own spontaneous ideas rarely leads to success, but often to unnecessary additional radiation exposure.

Technique for Panoramic Tomography for Basic Information and Special Radiographs for Supplemental Examination.

1940s Paatero developed the fundamentals of panoramic tomography from the principles of tomography. Three peculiarities characterize *classic tomography*:

- the movement in opposite directions of the x-ray tube and the film along the object determine the degree of elimination of undesired structures located outside the surveyed layer;

- the thickness of the surveyed layer depends upon the angle between the layer to be surveyed and the central x-ray;

- the choice of the surveyed layer position is achieved by shifting the center of rotation of the system.

Derived from these principles, *panoramic tomography* is characterized by the following:

- x-ray source and film holder move clockwise around the approximately elliptically shaped dental arches;

- structures close to or distant from the film, as well as the thickness of the surveyed layer are determined by the relationship of the speed of the film cassette (mounted on the film holder) to the speed of the x-ray source.

Advantages of panoramic radiography

- Presents a comprehensive dental examination by means of a panoramic representation of the masticatory system, including the temporomandibular joints (TMJ) and the maxillary sinuses.

- Permits detection of functional and pathologic relationships and of their effects on the masticatory system.

- Provides a documentary overview for treatment planning and follow-up.

- Reduces radiation exposure by means of a rational examination strategy.

Disadvantages of panoramic radiography

- Extreme class II and III anterior tooth relationships make it impossible to depict optimally the maxillary and the mandibular anterior segments simultaneously.

- The ratio of the focus-object distance to the object-film distance is not everywhere identical, resulting in a varying enlargement factor.
- Precise measurements are not possible.
- Structures that reside outside of the in-focus layer may be superimposed upon the normal structures of the jaw and mimic pathology.

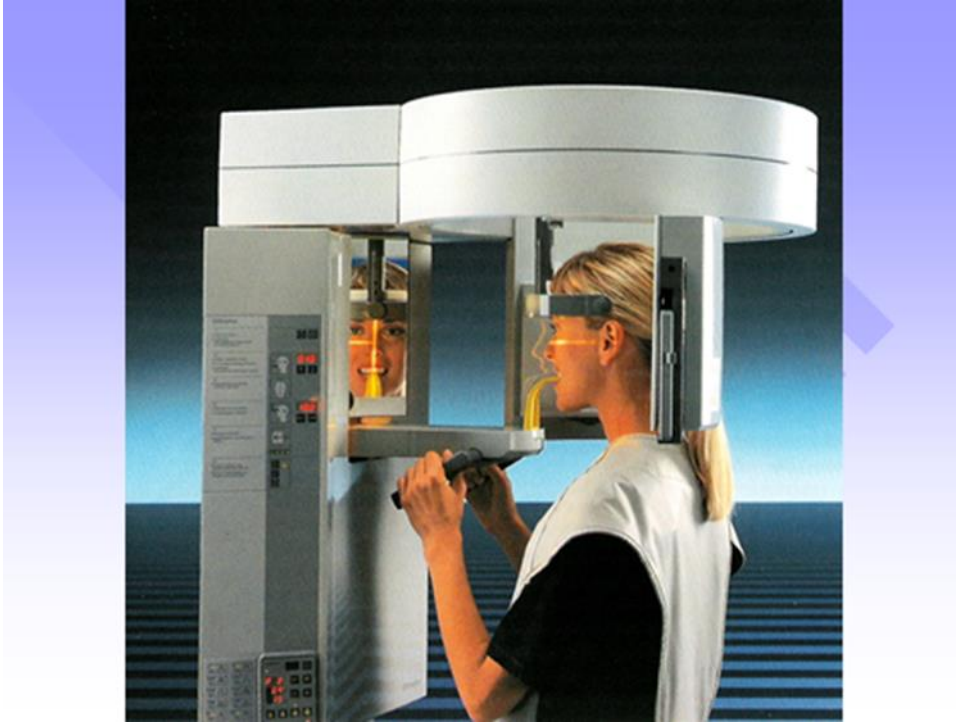


Fig. 1.1. Panoramic Tomograph



Fig. 1.2. Panoramic film. Improved resolution of the tooth buds in the maxilla of an 8-year-old boy. This film shows the double buds of the maxillary central incisors very well; this situation would not be clearly represented on a single periapical radiography.

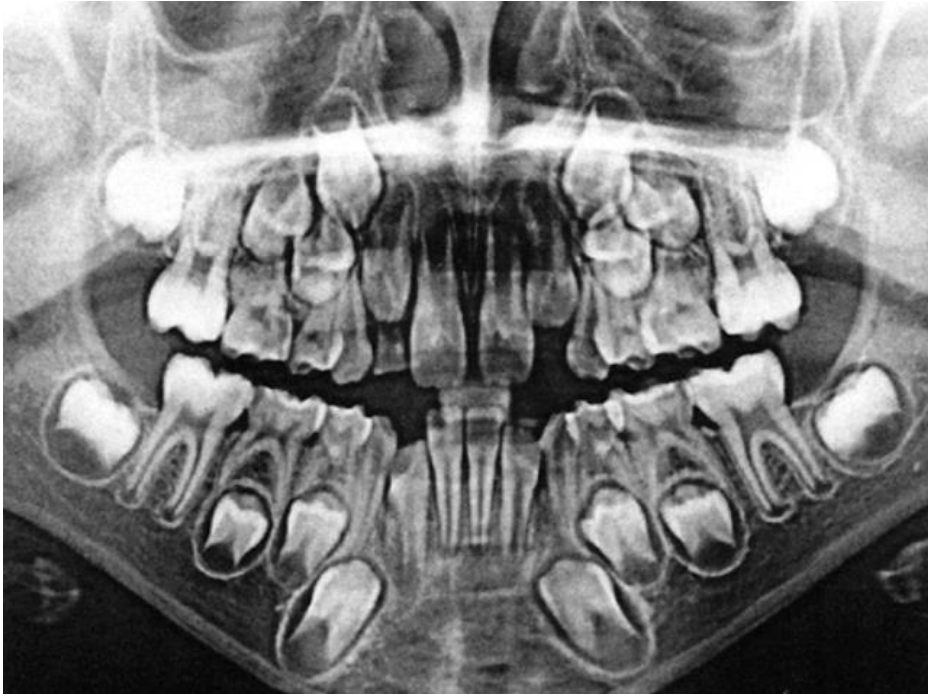


Fig. 1.3. Digital panoramic radiograph of a young child post-processed. Note the good harmonisation of the contrast between the different portions of the arches, with good visibility of central and molar regions as well.

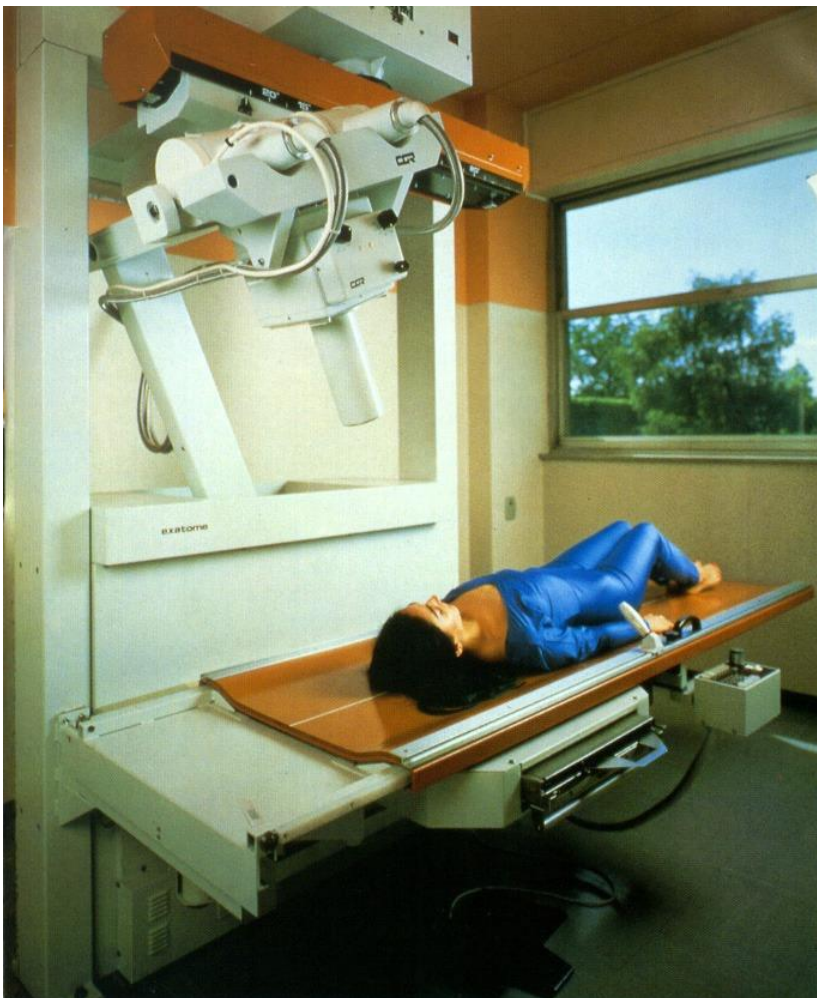


Fig. 1.4. Classical Tomograph



Fig. 1.5. CT unit

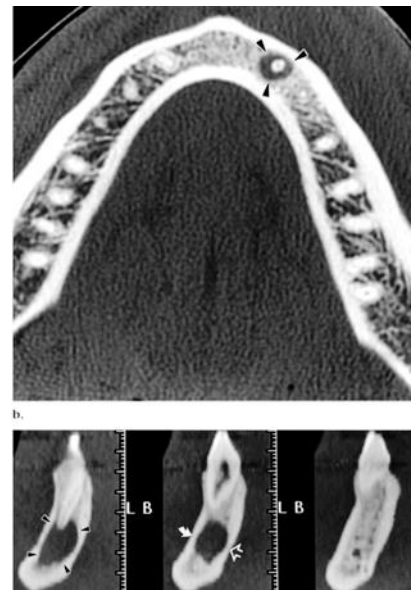


Fig. 1.6. Dental CT scans of woman with periapical radiolucency in the left canine tooth from endodontal disease.

Computed tomography (CT) is the modality of choice for the evaluation of facial trauma because it helps accurately identify and characterize fractures and associated complications, thereby aiding timely clinical management and surgical planning. In particular, CT clearly depicts clinically relevant fractures in the eight osseous struts or buttresses that function as an underlying scaffold for facial structures.

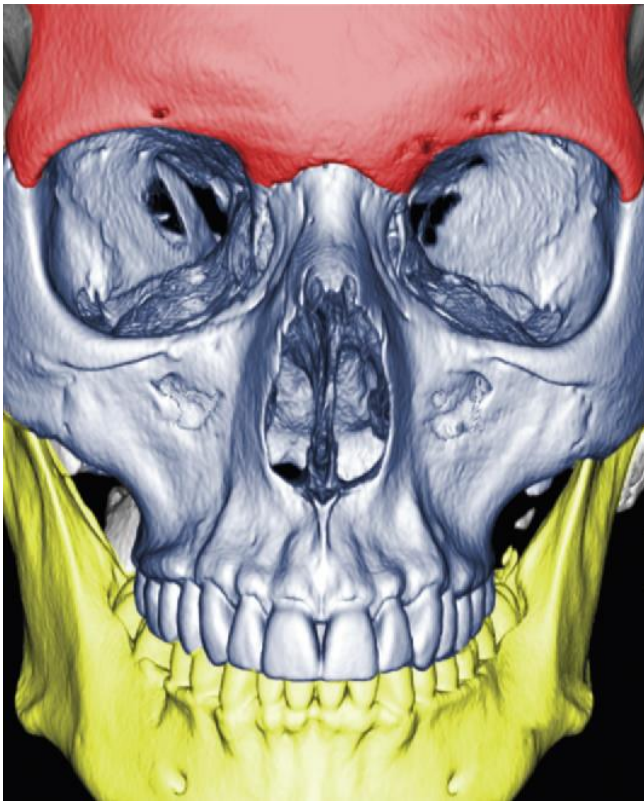


Fig. 1.7. System of facial partitions. Three-dimensional CT image of an adult skull with color overlays shows partition of the facial anatomy into upper (red), middle (blue), and lower (yellow) thirds, the system used by otolaryngologists to describe locations of fracture in the facial anatomy.

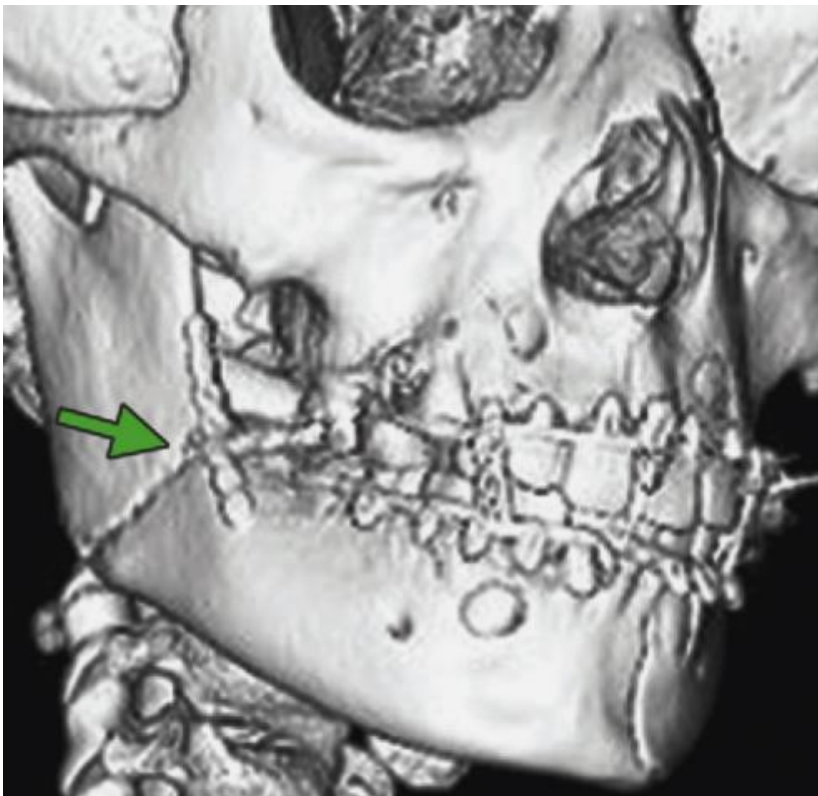


Fig. 1.8. Three-dimensional CT image of the mandible after internal fixation of the right posterior aspect of the upper transverse mandibular buttress across the mandibular angle fracture (green arrow) and maxillomandibular fixation shows reapproximation of the right mandibular body fracture fragments.

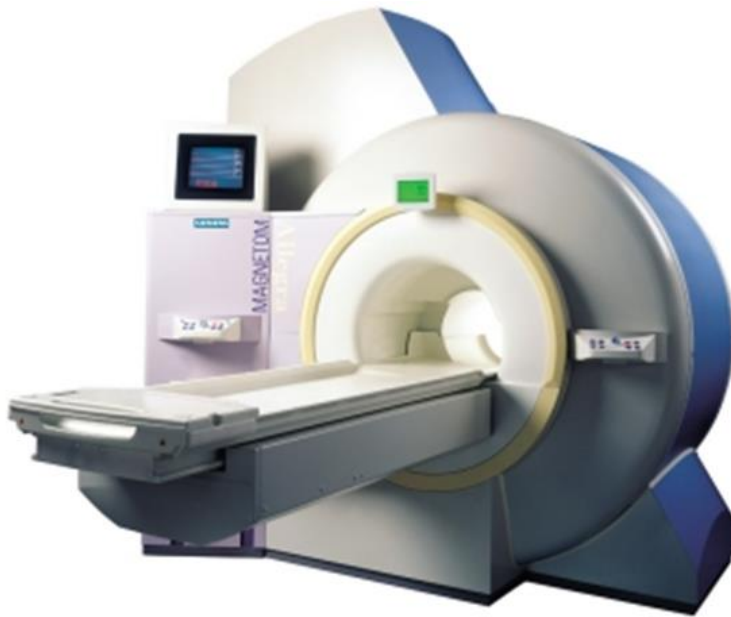


Fig. 1.9. Magnetic resonance (MR) unit

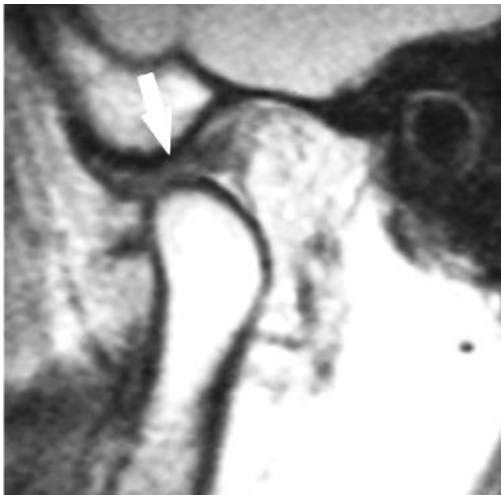


Fig. 1.10. MR images of TMJ disk displacement with reduction (arrow).



Fig.1.11. Conventional dental x-ray unit.

02 Radiographic Examination of the Patient in the Dental Office

Panoramic Radiography for Basic Information and Supplemental Examination Using Special Radiography

Examination Strategy and Active Protection Against Radiation Exposure

With the gradual introduction of a systematic radiographic examination came the firm intention to optimize patient examinations. The corollary goal was to perfect the system because radiography provides the basis for treatment planning and evaluation of therapy. Furthermore, it is recognized that it is the medical obligation of the dentist to detect pathologic alterations as early as possible and to institute timely therapy for developmental anomalies. However, because no radiographic survey comprised of individual films can provide a complete view of the masticatory apparatus with all its components and with its relationships to adjacent regions, the panoramic radiograph is now beginning to play a more significant role as the basis for a systematic and economically favorable method for data collection that also protects the patient from unnecessary radiation.

During the initial examination, radiography should be used to examine not only the teeth but also the jaws, including the angles of mandible and the temporomandibular joints. Failing this, the dental examination, the treatment plan and in some cases even the treatment itself may be incomplete and therefore in error. Some have argued that the fulfillment of these requirements would lead to excessive cost and increased radiation dosage, but this is not true because early diagnosis of dental and jaw anomalies as well as other diseases of the jaws is associated in the final analysis with less cost and less radiation exposure. In addition, there are advantages in terms of the patient's general health. Taken together, these facts clearly support the use of panoramic radiography as the source of basic information; today there is a growing tendency to replace the conventional dental radiographic survey with the panoramic radiograph. The use of supplemental individual dental X-rays serves only to complete the overall survey in special situations, e.g., for the examination and treatment of periodontal diseases. Supplementing the panoramic radiograph with specific conventional skull films and other imaging techniques must be carried out or arranged for with knowledge of the technical and diagnostic possibilities, and with full consideration of the regulations pertaining to protection from excessive radiation.

The term "examination strategy" stands for the rational selection of proven radiographic examination methods, depending upon the particular indication, in order to avoid unacceptable radiographs and unnecessary radiation exposure. Today

it can already be stated that the use of panoramic radiography is mandatory in the following cases:

- initial examination of new patients in all age groups (including orthodontic and periodontal patients);
- early diagnosis of developmental anomalies of the dental apparatus (recommended especially at ages 10, 15 and 20) to check the dentition and to diagnose early any odontogenic cysts and tumors;
- to clarify the cause of missing teeth;
- radiographic examination of nonvital teeth;
- suspicion of odontogenic diseases of the sinuses;
- temporomandibular joint disturbances caused by malocclusion (in such cases, a panoramic radiograph should be taken with the patient in habitual occlusion);
- asymmetries of the face and the jaw;
- pressure sensitive, painful as well as asymptomatic swellings;
- poorly healing extraction wounds and suspicion of osteomyelitis;
- examination of nonodontogenic cysts, tumors and tumor-like lesions;
- suspicion of intraosseous or invasive growth of tumors, and suspicion of metastasis;
- paresthesia of the mandibular nerve;
- examination of systemic diseases and syndromes;
- maxillofacial fractures, and suspicion of fracture following trauma;
- before and after the performance of surgical interventions;

This strategy evolves from the panoramic film; this is the basic radiograph, which can be classified into four diagnostic regions;

Dentoalveolar region (Figure 2.1),

Maxillary region (Figure 2.2),

Mandibular region (Figure 2.3),

Temporomandibular joint region (including the retromaxillary and cervical regions) (Figure 2.4).

Special Radiographs for Examination of the Dentoalveolar Region (Figure 2.1)

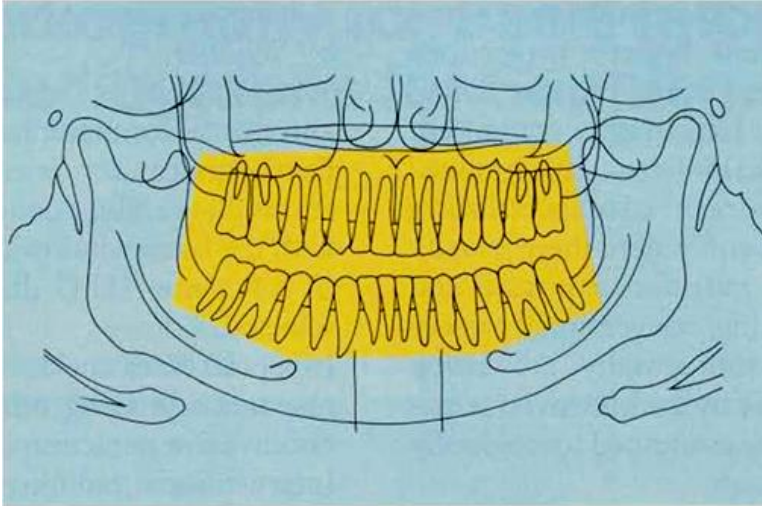


Fig. 2.1. Dentoalveolar region.

Depending upon the situation, supplemental radiographs of the following types may be indicated:

- bite-wing radiographs for caries diagnosis;
- periapical dental radiographs for examination of periapical lesions and endodontic problems;
- dental radiographs for periodontal diagnosis (depiction of the root apex is not always necessary);
- dental radiographs and possibly occlusal radiographs to determine position in cases where localization is difficult.

To complement the panoramic radiograph, in specific situations occlusal radiographs or periapical films precisely positioned with a film holder are employed.

Special Radiographs for Examination of the Maxillary Region (Figure 2.2)

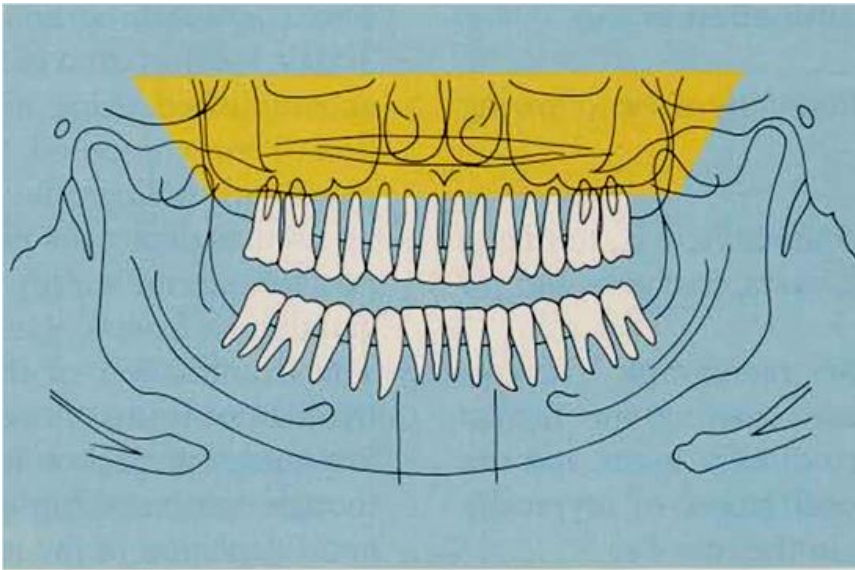


Fig. 2.2. Maxillary region.

Depending upon the situation, supplemental radiographs of the following types may be indicated:

- occlusal radiographs of the maxilla, e.g., for depiction of pathologic structural detail, depending on the indication;
- cephalometric radiographs using lateral and postero-anterior projection, e.g., for problems of localization in the maxilla;
- projections of the facial skeleton with maximum jaw opening, e.g., for examination of the maxillary sinuses in cases of dentogenic involvement;
- computed tomography.

Special Radiographs for Examination of the Mandibular Region (Figure 2.3)

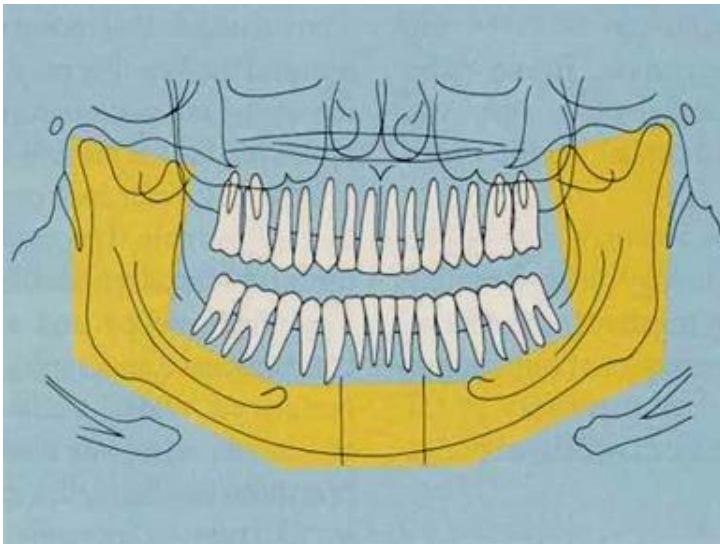


Fig.2.3. Mandibular region.

In certain cases, additional radiographs of the following types may be indicated:

- occlusal radiograph of the mandible, e.g., to depict pathologic structural details, cysts, fractures and for localization;
- mandibular posteroanterior radiograph with maximum jaw opening for frontal depiction of the temporomandibular joints and the ascending rami, and for localization of atypically impacted third molars (also in the maxilla).

In addition to occlusal radiographs the mandibular posteroanterior radiograph best serves to depict the anterior segment. In special cases, the “unilateral mandibular technique or computed tomography may be employed as appropriate to complement panoramic radiography. In some cases (see above), however, it may be prudent to refer the patient to a radiology clinic. Examination of the mandibular region by means of conventional radiographic technique and conventional tomography is also being replaced for the most part today by CT, except in patients with metal implants and metal bridge- work, which cause artifacts.

Special Radiographs for Examination of the Temporomandibular Joints Regions (Figure 2.4)

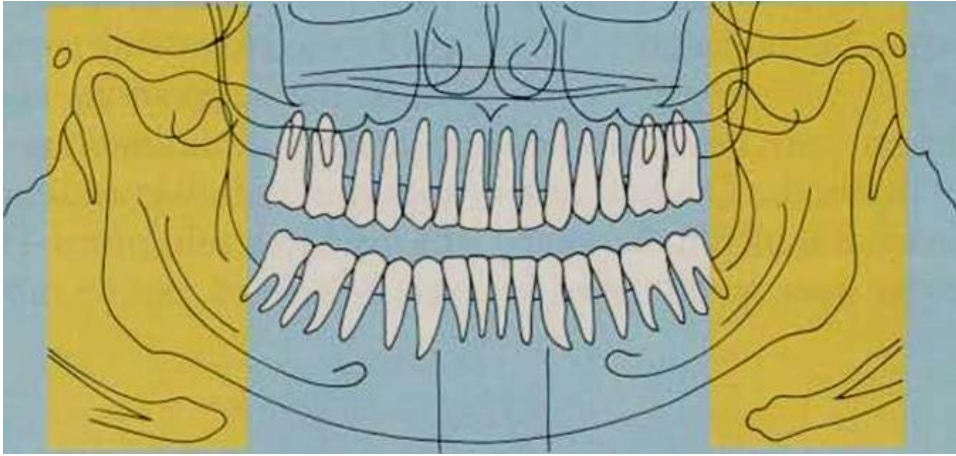


Fig. 2.4. Temporomandibular Joints Regions.

The temporomandibular joints can be examined using *noninvasive* or *invasive* methods. The noninvasive technique begins with an axial skull film to determine the angle of the condylar axes to the median sagittal plane.

In certain cases, additional radiographs of the following types may be indicated:

- subsequent films consist of radiographs as described by Schuller.
- these may, however, also consist of a series of lateral and frontal tomographs.
- furthermore, for temporomandibular joint alterations that exhibit a density similar to that of bone, CT with the bone window can be used; for the depiction of soft tissue (TMJ disc) the soft tissue window is selected.
- in special cases magnetic resonance imaging offers additional possibilities for noninvasive depiction of the TMJ disc.
- interventional radiology of the temporomandibular joint continues to defend its position using arthroscopic and arthrographic methods.
- today, the depiction of salivary glands is still frequently accomplished using sialography, despite competition from computed tomography.

The Bite-Wing Radiography

The bite-wing radiography is without doubt the most important supplemental film for data collection in addition to the panoramic film. Even though, thanks to modern preventive dentistry, the prevalence of dental caries has been dramatically reduced, early diagnosis of caries using the bite-wing radiography continues to be of central importance for the early detection of incipient proximal caries. Clinical experience shows, of course, that radiographic examination for fissure caries is helpful only in late stages of lesion development, while buccal and lingual or palatal lesions are hardly ever seen on radiographs; in these cases, careful clinical inspection plays the most important role. The reason for this fact can be explained by the mechanism of

action of X-rays; only those tooth surfaces that are not superimposed by dense, healthy tooth substance and that are struck tangentially by the central ray will appear as radiolucencies, thus signaling incipient loss of hard tooth structure. Tooth surfaces that are perpendicular to the central ray or which are superimposed by the entire thickness of an intact crown, e.g., fissure caries, elicit no radiographic sign of early carious lesions. On the other hand, because it functions according to the principles of tomography, panoramic tomography can reveal loss of tooth substance with surprising clarity if taken with precise positioning. This should not, however, be taken as a reason to disregard the bite-wing radiography when it comes to checking for proximal caries.

In summary, the bite-wing radiograph can provide the following information:

- early diagnosis especially of proximal caries;
- checking the marginal closure of restorations and crowns in the proximal area;
- evidence of existing endodontic treatments in the posterior segments;
- documentation of calculus accumulation in the proximal spaces of posterior teeth;
- condition of the alveolar ridge in the posterior region, if the projection relationships are ideal;
- existence of malocclusion in the posterior region caused by missing teeth, missing antagonists or premature contacts.

Good radiographic depiction of caries and malocclusion requires a higher energy exposure, while the depiction of restoration margins as well as cervical and periodontal problems require lower energy. Depending upon the age of the patient, various sizes of bite-wing films are available. The dentition from the distal surface of the canine to beyond the second molars should be captured on the bite-wing radiograph. In order to display the alveolar ridge as completely as possible, the elevation must be optimum, which necessitates using only those film holders with bite tabs no thicker than paper. Used in this way the bite-wing radiography and the panoramic film not only provide the basis for data collection but also serve as an excellent radiographic survey for the regular evaluation of the condition of the posterior teeth, while providing minimum radiation exposure.

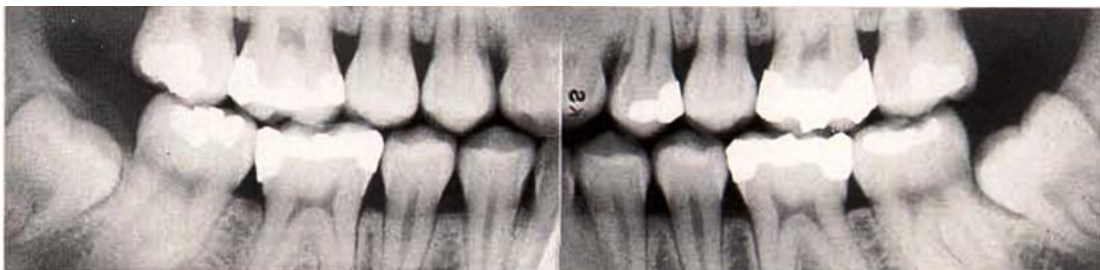


Fig. 2.5. Example. These bite-wing films were taken using the long (2.5 \times 5.5cm) bite-wing film. If the paper tab is pulled too tightly, the distal edge of the film will be pushed inferiorly when the patient bites in centric occlusion. If the film is positioned too far anteriorly, the mesial edge of the film will be pushed upward during closure. Both of these errors will result in the occlusal plane appearing oblique on the finished radiogram.

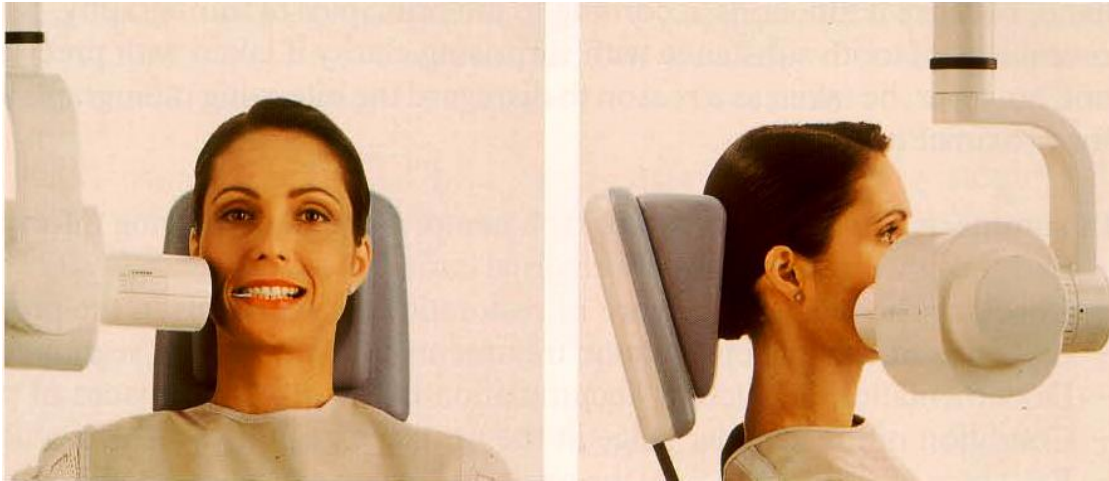


Fig. 2.6. Proper central ray targeting depicted from frontal and lateral views. Note the patient's head position and the position of the film axis. Note also that the central ray is positioned at a 5-7° angle from the horizontal plane, vertically. The horizontal targeting appears "mesial eccentric", but it is in fact perpendicular to the film surface.

Examples of Diagnosis Using Bite-Wing radiography

The bite-wing radiograph films presented on this page clearly show that the long bite-wing film from Kodak has distinct advantages over the normal periapical-size film for the examination of older adolescents and adults. Careful technique is worth the time! An ideal bite-wing radiograph that can also reproducibly reveal deeper periodontal lesions in the entire posterior segment should be taken using a 3.5x5 cm film, or the 4x5 cm film.

Here again we point out the importance of properly choosing the exposure data; see the example in Figure 2.7. High energy exposure can lead to the burn-out effect, especially in the proximal areas of the cervix of the tooth; such teeth appear in the radiograph to be somewhat narrower at the neck. If a metal restoration is present in such teeth, the burn-out effect will give the optical illusion of an overhang. In doubtful cases, of course, this should be checked clinically.

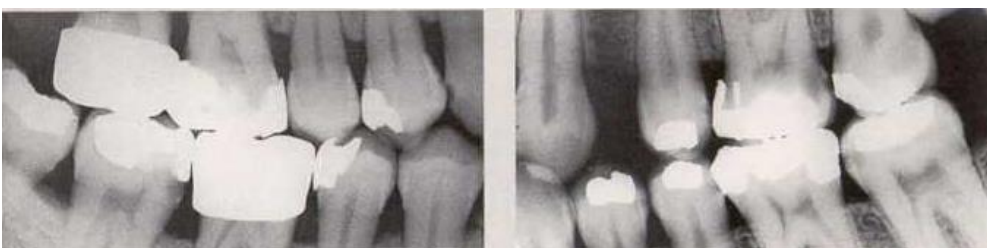


Fig. 2.7. These two films, from separate patients, show typical radiographic signs of overhanging restorations and crown margins in the proximal areas, proximal caries of varying severity, and an area of secondary caries resulting from a poor contact between teeth 47 and 46 (*left*).

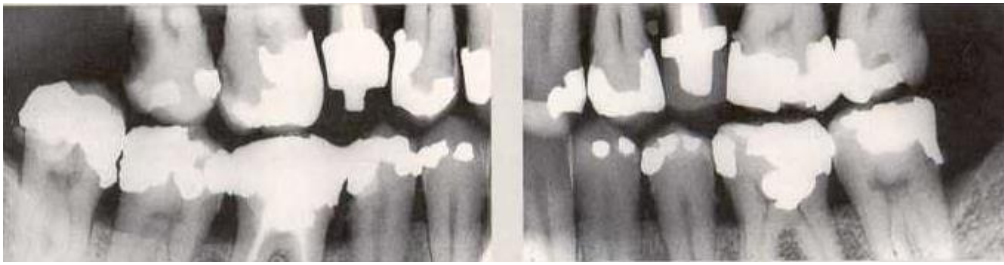


Fig. 2.8. Both these films reveal not only various stages of proximal caries, but also the condition of the restorations with overhanging margins of the post-and-core, a supererupted tooth 48 and periodontal destruction resulting from advanced marginal periodontitis. With a film height of 3.5 or 4 cm, it would be possible to achieve ideal illustration of periodontal lesions of the posterior segment.

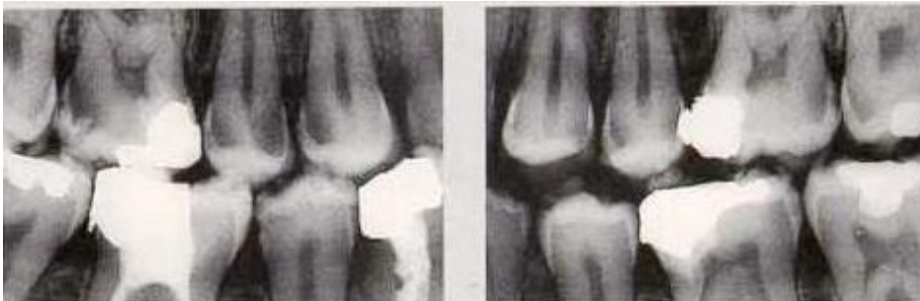


Fig. 2.9. These films were taken of a 20-year-old man 2 weeks after he had been examined clinically using mirror and probe, and dismissed as “caries free”! The bite-wing radiographs reveal numerous deep carious lesions.

Apical and Periodontal Radiographic Technique

Special radiographic techniques are necessary to show the apical and periodontal structures adequately, for two reasons:

- the best resolution as well as the least distortion will appear on the radiograph at the area where the central ray traverses the tissue;
- only those tissues that have been exposed appropriately with regard to their thickness and density will be optimally depicted in the radiograph.

For these reasons, in order to produce a high-quality apical or periodontal radiograph, the central ray must pass through either the root apex or the alveolar crest. The exposure data must be selected corresponding either to the thickness of the bone at the level of the root apices or for proper depiction of the thinner alveolar crest. Taken to extremes, this means that if perfect depiction of the apical region is desired, the depiction of the tooth crown and the alveolar crest must be sacrificed to some degree; on the other hand, for a perfect periodontal projection, the depiction of the root apex will be compromised.

In reality, of course, nobody who is preparing a conventional radiographic survey will be prepared to consciously renounce the simultaneous depiction of the tooth crown and the root apex! However, since the introduction of the panoramic radiograph as the basic diagnostic film, new ideas concerning targeted application for the periapical radiograph have begun to evolve. On the other hand, because the concept of a more modern examination strategy using panoramic radiography does not yet enjoy general acceptance, a compromise must be found. One realistic approach to improve the still often used conventional radiographic survey is the regular use of a film holder that guarantees optimum positioning. In this regard, systems that position the film at a right angle to the X-ray tube have proved themselves in clinical practice; in this way, the separate, tiresome, and “free-hand” positioning of the film and the X-ray tube can be replaced by a compact targeting mechanism that virtually guarantees accuracy. In addition to improving conventional radiographic technique, film quality is improved and radiation dose is reduced.

Apical and Periodontal Survey in Adults

This is achieved via a system in which the film is held in a sterilizable and interchangeable film holder attached to an adapter ring that can be connected to the tube of almost any dental radiographic equipment. This guarantees that the film is always at a right angle to the central ray and fixed in the center of the perfectly shielded X-ray beam; in addition, this insures proper positioning of the unit and the film, as well as maximum radiation protection with each exposure.

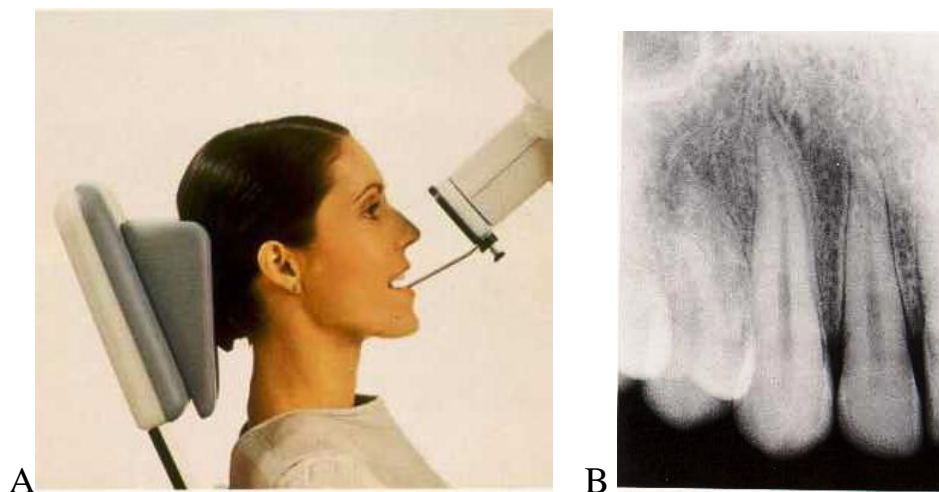


Fig. 2.10. (A) Positioning for the maxillary anterior region. The picture shows the use of the film holder. Note also the head position for radiography in the maxilla. (B) Radiograph of the region for a simple depiction of the canine.

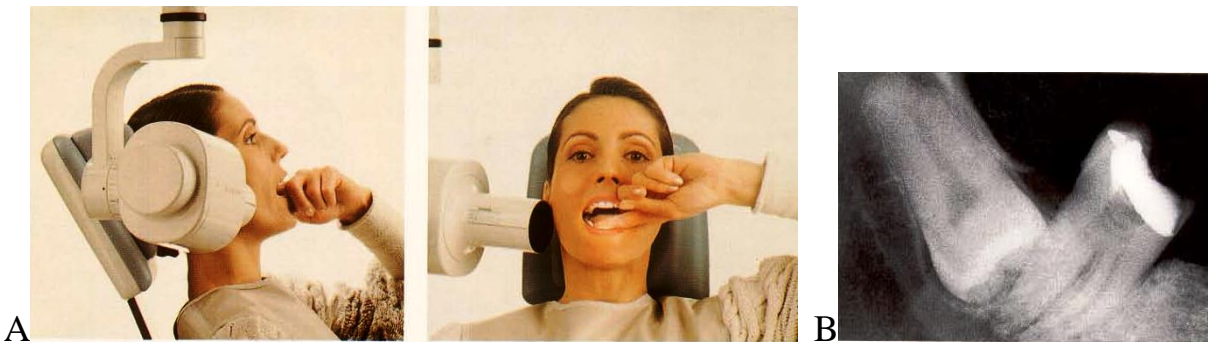


Fig. 2.11. (A) Positioning for depiction of a mandibular third molar. If the tooth is not completely depicted on the film, it is again unlikely the fault of film positioning, rather one of central ray projection. The central ray must be projected upon the object (lower third molar) such that it is directed somewhat from posteriorly and superiorly to inferior and anteriorly. (B) Radiograph of a horizontally impacted mandibular third molar. As in the maxilla, the 3x4 cm film packet is used horizontally.

Radiographic Technique with the Occlusal Film

Occlusal films can be employed intraorally as well as extraorally to depict the third dimension for diagnostic purposes. In children, periapical films or a 4x5 cm occlusal film may be used as occlusal radiographs.

Intraoral occlusal radiographs permit axial projections of the mandible and modified axial projections of the maxilla. With regard to the long axes of the teeth, periapical radiographs and panoramic films provide orthoradial or eccentric views only. Depiction of the third dimension can be of utmost diagnostic significance if the indication is appropriate and if the technique is performed precisely. The occlusal radiograph is most often used for localization, as well as in the diagnosis of tumors and fractures. It is important that the occlusal radiograph be taken with a strictly axial projection with regard to the long axes of the teeth in the jaw being examined. The use of occlusal radiographs taken with the central ray not projected precisely axially (e.g., in the maxilla) may lead to incorrect diagnosis, for example in attempts to localize impacted teeth.

For edentulous patients examined in dental offices not yet equipped for panoramic radiography, an intraoral occlusal radiograph of the maxilla or the mandible may be employed to examine the jaws for the presence of root tips, retained or impacted teeth, cysts, tumors and tumor-like lesions. In young children, the standard periapical film packet may be used as an adequate occlusal film. In such cases, the goal is a simple illustration of the anterior teeth, often following trauma; therefore the projection of the teeth may be dealt with using the conventional bisecting angle technique. On the other hand, if a film holder is available for the right-angle system, it is possible to position the film in the central ray in all anterior regions, with minimum patient discomfort. In the case of fearful or traumatized children, this method may have psychological advantages.

Extraoral occlusal films can be employed for various special indications. For example, lateral depiction of the nasal bone of the maxillary anterior jaw region can be useful after trauma, in addition to localization of ectopic maxillary anterior teeth. Furthermore, lateral soft tissue projections of the lips may also be prepared. The occlusal film may also be used for depiction of the chin region without superimposition effects, for example to enhance panoramic radiography following trauma. Worthy of note is that the occlusal film used as a foil-free “periapical” film necessitates a relatively long exposure time; however, use of the special small cassette keeps exposure time within limits.

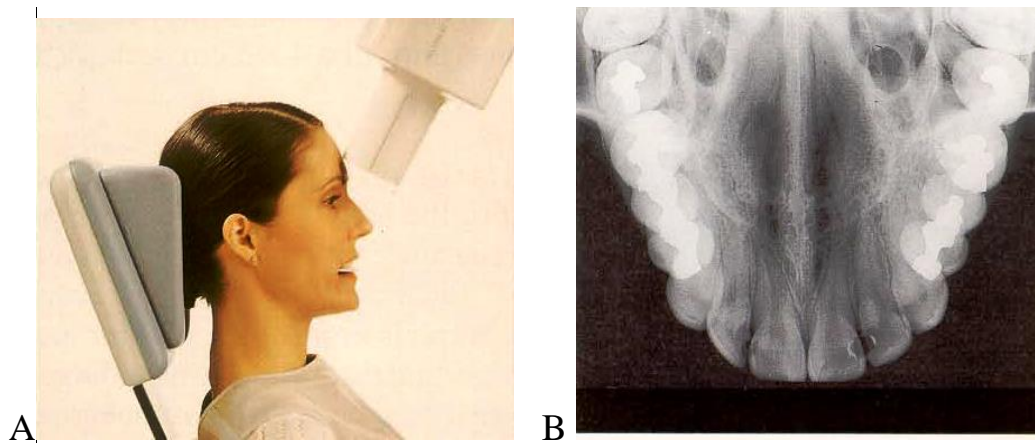


Fig. 2.12. (A) Correct positioning for a maxillary occlusal radiograph. Note the film packet position and the central ray direction (*left*). Viewed laterally, the central ray is targeted through the maxillary first molar. (B) Radiograph of the region. The 7.5x5.5 cm film packet is generally used for occlusal radiographs. For small children the 3x4 cm periapical film packet can be used, and for special situations the 4x5 cm periapical film.

Examination of the Masticatory Organ Using Panoramic Radiograph

To depict *occlusal relationships* simultaneously with the *position of the condyles*, it is necessary to take the radiograph with the patient in normal occlusion. The positioning of the patient demands particular attention: The position of the median sagittal plane at the back of the head must be checked precisely to avoid asymmetries of projection and resultant incorrect diagnosis.

For examination of *shape and structure of the condyles*, the patient is placed in the usual standard position and a bite plane is employed. A radiograph taken in this way generally depicts the condyles quite well in a zonographic layer of about 20 mm thickness. Perfect diagnosis of the condyles is only possible if the mandible is symmetrically positioned in a protruded position. It is well to remember that before proceeding to relatively more complicated radiographic examination, the possibilities provided by clinical examination, analysis of mounted study models, and panoramic radiographic analysis should be exhausted first. In many cases these will provide sufficient information to address any malocclusion.

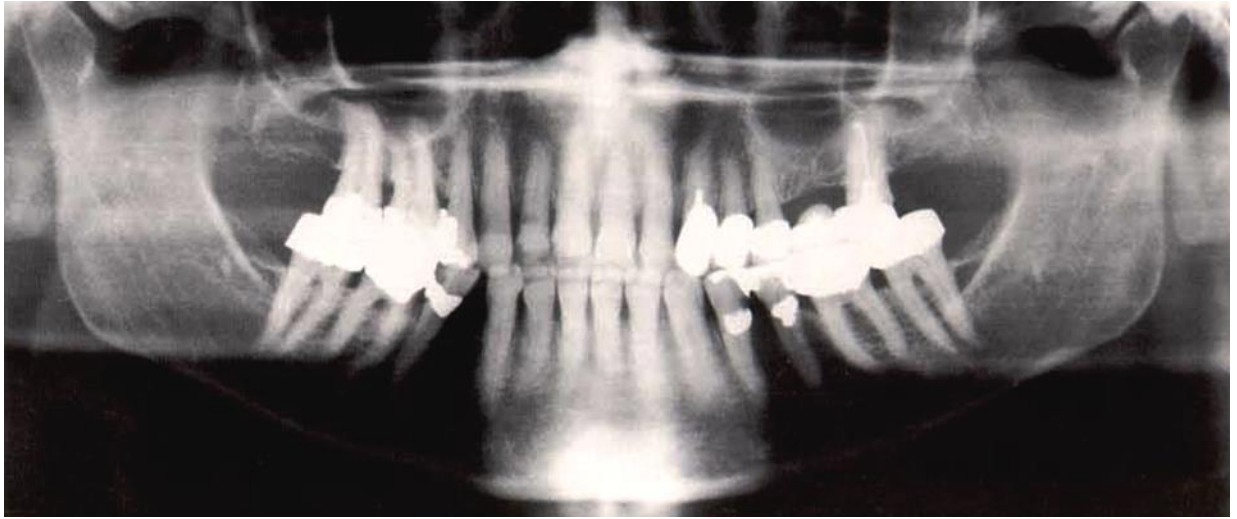


Fig. 2.13. Examination of occlusion with regard to condylar position in a fully dentulous patient. It is recommended to take the radiograph at high energy. This figure depicts a case of temporomandibular joint pathology on the right side accompanied by malocclusion. Note the differing positions of the condyles at the articular eminences.

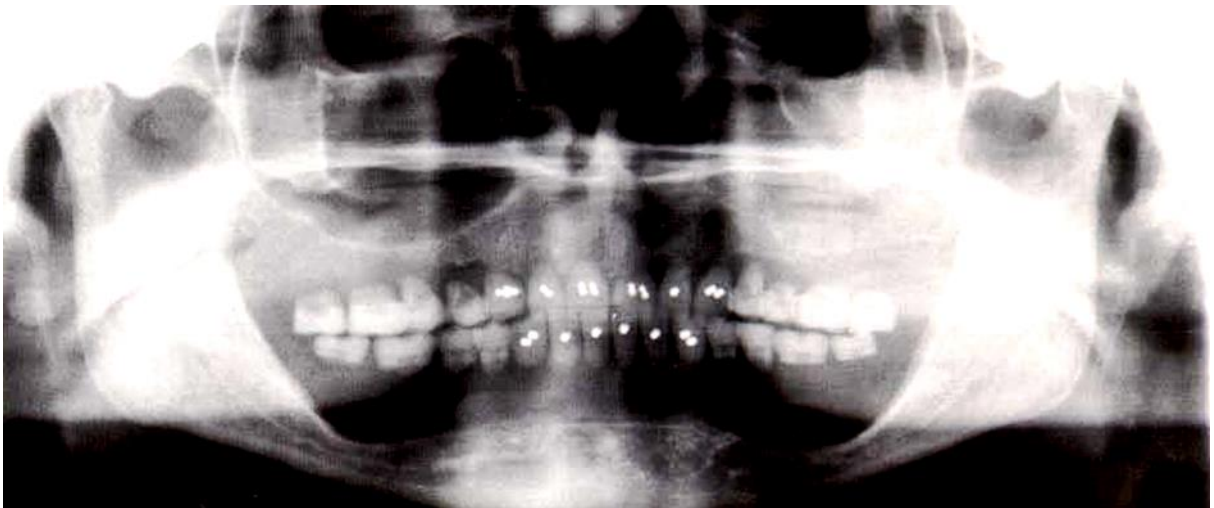


Fig. 2.14. Examination of occlusal relationships with regard to condyle position in an edentulous denture wearer. In this case it was necessary to leave the denture in place during exposure of the film. This panoramic film depicts a case with temporomandibular joint problems on the right side, and with poor occlusal support on the left side. Note the differing positions of the condyles at the articular eminences.

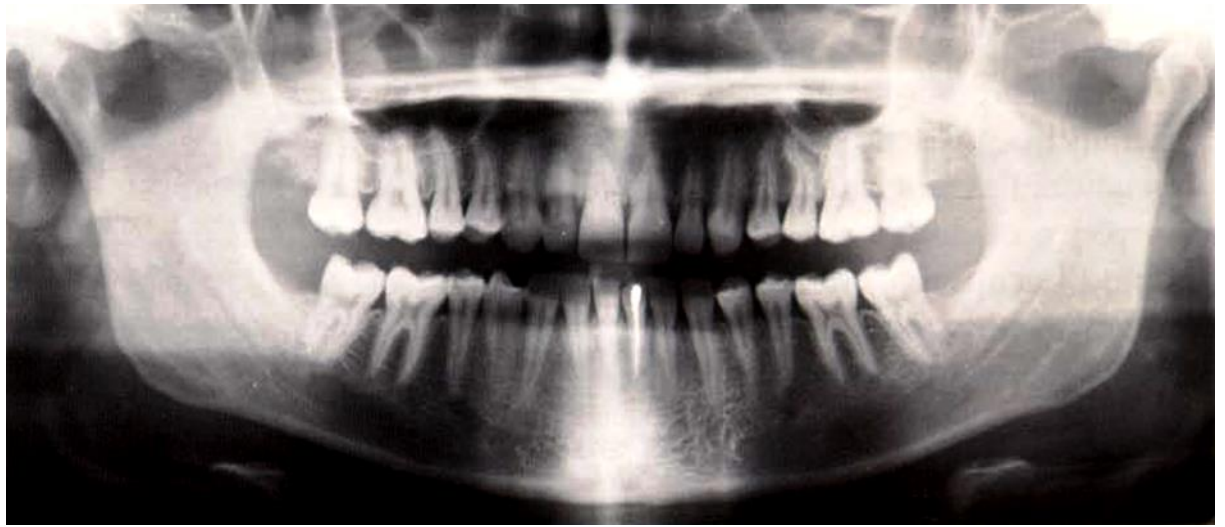


Fig. 2.15. Examination of the condyles in normal position with a bite plane in place. The slightly open mandible usually positions the condyles so that they can be observed without overlapping structures. In this 18-year-old female, the right condyle exhibits an osteochondral exostosis with a large cartilage component. Care must be taken to avoid asymmetric protrusive positioning of the mandible before taking the film.

Digital panoramic radiography: a clinical survey

Digital techniques have found increasing applications in radiology since the early 1980s, when digital subtraction angiography (DSA) was first introduced into clinical practice. In the recent past the use of photostimulable storage phosphor plates (IP) that can be exposed to X-rays like a standard film have extended the application of digital imaging to almost all the investigations of conventional radiology. The possibility of contrast modulation and the reduction of the radiation dose to the patient make digital storage techniques very promising in dental radiology also. This particular field is very demanding in terms of image quality.

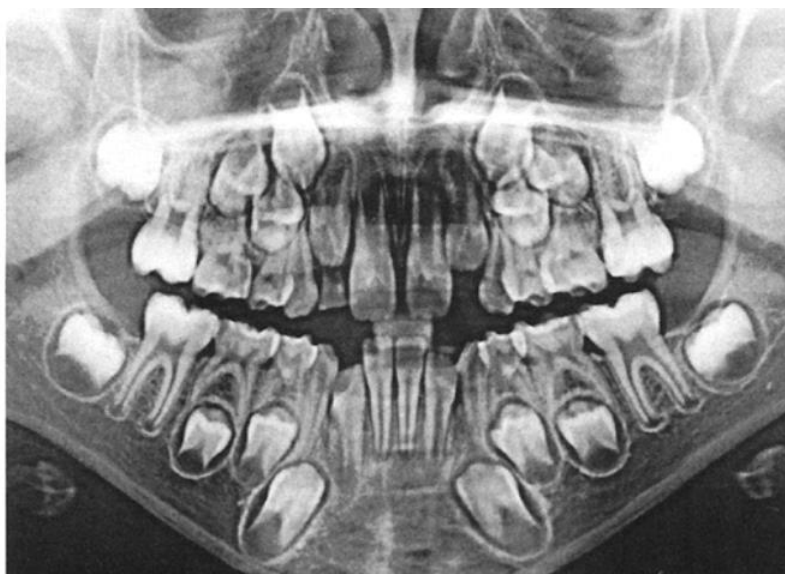


Fig. 2.16. Digital panoramic radiograph of a young child post-processed with an analogue-like **a** and a xerograph-like curve **b**. Note the good harmonisation of the contrast between the different portions of the arches, with good visibility of central and molar regions as well. This

feature is present in both images, but more marked in the xerograph-like image (b): the latter also improves the visibility of soft tissues and of the gingival border.

Film Tomography of the TMJ

Destructive parafunctions and unorthodox chewing habits as well as improperly contoured restorative work and occlusal wear can result in malocclusion. This can lead to functional disturbances, with ultimate trauma- induced degenerative changes within the TMJ. In this condition, during closure the mandible usually rotates around one of the joints, resulting in anterior, posterior, lateral or medial malpositioning of the condyles; the result is often lesions in the articular disc, with subsequent joint pathology.

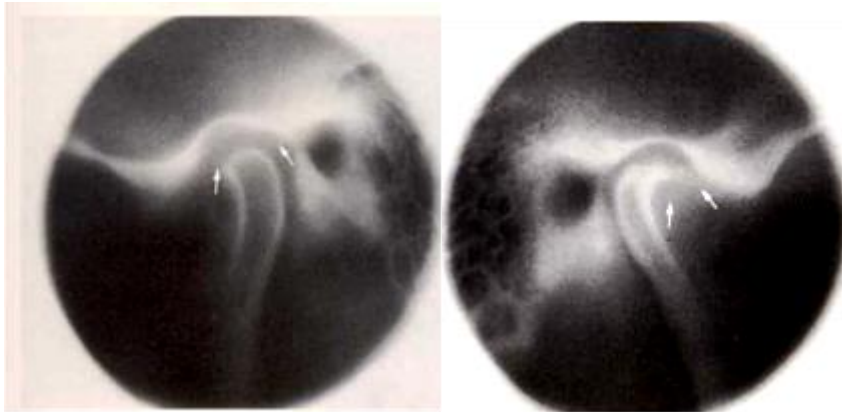
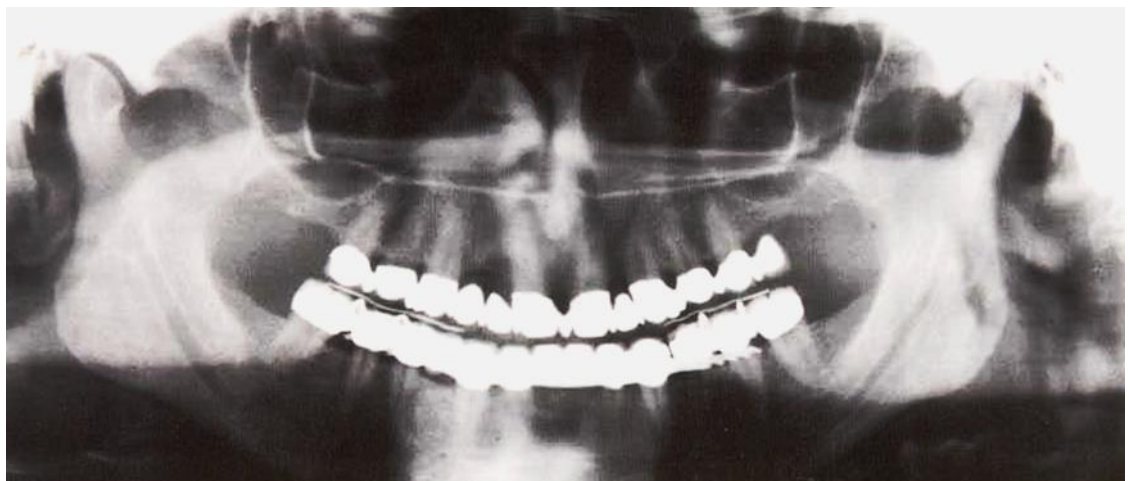


Fig. 2.17. Spiral tomography of left and right joints in normal occlusion. The left disc resides anteriorly (arrows), and the condyle resides in a “compressed” position deep in the fossa; arthropathy is obvious. The right condyle is normally configured but displaced medially. The disc (arrow) is in its normal position.



473

Fig. 2.18. Confirming radiograph of the same case, taken with a bite plane in situ. Note the positions of the condyles. After wearing the bite plane for 9 months, and after stabilization of the new occlusal position with temporary acrylic bridges, the patient could be dismissed without TMJ symptoms, despite irreversible joint pathology.

Computed tomography (CT)

Computed tomography (CT) is the modality of choice for the evaluation of facial trauma because it helps accurately identify and characterize fractures and associated complications, thereby aiding timely clinical management and surgical planning. In particular, CT clearly depicts clinically relevant fractures in the eight osseous struts or buttresses that function as an underlying scaffold for facial structures.

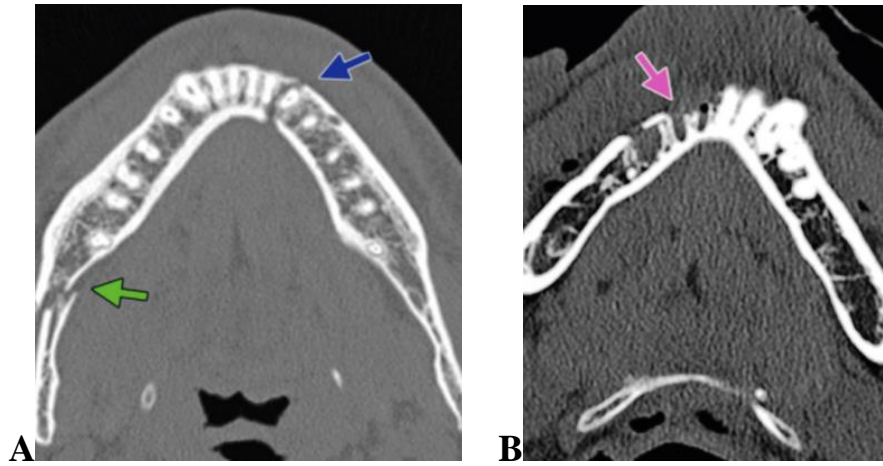


Fig. 2.19. Mandibular fractures. (A) Axial CT image of the mandible depicts a nondisplaced left parasymphyseal fracture (blue arrow) and mildly displaced fracture of the right mandibular body (green arrow) with distraction of the mandibular canal. (B) Axial CT image demonstrates a fracture of the right alveolar process (magenta arrow) with multiple missing teeth.

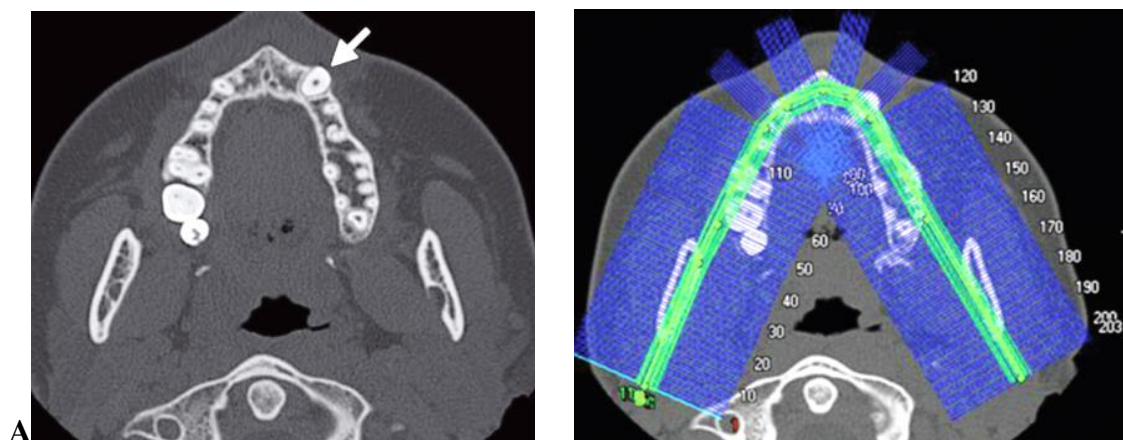


Fig. 2.20. Reformation of facial CT images in a 19-year-old woman. (a) Axial CT image obtained at the level of the alveolar process of the maxilla shows a nonerupted left maxillary canine (arrow). (b) Dental panoramic curved planar reformatted CT image created to prepare for surgical and orthodontic eruption shows the contour lines of the jaw, which were added with software.

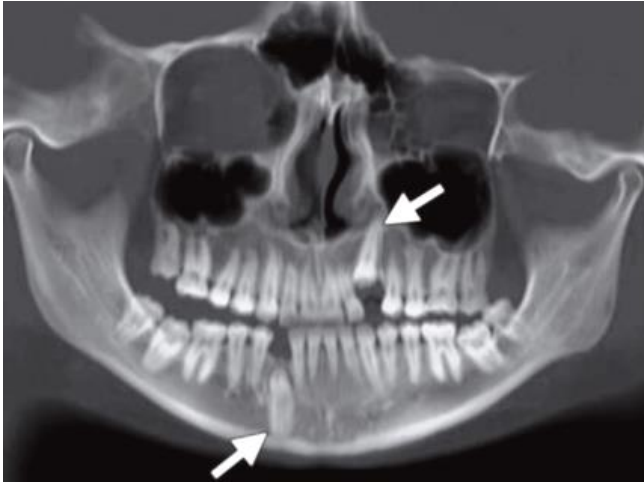


Fig. 2.21. Dental panoramic reconstructed CT image shows nonerupted left maxillary and right mandibular canines (arrows).

Computed Tomography for Supplemental Diagnosis

Regardless of its origin, a more or less asymptomatic chronic maxillary sinusitis is not always easy to detect on the panoramic radiograph, where other diagnostic problems assume primary importance. Only a carefully documented medical history and thorough clinical examination will provide the clinician with sufficient information to justify further radiographic examination. In addition to the radiographs, CT is often employed now to provide an axial depiction of the maxillary sinus without superimpositions; this permits diagnostically important left-right comparison.

Dental CT Imaging: A Look at the Jaw

The jaw comprises two complex bony structures: the mandible and maxilla. Their curved or archlike configuration makes radiographic imaging difficult. Furthermore, the superimposition of dense teeth and roots may obscure underlying tissues, and streak artifacts from dental restorations often degrade computed tomographic (CT) images. Recently, dental CT reformatting programs that use thin transverse images of the jaw to reformat multiple panoramic and cross-sectional views were developed.

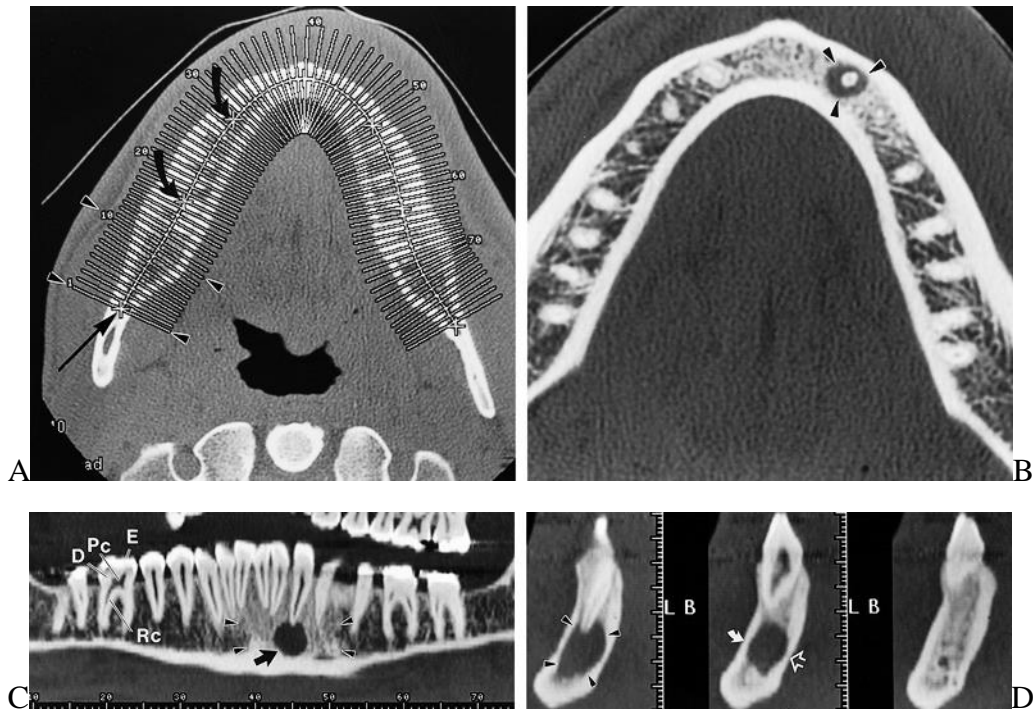
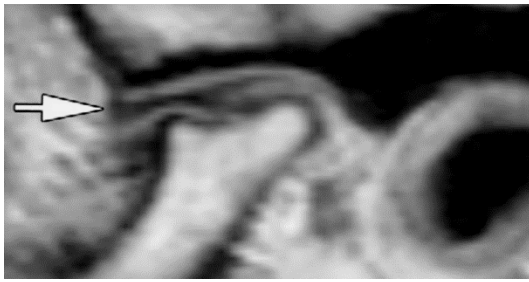


Fig. 2.22. Dental CT scans in 24-year-old woman with periapical radiolucency in the left canine tooth from endodontal disease. **(a)** Transverse image shows where the cursor is deposited (curved arrows) for the program to produce a curved line (straight arrow) that defines the location for reformatting the panoramic image in **c**. Perpendicular numbered lines (arrowheads) define where cross-sectional images in **d** are reformatted. **(b)** Transverse image shows the appearance of the target due to the opaque root in the center of the radiolucency (arrowheads). **(c)** Panoramic image shows an area of sclerotic condensing osteitis (arrowheads) surrounding a periapical radiolucency (arrow). The dentine (*D*), dense enamel (*E*), pulp chamber (*Pc*), and root canal (*Rc*) are nicely depicted. **(d)** Cross-sectional views show the relation of the periapical radiolucency (arrowheads) to the buccal (solid arrow) and lingual (open arrow) cortex.





C

Fig. 2.23. JIA in TMJ of 34-year-old woman. (A) Coronal CT image shows condylar concavities in both TMJs (arrows). (B) Oblique-sagittal CT image shows condylar concavity and flat wide fossa (arrow). (C) Oblique-sagittal intermediate-weighted MR image shows thin but intact disk (arrow), adapted to condylar deformity.



A



B



C

Fig. 2.24. (A) Axial contrast-enhanced CT image obtained with soft-tissue window settings shows the mass in the right mandibular ramus. The mass demonstrates low attenuation (20 HU) and is cystic with enhancing soft-tissue septations (black arrowheads) and mural nodules (white arrowheads). (B) Axial unenhanced CT image obtained with bone window settings shows the unerupted wisdom tooth (black arrow) centered in the cystic expansile mass. (C) Sagittal contrast-enhanced reformatted CT image shows the overall size of the mass and its cystic and solid components, as well as the unerupted tooth (black arrow). Arrowheads = septations, white arrow = large mural nodule.

03 Radiographic dental Anatomy

For all intraoral or extraoral dental radiographs, the radiographic anatomy as well as the general principles of radiology apply, as described in the section on radiographic anatomy in panoramic radiographs.

The *tangential effect* and the *summation effect* play decisive roles in the depiction of structure borders, and ascertainment of three dimensional relief. Any change in the central ray projection leads to an alteration of the radiographic illustration of the relationships among and between anatomic structures. This is why a single film can be insufficient and may even lead to incorrect interpretation when special examinations are performed using conventional radiographs. One need only consider the problems of localization. Dense, thick structures such as tooth roots may obscure thinner structures such as vestibular or lingual (palatal) alveolar walls because of increased X-ray absorption; on the other hand, the superimposition of such structures by air- or soft tissue-containing spaces may lead to radiolucency as a result of less X-ray absorption. An example of this is the possible superimposition of mandibular premolar roots by the mental foramen.

In this context, as already mentioned above, the *radiographic technique* used is of critical importance. In contrast to panoramic radiography, in which the patient is more or less immobilized by the cephalostat and the stationary X-ray beam

positioning, the free-hand positioning of the film packet and the central ray vis-a-vis the random positioning of the skull during periapical radiograph presents a broad variety of projection possibilities. As a consequence, projection variation causes structural details to shift in the third dimension, and may significantly alter the appearance of a radiograph in many different ways. To completely depict anatomic structures in various possible projections, it was important in this chapter to present not only normal projections but also the results of incorrect techniques.

Radiographic anatomy represents the basis for radiographic interpretation. It follows its own rules and demands understanding and knowledge of how X-rays work, as well as the normal anatomy of the irradiated spaces, depending on the radiographic technique used. Analogous to this essential knowledge, the following basic rules must be obeyed for every type of radiograph:

The *tangential effect* of X-rays renders clearly visible in the irradiated space only those hard tissues with either high density or significant thickness; thin lamella which, at the moment of the exposure, are parallel or nearly parallel to the central ray simulate hard tissue of significant thickness and therefore appear in the radiograph as densely opaque. On the other hand, similar structures which, at the moment of exposure, are perpendicular to the central ray or nearly so may, even though they are relatively thick, appear transparent in the radiograph because of the exposure data necessary to penetrate the tissue (Figure 3.1).

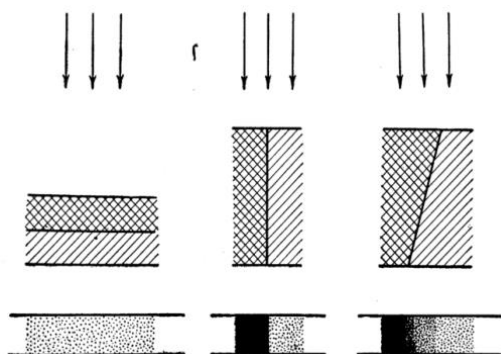


Fig. 3.1. Tangential effect.

Superposition effect can lead to a false image in the image of tissue density. The area of the image may look more dense, depending on the summation of the shadows from the two anatomical structures located one above the other. The situation in such cases is completely unrelated to the x-ray signs of "sclerosis" (Figure 3.2).

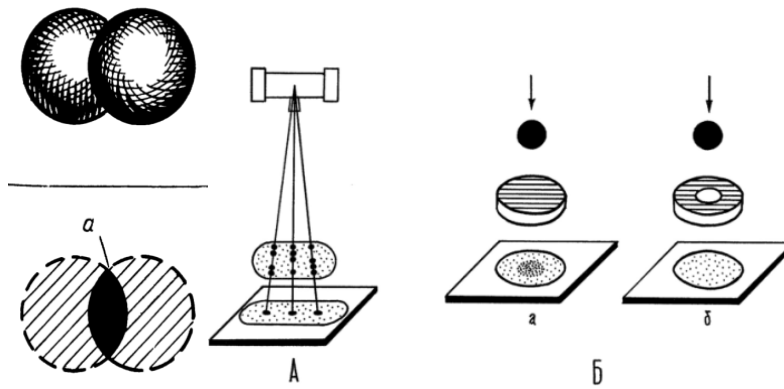


Fig. 3.2. Superposition effect

The effect of geometric deformation of images. Anatomical structures may have a deformed appearance on X-rays depending on their location in the flux of X-rays (Figure 3.3).

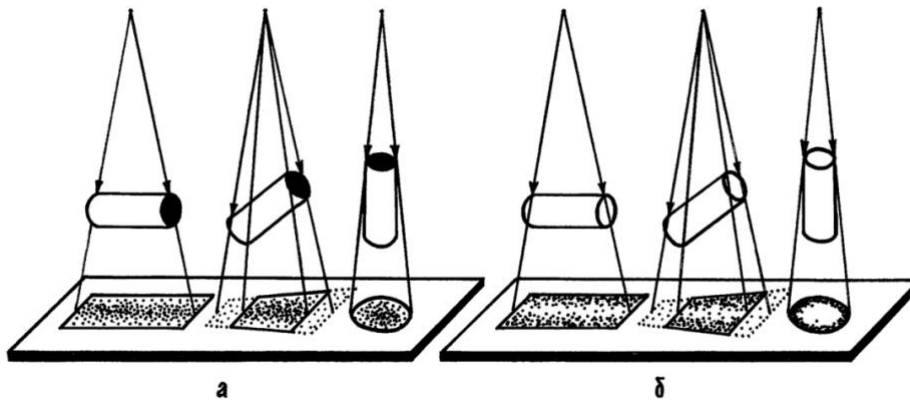


Fig. 3.3. The effect of geometric distortion of images.

If a film holder is routinely employed, it is possible to reduce the many possibilities for incorrect depiction of anatomic structures, which can lead to more standardized films that are easier to interpret. Finally it is important to note that certain special positioning cannot be accomplished even using a universal film holder; it is therefore necessary to have knowledge unexpected structures.

Teeth

Disease of the teeth and their support structures is common and frequently seen at imaging of the head and neck. Recognition of dental disease by the interpreting radiologist has the potential to alter the course of patient care, such as when periapical disease is identified as the cause of sinusitis or pericoronitis is identified as the cause of deep neck infection.

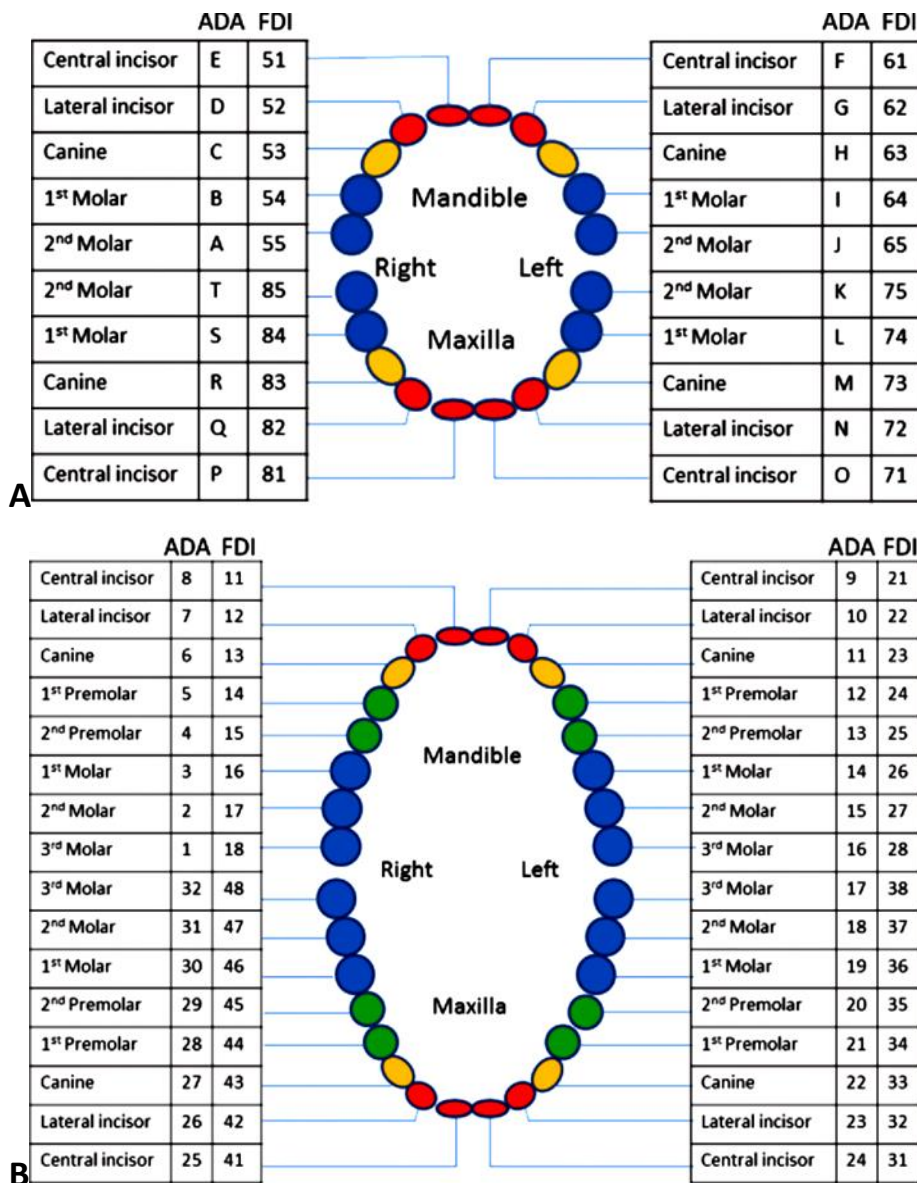


Fig. 3.4. Tooth numbering nomenclature for primary and permanent teeth. **(A)** Illustration shows the universal numbering system (ADA), which uses letters A–T, and the FDI numbering system, which uses numbers 51–55, 61–65, 71–75, and 81–85, for primary teeth. Blue = molars, red = incisors, yellow = canines. **(B)** Illustration shows the universal numbering system (ADA), which uses numbers 1–32, and the FDI numbering system, which uses numbers 11–18, 21–28, 31–38, and 41–48, for permanent teeth. Blue = molars, green = premolars, red = incisors, yellow = canines.

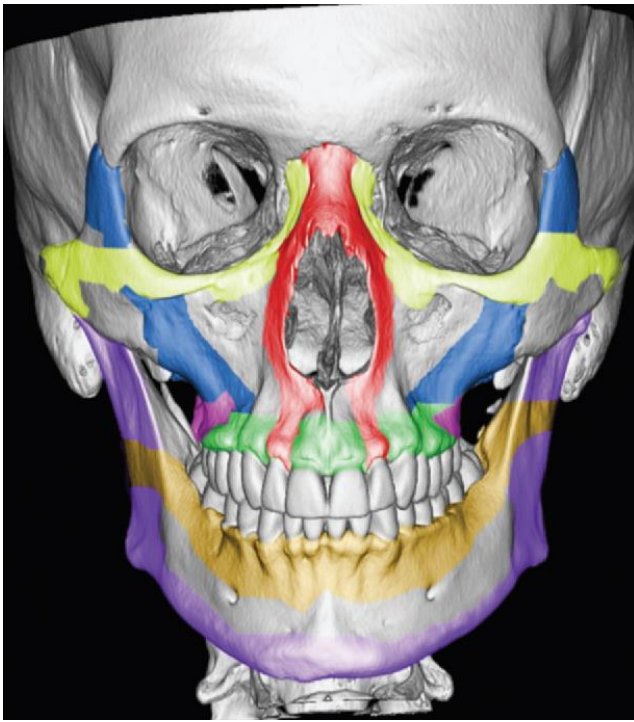


Fig. 3.5. Four systems of facial partitions. Three-dimensional CT image of an adult skull with color overlays shows partition of the facial anatomy into upper (red), middle (blue), and lower (yellow) thirds, the system used by otolaryngologists to describe locations of fracture in the facial anatomy.

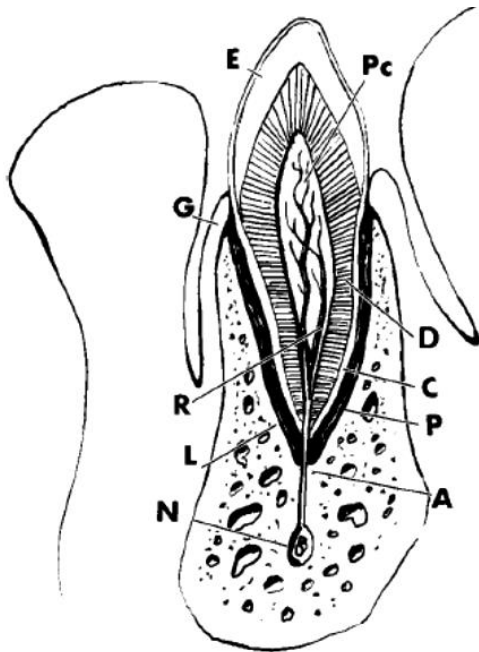


Fig. 3.6. Illustration of normal tooth anatomy. A = apical foramen, C = cementum, D = dentine, E = enamel, G = gingiva, L = lamina dura, N = neurovascular bundle, P = periodontal ligament. Pc = pulp chamber, R = root canal,

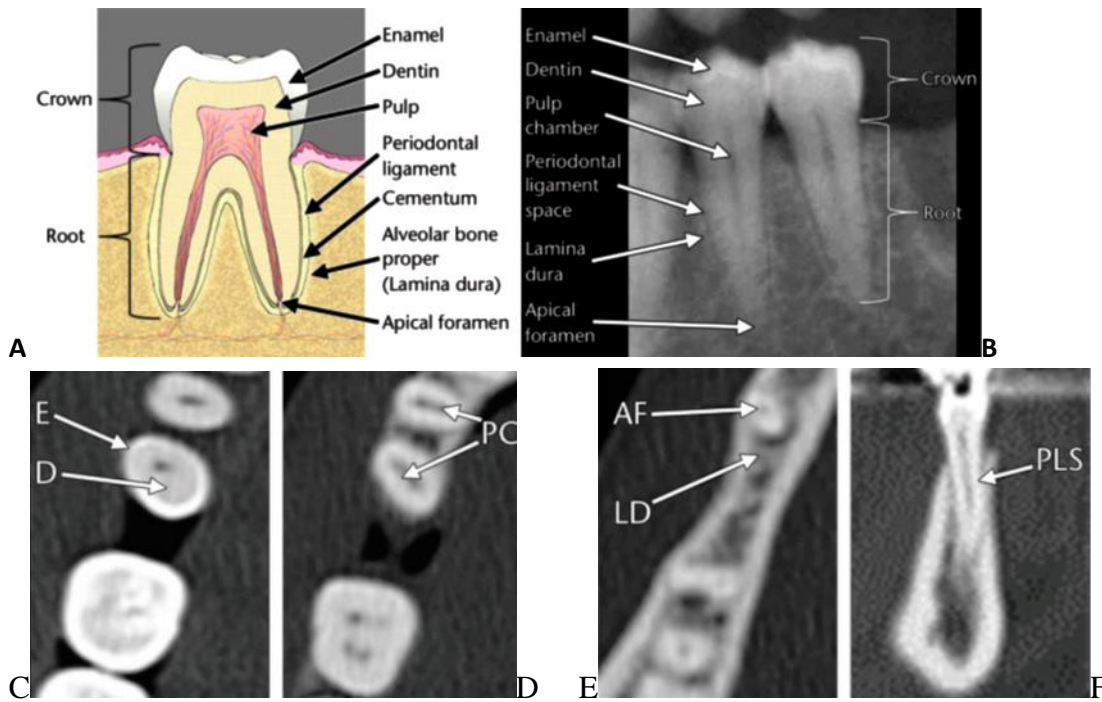


Fig. 3.7. Schematic (A), radiographic (B), and CT (C–E [axial], F [sagittal reformation]) anatomy of the tooth. The extremely opaque enamel encases less opaque dentin in the crown. The more lucent pulp chamber and root canal are located within the center of the tooth. The apical foramen is the lucent central aspect at the tooth apex. The lamina dura is a layer of cortical bone that lines the tooth socket and separates it from adjacent cancellous bone. The periodontal ligament is the connective tissue located between the tooth apex and the lamina dura. **AF** = apical foramen, **D** = dentin, **E** = enamel, **LD** = lamina dura, **PC** = pulp chamber, **PLS** = periodontal ligament space.

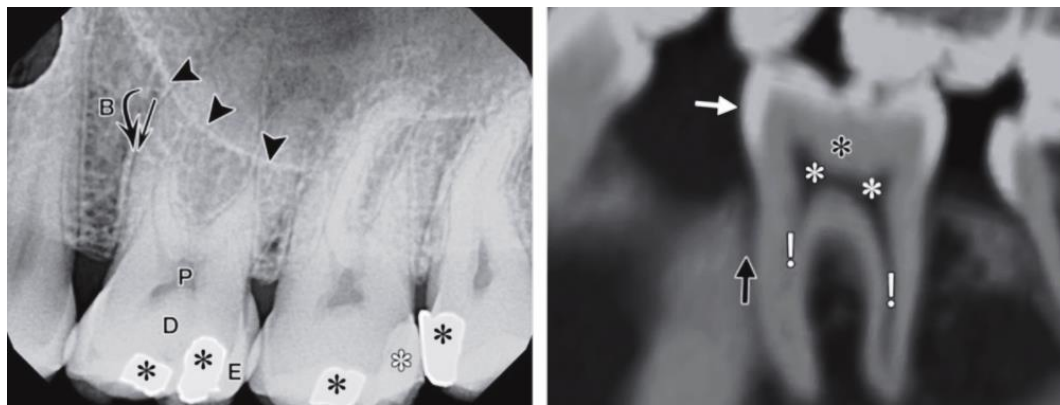


Fig. 3.8. Normal tooth anatomy. Digital periapical radiographs of maxillary molars shows enamel (E), dentin (D), pulp chamber (P), alveolar process (B), lamina dura (curved arrow), and periodontal ligament space (straight arrow). Amalgam (black *) and composite fillings (white *) are also seen. Arrowheads = superimposed maxillary sinus wall. (c) Magnified sagittal oblique CT image of a mandibular molar shows the enamel (white arrow), dentin (black *), pulp chamber (white *), pulp or root canal (!), and periodontal ligament space (black arrow), which is radiolucent.

Radiographic Anatomy During Tooth Development

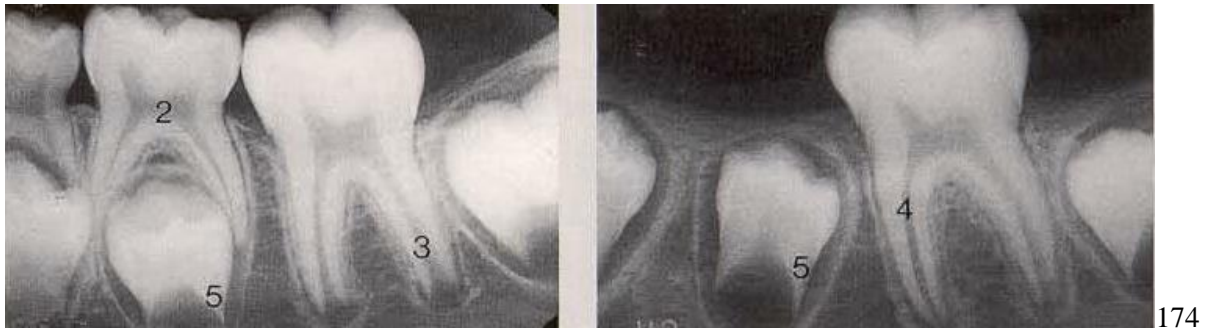


Fig. 3.9. Normal eruption (*left*) in this 7-year-old child. The apices of tooth are not yet fully formed. *Right*: 9-year-old child after extraction. The root formation has begun. The apices of tooth have formed. The root canals of this tooth remain widely open.

(2. Normal eruption, with incipient resorption of the roots of deciduous tooth. 3. Root formation not yet complete. 4. Root apex and the root canal remain wide open. 5. Incipient root formation.)

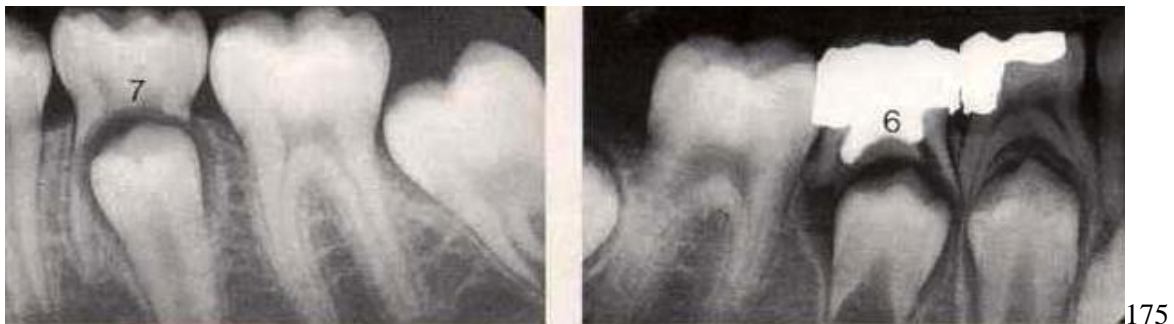


Fig. 3.10. Disturbances of tooth eruption (*left*): This radiograph gives the impression that the mesial root tip of tooth 75, which shows signs of resorption, remains isolated in the alveolar bone. This and similar situations can lead to rotation and axial deformation of the permanent teeth. Root canal fillings, apical periodontitis and trauma to the deciduous teeth may also lead to displacement of permanent teeth.

(6. Apical periodontitis on tooth, which disturbs normal eruption of permanent tooth. 7. Asymmetric root resorption on tooth.)

Radiographic Anatomy in Periapical and Occlusal Radiographs

Radiographic Anatomy of Special Regions

Maxillary Anterior Region

The characteristic radiographic appearance of this region results from the varying thickness and density of the tissues. Anterior teeth exhibit shadowing, caused by enamel and superimposed bone, as well as radio lucencies at the cervical region of the tooth, which is not superimposed by other structures. The cervical dentin, which is not superimposed by alveolar bone or the enamel, is easily penetrated in its lateral aspects by the X-ray beam and therefore presents as a radiolucency (“burn-out effect”). The tip of the nose and the nasal orifices also contribute to both addition and subtraction effects; frequently the anterior portions

of the floor of the nose and the median suture are clearly visible. Often it is difficult, however, to visualize the incisive foramen.

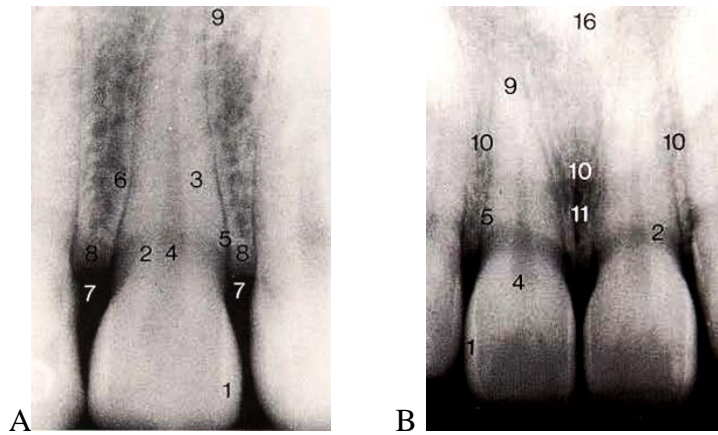


Fig. 3.11. (A) X-ray film of an intact tooth 22. This figure exhibits well the addition effects caused by enamel and alveolar bone, as well as the subtraction effects due to the periodontal ligament space and the pulp canal. (B) X-ray film of the maxillary central incisor.

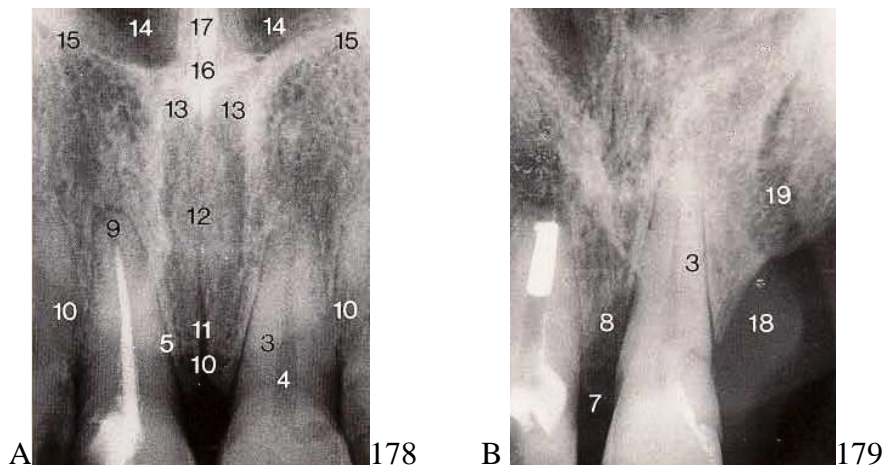


Fig. 3.12. (A) Radiograph of the nasopalatine canal system apical to teeth 11 and 21. (B) Addition and subtraction effects caused by nasal soft tissues.

(1. Coronal enamel made visible via tangential effect, 2. cervical area of the tooth between the enamel layer and the entrance to the alveolus, 3. tooth root, 4. pulp canal, 5. periodontal ligament space, 6. lamina dura, 7. vestibular margin of the alveolar bone, 8. palatal margin of the alveolar bone, 9. apex of the tooth root, 10. tip of the nose, 11. median suture, 12. incisive foramen, 13. nasopalatine canal, 14. nasal foramen of the nasopalatine canal, 15. piriform aperture, 16. anterior nasal spine, 17. nasal crest of the maxillary bone, 18. nasal cartilage, 19. nasal introitus.)

Maxillary Canine Region

Figures 180 to 183 present eccentric views of the maxillary anterior region. In addition to the teeth, some of these films therefore exhibit other structures such as the nasal process of the maxilla and the nasal soft tissues, which result from the addition effect. The nasopalatine canal and the incisive foramen also often appear superimposed upon a central incisor. In this projection, both roots of the first premolar appear, and sometimes a portion of the anterior lobe of the maxillary sinus is visible. The structure of the bone appears small meshed. This form is typical

for the maxilla. Incisor teeth that are rotated or oblique in the central ray exhibit the burn-out effect at the cervical area of the crown.

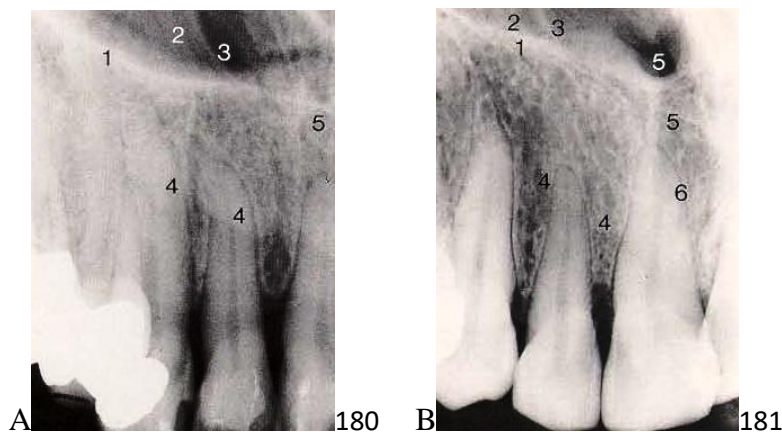


Fig. 3.13. (A) Distal eccentric projection, targeted on tooth 12. (B) Distal eccentric projection, targeted on teeth 11 and 12. The incisive canal is superimposed upon the root of tooth 11.

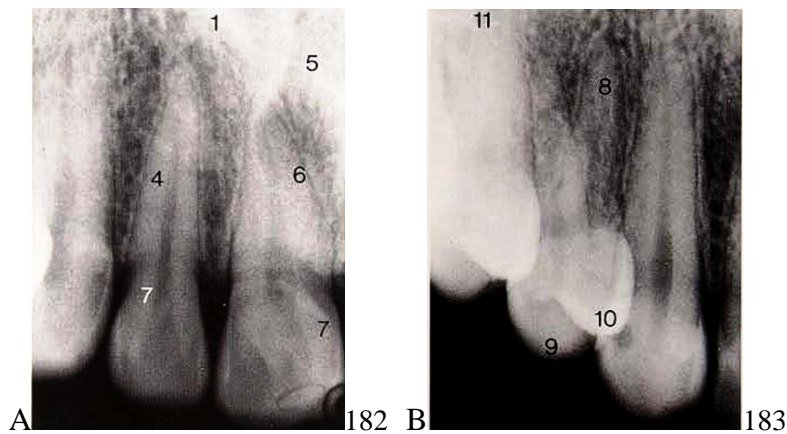


Fig. 3.14. (A) Distal eccentric projection, targeted on teeth 11 and 12. In addition to the subtraction effect caused by the incisive foramen, tooth 12 also exhibits a burn-out effect at the cervical area, mesial and distal on the crown of the tooth. (B). Mesial eccentric projection targeted on tooth 13.

(1. Laterobasal boundary of the nasal cavity, 2. frontal process of the maxillary bone, 3. piriform aperture, 4. lateral nasal border, 5. nasopalatine canal. 6. incisive foramen. 7. burn-out effect, 8. palatal root of tooth 14, 9. buccal cusp of tooth 14, 10. palatal cusp of tooth 14. 11. anterior lobe of the maxillary sinus.)

Maxillary Premolar Region

The possible relationships of the premolars and the molars to the maxillary sinus are so extraordinarily variable that it will not be possible to discuss them extensively here. Not only do the maxillary premolars exhibit quite variable root forms, the size and shape of the maxillary sinus also vary considerably. Of note is that the periapical film only provides an orthoradial view of the region. The view is from lateral and superior onto the tooth roots and the floor of the sinus; it is for this reason that the floor of the sinus is never precisely outlined by the radiographically visible borders.

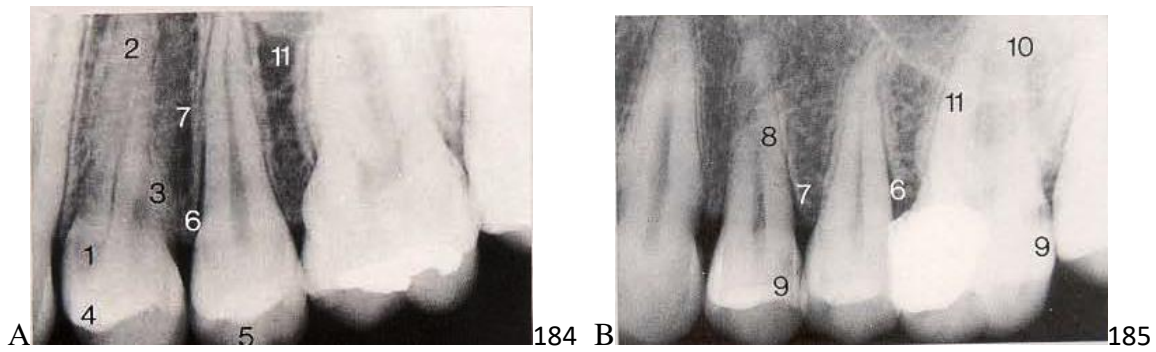


Fig. 3.15. (A) Radiograph of the region of teeth 24 and 25. Note the burn-out effect in the crown of tooth 24. (B) Radiograph of the maxillary left premolars. Note the root formation of tooth 24. Proximal caries is difficult to detect in periapical radiographs (note distal of tooth 24).

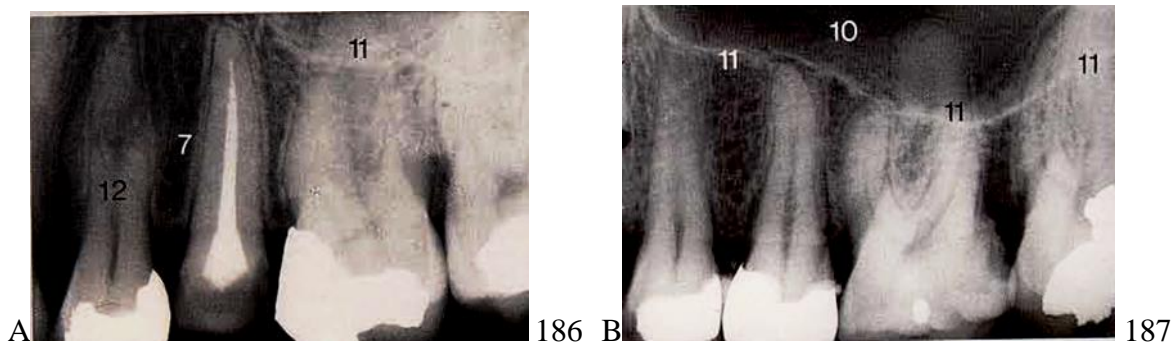


Fig. 3.16. (A) Radiograph of the region of teeth 24 and 25. Note that tooth 24 exhibits three roots! (B) Radiograph of teeth 24, 25 and 26. Note the position of the floor of the sinus, which must be located between the buccal root tips and the palatal root tip of tooth 26.

(1. Burn-out effect, 2. palatal root of tooth 24, 3. buccal root of tooth 24, 4. palatal cusp of tooth 24, 5. buccal cusp of tooth 25, 6. periodontal ligament space, 7. lamina dura, 8. dilacerated buccal root, 9. proximal caries, 10. floor of the maxillary sinus, 11. laterobasal border of the maxillary sinus, 12. tooth 24, exhibiting three roots.)

The radiographs of the premolar region presented on this page were not taken using the standard technique. Because of the steep projection angle, these films exhibit numerous anatomic details. The view is obliquely from above onto the floor of the nasal cavity and maxillary sinus. The palatal portion of the alveolar process of the maxilla is projected on the floor of the maxillary sinus, where it is seen as background formation. Usually a sinus is traversed by a septum that is often projected in the region of the root tip of the maxillary second premolar. The laterobasal walls of the nasal cavity often appear as a more or less horizontal opaque line at the upper border of the radiograph if the projection angle is steep or if the film has been bent.

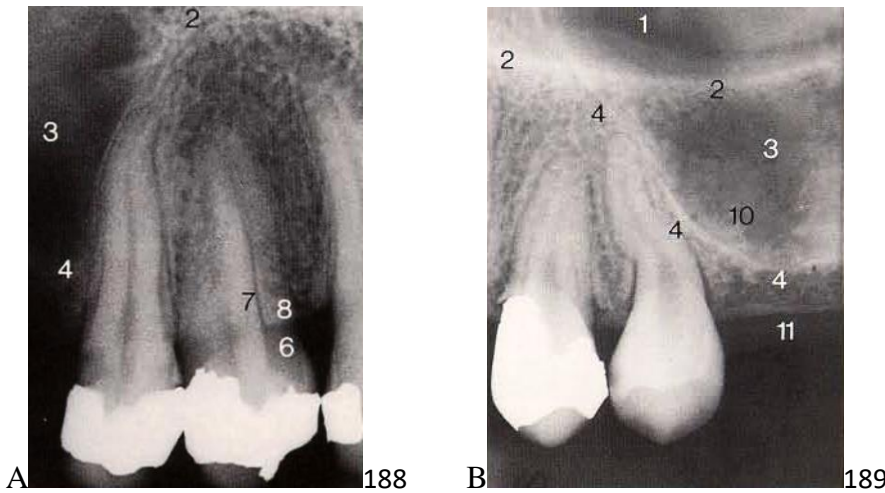


Fig. 3.17. (A) Radiograph of the region of teeth 15 and 14. (B) Radiograph of the region of teeth 24 and 25. After the loss of one or more molars, the maxillary sinus has expanded toward the alveolar crest and thus appears "far down" in the periapical radiograph.

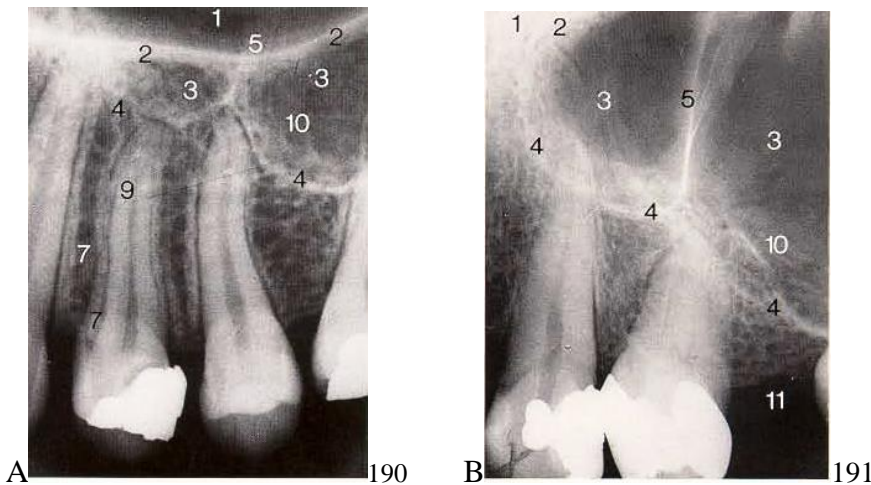


Fig. 3.18. (A) Radiograph of the region of teeth 24 and 25. Figures reveal how the septum divides the anterior recess from the alveolar recess of the sinus. (B) Radiograph of the region of teeth 23 and 24.

(1. Floor of the nasal cavity, 2. laterobasal border of the nasal cavity, 3. floor of the maxillary sinus, 4. laterobasal border of the maxillary sinus, 5. septum dividing the anterior recess from the alveolar recess of the sinus, 6. burn-out effect, 7. periodontal ligament space, 8. interradicular bone septum anterior to the palatal root of tooth 14, 9. superimposed roots of tooth 24; the longer root is the palatal, 10. alveolar process appears as the "background" on the sinus floor, 11. alveolar crest.)

Maxillary Molar Region

Here again it is important to keep in mind that when viewing a periapical radiograph one is looking from above and laterally onto the zygoma, the molars and the tuberosity region. If the projection angle is excessively steep, and if the apical base of the alveolar process is low, the zygoma is often root tips of the molars are obscured. Sometimes the pyramidal process of the palatal bone and the pterygoid process appear in the film. Sometimes the coronoid process of the mandible encroaches on the film, appearing as the so-called "radix relicta" projected on the tuberosity.

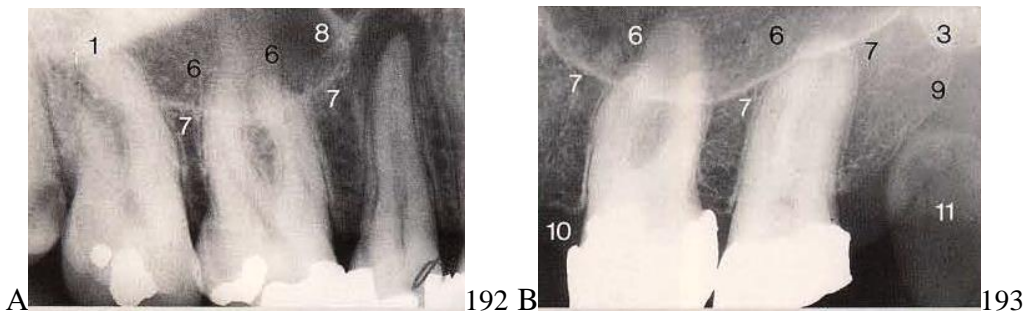


Fig. 3.19. (A) Periapical radiograph of the maxillary right molar region. A well-demarcated chronic apical periodontitis on tooth 15 displaces the maxillary sinus and shows signs of reactive sclerosis. (B) Radiograph of the tuberosity region, maxillary left.

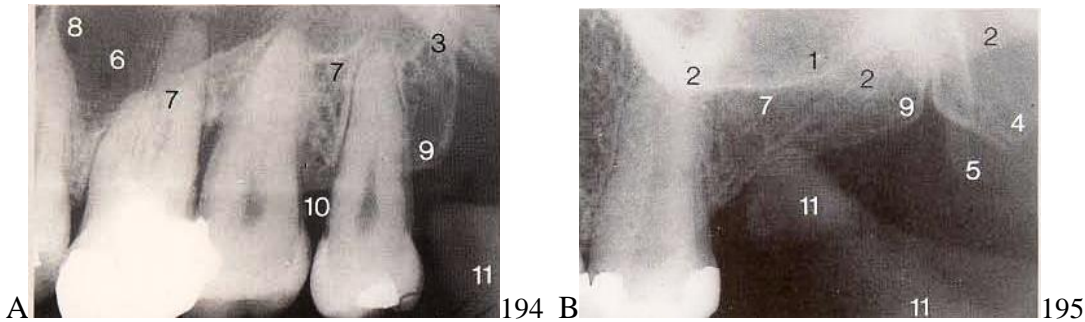


Fig. 3.20. (A) Radiograph of the molar and tuberosity regions, maxillary left. (B) Radiograph of the tuberosity region, maxillary left. The zygomatic process of the maxilla and the body of the zygoma shadow the root tips of 27 and the tuberosity region.

(1. Body of the zygoma, 2. zygomatic process of the maxilla and shadow of the zygomatic bone, 3. pyramidal process of the palatal bone, 4. lateral lamina of the pterygoid process, 5. hamulus of the medial lamina of the pterygoid process, 6. floor of the maxillary sinus, 7. laterobasal border of the maxillary sinus, 8. septum of the sinus, 9. maxillary tuberosity, 10. alveolar crest, 11. coronoid process of the mandible.)

Mandibular Anterior Region

It is usually possible to depict the four mandibular incisor teeth in a single periapical radiograph. If the mental fovea is deep and broad, a rather well-demarcated radiolucency will appear toward the alveolar crest; without perfect knowledge of the anatomic structures, such radiolucencies have been described as “cystoid.” Especially in cases of advanced chronic marginal periodontitis, well-demarcated radiolucent bands appear to course apically between the roots of the anterior teeth. Such radiolucencies represent vascular canals.

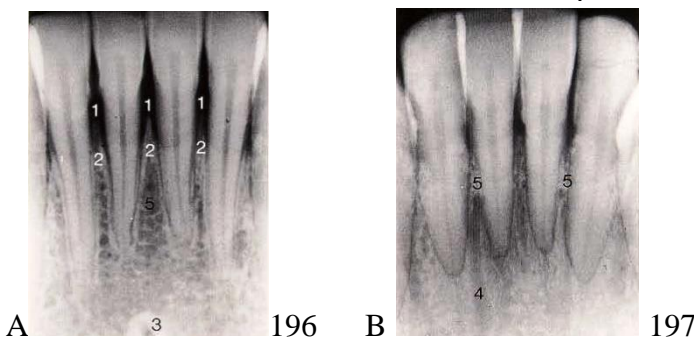


Fig. 3.21. (A) Normal periapical radiograph of the mandibular anterior teeth. (B) Periapical radiograph depicting vascular canals.

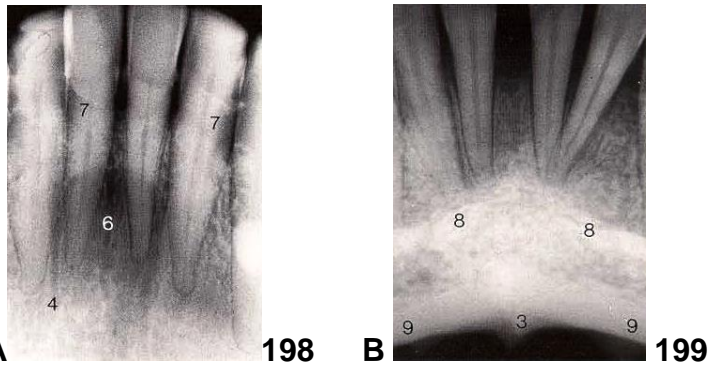


Fig. 3.22. (A) Radiograph of a mandibular anterior segment clearly exhibiting the mental fovea. (B) This periapical radiograph of the mandibular anterior region was taken with a steep projection angle and depicts the mental spine.

(1. Labial portion of the interdental septum, 2. lingual portion of the interdental septum, 3. mental spine, 4. vascular canals depicted longitudinally, 5. cross sections of vascular canals, 6. mental fovea, 7. burn-out effect, 8. shadowing caused by the chin prominence, 9. compact bone.)

Mandibular Canine Region

The bony structure of the mandible and the mandibular alveolar process is trabecular and unremarkable, but depending upon the radiographic projection angle, the canine tooth may exhibit several periodontal ligament spaces because of its flat and oval root form. Not infrequently one sees two completely developed roots; in an orthoradial projection, these may be almost perfectly superimposed upon each other and therefore be difficult to ascertain. The same holds true for the first premolars. Enostoses are sometimes observed around the mental foramen.

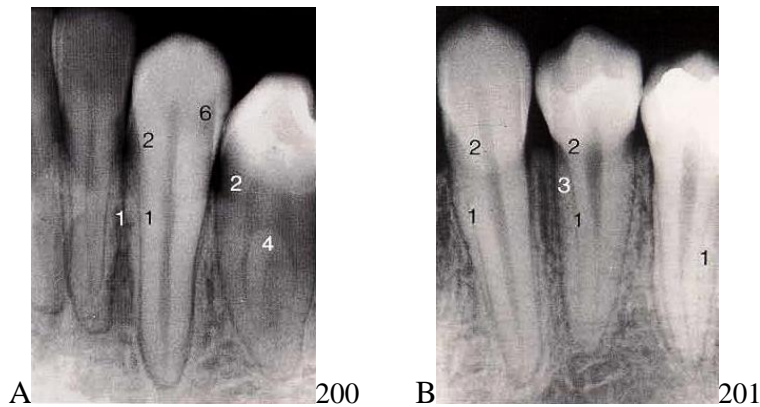


Fig. 3.23. (A) Radiograph of tooth 33 and a two-rooted 34. (B) Radiograph of the region of teeth 33 and 34. Note the multiple periodontal ligament spaces resulting from the root form.

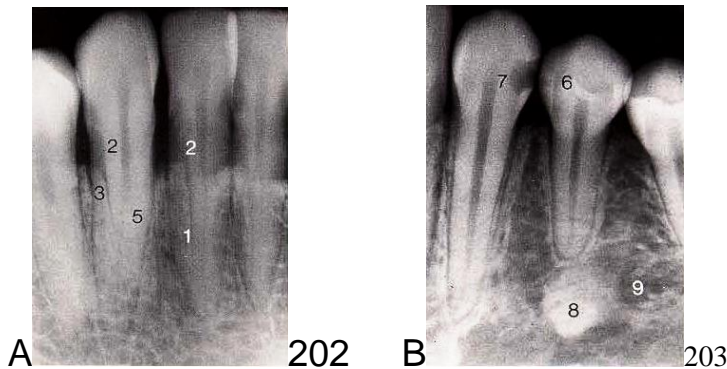


Fig. 3.24. (A) Radiograph of a two-rooted tooth 43. Note the easily visible course of the lingual portion of the alveolar ridge. (B) Radiograph of the region of teeth 33 and 34, with enostosis.

(1. Multiple periodontal ligament spaces on flat or slightly indented root surfaces; the alveolar walls are projected onto the lateral surfaces of the root, 2. burn-out effect, 3. interdental septum, 4. two-rooted premolar, 5. two-rooted canine, 6. dental caries, 7. prepared cavity with a non-radiopaque filling material, 8. enostosis, 9. mental foramen.)

Mandibular Premolar Region

The typical, somewhat trabecular bony structure of the mandible persists down to about the level of the root tips. Apical to this area are located marrow-rich, trabecular-poor cavities that therefore appear strongly radiolucent. Often this radiolucency is enhanced more by the submaxillary and sublingual fovea. The mental foramen is almost always observed between the roots of the premolars, but is often very difficult to discern because of the strongly radiolucent surroundings and the background of the lingual bony structures. Rarely, a variation of the root form, the “taurodont,” is observed.

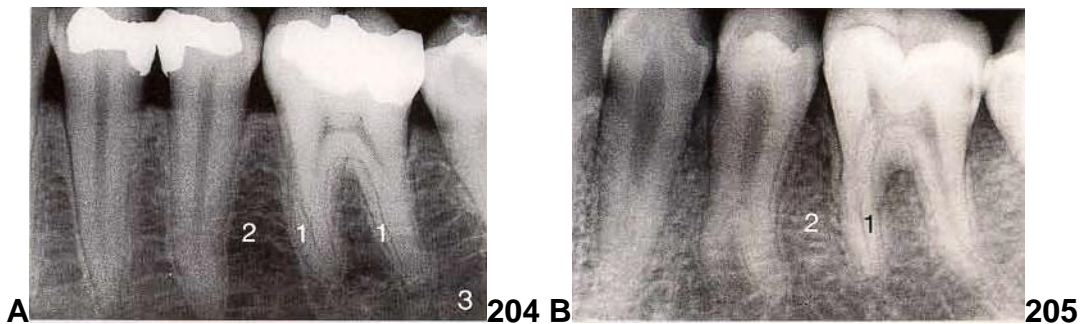


Fig.3.25. (A) Periapical radiograph of the premolars, mandibular left. (B) Radiograph of the left mandibular premolar region, exhibiting a taurodont.

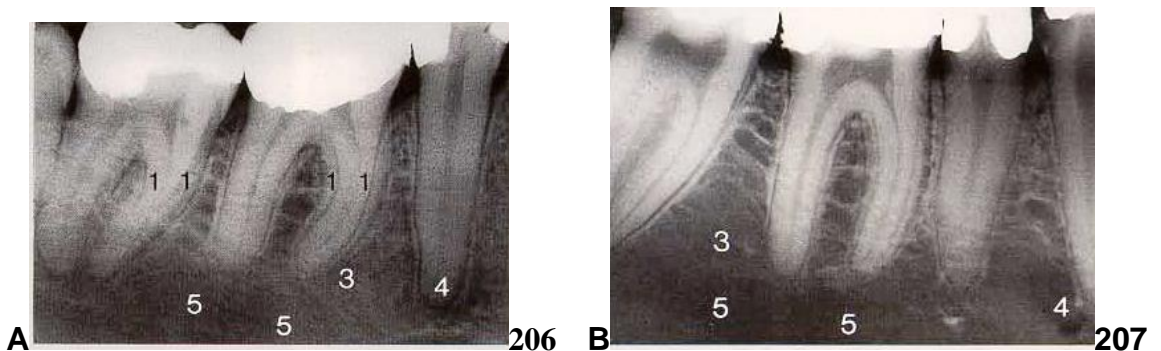


Fig. 3.26. (A) Radiograph of tooth 44 with superimposition of the mental foramen. (B) Radiograph of the region of teeth 45 and 46, showing sparse trabeculation.

(1. Depiction of multiple periodontal ligament spaces in this lateral projection of root surfaces, 2. typically trabeculated bone structure of the mandibular alveolar process, 3. zone of poor or no trabeculation in the body of the mandible, 4. mental foramen superimposed upon the tips of the premolars, 5. the course of the mandibular canal can scarcely be discerned in this radiograph.)

The periapical radiographs depicted on this page were not taken using the standard technique for the premolar region. Because of the steep projection angle, these films depict anatomic details that are hardly visible in standard projections. Especially interesting is the apparently variable position of this foramen cannot be unequivocally located in periapical films as compared to panoramic radiographs. For the non-dentist examiner, the superimposition of the mental foramen on or near the root tip of a premolar may present diagnostic problems. Figure 4.27 provides the criteria for differentiating the radiographic subtraction effect from a chronic apical periodontitis.

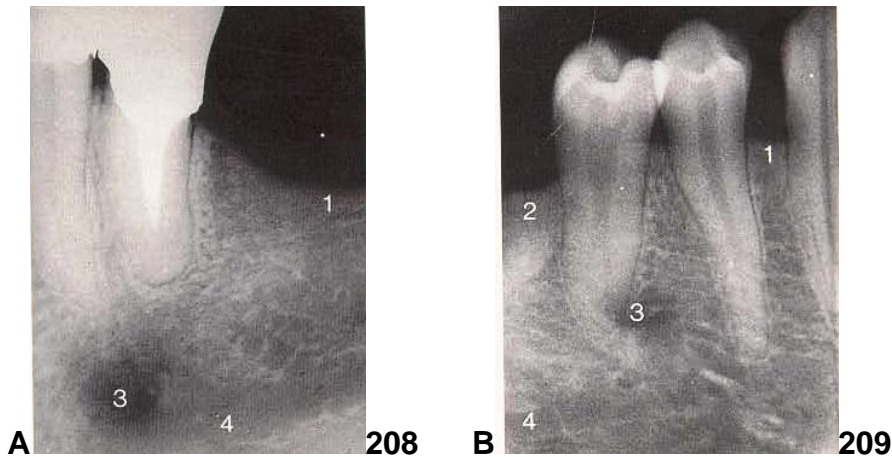


Fig. 3.27. (A) Radiograph of the region of teeth 34 and 35, with a steep projection angle. (B) Radiograph of the region of teeth 45 and 44, with a steep projection angle. The mesial inferior corner of the film packet was bent.

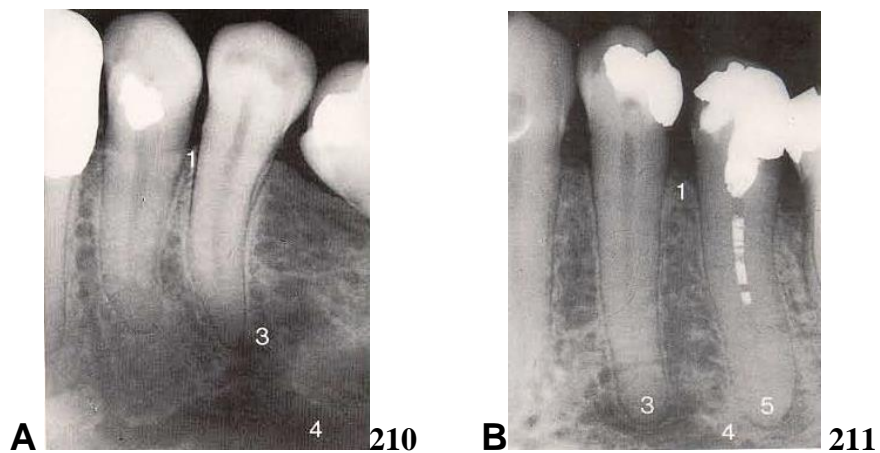


Fig. 3.28. A. Radiograph of the region of teeth 34 and 35. In addition to the excessively steep projection angle, the inferior margin of the film packet was bent. B. Radiograph of the region of teeth 34 and 35. The appearance of the excessively long roots reveal that the bottom portion of the film packet was bent.

(1. Buccal portion of the alveolar ridge, 2. root fragment, 3. mental foramen partially superimposed upon the root tips of the premolars; note the intact periodontal ligament space. 4. mandibular canal, 5. periapical lesion with reactive sclerosis; note the apparent loss of the periodontal ligament space in the region of the osteolysis.)

Mandibular Molar Region

Periapical radiographs of the molar area exhibit numerous anatomic structures that are often difficult to interpret because such films represent only a small section of the mandible. The location of the mandibular canal can often only be detected, if at all, by the radiographic appearance of its floor, because the roof of the canal is porous. The mylohyoid line often obscures the course of the canal, leading to incorrect interpretation; it also suggests excessive transparency of the submaxillary fovea. The external oblique line dominates and obscures the internal oblique line with the retromolar tuberosity.

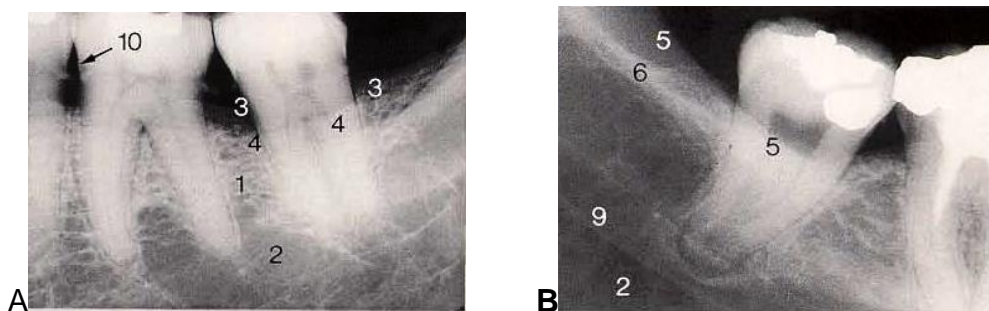


Fig. 3.29. (A) Periapical radiograph of the region of teeth 36 and 37. (B) Radiograph of the region of tooth 48. The apex of the nonvital tooth 48 is superimposed on the mandibular canal.

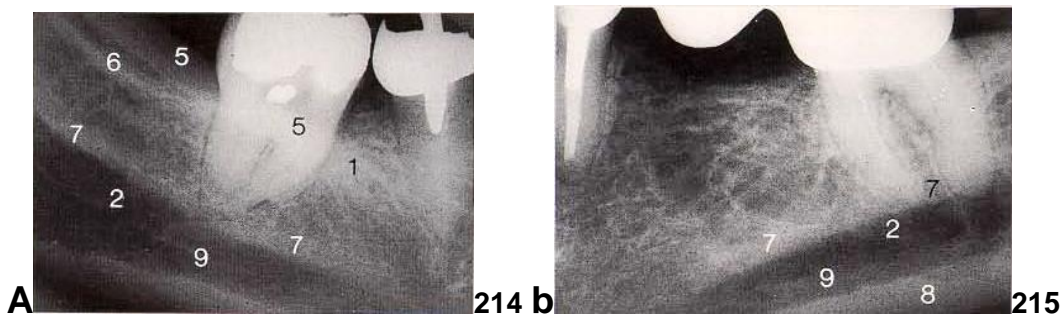


Fig. 3.30. (A) Periapical radiograph (steep projection angle) of the region of tooth 46. In this film and also in Figure 215 the mylohyoid line appears superimposed upon the mandibular canal because of the steep projection angle. (B) Periapical radiograph of the region of tooth 37.

(1. structures of the alveolar process, 2. region of the body of the mandible exhibiting poor trabeculation, 3. buccal portion of the alveolar ridge, 4. lingual portion of the alveolar ridge, 5. external oblique line (anterior border of the ascending ramus), 6. internal oblique line (temporal crest), 7. mylohyoid line, 8. compact bone of the mandible, 9. floor of the mandibular canal, 10. calculus.)

In addition to the anatomic details provided on the previous page, it is important to note the following variations: In elderly patients (especially women) and following tooth extractions, the fat-filled marrow space often expands into the region of the alveolar process. The clearly visible and well-demarcated radiolucency should not be

mistaken for a “cystoid” lesion. Just below the pulp chamber of lower molars, one sometimes observes roundish radioopacities, but these should not be confused with “enamel pearls”; rather they are created by the addition effect resulting from superimposition at the root trunk. This phenomenon disappears if the central ray projection is altered.

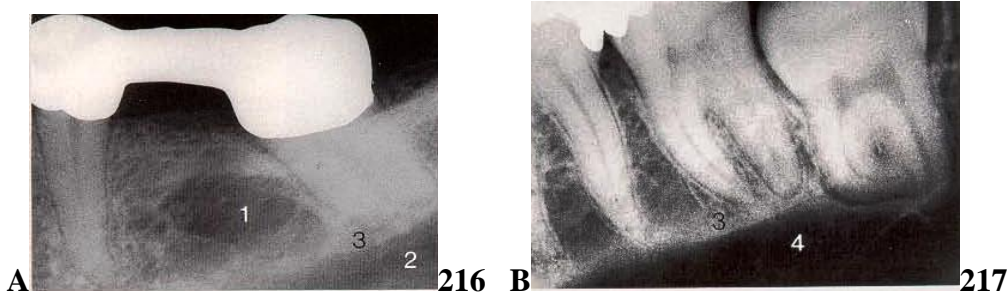


Fig. 3.31. (A) Radiograph of the molar region revealing an island of bone marrow. (B) Periapical radiograph of the molar region showing the submaxillary fovea. This region of poortrabeculation in the body of the mandible is in sharp contrast to the well-trabeculated alveolar process.

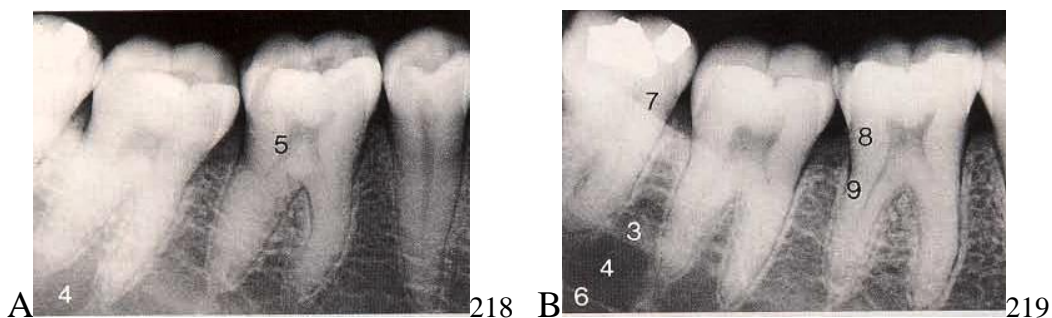


Fig. 3.32. (A) Radiograph of the molar region showing an apparent “enamel pearl” on tooth 46. (B) Radiograph of the same tooth with a different central ray projection. **In the molar region, with a slightly eccentric projection, the phenomenon of “enamel pearl” is sometimes visible.**

(1. Bone marrow island, 2. mandibular canal superimposed on the submaxillary fovea, 3. mylohyoid line, 4. submaxillary fovea, 5. enamel pearl" as an addition effect at the root trunk near the bifurcation on tooth 46, 6. floor of the mandibular canal, 7. external oblique line, 8. buccal portion of the alveolar ridge, 9. lingual portion of the alveolar ridge.)

Radiographic Anatomy in the Panoramic Radiograph

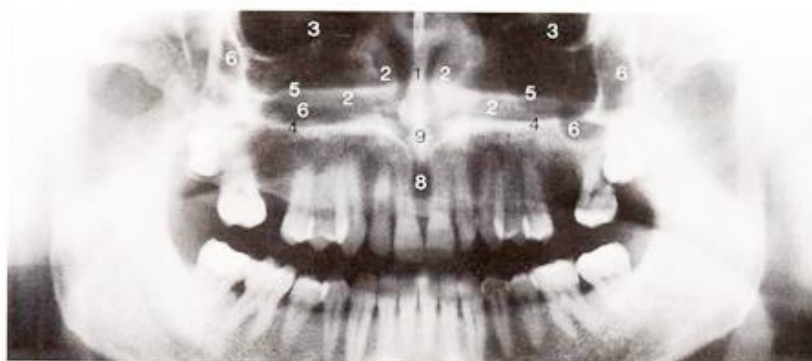
Panoramic radiography is not an exception; it depicts in-focus layers of various thickness (but always thicker than 5 mm), and thus may be classified as a type of zonography. In the panoramic radiograph, the picture of the irradiated tissues is determined by the tangential effect and the summation effect; however, in keeping with the principle of tomography, all of the structures within the in-focus layer are shown relatively distinctly and somewhat enlarged, while all structures outside of the layer are depicted as blurred and reduced in size or as blurred, broadened and enlarged superimpositions; such appearance will depend upon whether the superimposed structures are between the in-focus layer and the film or between the in-focus layer and the focal spot.

Survey of the Anatomic Structures Visible in a Panoramic Tomography

Ventral Portion of the Facial Skeleton

Depending upon the individual development of the facial skeleton and the positioning of the patient in the apparatus, the structures of the orbit and the nasal cavity appear in the picture. But regardless of whether or not these structures are visible or invisible in the radiograph, they do play a role in the overall appearance.

Taking as an example the inferior nasal concha, it is easy to imagine that the panoramic radiograph, as already mentioned, really consists of two broad lateral and one narrow frontal view of the facial skeleton; structures lying further medial and superiorly, e.g., the superior nasal concha, are completely invisible. In the inferior portion of the orbit, foreign bodies are sometimes observed, and these appear to lie within the maxillary sinuses.



46

Fig. 3.33. **Structures of the nasal cavity, the floor of the nose/palatal roof and the ventral portion of the maxilla.** Depiction of the borders of the floor of the nose will depend upon the vertical angulation of the skull in the cephalostat.

(1. Nasal septum, 2. inferior nasal concha, 3. orbit, with right infraorbital canal, 4. laterobasal border of the nasal cavity, 5. horizontal portion of the pyramidal bone with the posterior border of the nasal cavity; the palatal roof itself, when it is visible at all, will be found between 4 and 5, 6. maxillary sinus, 7. nasal entrance into the incisive canal, 8. incisive foramen, 9. anterior nasal spine with the nasal crest of the maxilla.)

Ventral Portion of the Facial Skeleton in the Maxilla

Sometimes soft tissue structures appear clearly in the radiograph; this demonstrates that the addition effect must always be considered. On the other hand, the orbits and the maxillary sinuses, together with the nasal cavity and the epipharynx are easily penetrated by the X-ray beam, and this leads to darkening of the radiograph.

Although our primary purpose is not depiction of the soft tissues, an appropriate example will serve to emphasize the result of the addition effect caused by soft tissues. This is emphasized because the shadowing influence of soft tissue may be of significance in diagnosis, especially if the exposure data were at or below the lower limit.

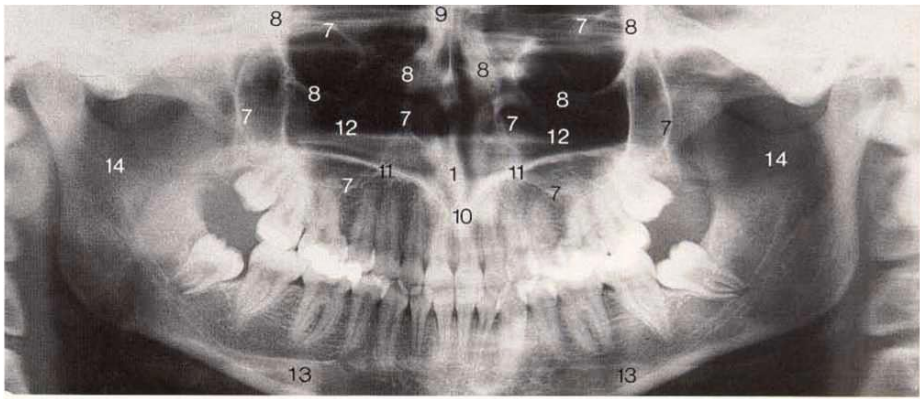


Fig. 3.34. Subtraction effect. This film shows the result of the subtraction effect on the borders of the orbits caused by the influence of the superimposition of the air-containing maxillary sinuses. This radiograph was taken with the patient in maximum intercuspation.

(1. Nasal septum and maxillary nasal crest, 2. atlanto-occipital articulation, 3. nasolabial fold of the cheek, 4. cheek, 5. body of the mandible (distant from the film), 6. plastic positioning device, 7. maxillary sinus (borders), 8. orbit (borders), 9. nasal bone, 10. anterior nasal spine, 11. laterobasal border of the nasal cavity, 12. horizontal portion of the palatal bone and dorsum of the tongue, 13. shadow of the hyoid bone, 14. air-containing epipharynx.)

External Ear and Temporomandibular Joint Region

Often the auricle and the external acoustic opening are projected onto the articular process in such a way that the shadows caused by the soft tissues create an addition effect while the opening itself elicits a subtraction effect in the condyle; this is a situation that is easy to confuse with “arthritic manifestations.”

The panoramic radiograph taken with the patient in maximum intercuspation is the only radiograph that permits an information-rich examination of the occlusion in relation to the position of the condyles. One must also note, however, that the individual shape and axis angle of the joints make evaluation more difficult. On the other hand, if the radiograph is taken with the anterior teeth in edge-to-edge relation, the position of the condyles in the fossae can of course not be evaluated. Radiographs taken symmetrically with the jaws closed can provide the opportunity to examine the condylar positions if the distance from the dorsal edge of the articular process to the ventral border of the condyle can be ascertained. However, definitive statements about condylar position and the shape of the roof of the joint capsule are usually not possible.

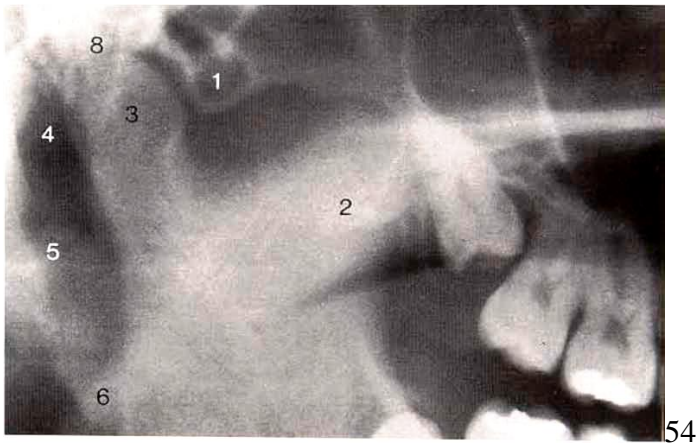


Fig. 3.35. A particularly clear illustration of a pneumatized articular tubercle of the temporal bone. This figure show the radiographic anatomy in this region. Note that in this and the subsequent figure the teeth were not in contact during the exposure.

(1. Articular tubercle, pneumatized, 2. coronoid process superimposed upon the pterygoid process and portions of the soft palate, 3. condyle, 4. entrance of the auricle with external auditory opening, 5. soft tissue of the auricle, 6. ear lobe.)

Chin Region

This region is often poorly depicted in panoramic radiographs, either because of the addition effect caused by the cervical vertebrae or the hyoid bone, or because of the subtraction effects if the mental fovea is positioned within the in-focus layer or the intervertebral spaces. Clear and sharp projections of this region, which are possible in young patients because of the low hydroxyapatite content of the vertebral column, nevertheless exhibit radiologically the complex structure of the symphysis following integration of the mental ossicles and the eruption of the permanent anterior teeth. It is therefore not surprising that in this region ossifying fibroma and osteochondroma can be found in addition to the often observed post-traumatic pseudocyst and reparative granuloma.

Also here, it is important to remember that the panoramic tomogram can only provide an anterior summation picture of this region. Individual cases may demand depiction of the third dimension, either via occlusal radiographs or CT.

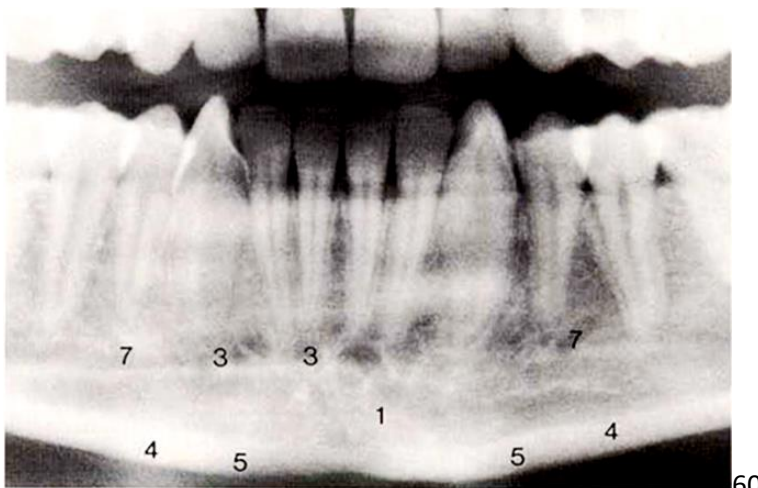


Fig. 3.36. This section from a panoramic tomogram depicts particularly well

all of the possibilities for the existence of pathologic lesions. The previous symphysis, with the mental ossicles and the endochondral growth from the Meckle's cartilage have left traces of their former existence.

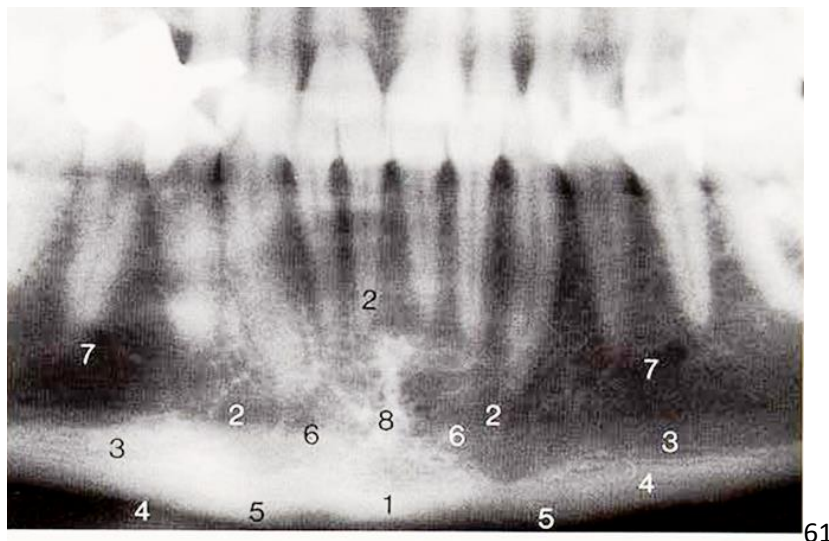


Fig. 3.37. This section from a panoramic tomogram again shows the chin with the typical triangular shadowing of the protuberance and the hyoid bone. The mental foramen can be seen within the poorly trabeculated bony structure of the body of the mandible.

(1. Mental protuberance, 2. mental fovea, 3. shadow of the hyoid bone, 4. compact bone of the mandible, 5. mental tubercle, 6. digastric (lingual) fovea. 7. mental foramen, 8. internal mental spine.)

Figure 3.34 displays particularly well how the mental fovea may appear as a poorly demarcated osteolytic area if it is serendipitously located directly in the in-focus layer. Class II patients and those with pronounced fovea often exhibit this phenomenon. It is as well to mention that cystoid alterations in this region always depict a clear and typical margin contour if inflammation is not present. Malignant changes are extremely rare, with exception of the osteoclastoma.

Additional radiolucencies in this region may be caused by the intervertebral spaces between the first and the fourth cervical vertebrae. Depending upon the position of the skull in the cephalostat, these may present as narrow, roof-like radiolucencies, and may also be projected onto the anterior region of the maxilla.

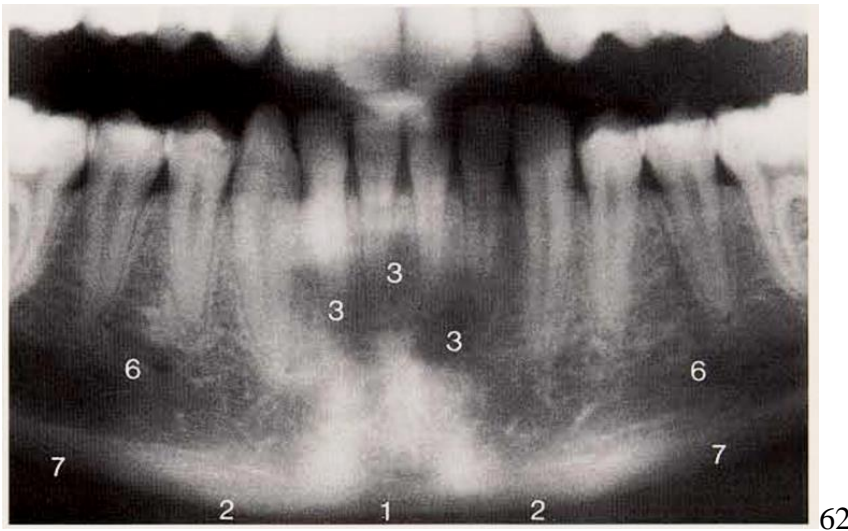


Fig. 3.38. Section from a panoramic tomogram. The buccolingual dimension of the bone is especially narrow in this area, and therefore often exhibits a well-demarcated radiolucency that is often difficult to distinguish from a pathologic lesion such as the traumatic pseudocyst. Note the reactive sclerosis in the periapical region. This followed disturbed eruption of vital tooth 44.

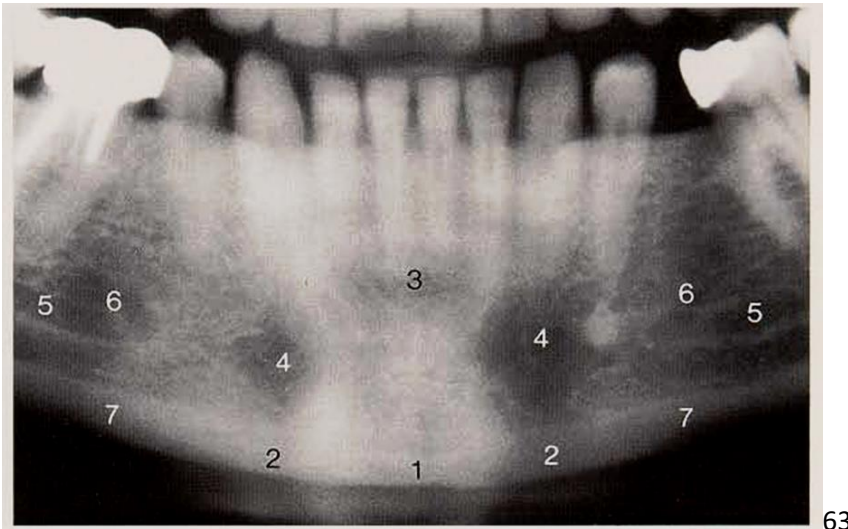


Fig. 3.39. Section from a panoramic tomogram. The mental fovea appears very frequently as a confusing radiolucency if the fovea itself is positioned directly in the in-focus layer. Note the small enostosis apical to tooth 34.

(1. Mental protuberance, 2. mental tubercle, 3. mental fovea (upper portion), 4. lower portions of the mental fovea as it encompasses the protuberance, 5. mandibular canal, 6. mental foramen, 7. compact bone of the mandibular border.)

Chin Region and the Body of the Mandible

The section from a panoramic radiograph also exhibits a view of the chin region with an additional variant in terms of radiolucency. If the submaxillary fovea is especially pronounced, a significantly radiolucent and poorly trabeculated region may be observed beneath the clearly demarcated mylohyoid line. It is not infrequently diagnosed as a cystic alteration when observed in periapical films because of the lack of a broader view. The mandibular canal is often invisible if the body of the mandible is excessively radiolucent, and often only the floor of the canal can be identified. On the other hand, the mylohyoid line may be

superimposed upon the course of the mandibular canal and render its identification more difficult.

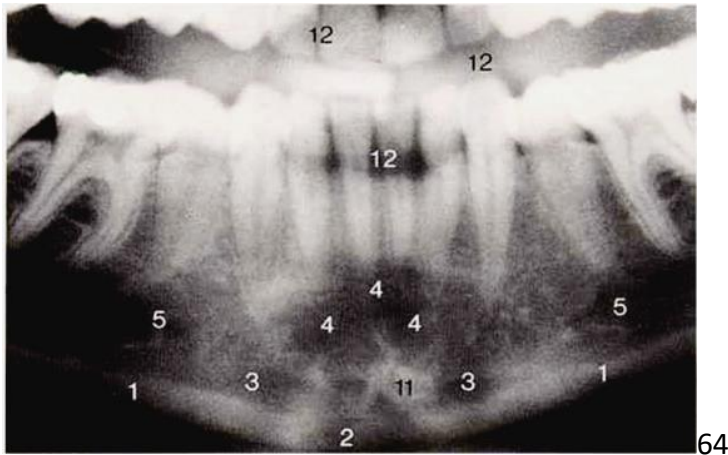


Fig. 3.40. Digastric fovea. This section from a panoramic tomogram reveals the pronounced depressions that represent the attachments of the lingual digastric muscle, creating bilaterally the digastric fovea. Note also the small osteoma left of the midline on the inferior border of the mandible.

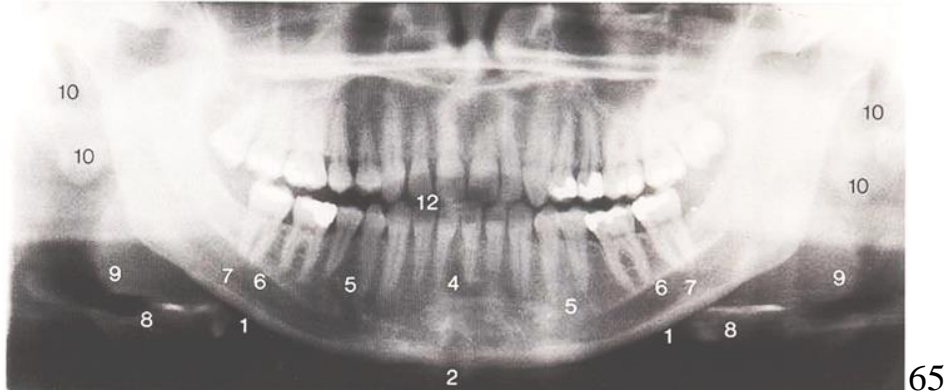


Fig. 3.41. Mylohyoid line. This panoramic tomogram shows a clearly formed mylohyoid line on both left and right sides of the mandible. This structure is the attachment point for the mylohyoid muscle and is immediately coronal to the submaxillary fovea, which appears as a radiolucency on both sides.

(1. Compact bone of the mandible, 2. Mental protuberance, 3. Digastric fovea, 4. Mental fovea, 5. Mental foramen, 6. Mylohyoid line, 7. Submaxillary fovea, 8. Hyoid bone, 9. Base of the tongue, 10. External auditory opening and soft tissues, 11. Small osteoma, 12. Radiolucency created by the lips.)

Mandibular Canal, Mandibular Rami and the Cervical Vertebrae

The mandibular foramen is usually difficult to discern on a panoramic radiograph because of the super imposition of the contralateral side of the jaw. Exceptions do occur, as shown in Figure 66, where the mandibular foramen is more inferior than normal and therefore readily visible. The course of the mandibular canal is usually readily visible in younger individuals to the second molar. From there to the mental foramen it is seldom readily visible because of the porosity of the canal walls, the superimposition of the highly radiolucent submaxillary fovea and the lack of trabeculation.

If the canal is visible, it appears as a fine radiopaque line. The mental foramen, located buccally, is superimposed by the bony lingual structures and is seldom clearly visible, but topographically more adequate than in periapical radiographs.

Examination of the mandible in panoramic radiographs is also complicated due to the addition effects by superimposition of the mandibular ramus onto the angle of the mandible on the opposite side; subtraction effects also may interfere due to the air-containing epipharynx, especially if the patient inhales deeply.

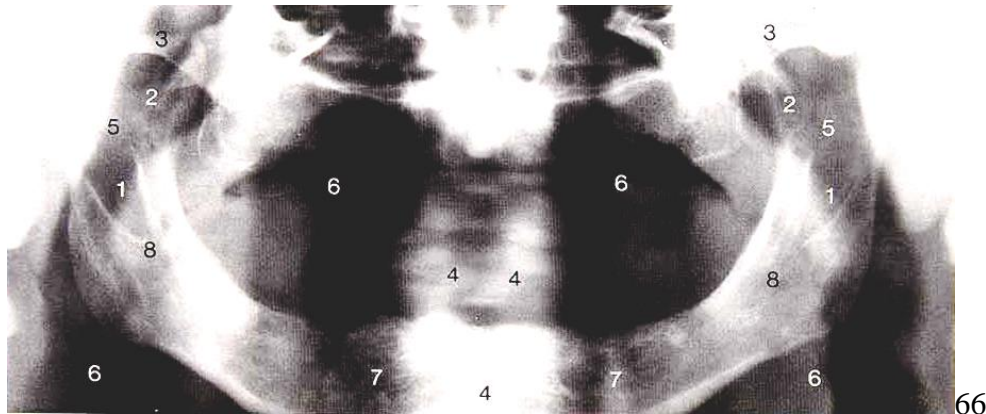


Fig. 3.42. Mandibular foramen. This panoramic tomogram exhibits bilaterally well-formed mandibular foramina that are located more inferior than normal. This could be mistaken for osteolysis if the radiographic resolution of the ascending ramus were not sharp, because the depression is covered only by a lateral bony plate without spongy bone. Note also the depiction and superposition of the highly hydroxyapatite-containing cervical vertebrae, a phenomenon of age.

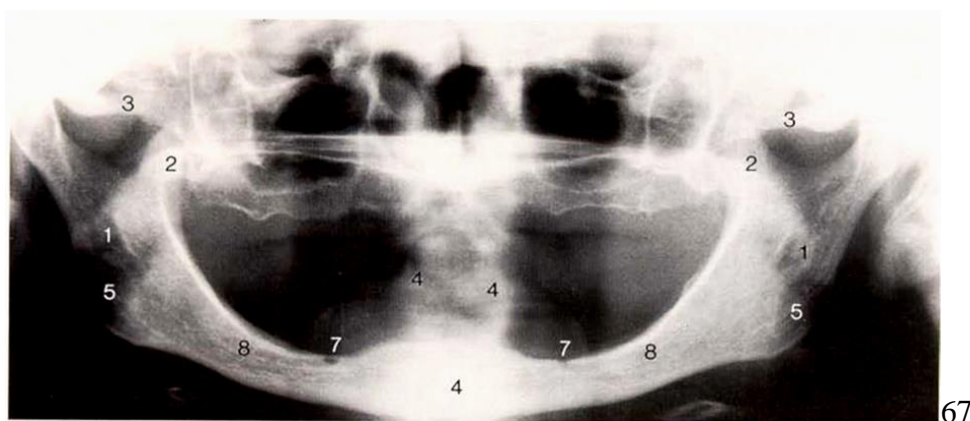


Fig. 3.43. Course of the ventral segment of the mandibular canal in an edentulous patient. The atrophy of the alveolar process of the mandible has created a situation in which the mental foramen is at the crest of the ridge. This film also shows the subtraction effect caused by the air-containing epipharynx.

(1. Mandibular foramen, 2. coronoid process, 3. zygomatic arch, 4. frontal view of cervical vertebrae, 5. subtraction effect caused by air-containing epipharynx, 6. base and dorsum of the tongue, 7. mental foramen, 8. mandibular canal.)

Mandibular Canal and Retromolar Structures

The structures of the body of the mandible and the retromolar region are usually targeted too steeply caudally when dental X-ray equipment is used. In addition, the long axes of the molars are inclined lingually. The panoramic

tomograph provides a less distorted view of these structures because the central ray is targeted lingually and slightly from below in this region. In addition, if the mandibular canal and the mental foramen are visible despite the summation effect, the distance from these structures to the crest of the ridge is more faithfully reproduced. A lateral tomogram can provide a better projection (as might be needed by an implantologist), but only if the skull is properly positioned with the mandibular canal parallel to the film. In addition, the use of low energy exposure is recommended because this will help to eliminate the summation effect on regular films and zonographs.

When making interpretations concerning retromolar structures, note that the lingual aspect of the retromolar area is projected upward.

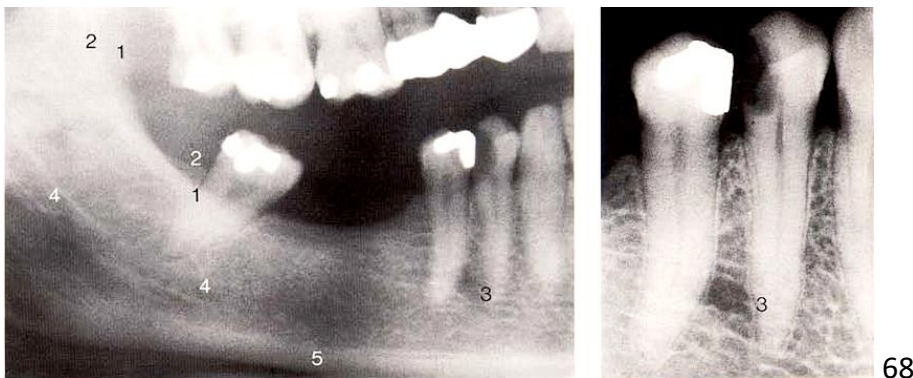


Fig. 3.44. Position of the mental foramen. In this section from a panoramic tomogram (*left*) the mental foramen is depicted in its normal location. In the periapical film (*right*), however, the mental foramen appears more coronal than normal. The external oblique line together with the temporal crest comprise the retromolar trigone.

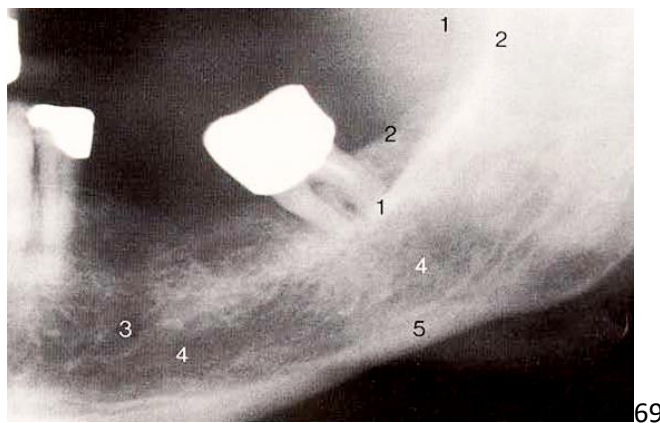


Fig. 3.45. Radiographic anatomy in the dorsal section of the body of the mandible at the transition into the angle of the mandible. This section from a panoramic tomogram and that above (Fig. 3.16) demonstrate that the mandibular canal often cannot be discerned clearly along its entire length.

(1. External oblique line (continuation of the anterior margin of the ascending ramus), 2. temporal crest with retromolar trigone, 3. mental foramen, 4. mandibular canal, 5. compact bone of the mandible.)

Examination of Children and Adolescents Using the Panoramic Tomography

The prevalence of dental diseases has decreased in recent years because of the effect of dental preventive measures. Bite-wing radiographs are indicated for detection of coronal caries but they are not suitable for the examination of the *jaws*. The method of choice today to examine the jaws for anomalies and pathologic processes is panoramic tomography, and should be performed at a minimum during the 9th, 15th and the 20th years of life.

Summarized simply, the following developmental anomalies can be expected in children and adolescents:

- Disturbance of the normal developmental morphogenic processes of the bony structures of the jaw, including the temporomandibular joints in early childhood as well as during the course of the first and second decades of life, with formation of typical tumors and tumor-like lesions;

- Improper development of the dental structures during the growth-intensive mixed dentition stage, with congenitally missing or supernumerary teeth as well as formation of typical odontogenic cysts and tumors, especially in the second decade of life;

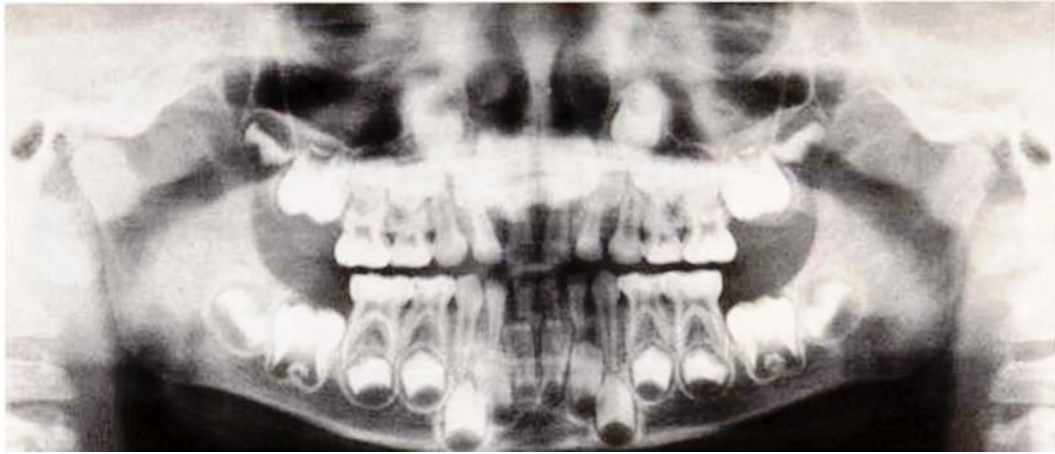
- Dysgnathia;

- Systemic diseases.

Specific dental diseases and inflammatory processes in the jaws may also play additional roles.

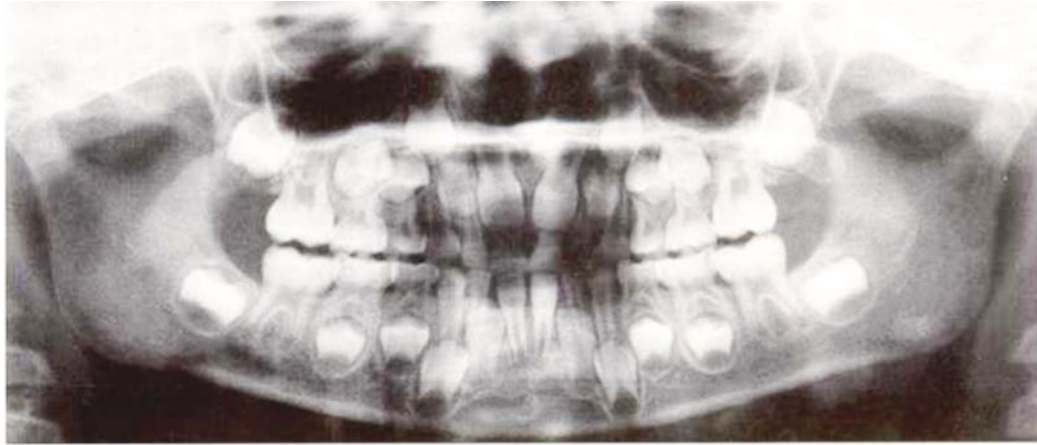


Fig. 3.46. Panoramic tomogram of a 3-year-old girl with deciduous dentition. While the formation of the crowns of the first permanent molars is complete, formation of the cusps of the second molars has only begun.



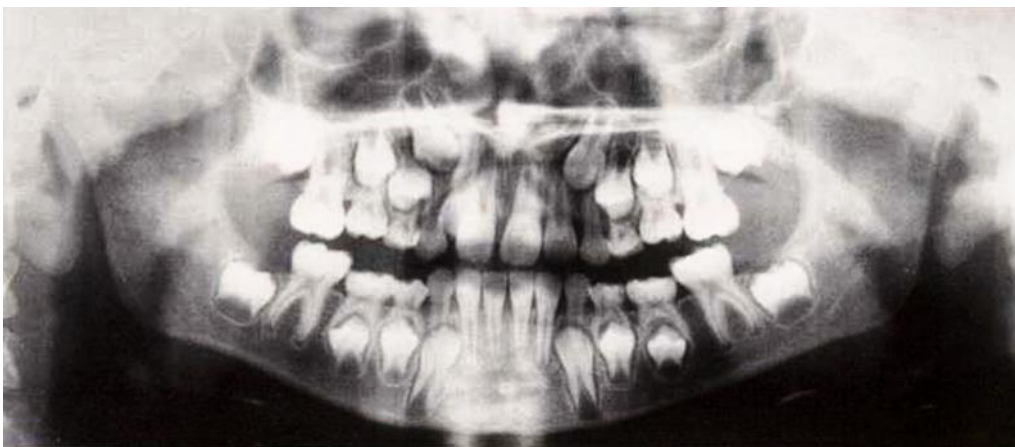
77

Fig. 3.47. Panoramic tomogram of a 5-year-old boy with deciduous dentition. While root formation of the first permanent molars, the incisors and the canines is already in process, the formation of the crowns of the second permanent molars is not yet complete. Clearly visible are the maxillary sinuses.



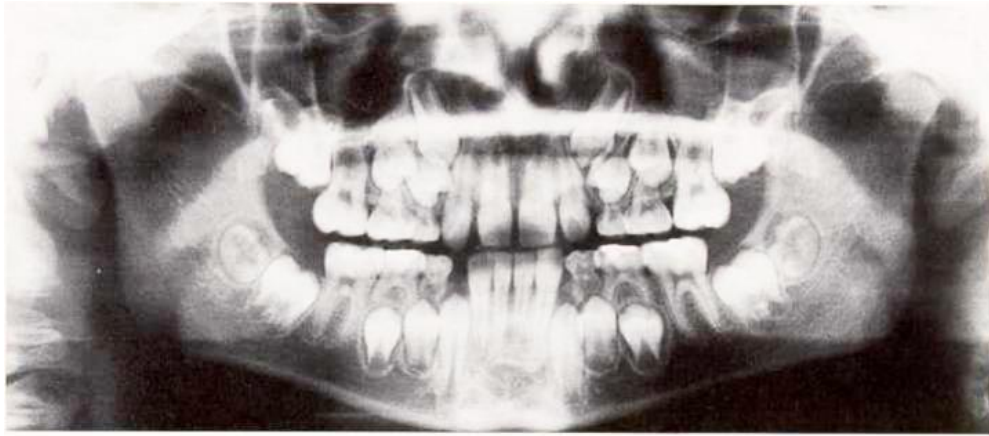
78

Fig. 3.48. Panoramic tomogram of a 6-year-old girl in early mixed dentition stage. The first permanent molars and partially also the incisors have erupted; root formation is almost complete. The articular process has obviously begun to elongate.



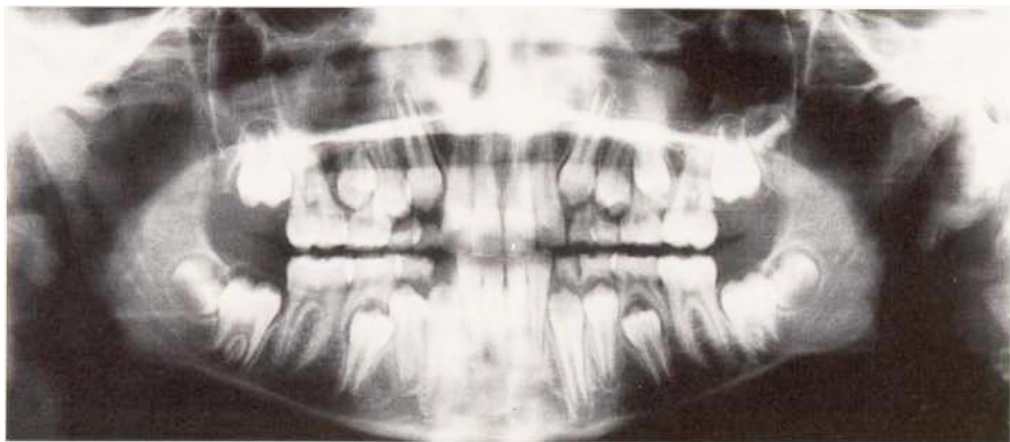
79

Fig. 3.49. Panoramic tomogram of an 8-year-old girl in the mixed dentition stage. **The apices of the roots of the first permanent molars are forming. Root formation of the other permanent teeth is progressing.**



80

Fig. 3.50. Panoramic tomogram of a 10-year-old girl in the mixed dentition stage. The formation of the apical foramina of the roots of the first permanent molars is complete. The crowns of the extremely variable third molars are visible.



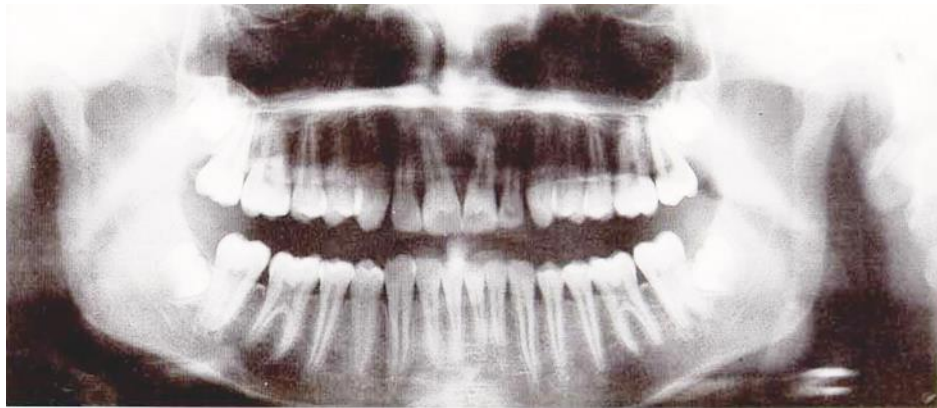
81

Fig. 3.51. Panoramic tomogram of a 12-year-old girl in the mixed dentition stage. The deciduous canines and the deciduous molars are being resorbed by the erupting permanent teeth. The second permanent molars are erupting. The condyles no longer exhibit the round shape characteristic of children.



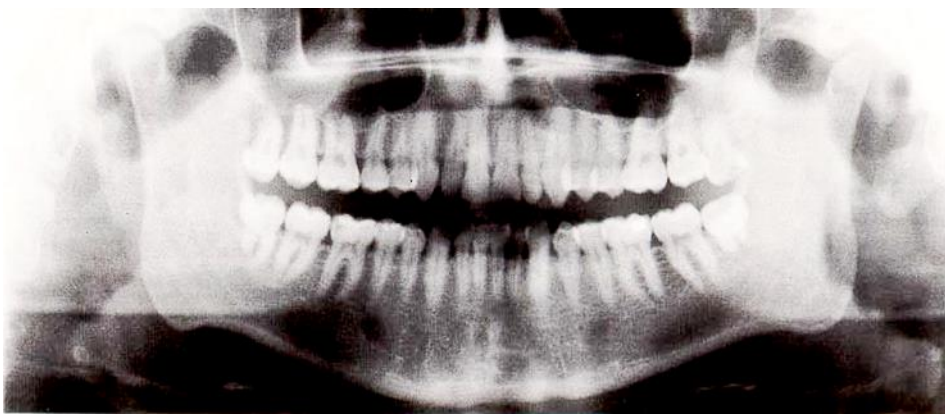
82

Fig. 3.52. Panoramic tomogram of a 14-year-old male with permanent dentition. The roots of the permanent teeth and most of the apical foramina have formed.



83

Fig. 3.53. Panoramic tomogram of a 16-year-old female with permanent dentition. The root canals of the most recently erupted teeth are becoming narrower. The extremely variable third molars appear in various stages of development.



84

Fig. 3.54. Panoramic tomogram of an 18-year-old male with fully developed permanent dentition.

Temporomandibular joint (TMJ)

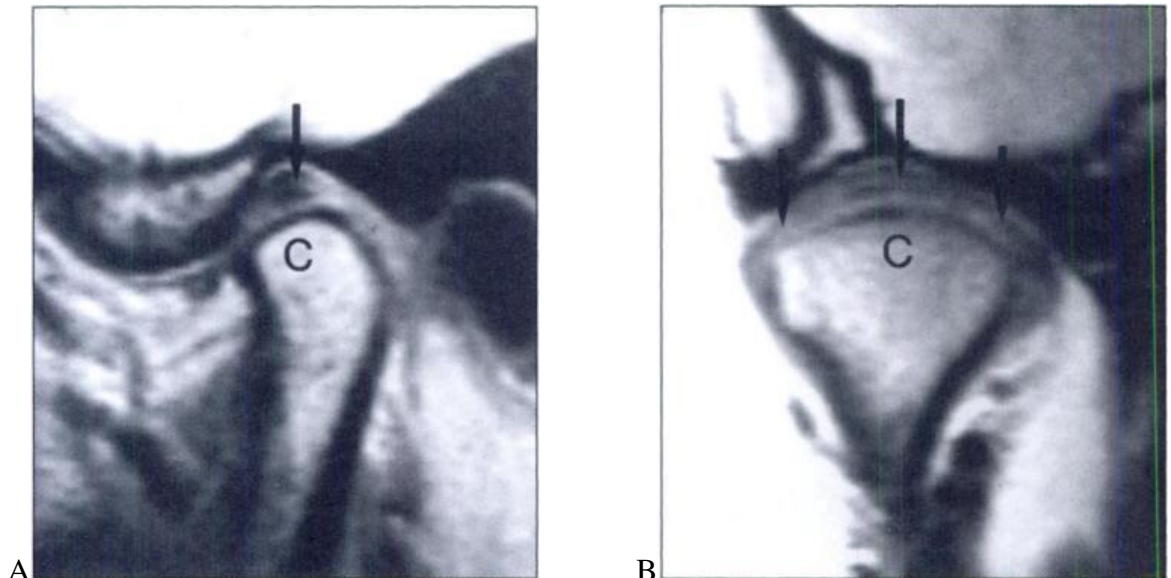


Fig. 3.55. (A) Sagittal MR images of 37-year-old female patient with no temporomandibular joint (TMJ) symptoms shows posterior band of disk (arrow) located in 12-o'clock position above condyle (C). (B) Coronal MR of 38-year-old healthy male volunteer shows disk (arrows) located on top of condyle.

04 Anomalies of Dental Development and the Teeth

Endogenous as well as exogenous factors can directly or indirectly elicit abnormalities of the dental lamina, which develops in close harmony with the surrounding tissues. Viewed in this way, the goal of this chapter is to summarize a large number of anomalies of the teeth that the dentist in daily practice may encounter as isolated cases or as serendipitous radiographic observations.

The list of abnormalities is long, and includes, for example, hyperodontia, hypodontia and anodontia, as well as the persistence and the inclusion of deciduous teeth, the retention of permanent tooth buds and the tooth primordia of supernumerary teeth such as the mesiodens, supernumerary premolars of the mandible and supernumerary molars of the maxilla. Such abnormalities can be considered as odontoma-related forms.

Also included are dysplasias of the tooth crowns such as dens in dente, double tooth buds and “twinning” of the tooth crowns, as well as abnormal development of the tooth roots such as concrescence and the taurodont. Concrescences of maxillary molars call to mind the complex odontoma of this region that occurs preferentially in women.

Amelogenesis imperfecta or hereditary enamel hypoplasia assumes a particular place in the category of anomalies of dental development, as do the other enamel hypoplasias with their sex-linked inheritance pattern of incomplete dominance as an ectodermal odontopathy. The radiographic examination of such lesions is of importance mainly for forensic reasons, and is of little diagnostic significance.

On the other hand, osteogenesis imperfecta is a mesodermal malformation with simple dominant inheritance. It is characterized by dentin malformation and by shortened roots and altered root form. Anomalies of this kind may be associated with corresponding developmental anomalies of the skeleton, and it may therefore be more reasonable to discuss them under the rubric “osteopathy.” The features of such lesions are usually only described in radiographic terms, because a targeted histologic examination is usually not performed in a living patient.

Numerous syndromes are accompanied by odontodysplasias. Their appearance in radiographs should therefore always lead the practitioner to a careful search for their origins. The various forms may be reviewed in the appropriate literature.

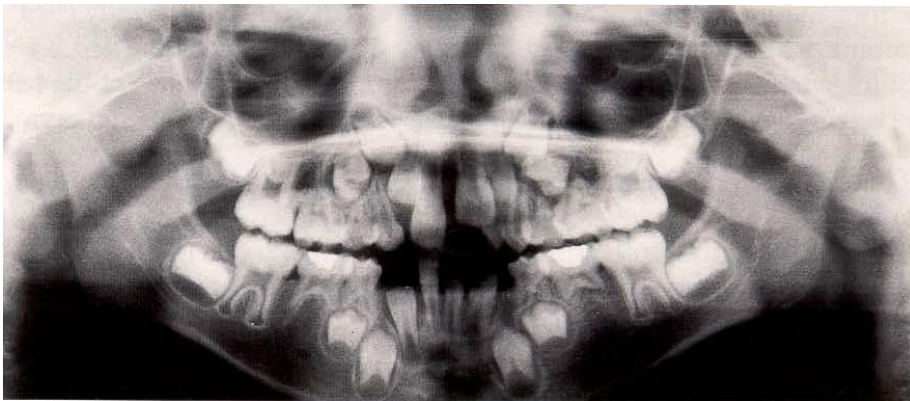
Most developmental malformations can only be correctly diagnosed by means of a complete radiographic examination of the dental structures. For definitive diagnosis in the individual case, the use of panoramic radiography as well as foil-free films for targeted or special projections is recommended.

Congenitally Missing Teeth, Retention and Inclusion

We have selected three typical examples from the myriad of cases: The relatively common congenitally missing second premolar, which often leads

- 1) to the persistence of the second deciduous molar,
- 2) the tipping of the first permanent molar and the other molars, and
- 3) the inclusion of deciduous molars in their original location at the deciduous occlusal plane.

Note that retained deciduous molars and retained tooth buds of permanent molars must be followed up using panoramic tomography at regular intervals if surgery is not immediately indicated.



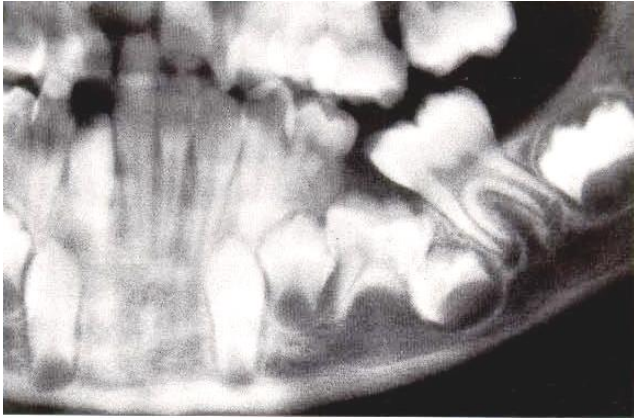
344

Fig. 4.1. Hypodontia in a 7-year- old female. Note the complete congenital absence of all permanent tooth buds of the second premolars and the retarded eruption in the maxillary and mandibular anterior areas.



345

Fig. 4.2. Inclusion of a persisting deciduous tooth 75. Permanent tooth 35 was congenitally absent. Note that tooth 34 as well as teeth 36, 37 and 38 have tipped toward the deciduous molar in this 23-year-old female. As a consequence of a tongue thrust habit, this patient also exhibited a lateral open bite.



346

Fig 4.3. Entrapment of deciduous tooth 75. The mesial tipping of tooth 36 enhanced the intrusion of the already entrapped tooth 75. This appears to have led to retention of permanent tooth 35 and inhibition of its further development.

Retention, Malocclusion and Resorption

Because early retention of teeth often leads to malocclusion and TMJ problems in younger individuals, it is important to remember that at every initial examination all teeth must be accounted for. Retained teeth, which are often discovered accidentally on panoramic radiographs, may have been problems that patients experienced over many years. Failure to perform a complete examination of all patients may sometimes lead to uncomfortable surprises and to an unnecessary loss of confidence by the patient.



347

Fig. 4.4. Retention of tooth 37 by the horizontally impacted tooth 38 in this 26-year-old male. Note the incomplete formation of the mesial root of tooth 37 and the opening of the interdental space between teeth 26 and 27, the latter caused by a premature occlusal contact between 36 and 27.



348

Fig. 4.5. Retention of tooth 44 in a 74-year-old female. The crown of the retained tooth is positioned buccally.

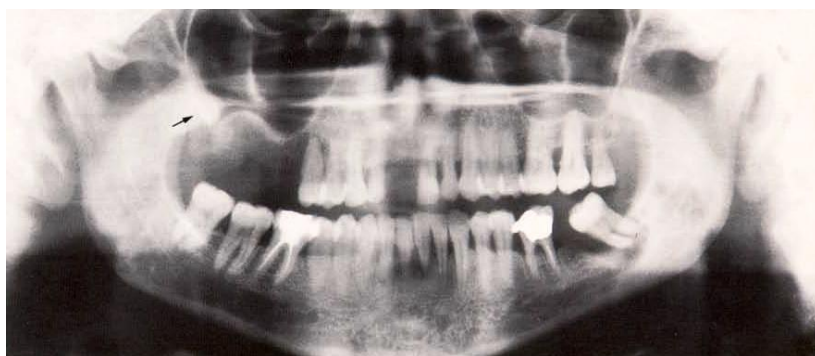


349

Fig. 4.6. Retention of tooth 43 in a 53-year-old female. Note the loss of the follicular sack. This is always an indication of the initiation of crown resorption or the formation of an ankylosis.

Retention of Supernumerary Teeth, Resorption of Retained Teeth

Supernumerary maxillary molars such as upper fourth or fifth molars are almost never detected in the conventional radiographic survey. Such supernumerary teeth represent a focus for the formation of follicular cysts developing in the sinus, and must therefore be removed. The syndrome of cleidocranial dysostosis is mentioned in this context because it is typified by hyperodontia as well as skeletal developmental disturbances. Retained teeth whose crowns resorb often represent the etiology of undiagnosed problems over many years. Only the panoramic radiographic technique can routinely permit detection of such processes.



350

Fig. 4.7. Retained tooth 18 in a 42-year-old female. The extreme position (arrow) of this impacted tooth provides evidence why such teeth that often elicit "pains of unknown origin" cannot be detected without panoramic radiography. Note especially the reactive sclerosis on the floor of the sinus! However, the precise location of this tooth cannot be defined from the panoramic film alone.



Fig. 4.8. Duplication of tooth primordia extending into the premolar region. This observation is a signal symptom of hereditary cleidocranial dysostosis. The syndrome also manifests the lack of collar bones, skeletal anomalies, follicular cysts with tooth impaction and hyperodontia, as in this 13-year-old male..

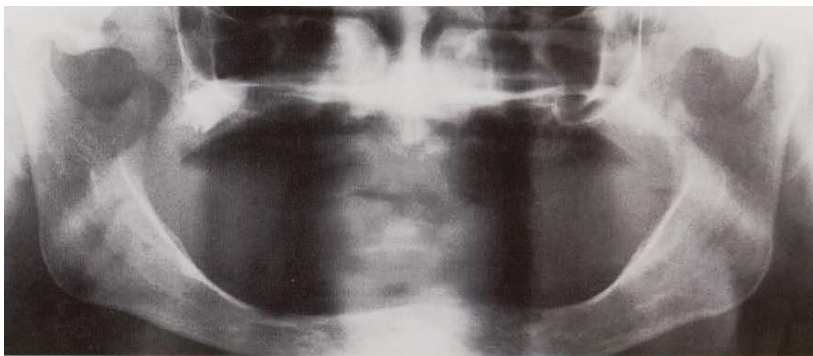


Fig. 4.9. Retained tooth 18 exhibiting substantial crown resorption. This 83-year-old female had complained for years of nebulous pain in the TMJ region.

Retained and Ankylosed Teeth

Presented here is an additional case of an impacted tooth in an unusual location; this tooth was the cause of undiagnosed difficulties throughout many years. Ankylosed teeth are, by definition, teeth whose roots are fused with the alveolus in such a way that no periodontal ligament space can be detected on the radio graph. Such teeth are therefore usually diagnosed as retained or impacted. Retained teeth whose crowns lack a follicular sac surrounding them are classified under the term ankylodontia because they appear to be fused with the surrounding bone.

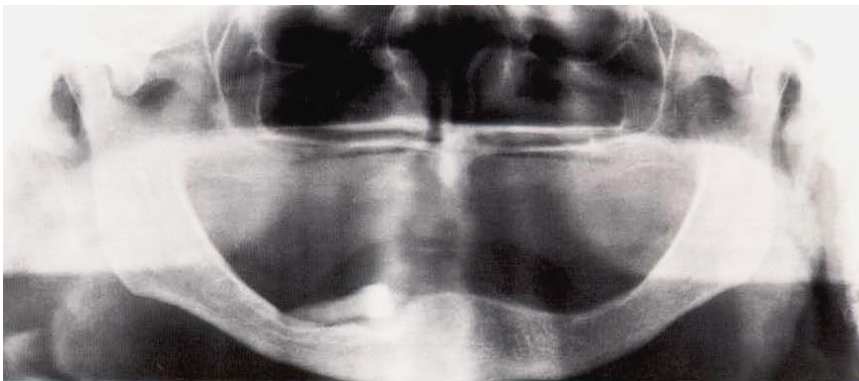


Fig. 4.10. Retained tooth 45 in a 74-year-old female. This tooth was completely covered by mucosa. Its crown rested upon the mental foramen.



Fig. 4.11. Tooth 25 ankylosed at the floor of the sinus following persistence of deciduous tooth 65 in a 25-year-old female. Note the tipping of the adjacent permanent teeth.

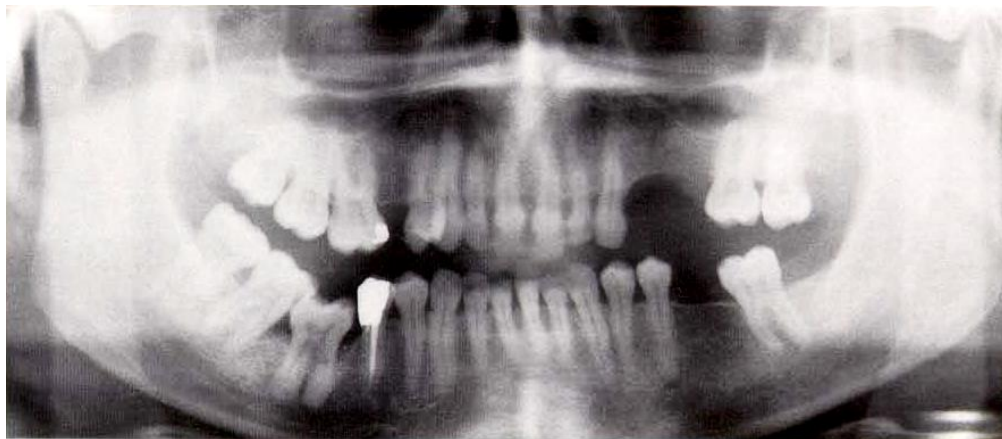


Fig. 4.12. Ankylosed tooth 46 in an included position in a 36-year-old male. Note the lack of a periodontal ligament space. The exact depiction of periodontal ligament space is impaired by the printing process.

Mesiodens, Gemination, Taurodontism and Dens in dente

The supernumerary central incisor has inherited the special designation of mesiodens because of its relatively common occurrence. The mesiodens is the result of a developmental anomaly of the dental organ in the area of the median suture. This supernumerary tooth is often very poorly developed and should be localized radiographically using the so-called tube shift principle and not only with an occlusal film. Gemination is very rare, being observed almost exclusively in the region of the mandibular molars. Additional dental developmental anomalies are represented by the taurodont and the invagination of the dens in dente.



Fig. 4.13. Mesiodens as seen in an occlusal film of a 44-year-old female. **Detection of mesiodens can be achieved with an occlusal film, but this will not provide precise localization. The mesiodens can be visualized using the horizontal localization technique.**



Fig. 4.14. Gemination of teeth 48 and 47. **The two mandibular molars developed simultaneously in a single follicular sac.**



Fig. 4.15. Taurodont. **Tooth 37 exhibits a typically elongated pulp chamber and short, dilacerated roots.**



Fig. 4.16. **Dens in dente.** A particularly remarkable case of dens in dente exhibiting pulpal necrosis with its attendant periapical lesion.

Hypercementosis and Enamel Pearls

Hypercementosis is observed relatively frequently on nonvital teeth. Its presence represents an expression of host defense against chronic infection. If hypercementosis occurs adjacent to vital teeth, the differential diagnosis must include osteopathy, e.g., Paget's disease, which is sometimes detected in elderly males. Enamel pearls can only be well detected radiographically if they extend

into the interdental area. Enamel pearls may be incorrectly diagnosed when they appear as the result of superimposed radicular processes of molar teeth.

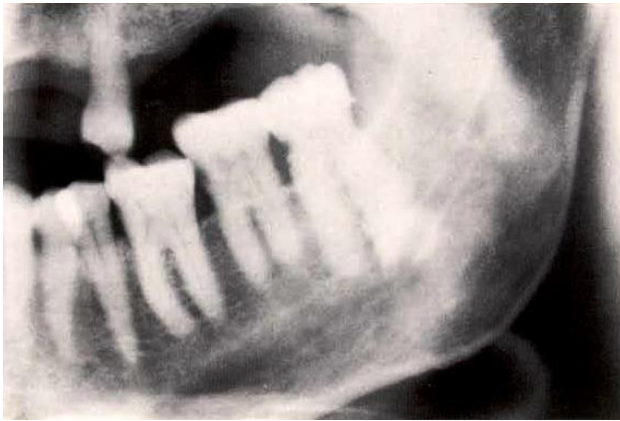


Fig. 4.17. Hypercementosis shown on panoramic and periapical radiographs for comparison. If cemental hypertrophy is detected in elderly men, one must consider the possibility of osteitis deformans (Paget's disease).

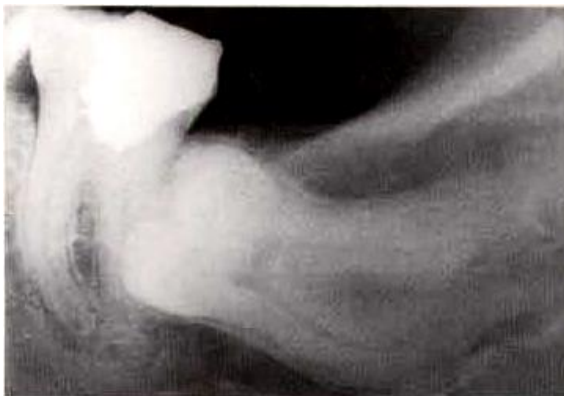


Fig. 4.18. Hypercementosis. This condition occurs most frequently in nonvital teeth as an expression of host defense. However, it may also occur near vital teeth, either as a corollary condition of osteopathy or an idiopathic lesion.



Fig. 4.19. Enamel pearl. Enamel pearls often occur near the cemento-enamel junction (tooth 18, mesial), as a hamartoma in the category of odontogenic tumors.

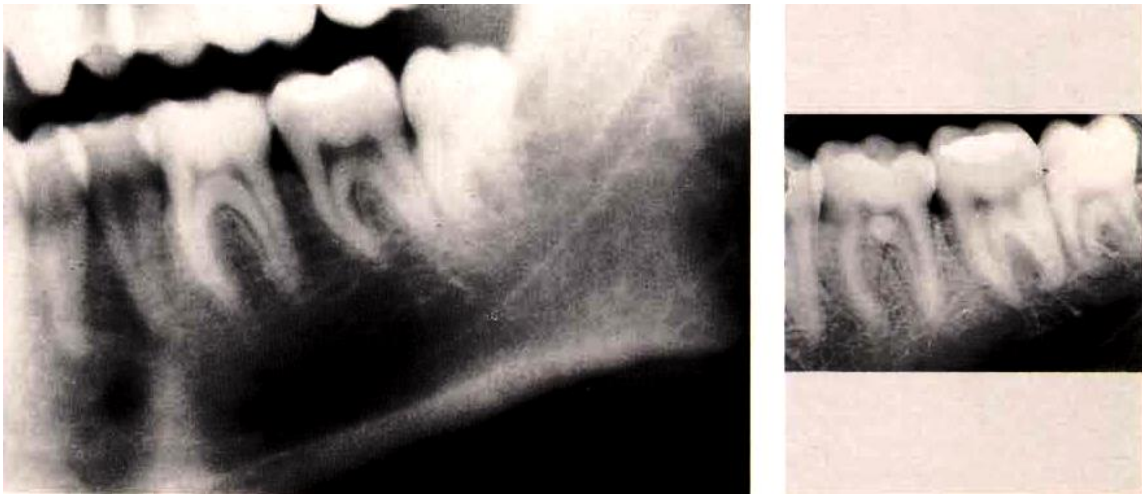


Fig. 4.20. Enamel pearl. The enamel pearl is often incorrectly diagnosed because of the angle of the radiographic projection, for example in bi- and trifurcations of molars, where an apparent pearl may result from the addition effect. Right: An apparent enamel pearl on tooth 36 is not visible on the panoramic radiograph (left) because of the different radiographic projection.

Amelogenesis Imperfecta

Amelogenesis imperfecta or hereditary enamel hypoplasia is an ectodermal odontopathy with incomplete dominance and sex-linked heredity. It presents clinically as a typically brown discoloration of the enamel, which is either relatively smooth and thin (typical in males), or vertically ridged (typical in females). While classical examples of enamel hypoplasia need not be examined radiographically to arrive at a diagnosis, a forensic indication for radiographic analysis may exist.

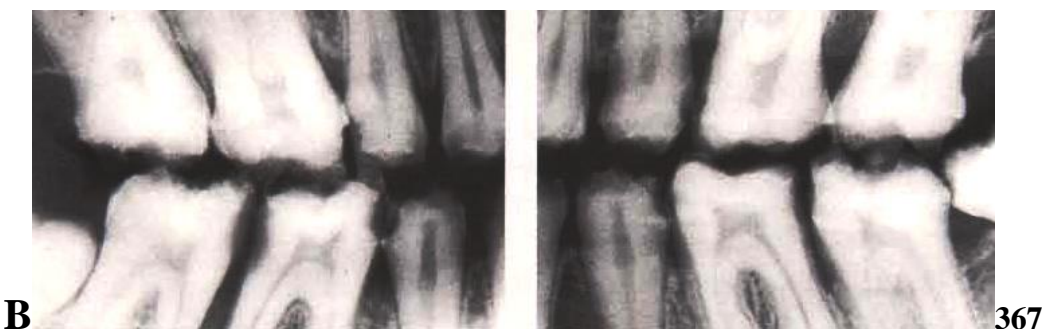
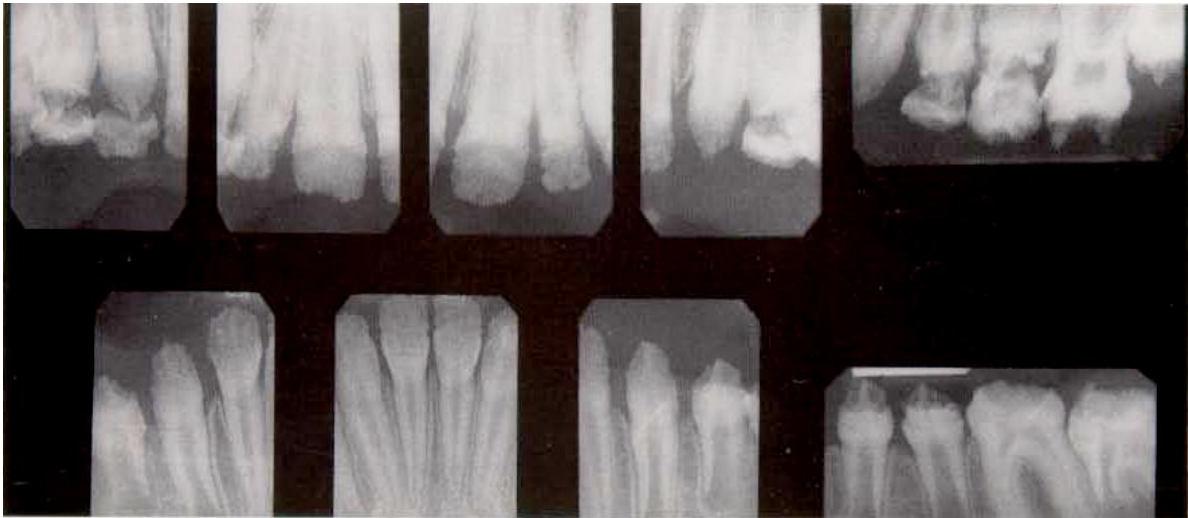


Fig. 4.21. Amelogenesis imperfecta as it appears in a panoramic radiograph and a bite-wing film of the same patient. Of note is the extremely thin layer of enamel on the tooth surfaces.



368

Fig. 4.22. Detail from the radiographic survey of a case of amelogenesis imperfecta. The enamel is vertically ridged and relatively thick (female form).

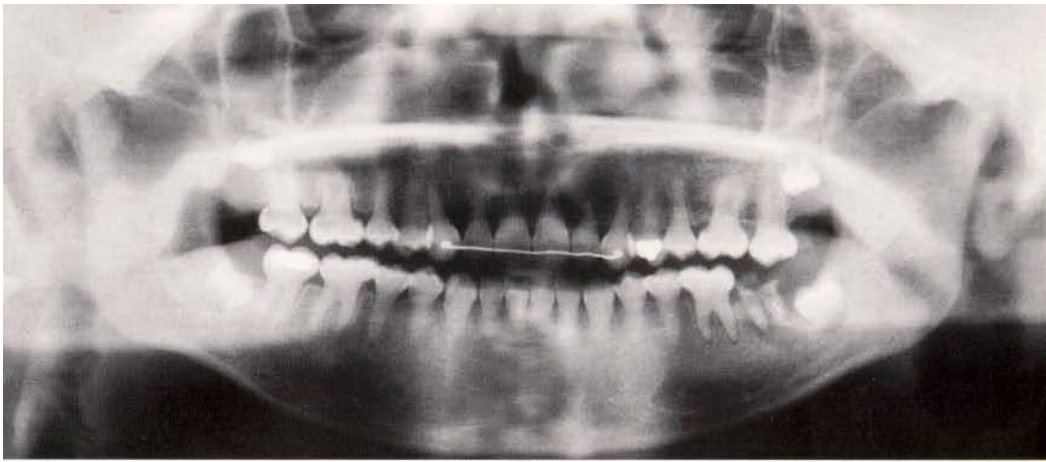
Dentinogenesis Imperfecta

Dentinogenesis imperfecta is the result of a mesodermal malformation with disturbance of dentin formation, and is a disorder that is inherited as a simple dominant trait. It may also be combined with osteogenesis imperfecta. Because of the short, conically deformed roots, the crowns of the teeth appear large and plump. A thin layer of enamel covers the malformed dentin; the dentin is completely insensitive. A typical sign of the malformation is the rapid reduction in size of the pulp chamber, which is initially quite large.



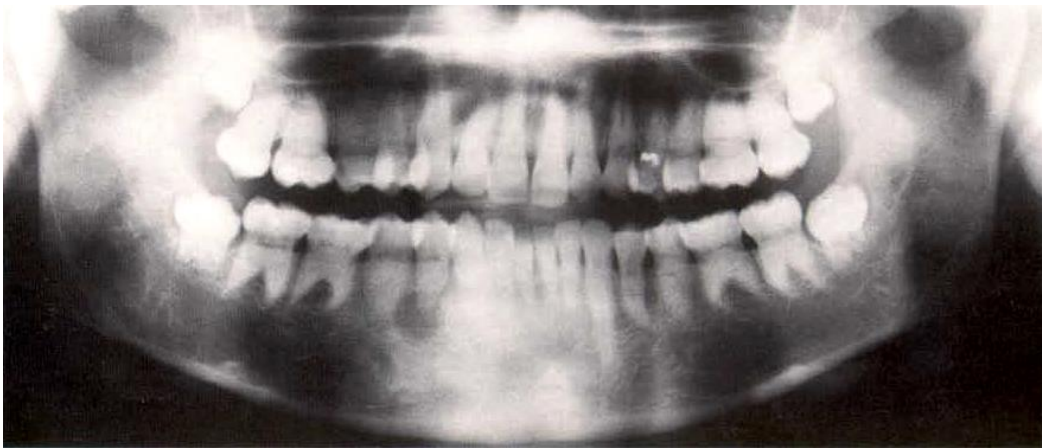
369

Fig. 4.23. Dentinogenesis imperfecta in a 38-year-old female. This case exhibits a mild form with slender roots. The condition is inherited as a simple dominant trait. The thin layer of enamel exhibits cracks. Enamel and dentin are gradually worn away due to attrition.



370

Fig. 4.24. Dentinogenesis imperfecta in an 11-year-old female. Note the typical disproportion between crowns and roots. Such patients may also exhibit signs of osteogenesis imperfecta. Note that the pulp chambers and the root canals have already become obliterated.

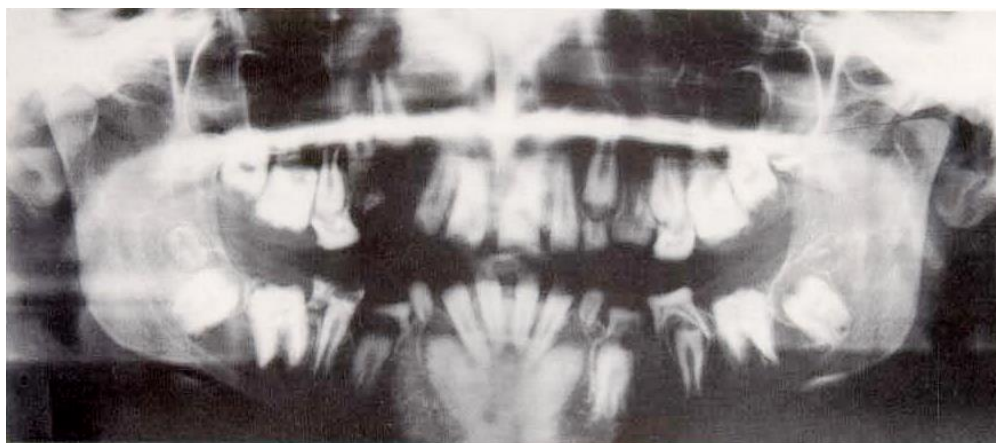


371

Fig. 4.25. Dentinogenesis imperfecta in a 19-year-old female. The pulp chambers, which were initially large, are already considerably reduced in size. The roots are shorter than normal and bizzare in shape.

Additional Dental Dysplasias

Odontogenesis imperfecta with its attendant malformation of teeth and disturbances in eruption patterns results from perturbation of odontoblast function. This is frequently combined with dysfunction of osteoblasts, a condition known as osteogenesis imperfecta. In addition to this genetically determined form, local odontogenic dysplasias of uncertain etiology may also occur. A peculiar form of odontogenic dysplasia is the so-called “shell tooth,” which is characterized by a completely formed layer of enamel with an apparently enlarged pulp chamber and complete absence of root formation.



372

Fig. 4.26. Odontogenesis imperfecta. Note that the pulp chambers vary considerably in size. The malformed teeth do not erupt. All parts of the teeth are involved. This condition is often observed in patients who also suffer from osteogenesis imperfecta.



373

Fig. 4.27. Odontogenic dysplasia localized to the right side of the mandible. Note that all dental structures are malformed, and the teeth have failed to erupt. The etiology is assumed to include early childhood trauma that led to local disturbance of odontoblast function.



374

Fig. 4.28. "Shell tooth". This is one form of dentinogenesis imperfecta in which the roots do not form at all and the pulp chamber appears to be enlarged.

Concretions, Calcifications, Ossifications

Combining these three topics permits discussion of various radiopaque objects and structures that are not always observed outside the jaws and that are relatively easy to detect there radiographically. In many cases during the production of periapical

films and especially in panoramic radiographs, the X-ray beam encounters these structures and they appear as superimpositions upon the teeth and jaws. Since radiographs represent only a two-dimensional picture and the third dimension is lacking, one is tempted to interpret such objects and structures that appear at various locations in the film not as results of addition but rather as actual alterations of structures in the jaws. Furthermore, radiopaque objects outside the jaws become much more clearly visible than would be possible without this apparent layering, due to the additive effect of X-ray beam dampening. One must keep in mind that individual periapical radiographs as well as the panoramic film can provide only a “summation” picture. Even panoramic radiography falls into the classification of zonography (more than 5 mm layer thickness) and not tomography (less than 5 mm layer thickness), which is why the summation effect cannot be completely excluded. All of the above-mentioned conditions make it clear that incorrect interpretations can be avoided only with great care. Everything depends upon recognition of the misleading addition effect and the elimination of the risk of incorrect interpretation by means of other projections to ascertain that third dimension.

The most important structures and situations that create confusing radiopacities include:

- Supra- and subgingival calculus, which is visible only on the proximal surfaces and in some cases masks the tooth root;
- Sialoliths from the submandibular gland, which may produce shadows at the angle of the mandible and in the premolar-molar area of the mandible if they reside within Wharton’s duct;
- Sialoliths from the sublingual gland; these are usually too small to produce any addition effect in the anterior region of the mandible;
- Sialoliths from the parotid gland, if they reside in the anterior portion of the gland, which may be projected onto the mandibular ramus in a panoramic film, or near the maxillary molars if they reside within Stensens’s duct;
- Multiple osteoma and calcified acne foci in the soft tissue of the cheek;
- Calcified lymph glands, which may cause apparent radiopacities in the mandible;
- Ossification in myositis ossificans;
- Ossification of the stylohyoid ligament;
- Superimposition upon the body of the mandible by the hyoid bone if a patient swallows during exposure of the panoramic radiograph.



Fig. 4.29. Supragingival calculus “spurs”. Periapical film of the left molar region of the mandible, taken at low voltage.

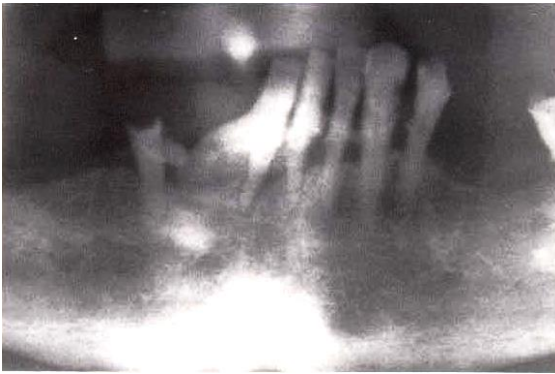


Fig. 4.30. Supragingival calculus in a 79-year-old female. This section from a panoramic radiograph depicts a massive accumulation of supragingival calculus.

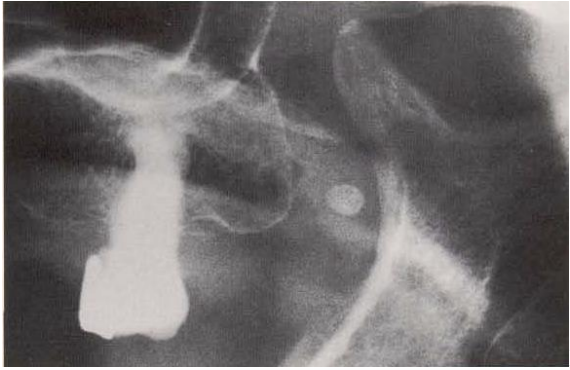


Fig. 4.31. Calcified cervical lymph nodes in a 79-year-old male. Calcified lymph nodes were often seen in earlier times following tuberculosis. Such calcified lymph nodes are still occasionally observed today in elderly patients.



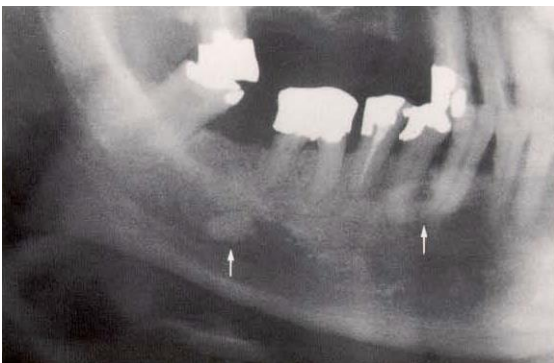
Fig. 4.32. Calcification in the parotid gland of a 54-year-old male following mumps. The use of sialography permits depiction of the configuration on the parotid gland in a panoramic

radiograph.



383

Fig. 4.33. Sialolith within Stensen's duct of the parotid gland in a 74-year-old female. Other calcifications, such as phleboliths or osteoma on the pterygoid process can occur in this region. With the help of a tangential zygoma projection (phleboliths) or an axial skull film, or with CT (osteoma on the pterygoid process), the differential diagnosis can be determined..



385

Fig. 4.34. Sialolith within Wharton's duct of the submandibular gland in a 56-year-old female. The comparison of a panoramic radiograph and a less than ideal occulusal film is instructive: The stone appears near the roots of teeth 40 and 43 in the panoramic film.



394

Fig. 4.35. Rhinolith in the maxillary sinus. Section from a panoramic radiograph showing a rhinolith located at the posterior wall of the right maxillary sinus (arrow).

Regressive Alterations of Teeth and Jaws

The term regressive is generally limited in use to alterations such as abrasion, atrophy, degeneration, necrosis or resorption.

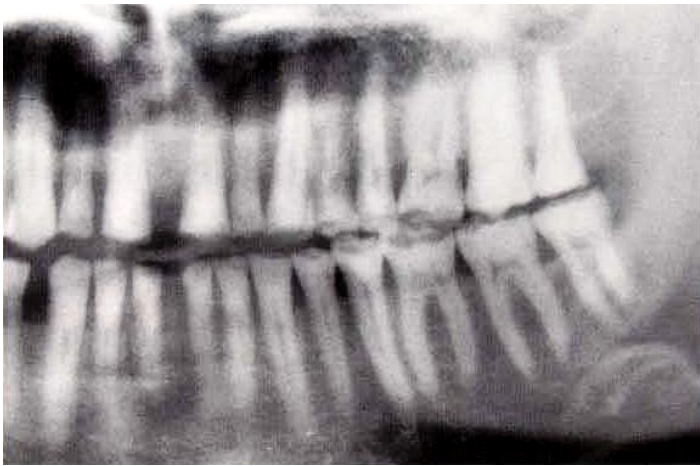
Abrasion, which can be diagnosed clinically and which therefore need not be examined radiographically, can result from either physiologic or nonphysiologic wear. For forensic reasons, documentation of certain cases may be indicated both

photographically and radiographically. Several characteristic examples will be presented in this section.

Wedge-shaped defects are quite easy to detect clinically, and also on radiographs when the defects extend toward the interdental area. On the other hand, resorption of the crowns of retained or impacted teeth as well as root resorptions on vital or nonvital teeth can be inspected only by means of radiographic examination. It must be emphasized that all abnormalities in the mixed dentition must be investigated using an appropriate radiographic projection (panoramic tomography!). This is also the case for any permanent tooth that apparently “failed to erupt” .

Enlarged pulp chambers in the teeth of adults indicate compromised formation of secondary dentin. Radiopacities in the pulp chamber usually represent free or adherent denticles, and radiographic differentiation is seldom possible because even adherent denticles may appear as free, and vice versa, depending upon their position in the projected X-ray beam. Of additional note is that the vestibular wall of the alveolus is projected upon the pulp chamber in periapical radiographs and may compromise the interpretability of the film.

Idiopathic root resorption may be localized centrally or peripherally. The central form has also been termed “internal granuloma”, and is usually the result of pulpa trauma, for example during tooth preparation. The peripheral form usually occurs following injury to the periodontal ligament, for example through accident or attempts to reimplant luxated teeth. It should be noted that the radiograph may also depict a central resorption if the defect is located peripherally but exactly on the vestibular or the palatal/lingual aspect. In such cases, an eccentric periapical projection using a horizontal localization will usually provide clarification. Even vital teeth may be affected, due to the growth pressure on retained teeth, abnormal tooth mobility or forced orthodontic treatment. In addition to regressive changes we should also include atrophy of age, even though some authors include such atrophy under the rubric osteopathy. Such age-related conditions should be studied radiographically using the filter effect and whenever possible with dentures in place and the jaws closed. Occlusal films should be used when necessary in such cases for examination and documentation where the mental spine is often considerably enlarged lingually.



398

Fig. 4.36. Generalized abrasion. Section from a panoramic radiograph of a 54-year-old male.



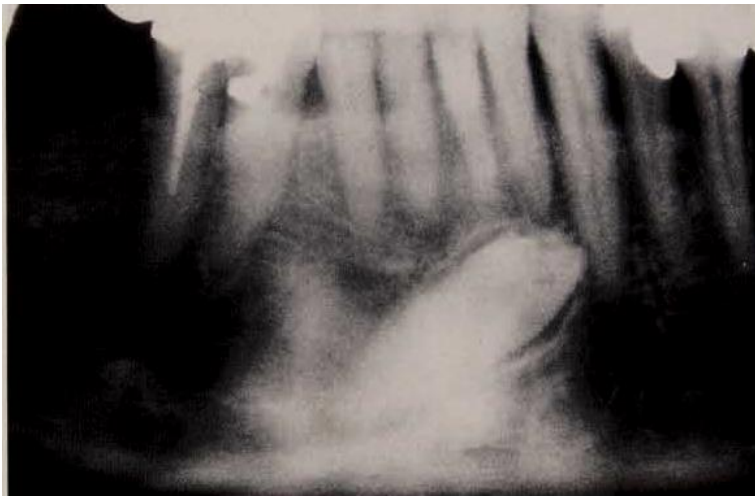
399

Fig. 4.37. Resorption of deciduous tooth 75 in a 12-year-old male. Normal physiologic resorption has been effected by previous endodontic treatment.



400

Fig. 4.38. Initial resorption of the crown in a 44-year-old female. This section of a panoramic radiograph reveals the initial resorption of the crown of impacted deciduous tooth 75, which has forced tooth 35 out of its normal path of eruption.



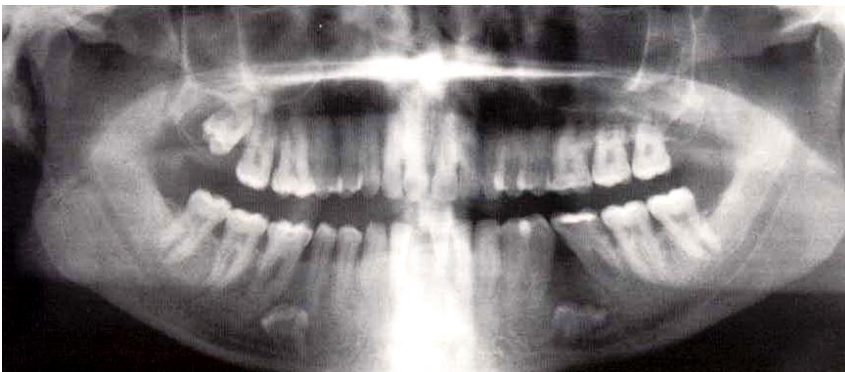
401

Fig. 4.39. Resorption of the crown of impacted tooth 43 in a 42-year-old male. It is likely that in early childhood the tooth bud was dislodged from its normal eruption direction through trauma. In this section of the panoramic radiograph, the impacted tooth appears enlarged and distant from the film, indicating that it is lingually displaced.



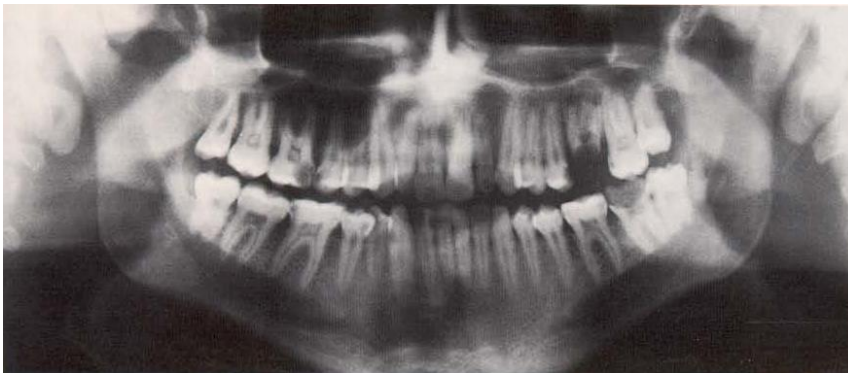
402

Fig. 4.40. Resorption of deciduous teeth 75 and 85 in a 14-year-old female. Tooth 45 was congenitally missing.



403

Fig. 4.41. Resorption of deciduous teeth 75 and 85 in a 22-year-old female. Note the eruption cyst on tooth 18.



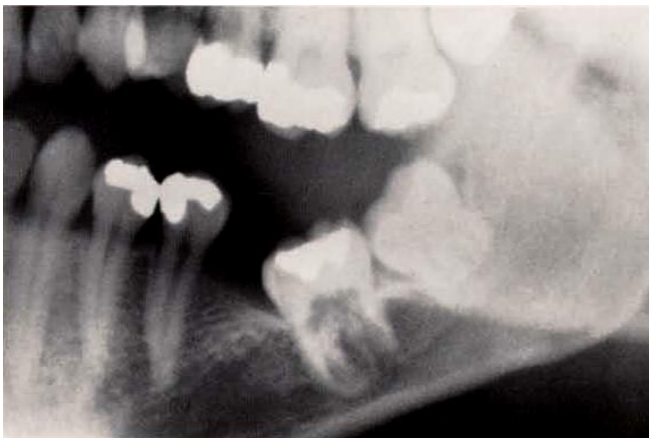
404

Fig. 4.42. Denticles. The radiograph depicts opacities in the pulp chambers of the molars. However, the radiographic picture does not permit differentiation between free or adherent denticles.



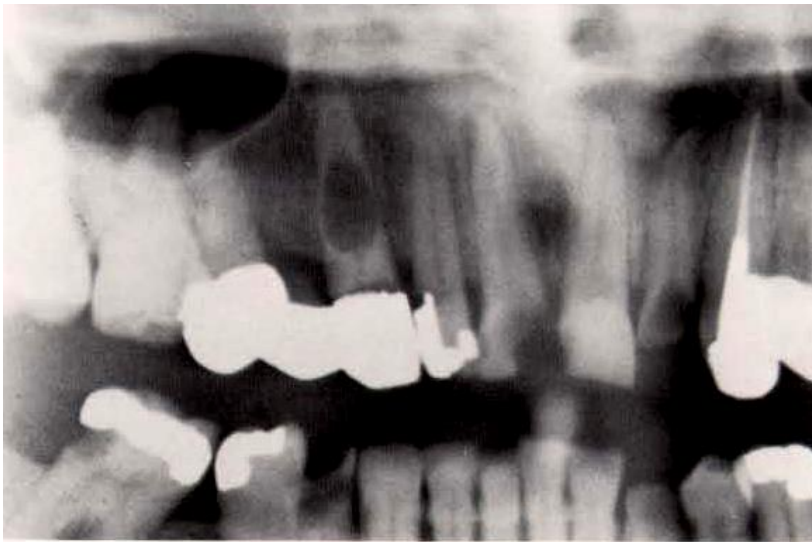
405

Fig. 4.43. Senile atrophy of the alveolar processes of both maxilla and mandible in a 77-year-old female. It appears that the mandibular nerve courses superficially in a depression. The alveolar processes can be more clearly depicted when the patient's prostheses remain in situ, especially the maxilla.



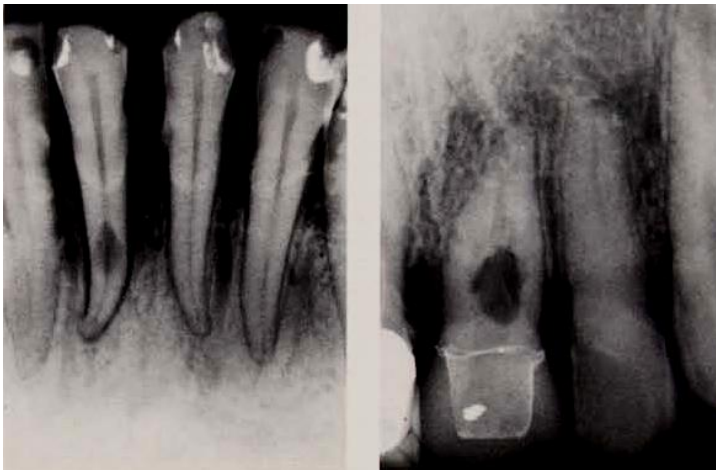
406

Fig. 4.44. Idiopathic resorption of the central type on ankylosed tooth 37 in a 25-year-old male. With advanced resorption such teeth become extraordinarily radiolucent and for this reason are often referred to as "ghost teeth."



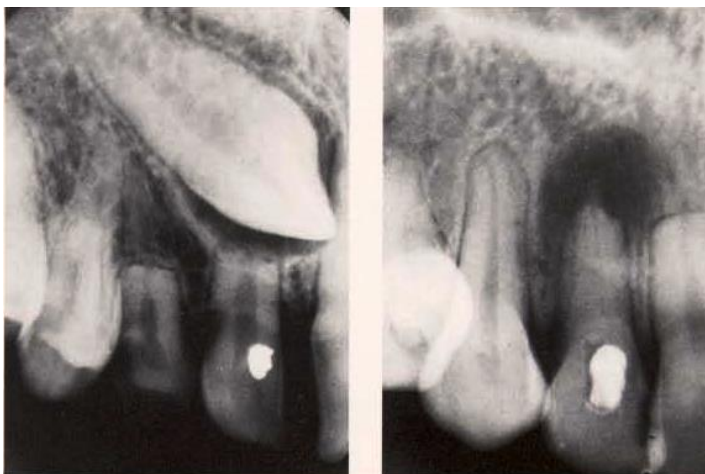
407

Fig. 4.45. Idiopathic resorption of the central type following trauma during tooth preparation and recurrent caries on tooth 13 in a 47-year-old female. The lesion is also known under the synonym "internal granuloma."



408

Fig. 4.46. Idiopathic resorption on maxillary and mandibular anterior teeth. Anterior teeth with abnormal mobility or after traumatic tooth preparation frequently exhibit the formation of "internal granuloma." The left figure depicts a central projection of such an internal granuloma located towards the vestibular aspect.



409

Fig. 4.47. Resorption of deciduous tooth 53 and root resorption on tooth 12. *Left:* The resorption was elicited by growth pressure from impacted tooth 13 and its follicular cyst.

Dentigerous cyst



Fig. 4.48. Dentigerous cyst in a 42-year-old man with painful third molars. A full-mouth radiographic series showed an abnormality; additional radiographic views were then obtained. Panoramic radiograph shows an ellipsoid, expansile, well-defined, corticated, lucent lesion with undulating margins in the right mandible. An associated tooth is seen within the lesion.

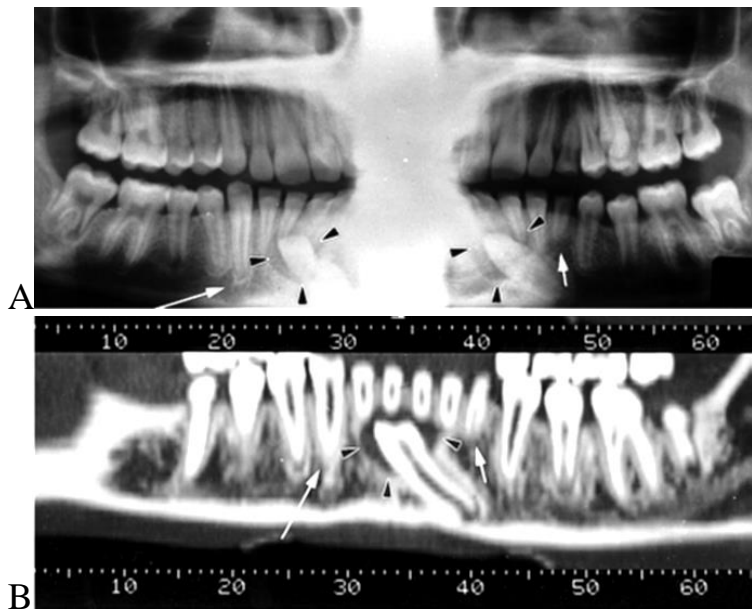


Fig. 4.49. Images in a 14-year-old male adolescent with a dentigerous cyst in an unerupted left cuspid. **(a)** Orthopantomogram shows the dentigerous cyst (arrowheads) twice because of distortion near the midline. Note that the root of the retained primary cuspid (baby tooth) on the left (short arrow) is much shorter than the root of the permanent cuspid on the right (long arrow). **(b)** Panoramic dental CT scan better delineates the unerupted left cuspid with the dentigerous cyst (arrowheads) that surrounds the crown of tooth. The primary left cuspid with a short root (short arrow) and the permanent right cuspid (long arrow) are again depicted.

Torus mandibularis

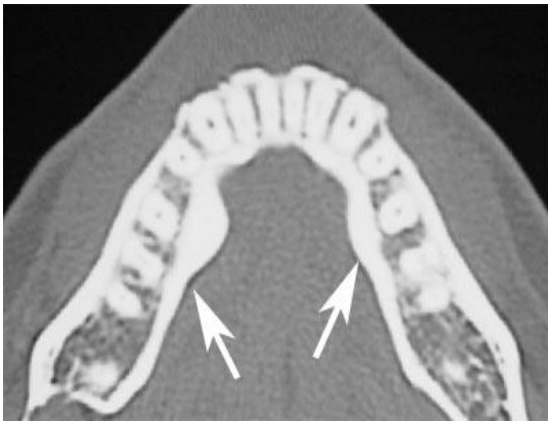


Fig. 4.50. Torus mandibularis in a 35-year old man. CT scan shows bilateral exostosis (arrows) in the lingual aspects of the mandible.

Arteriovenous Malformation (AVM)

Arteriovenous malformations are abnormal, direct communications between arteries and veins that bypass the capillary bed. They are uncommon lesions in the head and neck. Most lesions in the jaws occur in the ramus and posterior body of the mandible. It is important to recognize the hemorrhagic potential of these lesions because extraction of a tooth adjacent to an arteriovenous malformation may result in lethal exsanguination. The clinical features of arteriovenous malformations are variable. The lesion can cause soft-tissue swelling and can expand bone; the swelling is occasionally pulsatile. Aspiration will produce bright red blood.

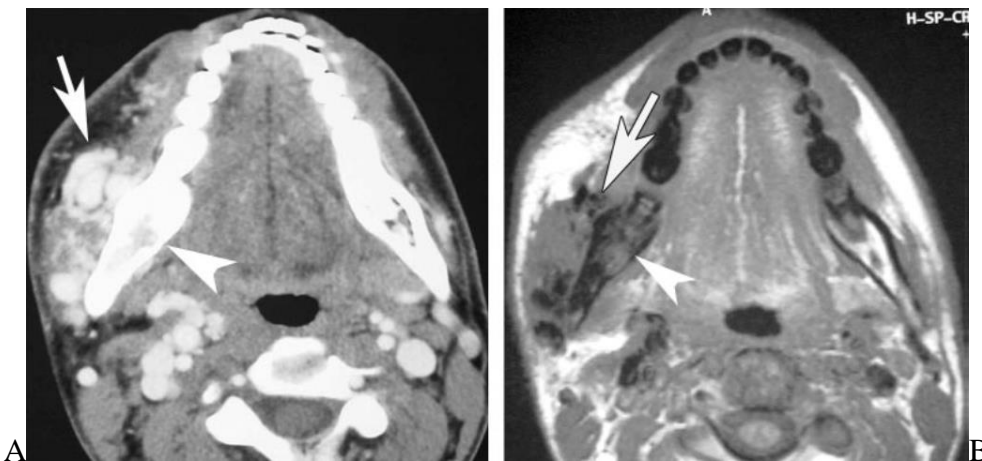


Fig. 4.51. AVM in a 28-year-old man. (A) Contrast-enhanced CT scan reveals multiple dilated and tortuous vessels (arrow) within the right masseter muscle. Note the abnormal enhancement (arrowhead) within the marrow of the mandible. (B) Axial T1-weighted MR image demonstrates a slightly expansile lesion (arrow) within the right mandibular angle and body. Multiple flow voids are present within the right masseter muscle. Note the loss of normal fatty marrow (arrowhead) within the mandible.

Mesiodens

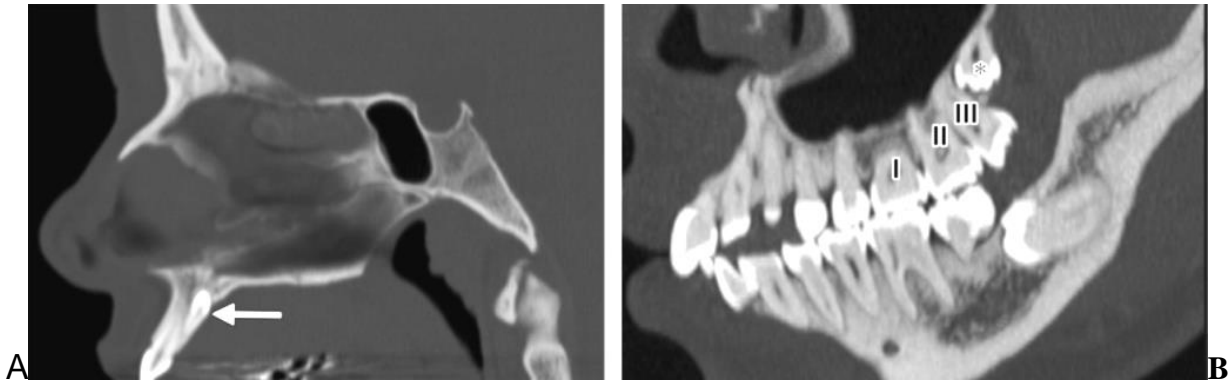


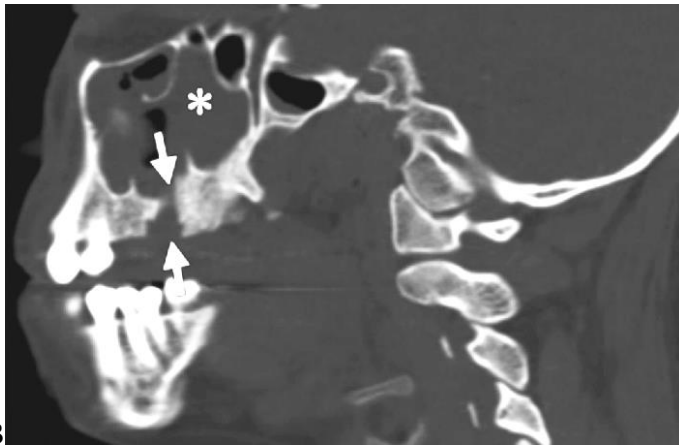
Fig. 4.52. (A) Mesiodens in a 34-year-old woman. Sagittal CT image shows a mesiodens (arrow) lingual to a maxillary incisor. The mesiodens appears peglike, with its crown facing superiorly, a common finding of this condition. (B) Supernumerary molar (distodens) in a 35-year old-woman. Sagittal oblique CT image shows an impacted supernumerary maxillary molar (*). I, II, III = normal three maxillary molars.

Hypereruption



Fig. 4.53. Hypereruption in a 21-year-old man. Sagittal CT image shows hypereruption of the third maxillary molar (arrow), which occurred after the third mandibular molar was extracted.





B

Fig. 4.54. Oroantral fistula. Axial (A) and sagittal (B) CT images show an absence of bone separating the first maxillary molar tooth socket from the maxillary sinus (arrows in B) and a loss of continuity of the palatal cortical plate (arrow in A). Fluid and mucosal thickening are also seen within the maxillary sinus (* in B), a characteristic finding of oroantral fistula.

Sclerosing osteomyelitis

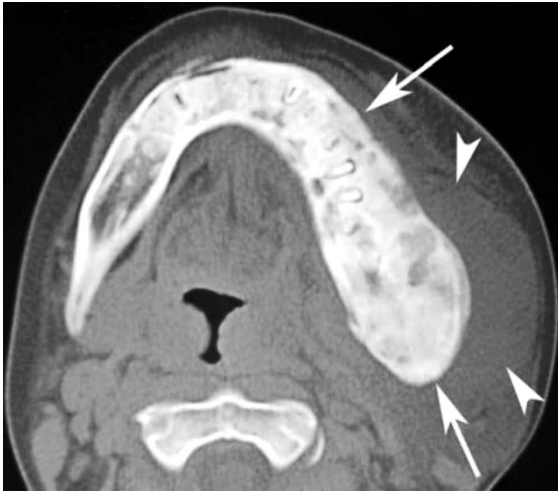


Fig. 4.55. Sclerosing osteomyelitis in a 10-year-old boy. CT scan shows diffuse sclerotic changes with expansion of the left mandibular body (arrows). Note the diffuse soft-tissue swelling (arrowheads).

Sinusitis from an ectopic tooth

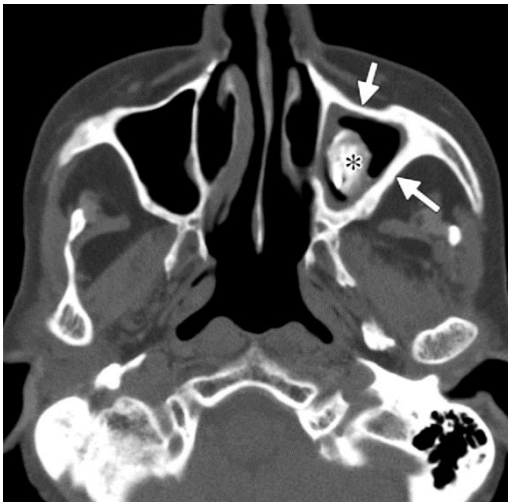


Fig. 4.56. Sinusitis from an ectopic tooth in an 81-year-old woman. Axial CT image shows an ectopic tooth in the maxillary sinus (*), with associated mucosal thickening and asymmetric cortical thickening (arrows), findings consistent with chronic sinusitis.

05 Inflammation and Osteonecrosis

Periapical Infection or Inflammation

In the initiating steps of cavity formation, lactic acid-producing microbes form a film on the surface of the tooth and create an acidic microenvironment. Enamel, although dense, is acellular and will eventually be penetrated by the bacteria, thus forming caries. At CT, a cavity appears as a discontinuous hypoattenuating defect within the enamel along the surface of the crown.

The anatomic structures of the functional elements of the jaws and their tooth-supportive alveolar processes provide numerous possibilities for the initiation and spread of infection. The variable trabecular structure of maxillary and mandibular alveolar processes may contribute here as well. Depending upon the cause and the location, the clinical manifestations of inflammatory processes may vary. It would be desirable to achieve comprehensive information from the radiographic examination of such conditions, which might range from a simple dentogenic infection all the way through osteomyelitis and osteoradionecrosis. Unfortunately, however, radiography can only provide basic documentation of the condition of the tissues *at the time the radiograph is taken*; a radiograph permits no speculative interpretation! Furthermore, radiographic findings often do not agree at all with the clinical picture. Nevertheless those radiographic signs that become visible, independent of the classification of the various etiologies, do show similarities with the documentable tissue changes, and this is the reason for discussing these issues under the above title.

Depending upon the virulence of the infectious agent and the location of the attack, inflammatory processes in the jaws and their radiographic signs can be classified simply as acute or chronic. In the case of *acute conditions* the radiograph begins to correspond to the clinical picture only after several days because serous absorption, the resultant edema, the incipient decalcification and finally the inception of necrosis require time to effect changes in the radiographic picture. These changes generally consist of radiolucencies with vague demarcation. In the case of *chronic conditions* one may see not only osteolysis but also reactive sclerosis; depending upon the host response, the virulence of the microorganisms and the length of time the condition persists, lysis and sclerosis may present a changing relationship. The radiographic picture can also be altered by an acute exacerbation or a superinfection. It is extremely important to avoid confusing the radiographic signs of chronic infection with connective tissue or osseous scar formation, and especially with radiographic subtraction effects in bone. The radiograph alone, without knowledge of the clinical situation and without the use of clinical methods of examination, will rarely provide the necessary diagnostic certainty. At best, it permits only speculation about what is possible or probable.

Thanks to early administration of antibiotic therapy, the widespread forms of acute as well as secondary chronic osteomyelitis, which were common previously, have become much more rare today. Most common today is the primary chronic

form, which may remain symptom-free for long periods of time.

Osteoradionecrosis, which has also been referred to as radio-osteomyelitis, results from latent damage to bone, and it exhibits a common tendency for sequestrum formation.

Periodontitis

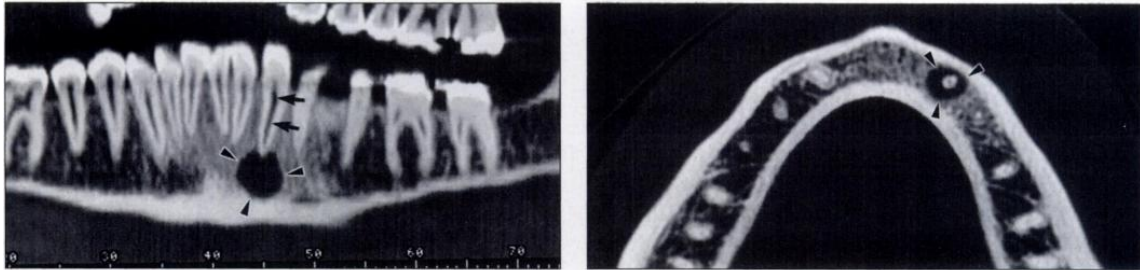


Fig. 5. 1. 24-year-old woman with periapical radiolucency of left canine tooth from endodontal disease. (A) Panoramic image shows periapical radiolucency (*arrowheads*). Note surrounding zone of relatively dense bone from condensing osteitis. Arrows show root canal. (B) Axial image shows target appearance from dense root in center of radiolucency (*arrowheads*).

Periapical Diseases

Apical periodontitis refers to a spectrum of diseases that occur around the tooth apex, including periapical granuloma, periapical abscess, and periapical (radicular) cyst. Infection of the pulp, which usually results from carious lesions that have reached the pulp chamber, increases pressure within the chamber and activates pain fibers within the pulp, causing extreme pain. Persistent high pressure within the pulp chamber leads to pulp death and devitalizes the tooth. Infectious or inflammatory material (even in the absence of infection) in the canal ultimately decompresses into the periapical bone, causing an acute phase of bone resorption. A subacute periapical granuloma may occur at a site of granulation tissue formation where there is a balance between the formation and neutralization of infectious and inflammatory material. A radicular cyst, an expansile epithelium-lined cavity that contains fluid or semisolid material, may ultimately form within the maxilla or mandible. Rarely, if the offending tooth is extracted and the periapical lesion is not curetted, the remaining cyst is referred to as a residual cyst. Keratocystic odontogenic tumors may have a similar appearance as periapical lesions, adding further diagnostic uncertainty.

Periodontal pocket

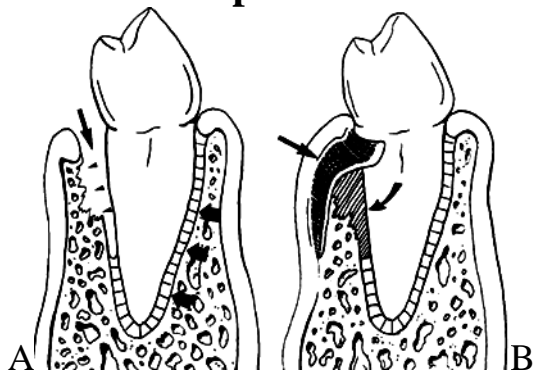


Fig. 5. 2. Illustrations of a periodontal pocket and its treatment. (A) On the right, a normal periodontal ligament is depicted (thick arrows). On the left, the portion affected by periodontal disease results in a periodontal pocket (thin arrow), with resorption of adjacent bone (arrowheads). (B) The periodontal pocket is treated by filling it with freeze-dried bone (curved arrow), by placing an expanded polytetrafluoroethylene membrane (straight arrow) between soft tissues, and by performing a bone graft to prevent soft-tissue ingrowth.

Periodontal Disease

Periodontal disease is the most common cause of tooth loss worldwide. When dental care is inadequate, bacteria-harboring plaque accumulates at the tooth-gingival (gum) interface, leading to inflammation of the gingiva, a condition known as gingivitis. Plaque infection may extend under the gingiva, creating a periodontal pocket. In marginal periodontitis, the infection spreads along the periodontal ligament toward the tooth apex, destroying the periodontal ligament and resorbing bone between teeth and at root furcations. Ultimately, general tooth loosening and root uncovering result.

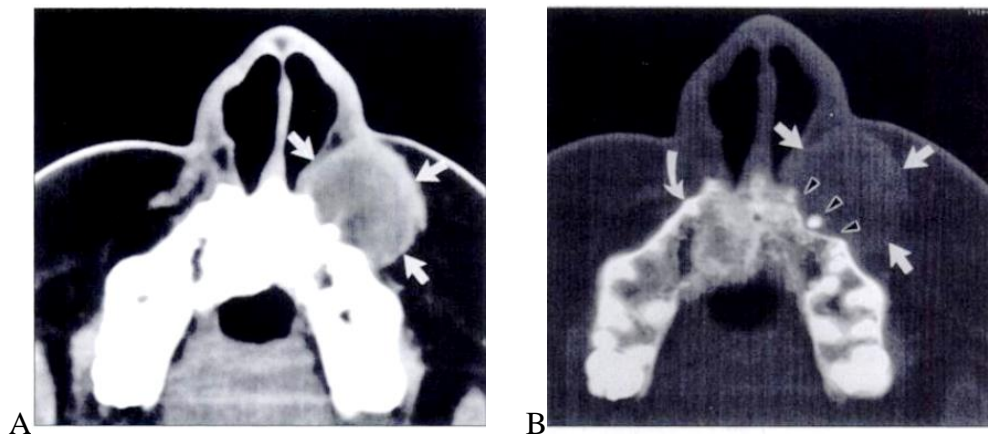


Fig. 5. 3. year-old woman with **periapical lesion causing soft-tissue mass** of face. (A) Soft-tissue window of axial CT scan shows soft-tissue mass (*arrows*). (B) Bone window of same axial CT scan as in A reveals that resorption of bone around root apex created peniapical radiolucency (*arrowheads*). Compare with normal root apex on right side (*curved arrow*). Straight arrows show soft-tissue mass.

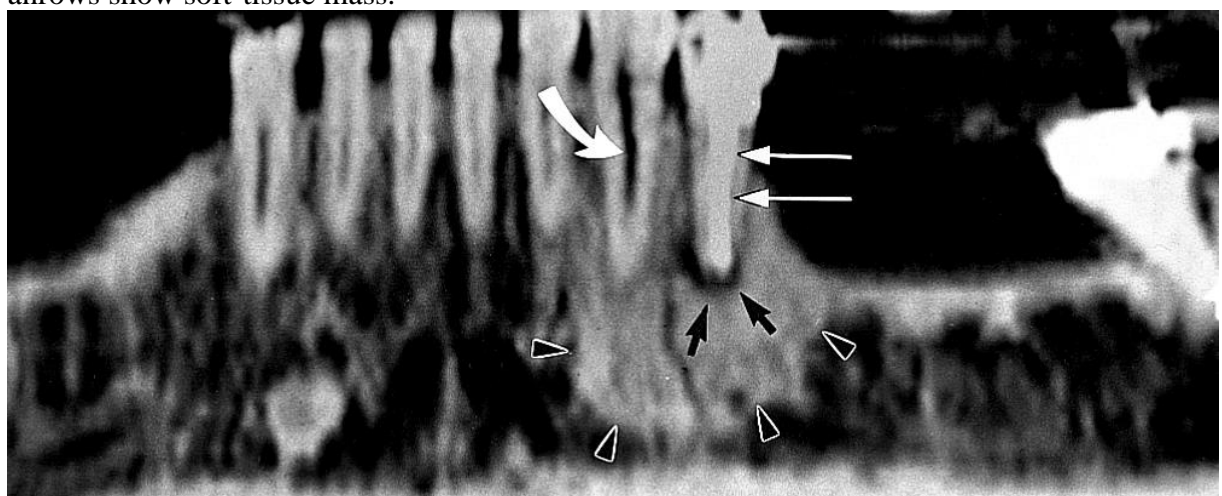


Fig. 5. 4. Panoramic dental CT scan in a 52-year-old man with a small periapical lesion (straight white arrows) from endodontal disease that surrounds a zone of condensing osteitis (arrowheads). Note that the radiopaque post (black arrows) from a root canal procedure fills the

root canal. Compare this with the normal radiolucent root canal in the adjacent tooth (curved white arrow).

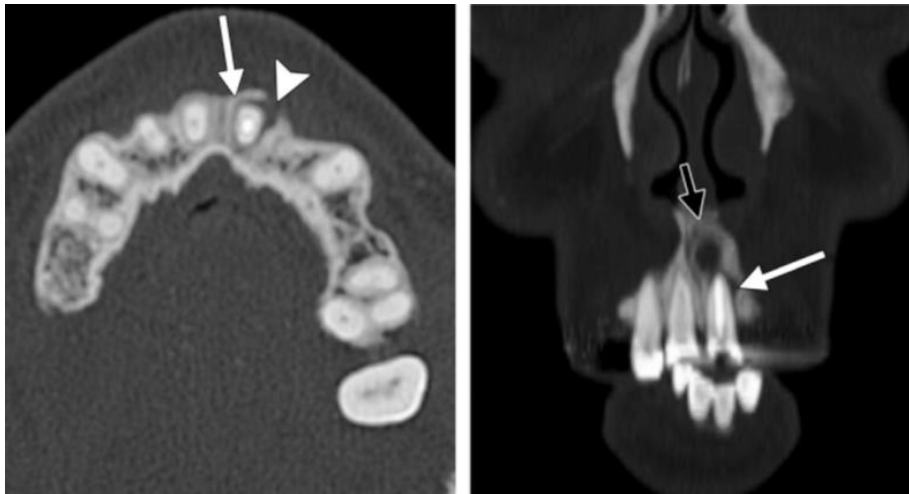


Fig.5.5. Failed root canal with periapical abscess in a 69-year-old woman with lip swelling. (a) Axial CT image demonstrates a periapical lucency (arrow) involving the left maxillary central incisor. Cortical breakthrough (arrowhead) occurred and led to recurrent cellulitis of the upper lip. (b) Coronal CT image shows the periapical lucency (white arrow) and additional ill-defined lucent lesion (black arrow) consistent with an abscess. Radiopaque material from prior root canal therapy fills the pulp cavity.

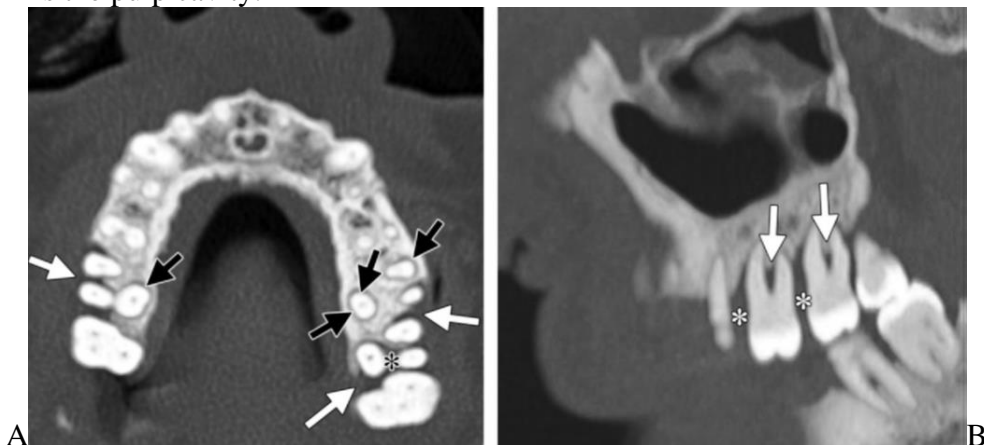


Fig.5.6. Periodontal disease in a 52-year-old man. (A) Axial CT image shows marked bone loss (white arrows) around the molar roots and widening of the periodontal ligament space, which is seen as a ring of low attenuation (black arrows) surrounding the molar roots. Bone loss is also seen at a molar furcation (*). (B) Sagittal oblique CT image shows bone loss between the teeth (*) and at furcations (arrows). (C) Three-dimensional surface-rendered CT image shows marked bone loss, with partial uncovering of the roots in multiple premolars and molars (*).

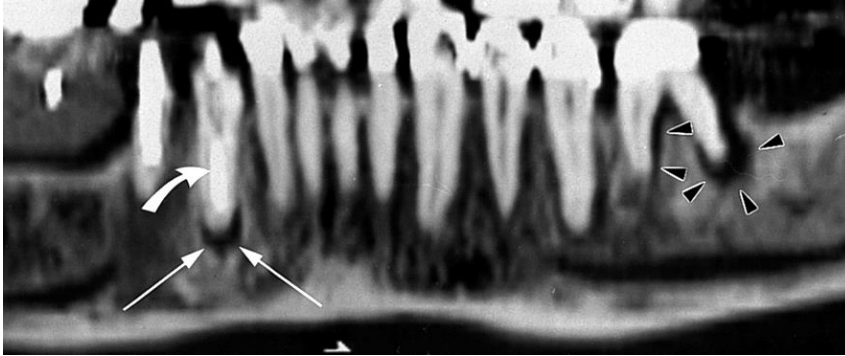


Fig.5.7. Panoramic dental CT scan in a 60-year-old man with advanced periodontal (arrowheads) and endodontal (straight arrows) lesions. Note how periodontal disease travels down the sides of the root, while endodontal disease affects the root apex. A radiopaque post from a root canal procedure is seen in a tooth with an endodontal lesion (curved arrow).

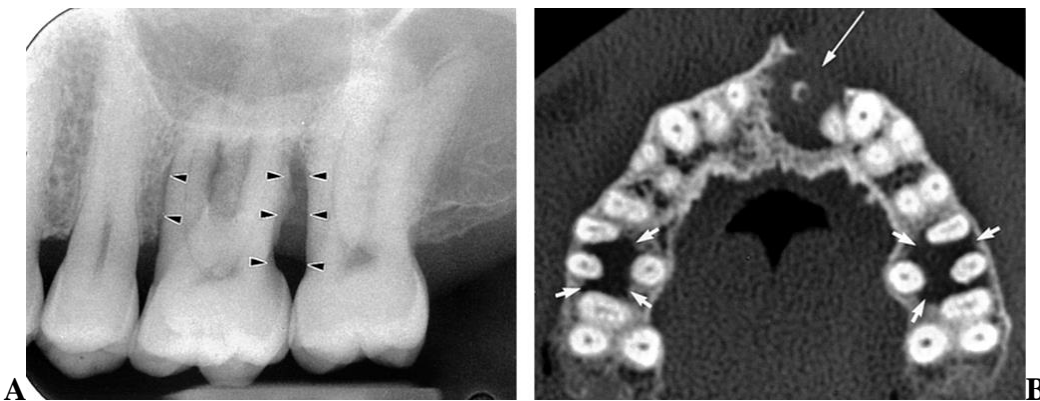


Fig.5.8. Images in a 46-year-old man with periodontal disease causing bone resorption of the right and left first molar root furcation and with endodontal disease causing periapical radiolucency in the left central incisor. (A) On the conventional dental radiograph, roots are superimposed, making it difficult to determine which roots have bone loss and whether periodontal disease affects root furcation. Bone resorption (arrowheads) is depicted along the sides of the roots. (B) Transverse CT image more easily reveals that radiolucency due to bone resorption involves the root furcations of the first molars (short arrows). Note also the large periapical radiolucency (long arrow) in the left central incisor caused by endodontal disease.

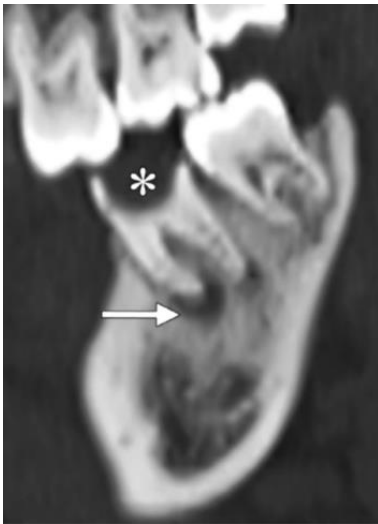


Fig.5.9. Cavity and periapical lucency (granuloma). Sagittal CT image demonstrates a large cavity (*) in the crown of a second mandibular molar, involving both enamel and dentin. Widening of the periodontal ligament (arrow) around the apex of the tooth is seen, consistent with apical periodontitis. Sclerosis of the bone surrounding the infected tooth suggests chronic inflammation.

Acute and Chronic Apical Periodontitis

As long as no structural alterations have occurred in the periapical tissues, the radiograph will reveal no reaction, despite acute clinical symptoms. Acute inflammatory processes that extend from the root apex often appear on the radiograph as diffuse periapical radiolucencies with apparent widening of the periodontal ligament space. Chronic apical periodontitis that often exhibits acute exacerbations may appear radiographically as sharply demarcated radiolucencies with reactive sclerosis.

If the practitioner suspects participation by a dentogenic focus of infection, the radiographic examination must be carried out with greatest care:

- A radiograph cannot provide information about the vitality of a tooth except in the case of previously performed endodontic therapy.
- Spreading inflammatory processes will only be detectable radiographically with delays, after osseous reactions have occurred.
- Obvious periapical lesions can, at best, be described by the radiologist as “possible” or “probable” foci of infection.

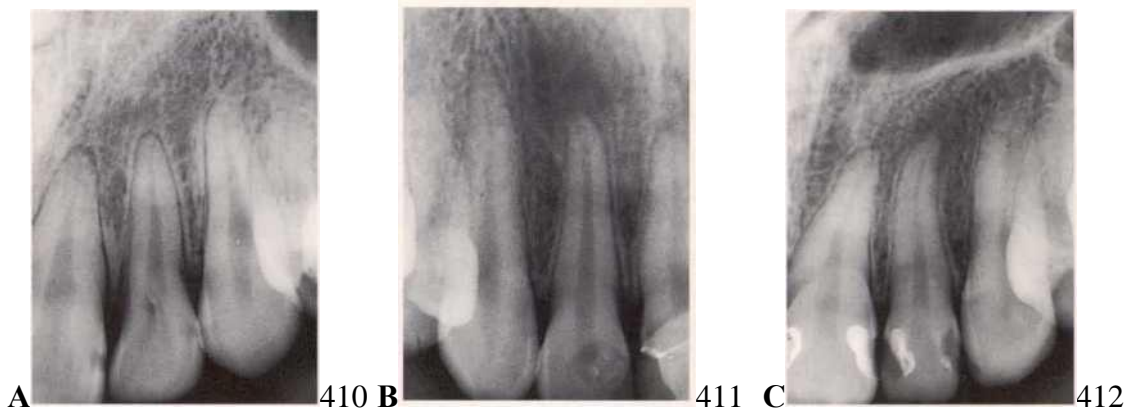


Fig. 5.10. (A) **Fully developed acute pulpitis.** No periapical alterations are apparent at the apex of tooth 22, which has undergone trepanation. (B) **Subperiosteal abscess.** Note the diffuse periapical radiolucency on tooth 12. (C) **Chronic apical periodontitis.** The lamina dura is widened apical to the poorly demarcated radiolucency.

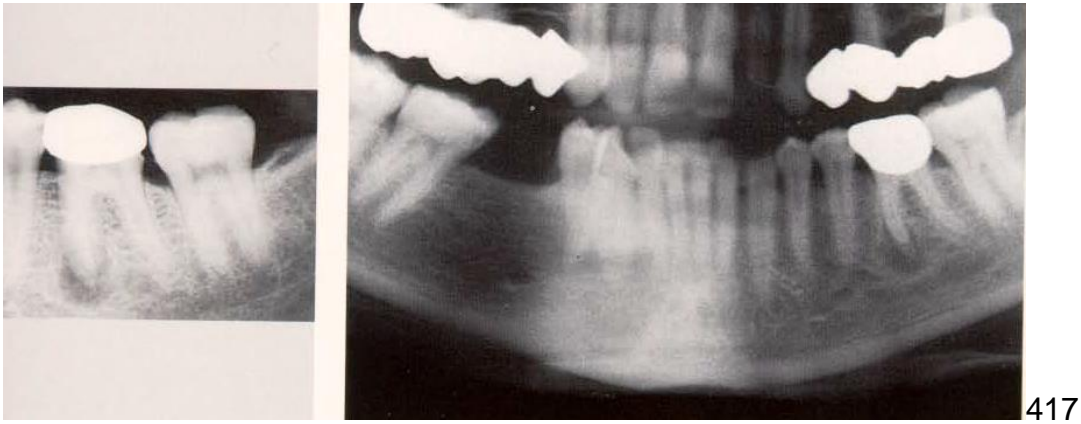


Fig. 5.11. **Following trauma during tooth preparation, pulpal necrosis and chronic apical periodontitis of tooth 36 ensued.** Comparison between periapical radiograph and panoramic film. The periapical film provides a clear picture of the lesion. Because of the summation effect, the lesion appears smaller radiographically when underexposed.



Fig. 5.12. Condensing osteitis in the former alveolus of tooth 46. Tooth 47 exhibits a terminal marginal periodontitis with chronic apical periodontitis on the distal root. The extremely wide periodontal ligament space of tooth 45 is a sign of the occlusal overload and resulting mobility.

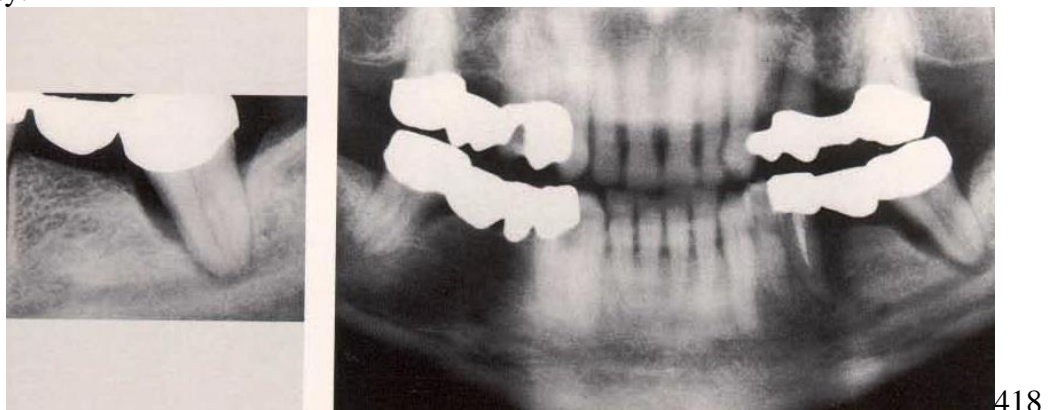


Fig. 5.13. **Late stage marginal periodontitis on tooth 37.** Comparison between periapical and panoramic films. Note the massive osseous reaction, which extends into the compact bone. The reaction becomes evident after comparison with the left side.

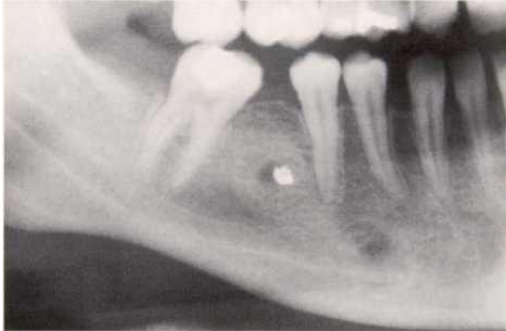


A 413



B 414

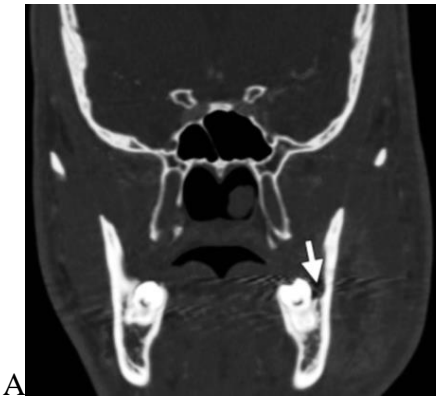
Fig. 5.14. A. Chronic apical periodontitis. **Obvious periapical osteolysis and radiopaque border of an incapsulated granuloma on tooth 22.** B. Chronic apical periodontitis. **Reactive sclerosis on the mesial and acute exacerbation on the distal root of tooth 36.**



415

Fig. 5.15. **Foreign body granuloma.** Reaction around the residual amalgam that persisted in the mesial alveolus after extraction of tooth 46. The reactive sclerosis is clearly discernible.

Pericoronitis



A



B



C



D

Fig. 5.16. Pericoronitis in two patients. (A) Coronal CT image obtained with bone window settings in a 24-year-old man shows an impacted left third mandibular molar and expansion of the

buccal coronal follicular space (arrow). **(B)** Coronal CT image obtained with soft-tissue window settings in the same patient shows an adjacent abscess in the masticator space (arrows). Streak artifact from dental amalgam extends through the abscess. **(C, D)** Sagittal **(c)** and axial **(D)** CT images obtained with bone window settings in a 31-year-old man show distocoronal chronic pericoronitis (arrow) involving the bone posterior to the mandibular third molar. A widened distocoronal follicular space and adjacent bone sclerosis are also seen, common changes, especially in young adults.

Abscess

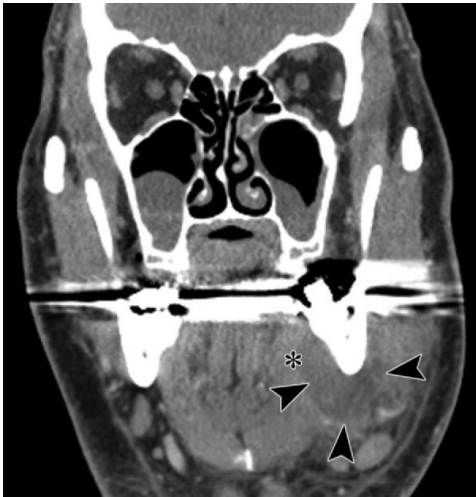


Fig. 5.17. Odontogenic submandibular abscess. Coronal CT image shows a submandibular abscess (arrowheads) adjacent to the left mandibular second molar and medial bowing of the mylohyoid muscle (*).

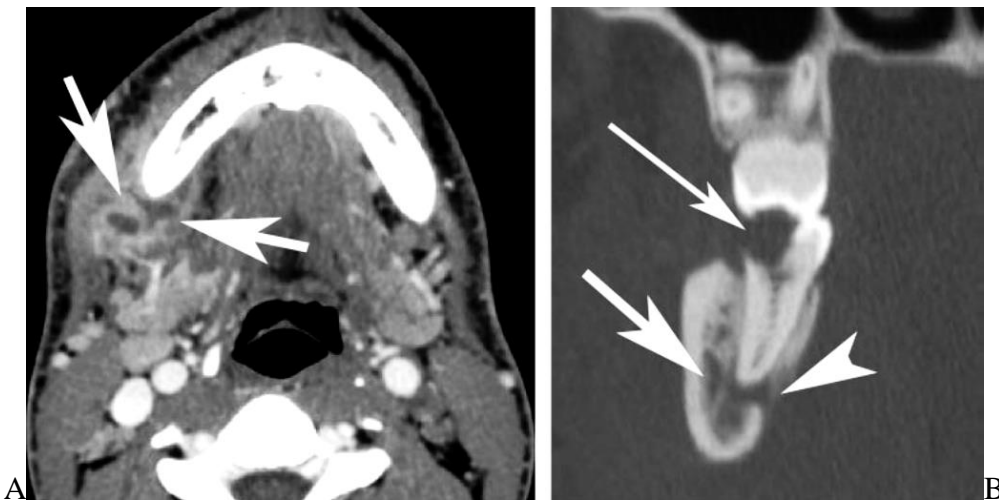


Fig. 5.18. Periapical and perimandibular abscess in a 10-year-old boy. **(A)** Contrast-enhanced CT scan demonstrates a rim-enhancing fluid collection (arrows) within the perimandibular soft tissues. **(B)** Oblique coronal reformatted CT image reveals a periapical abscess (thick arrow) within the mandibular body and a fistula (arrowhead) that extends to the lingual surface. Note the cavity (thin arrow) within the crown of the tooth.

Condensing osteitis

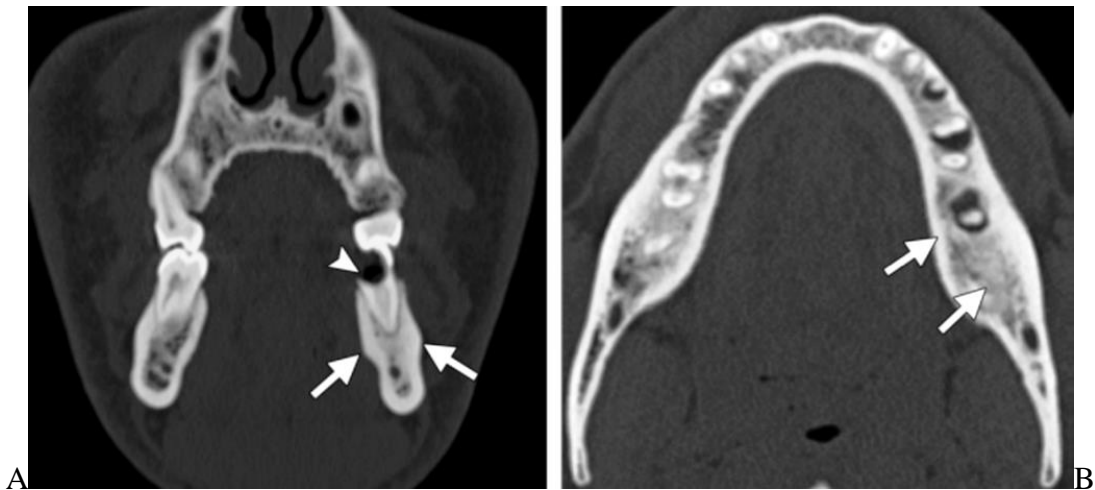


Fig. 5.19. Condensing osteitis in two patients. **(A)** Coronal CT image shows a poorly marginated nonexpansile sclerotic lesion (arrows), a finding indicative of condensing osteitis. The lesion is associated with a carious lesion (arrowhead). **(B)** Axial CT image obtained in a different patient shows two poorly marginated nonexpansile sclerotic lesions (arrows) associated with periapical inflammatory lesions, a finding indicative of condensing osteitis.

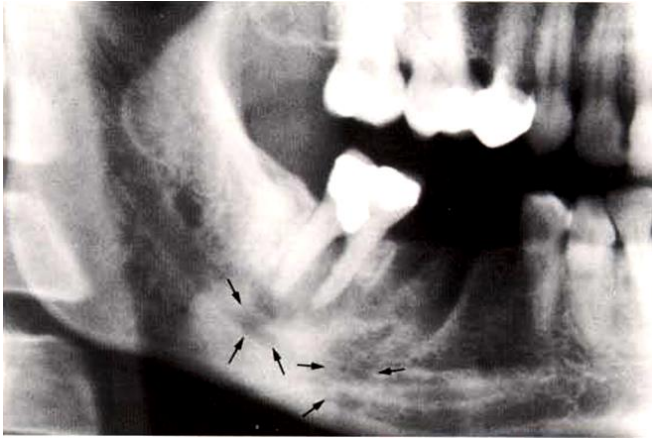
Osteomyelitis

Radiographic signs of osteomyelitis:

- Acute osteomyelitis: Radiographic signs can only be observed after structural alterations have occurred.
- Secondary chronic osteomyelitis: 1-2 weeks after onset, expansive necroses with pus formation predominate. Lesions become circumscribed and periosteal reactions are observed.
- Primary chronic forms of osteomyelitis: Radiolucencies (bone resorption) and radiopacities (bone formation) present a “cloudy” or “cottonlike”.

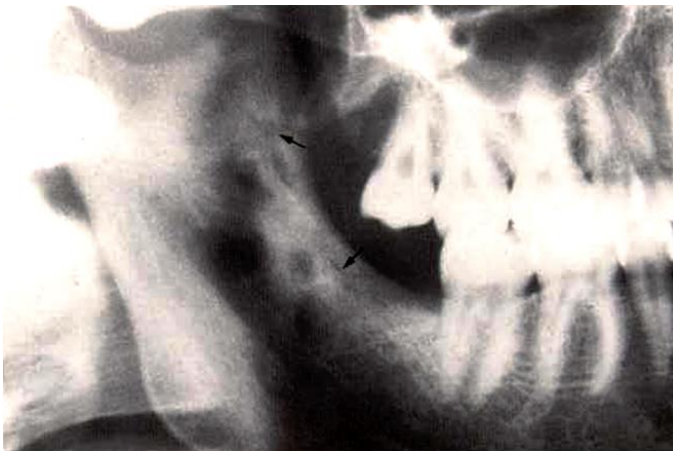
Acute Osteomyelitis

Despite the somewhat spectacular clinical picture that includes compromised general health, fever, swelling of the soft tissues, neurologic disturbances and characteristic “pounding” pain, acute osteomyelitis in its initial stage is not accompanied by any radiographically discernible manifestations. Additional clinical symptoms include increasing tooth mobility and a “woody” sound upon percussion of the affected teeth. The radiograph exhibits circumscribed radiolucencies only 1-2 weeks later as the first signs of initial demarcation of the necrotic areas.



424

Fig. 5.20. Acute osteomyelitis in an early stage, following extraction of tooth 46. In addition to the original signs of existing apical and periodontal lesions, the initial circumscribed radiolucencies are visible (arrows).



425

Fig. 5.21. Acute osteomyelitis in the ascending ramus following extraction of tooth 48 and a fracture (arrows). Initial and confluent areas of resorption surround the already sclerosed section as demarcation progresses.

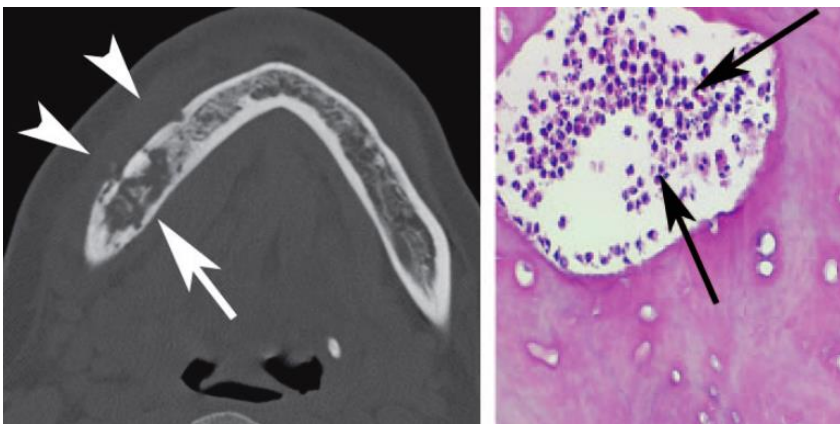


Fig. 5.22. Acute suppurative osteomyelitis in a 44-year-old woman. (a) CT scan (bone windowing) demonstrates a nonexpansile, osteolytic lesion (arrow) within the right mandible. Perimandibular soft-tissue inflammatory change (arrowheads) is also present. (b) High-power photomicrograph (H-E stain) reveals loss of osteocytes from lacunae and severe inflammatory cell infiltrates (arrows).

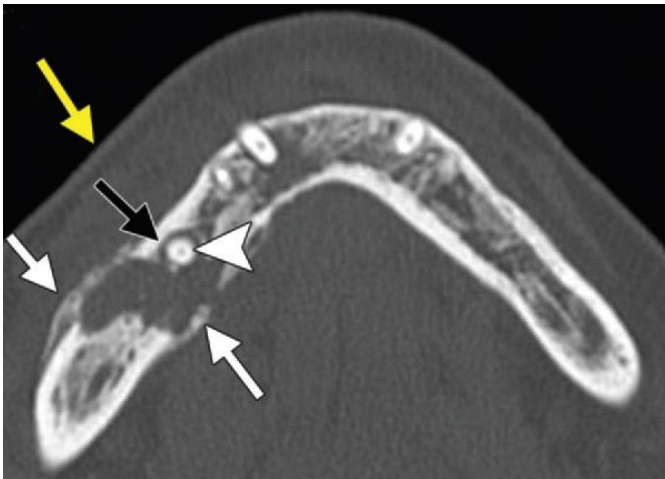


Fig. 5.23. Osteomyelitis in a 66-year-old woman with mandibular pain. Axial CT image shows an irregularly marginated lucent lesion (black arrow) adjacent to the root of the right mandibular second premolar (arrowhead). Thinning and breakthrough of the surrounding lingual and buccal cortices and periosteal reaction (white arrows) have occurred. Adjacent soft-tissue stranding and thickening (yellow arrow) and enlarged lymph nodes (not shown) suggest acute infection.

Chronic Osteomyelitis

The primary chronic forms of osteomyelitis are often seen today. Symptoms are rare early on, and massive remodeling within bone determines the radiographic diagnostic picture; this can be accompanied by massive distension of the bone that is undergoing vascular damage. However, the pathologic processes may present in various ways, with structural changes resembling clouds or cotton, as osseous resorption and formation persist and alternate within the bone.

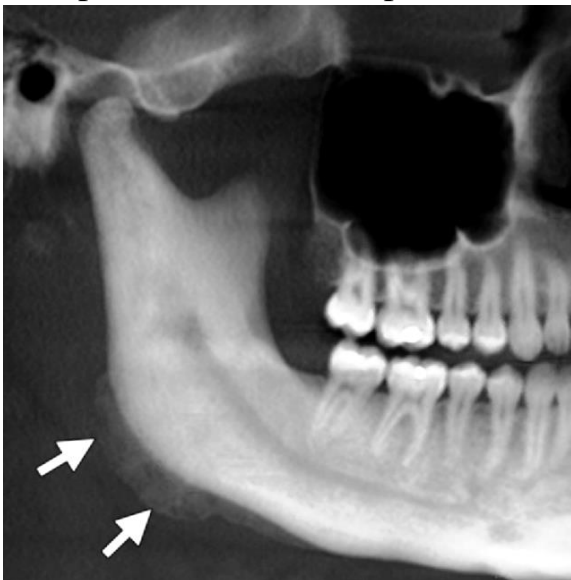
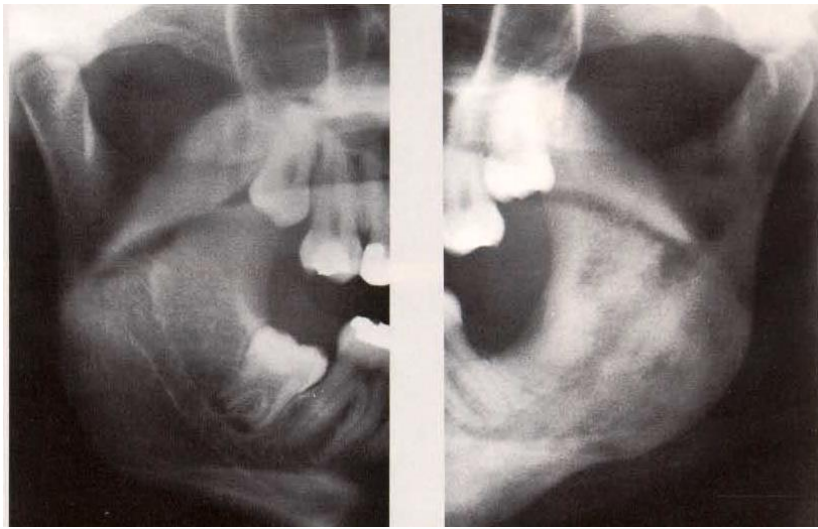


Fig. 5.24. Long-standing primary chronic osteomyelitis in an adult. Cropped and reconstructed CT panorex image shows diffuse mandibular sclerosis with fluffy periosteal new bone formation (arrows) at the mandibular angle.



429

Fig. 5.25. Primary chronic osteomyelitis in a left-right comparison following extraction of tooth 38 and delayed wound healing. Note the dense cloud/cotton-like structure and the loss of normal anatomic picture of the mandibular canal on the right; compare this with the ascending ramus of the mandible on the healthy side. Paresthesia is often reported by these patients, as well as distension of the bone on the affected side.



Fig. 5.26. Chronic osteomyelitis in a 47-yearold man. CT scan reveals an osteolytic lesion (arrow) containing a bony sequestrum (arrowhead) within the left mandibular body.

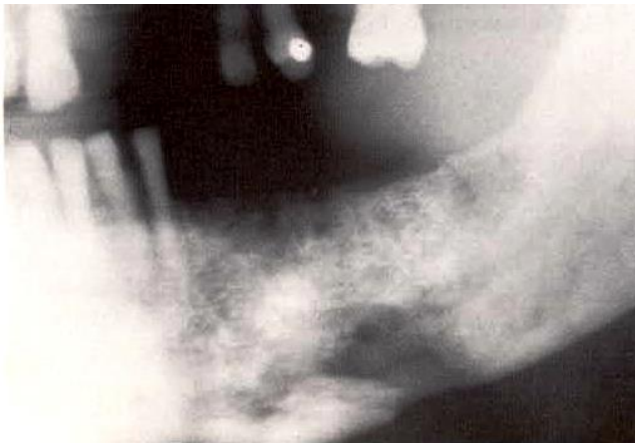
Secondary Chronic Osteomyelitis

If healing of acute, suppurative osteomyelitis does not occur, after approximately 2 weeks the secondary chronic form ensues. The radiographic picture of this form is dependent upon the localization and the effectiveness of therapy. Radiographically one may see confluent areas of bone resorption and demarcation of necrotic areas in the bone. In the absence of appropriate therapy, spontaneous fractures often occur. Thanks to modern antibiotic therapy, this form of osteomyelitis is seldom encountered today.



426

Fig. 5.27. Secondary chronic osteomyelitis after extraction of tooth 37 and delayed wound healing. Readily visible are the coalescing, poorly demarcated radiolucencies, which correspond to bone marrow necrosis, in addition to demarcation and sequestrum formation.



427

Fig. 5.28. Secondary chronic osteomyelitis with necrosis and sequestrum formation. The sequestrum is clearly visible near the bottom of this picture.



428

Fig. 5.29. Same case, as seen in a periapical film. This film points up how little can actually be observed in a periapical radiograph when, for example, soft tissue swelling makes it impossible to position the film packet correctly.

Diffuse Sclerosing Osteomyelitis in Chronic Apical and Marginal Periodontitis

The relatively mild bacterial infections typical of chronic apical and marginal periodontitis can lead to a special form of osteomyelitis with diffuse opacities of the surrounding bone, especially in young persons with good host response. For

example, the otherwise difficult to discern mandibular canal becomes easily visible because of its transparent contents and also because of the sclerosis of the canal wall. This form of osteomyelitis can sometimes occur following tooth extraction and delayed wound healing.

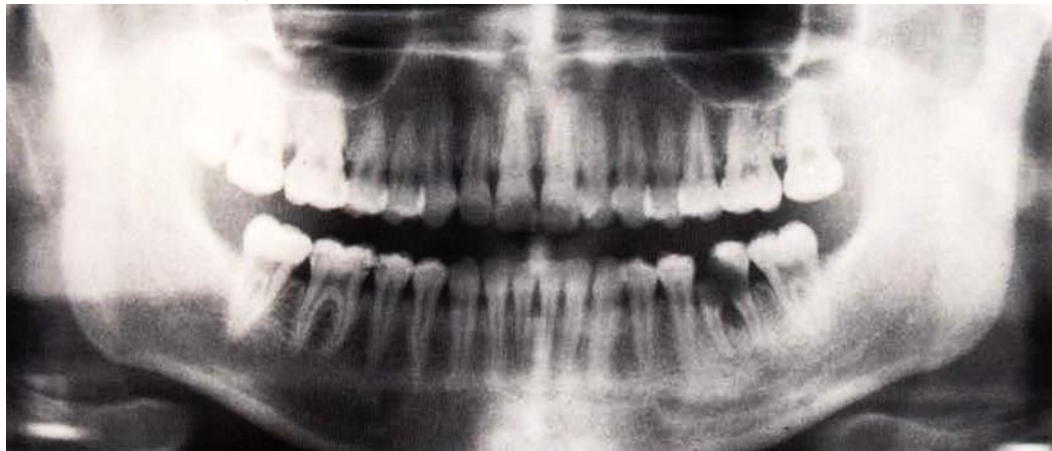


Fig. 5.30. Diffuse sclerosing osteomyelitis in the left mandible of a 22-year-old female following pulpal necrosis and interradicular osteolysis of tooth 36. Compare the opacities on the left side with the healthy right side.

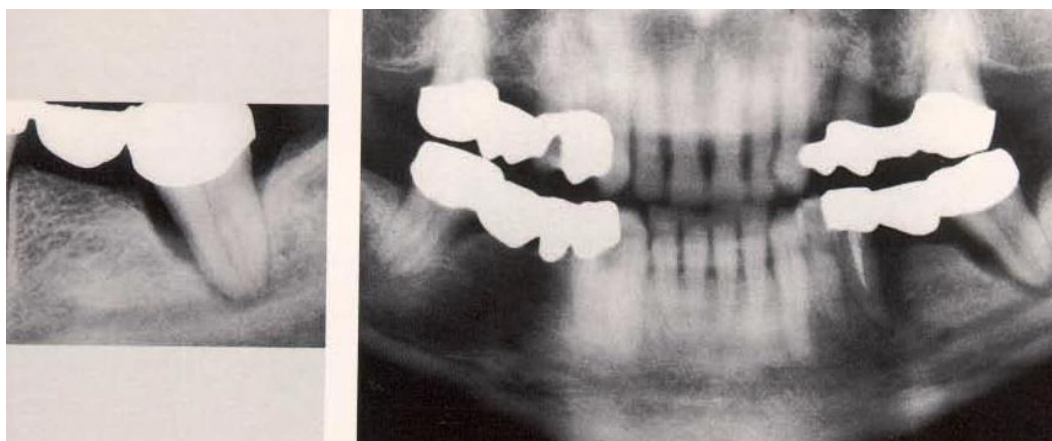
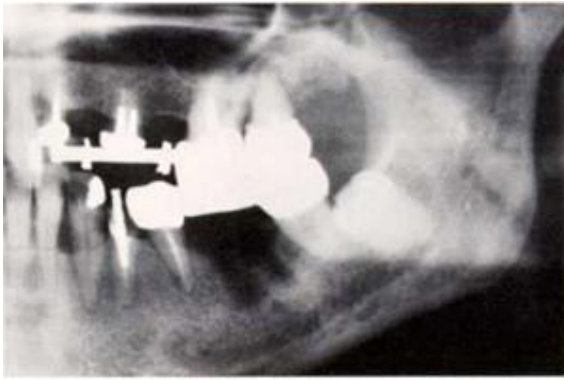


Fig. 5.31. Late stage marginal periodontitis on tooth 37. Comparison between periapical and panoramic films. Note the massive osseous reaction, which extends into the compact bone. The reaction becomes evident after comparison with the left side.

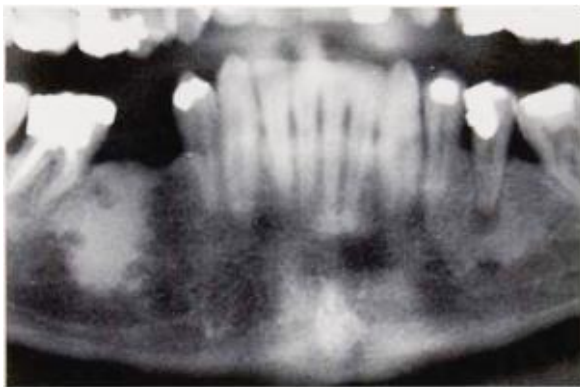
Sclerosing Osteomyelitis and Inflammatory Reactive Osteosis

Following chronic apical or marginal periodontitis, after tooth extraction and in cases of delayed wound healing, focal or a diffuse spreading primary chronic osteomyelitis sometimes ensue. Also often observed is an excessive reactive production of sclerosing bone, as in a bone scar. Such conditions are believed to result from the stimulation of new bone formation by low grade bacterial infection in the affected region. Because such compact bone formation is almost never resorbed spontaneously, it remains visible in the radiograph over the long term.



419

Fig. 5.32. Localized primary chronic osteomyelitis. Following tooth extraction and delayed wound healing, this picture persisted four months after placement of the bridge between teeth 35 and 37. Observe the reactive sclerosis around the mandibular canal and the poorly defined alveolar border.



421

Fig. 5.33. Reactive osteosis in the region of the former alveolus of extracted tooth 46. Histologically, such cases exhibit compact bone without marrow spaces. As a comparison, note the chronic apical periodontitis on tooth 35, with extensive reactive sclerosis.

Additional Signs of Dentogenic Infection

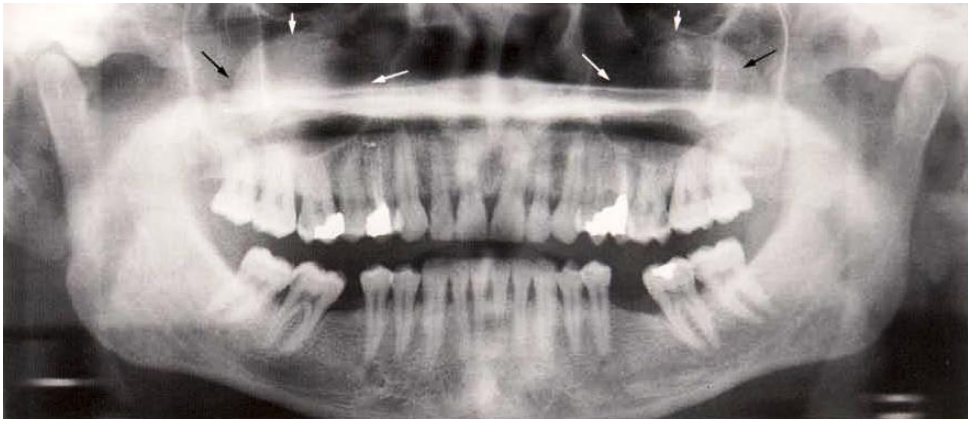
Any practical comparison between periapical radiographs and panoramic films will demonstrate that many types of mucosal reactions, e.g., the mucocele, can be satisfactorily depicted only in the panoramic film. The vague radiopacity sometimes seen on periapical films may lead to a suspicion of pathology, but even panoramic radiography does not permit perfect diagnosis in every case. Therefore it is necessary in any ambiguous situation to supplement with additional examination methods.



437

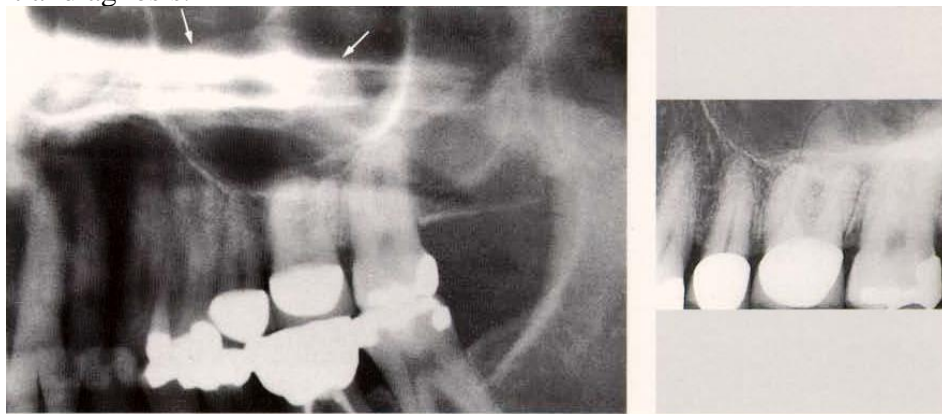
Fig. 5.34. **Periapical radiographs of the premolar-molar region.** The film depicts endodontic treatment of teeth 14 and 25, as well as deep proximal caries on the distal surfaces of

teeth 16 and 26. The floor of the sinus appears more radiopaque than normal, but interpretation of this observation is not possible without a more comprehensive depiction.



438

Fig. 5.35. Panoramic radiograph of the same case. Massive round opacities in both sinuses (arrows) indicate the presence of mucocoeles (mucosal retention cysts). In the periapical films (Fig. 6.25), these lesions shadow only the floor of the sinus, and thus do not permit a differential diagnosis.



439

Fig. 5.36. Development of a mucocoele around the root of nonvital tooth 26, with pulpal necrosis following trauma during tooth preparation. Comparison between the panoramic radiograph (arrows) and the periapical radiograph of the same case.

Osteomyelitis in Infants and Children

A life-threatening form of osteomyelitis may afflict babies and children. It takes the form of a severe toxic event that begins with a high fever and quickly develops into swelling in the facial area, especially in the maxilla. In the secondary chronic stage, osseous necrosis often occurs, as well as sequestration of the tooth buds. Preschool children often develop maxillary osteomyelitis following pulpal necrosis of the mandibular deciduous molars; this sometimes results in loss of the permanent premolar tooth buds.



422

Fig. 5.37. A 5-month-old child with osteomyelitis. **The arrow depicts the sequestration of a mandibular deciduous molar, as it is often seen in the later stages of this disease.**

Inflammatory Disease of the Jaw

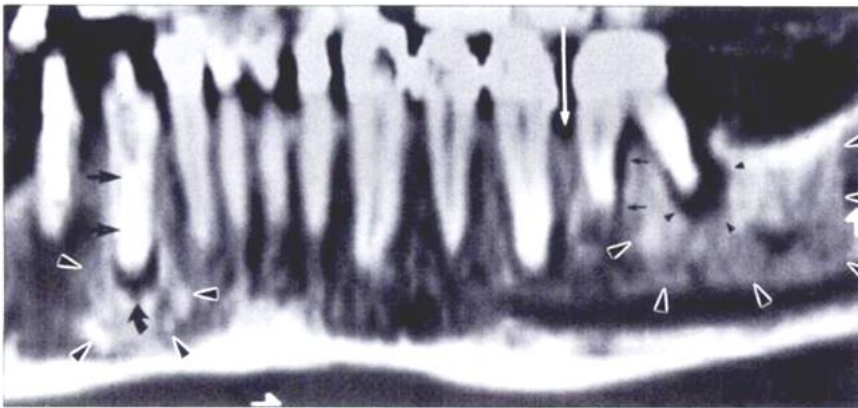


Fig. 5.38. Panoramic image of 60-year-old man with advanced periodontal and periapical lesions as well as areas of surrounding osteitis condensans. On patient's left, periodontal infection has resorbed bone and created radiolucency adjacent to root surface (*small black arrows*). Also seen is more atypical combined periodontal and periapical lesion (*small arrowheads*). Note surrounding zone of relatively dense bone from condensing osteitis (*large arrowheads*). Periodontal disease has also created wedge-shaped radiolucency adjacent to root at crest of interdenal bone (*white arrow*). On patient's right, note curvilinear periapical radiolucency (*curved arrow*), which also has surrounding zone of condensing osteitis.

Osteonecrosis

Bisphosphonate-related osteonecrosis

Bisphosphonate-related osteonecrosis of the jaw (BRONJ) is associated with the use of oral or intravenous bisphosphonates to treat various bone conditions such as osteoporosis, Paget disease, multiple myeloma and metastasis. BRONJ may also be associated with infection by *Actinomyces* organisms. Osteonecrosis may be spontaneous; it commonly occurs in the mylohyoid ridge or is precipitated by a traumatic procedure such as tooth extraction or dental surgery. BRONJ should be considered in patients undergoing bisphosphonate therapy with findings of bone necrosis and no history of radiation therapy. Bisphosphonates inhibit endothelial proliferation and interrupt intraosseous circulation. The risk for osteonecrosis is

higher with concurrent steroid therapy. BRONJ is typically painful, but some patients may be asymptomatic. Maxillary osteoradionecrosis and osteomyelitis are unusual because of the rich blood supply of the maxilla. At imaging, BRONJ is seen as a poorly marginated diffuse area of low attenuation with bilateral symmetric sclerosis.

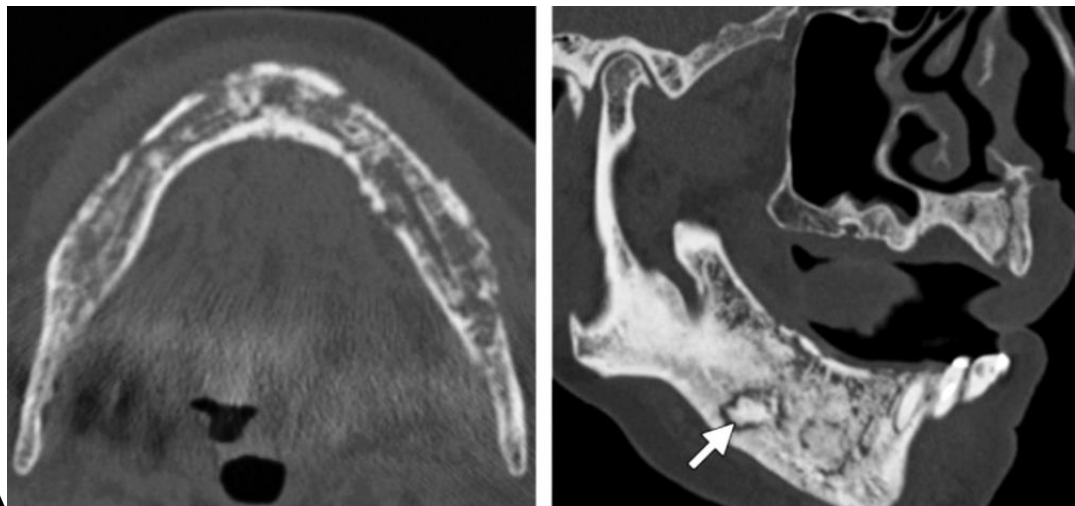


Fig. 5.39. BRONJ in two patients. Axial (A) and sagittal reformatted (B) CT images show symmetric, poorly marginated, mixed sclerotic and lytic lesions throughout the mandible with multiple cortical interruptions. The lesions are bilateral. An area of evolving sclerotic necrotic bone (arrow in b) is also seen.

Osteoradionecrosis

The presentation of osteoradionecrosis (ORN) after radiotherapy (RT) for head and neck cancer varies from small, asymptomatic bone exposures that may remain stable for months to years or heal with conservative management, to severe necroses necessitating surgical intervention and reconstruction. The risk of developing ORN depends on a number of factors, including primary site, T stage, proximity of the tumor to bone, dentition, type of treatment (external beam RT, brachytherapy, surgery, and chemotherapy), and RT dose.



430

Fig. 5.40. **Osteoradionecrosis with sequestration and spontaneous fracture.** The radiographic appearance in cases of osteoradionecrosis is generally similar to that of secondary chronic osteomyelitis. Of note is that following massive irradiation of the bone, the periosteum is no longer capable of mounting an effective reparative response because of the vascular damage. The periosteal reaction is a typical radiographic sign.

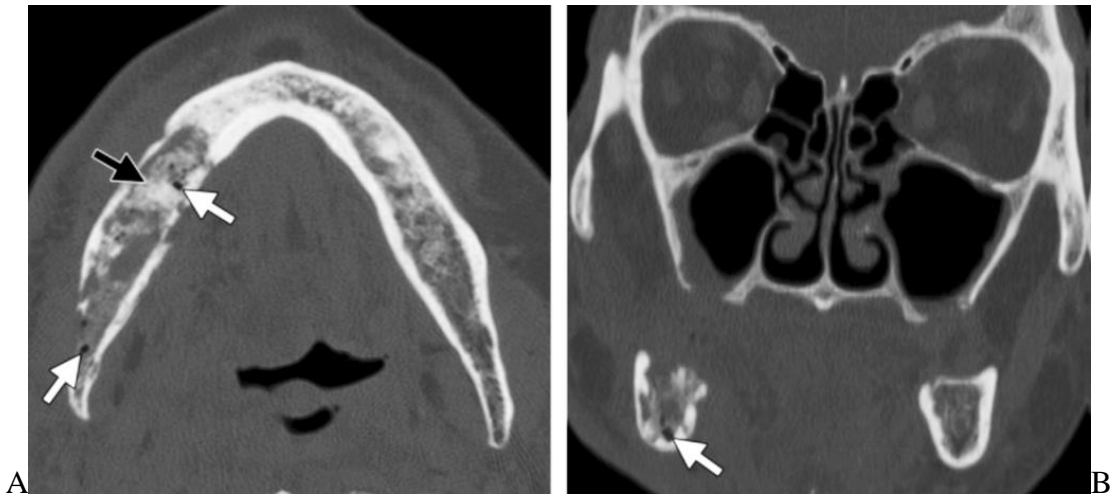


Fig. 5.41. Mandibular osteoradionecrosis in a patient with a history of radiation therapy. Axial (A) and coronal reformatted (B) CT images show sclerosis, loss of trabeculation, cortical interruptions, and areas of gas attenuation (white arrows) in the right mandible, findings consistent with osteoradionecrosis. More sclerotic necrotic bone (black arrow in A) is also seen.

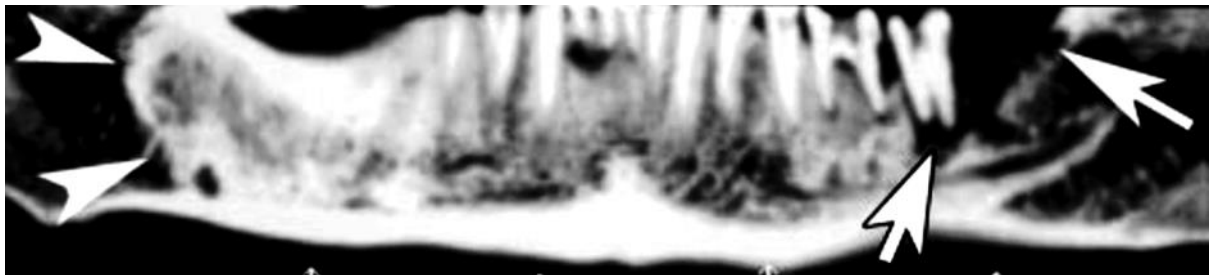


Fig. 5.42. Osteoradionecrosis in a 56-year-old man with a history of radiation therapy for oropharyngeal squamous cell carcinoma. Panoramic reformatted CT image shows ill-defined osteolytic lesions (arrows) within the left mandibular body, findings that represent osteonecrosis. In addition, a diffusely sclerotic region (arrowheads) is identified within the right mandibular body, a finding that represents osteitis.

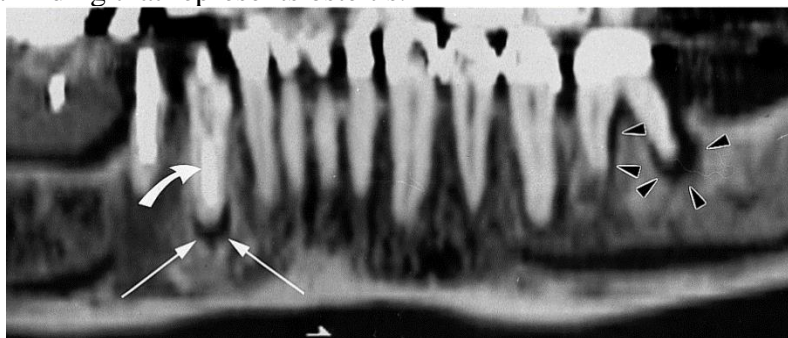


Fig. 5.43. Panoramic dental CT scan in a 60-year-old man with advanced periodontal (arrowheads) and endodontal (straight arrows) lesions. Note how periodontal disease travels down the sides of the root, while endodontal disease affects the root apex. A radiopaque post from a root canal procedure is seen in a tooth with an endodontal lesion (curved arrow).

06 Sinusitis

Dentogenic Sinus Pathology

Ninety percent of all sinus disorders are of rhinogenic origin and are therefore not usually treated by the dentist. The maxillary sinuses, on the other hand, represent an exception because the dentist's area of concern is immediately adjacent. Many normally encountered dental problems such as acute and chronic periapical or periodontal lesions in the maxilla can lead to collateral inflammation of the periosteum or to reactive swelling of the sinus mucosa. Foreign body reactions following endodontic therapy and inflammation of the maxillary sinuses accompanying dentogenic cysts, tumors or fractures of the maxilla are certainly possible. While there can be no doubt that the treatment of diseases of the maxillary sinuses resides in the hands of appropriate specialists, one must concede that the dentist is in an excellent position to observe and diagnose dentogenic disorders of the maxillary sinuses, based upon his specific knowledge. On the other hand, it is well known that patients often seek out the dentist first when they experience acute or chronic inflammation of the maxillary sinus, even when such inflammation is not of dentogenic origin. This is because in such conditions the maxillary premolars and molars are painful during chewing. The elevated percussion sensitivity and the reduced reaction to standard vitality tests can lead the dentist initially into diagnostic difficulties if only one vital and restored tooth is involved. If several vital teeth are involved, and if the roots of these teeth exhibit a close anatomic relationship to the floor of the sinus and if no additional clinical signs are observed, the appropriate clinical diagnosis is simplified but the radiographic picture will exhibit no changes, especially in acute or early cases.

Until a few years ago it was difficult, if not impossible, for the dentist to provide a radiologic diagnosis in this area because the periapical radiograph, as a result of its format and the special projection of the central ray, depicted at best only the floor of the maxillary sinus and only from an oblique angle. The typical periapical radiograph is not indicated for examination of the maxillary sinus because of the danger of incorrect interpretation. Only the panoramic radiograph has given us new possibilities in this realm; it can provide an appropriate view of at least the alveolar portion of the maxillary sinuses, which can enhance our clinical examinations in terms of possible dentogenic participation.

More sophisticated radiographic methods are available to the dentist only in special clinics or in particular cases because the techniques for radiographic examination have changed considerably in the last few years. The standard technique that is still used most commonly today is the Waters' projection. This is

being replaced more and more by computed tomography, which provides perfect observations of on-going pathology through bone and soft tissue windows. Despite these advances in technology, today's dentist should be aware of the possibilities and limitations of conventional examination methods in order to provide appropriate patient treatment and referral.

Panoramic Radiography of Dentogenic Sinus Pathology

Ninety percent of all sinus disorders are of rhinogenic origin and are therefore not usually treated by the dentist. The maxillary sinuses, on the other hand, represent an exception because the dentist's area of concern is immediately adjacent. Many normally encountered dental problems such as acute and chronic periapical or periodontal lesions in the maxilla can lead to collateral inflammation of the periosteum or to reactive swelling of the sinus mucosa. Foreign body reactions following endodontic therapy and inflammation of the maxillary sinuses accompanying dentogenic cysts, tumors or fractures of the maxilla are certainly possible. While there can be no doubt that the treatment of diseases of the maxillary sinuses resides in the hands of appropriate specialists, one must concede that the dentist is in an excellent position to observe and diagnose dentogenic disorders of the maxillary sinuses, based upon his specific knowledge. On the other hand, it is well known that patients often seek out the dentist first when they experience acute or chronic inflammation of the maxillary sinus, even when such inflammation is not of dentogenic origin. This is because in such conditions the maxillary premolars and molars are painful during chewing. The elevated percussion sensitivity and the reduced reaction to standard vitality tests can lead the dentist initially into diagnostic difficulties if only one vital and restored tooth is involved. If several vital teeth are involved, and if the roots of these teeth exhibit a close anatomic relationship to the floor of the sinus and if no additional clinical signs are observed, the appropriate clinical diagnosis is simplified but the radiographic picture will exhibit no changes, especially in acute or early cases.

Until a few years ago it was difficult, if not impossible, for the dentist to provide a radiologic diagnosis in this area because the periapical radiograph, as a result of its format and the special projection of the central ray, depicted at best only the floor of the maxillary sinus and only from an oblique angle. The typical periapical radiograph is not indicated for examination of the maxillary sinus because of the danger of incorrect interpretation. Only the panoramic radiograph has given us new possibilities in this realm; it can provide an appropriate view of at least the alveolar portion of the maxillary sinuses, which can enhance our clinical examinations in terms of possible dentogenic participation.

More sophisticated radiographic methods are available to the dentist only in special clinics or in particular cases because the techniques for radiographic examination have changed considerably in the last few years. The standard

technique that is still used most commonly today is the Waters' projection. This is being replaced more and more by computed tomography, which provides perfect observations of on-going pathology through bone and soft tissue windows. Despite these advances in technology, today's dentist should be aware of the possibilities and limitations of conventional examination methods in order to provide appropriate patient treatment and referral.

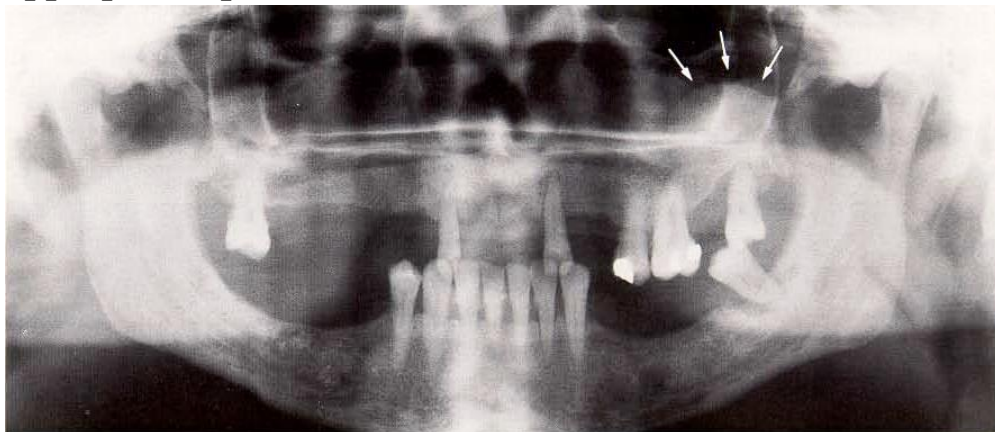
Collateral inflammation radiating from periapical lesions may elicit local osteomyelitis of the maxilla (in addition to periostitis and polyp-like alterations of the sinus mucosa), and can lead to acute and chronic inflammation of the maxillary sinuses. In contrast to inflammation of rhinogenic origin, such dentogenic sinus pathology is usually unilateral, but this rule also has its exceptions.

Inflammation radiating from periodontal lesions may also cause periostitis, polyp-like thickening of the sinus mucosa as well as acute and chronic inflammation of the maxillary sinuses.

In addition to rhinogenic sinus pathology, which will not be discussed here, incorrect positioning of the patient can also lead to masking of the sinus region, and this may lead the inexperienced to a diagnosis of sinusitis. Following thorough dental examination, radiographic evidence of sinus pathology should be referred to the appropriate medical specialist for clarification. The possibility that the teeth may be involved, however, **must not lead the dentist to premature devitalization and endodontic therapy. Careful observation may be more appropriate.**

During radiographic examination, the following must be noted:

- *only* the alveolar recess of the maxillary sinuses can be observed and examined in terms of possible relationship to a dentogenic etiology;
- care must be exercised during interpretation or observation of *all other* sections of the maxillary sinus;
- be certain that the patient is properly positioned and the central ray is properly aimed. If a *nondentogenic* cause is suspected, referral to the appropriate specialist is indicated.



431

Fig. 6.1. **Unilateral polyposis of the sinus mucosa, of dentogenic origin.** This lesion originated from advanced marginal periodontitis on tooth 28 (arrow).

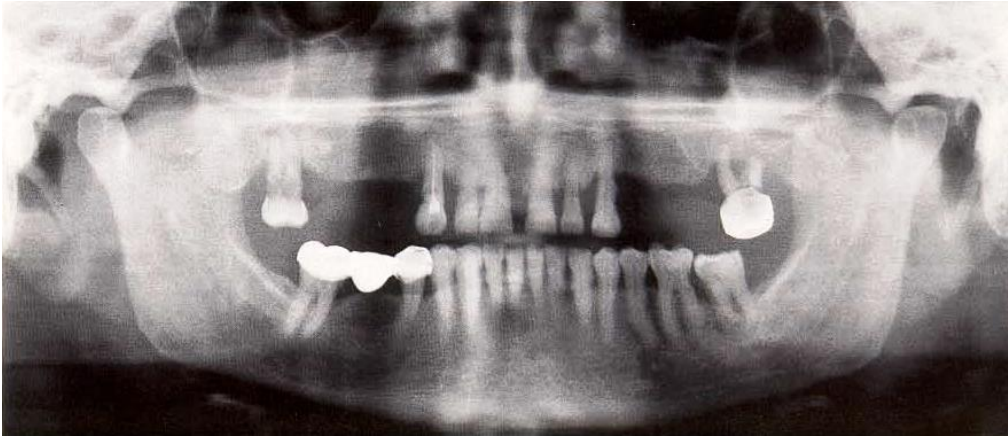


Fig. 6.2. **Bilateral sinus pathology of dentogenic origin.** Tooth 27, with severe periodontal involvement, appears associated with polyp-like thickening of the sinus mucosa, but without sinusitis. The nonvital, periodontally compromised tooth 17 is associated with radiopacity of the entire sinus, presenting as unilateral dentogenic sinusitis.

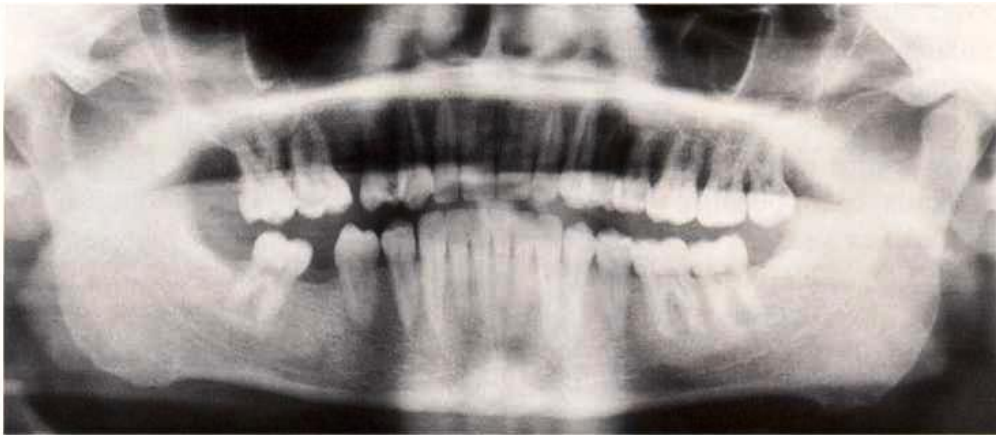


Fig. 6.3. **Incorrect positioning of the patient.** If the patient's chin is elevated, the radiograph will present a picture resembling radiopacity of the maxillary sinus, which could lead to an incorrect diagnosis.

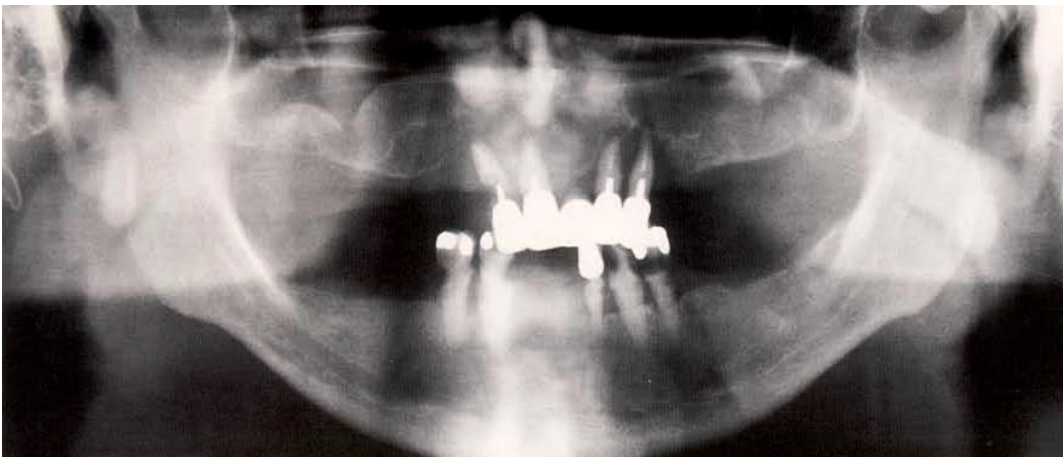


Fig. 6.4. **Polyposis of the maxillary sinus mucosa, of dentogenic origin.** The nonvital teeth 12, 11, 22 and 23 are associated with local periapical osteomyelitis. The result is a bilateral polyp-like thickening of the sinus mucosa. Aside from this, however, both maxillary sinuses contain air and are without symptoms.

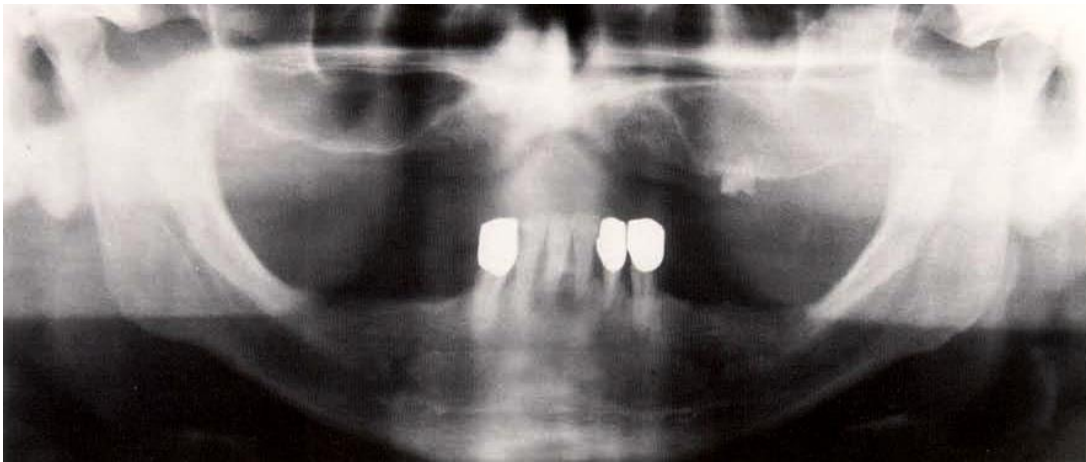


Fig. 6.5. Unilateral acute maxillary sinusitis of dentogenic origin. The retained root tip (tooth 25), displaying an apical radiolucency, has caused a unilateral dentogenic sinusitis. Compare the healthy, air-containing sinus on the right side.

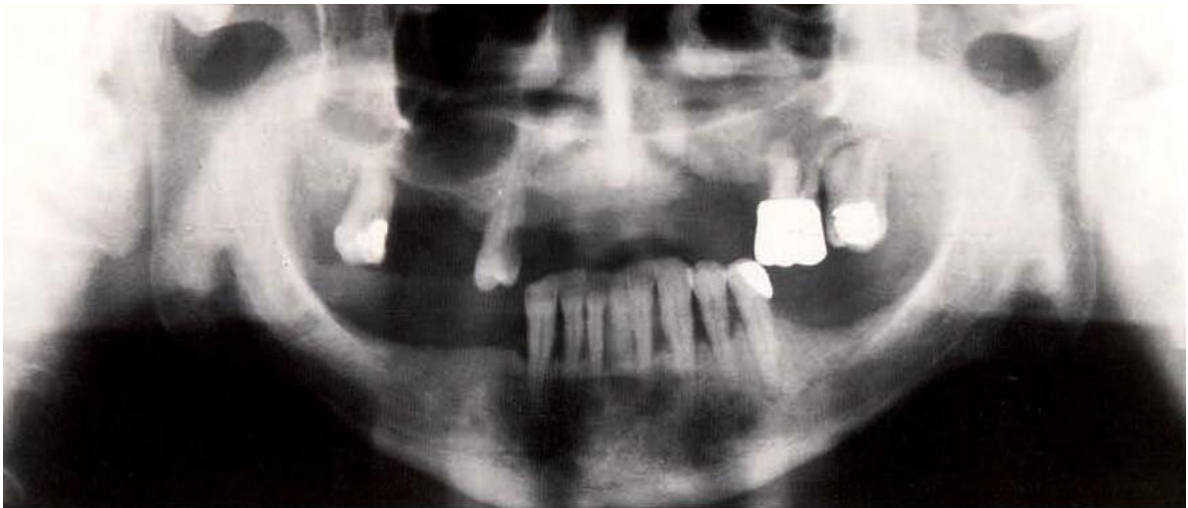


Fig. 6.6. Unilateral chronic maxillary sinusitis of dentogenic origin. The chronic apical periodontitis from tooth 27 has caused local osteomyelitis with loss of normal appearance of the inferior border of the sinus; in addition, the massive radiopacity (shadowing) of the left sinus is obvious.

Acute Unilateral Dentogenic Sinusitis

The comparison of both types of films clearly shows the possibilities and limitations of panoramic radiography, and the supplementary diagnostic possibilities provided by the Waters' projection in cases of acute dentogenic sinusitis. On the one hand, in the panoramic radiograph the opacity of the affected sinus is limited to the posterior segment of the sinus, while the Waters' projection depicts the complete expanse of the acute inflammation as seen in comparison to the healthy and air-containing left side. This is possible because of the posteroanterior central ray projection.

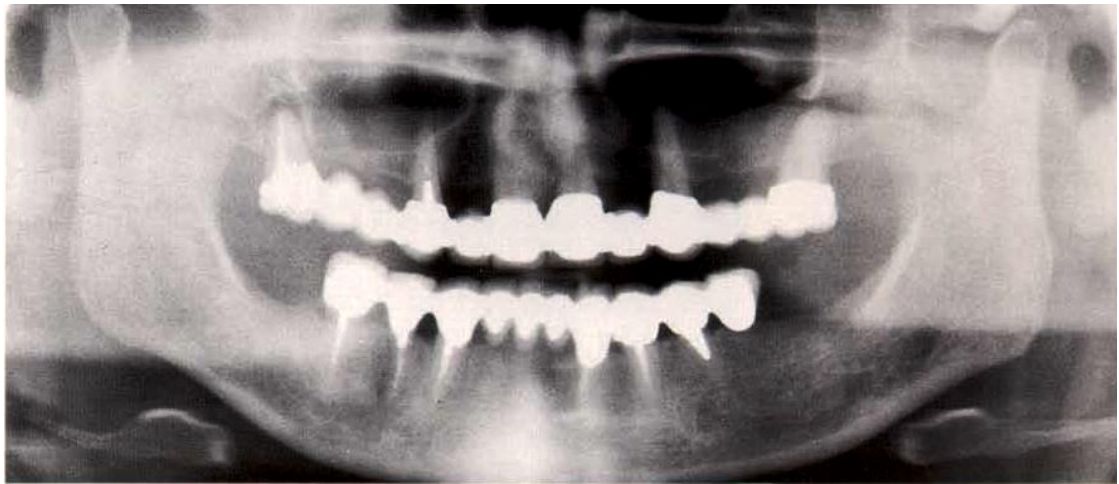


Fig. 6.7. **Acute unilateral dentogenic sinusitis as seen in the panoramic radiograph.** The affected tooth 17 reveals acute apical periodontitis. The anterior segment of the sinus appears free of radiopacity. Clinically, this was ascertained to be acute sinusitis in an early stage.

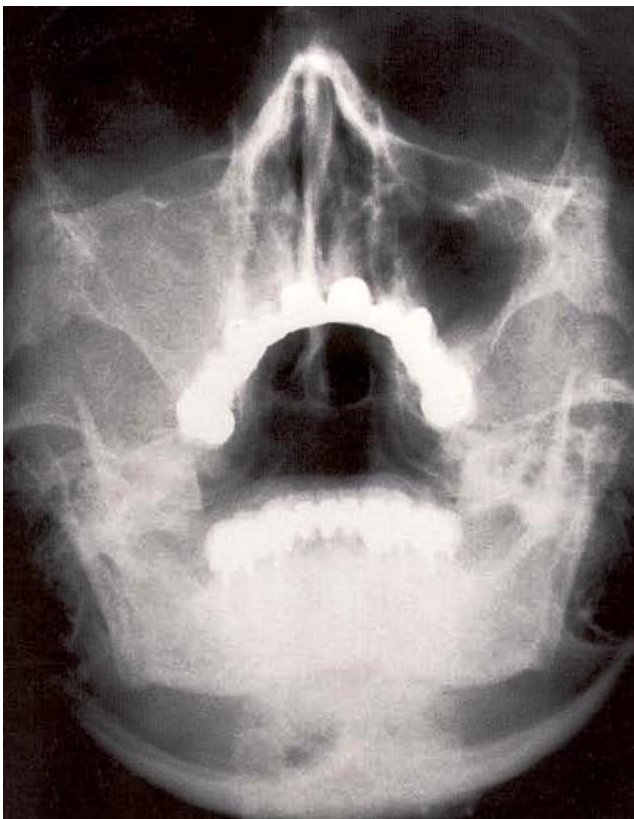


Fig. 6.8. **Acute unilateral dentogenic sinusitis as viewed in the Waters' film.** Same case as in Figure 6.7. The affected sinus is uniformly radiopaque and the borders of the sinus remain visible. In cases of progressive inflammation, the distinct boundaries of the sinus may disappear. Purulent inflammatory processes appear as a horizontal fluid "level." Chronic conditions are seen as a more or less clear thickening of the borders as a result of reactive sclerosis of the surrounding bone; this is especially apparent in the area of the zygomatico-alveolar crest.

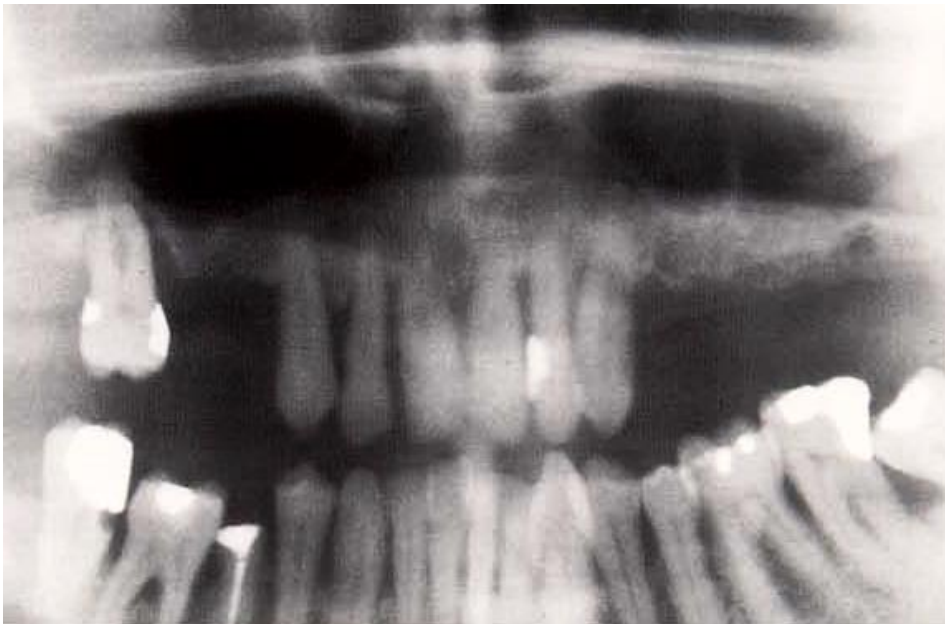


Fig. 6.9. **Chronic dentogenic sinusitis.** The radiograph compares the alveolar segment and the osseous structure. Only a slight radiopacity of the sinus and sclerosis of the alveolar ridge are visible on the left side.



Fig. 6.10. **Chronic dentogenic sinusitis as viewed by CT.** An axial CT with soft tissue window shows almost complete obliteration of the left sinus caused by the thickened mucosa. Clearly visible is the reactive sclerosis of the left sinus wall.

Acute Unilateral Dentogenic Sinusitis

The comparison of both types of films clearly shows the possibilities and limitations of panoramic radiography, and the supplementary diagnostic possibilities provided by the Waters' projection in cases of acute dentogenic sinusitis. On the one hand, in the panoramic radiograph the opacity of the affected sinus is limited to the posterior segment of the sinus, while the Waters' projection depicts the complete expanse of the acute inflammation as seen in comparison to the healthy and air-

containing left side. This is possible because of the posteroanterior central ray projection.

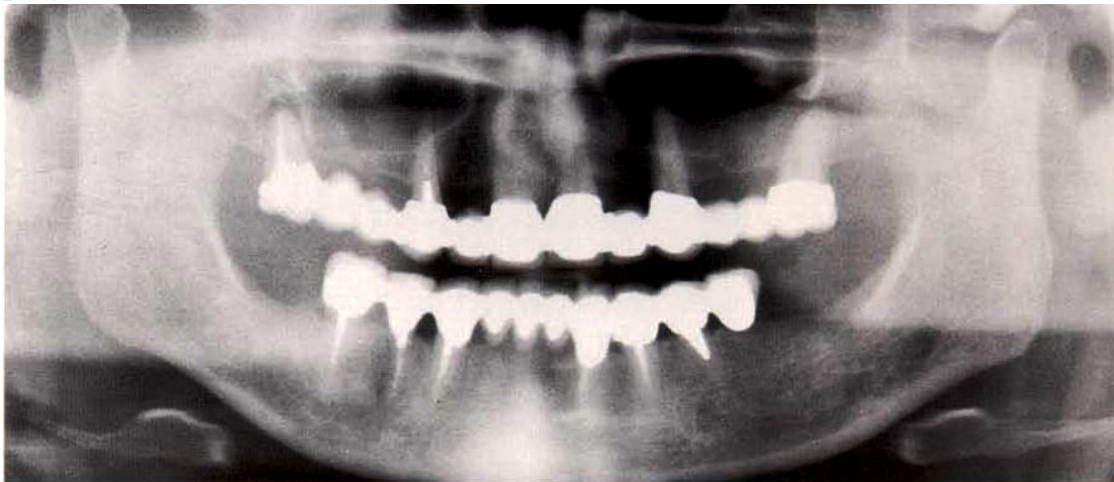


Fig. 6.11. **Acute unilateral dentogenic sinusitis as seen in the panoramic radiograph.** The affected tooth 17 reveals acute apical periodontitis. The anterior segment of the sinus appears free of radiopacity. Clinically, this was ascertained to be acute sinusitis in an early stage.

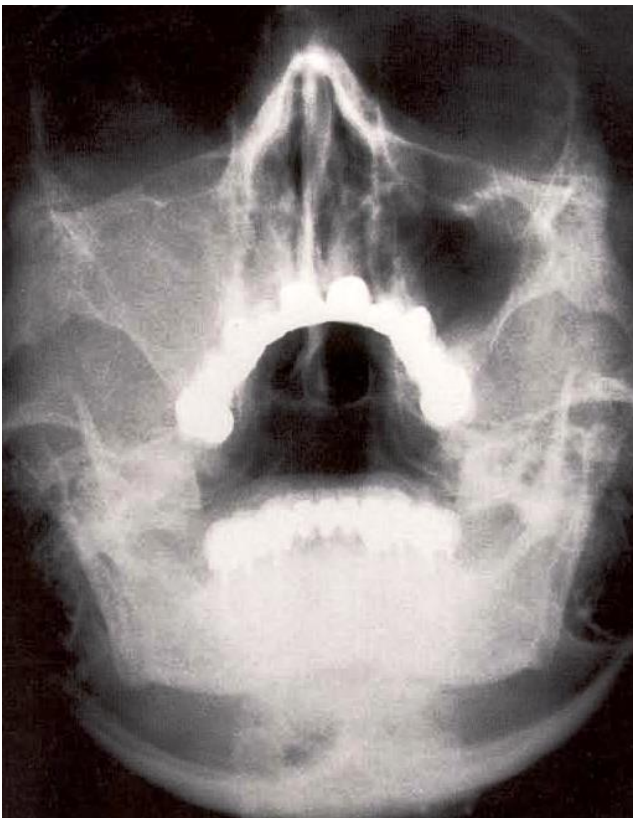


Fig. 6.12. **Acute unilateral dentogenic sinusitis as viewed in the Waters' film.** Same case as in Figure 6.7. The affected sinus is uniformly radiopaque and the borders of the sinus remain visible. In cases of progressive inflammation, the distinct boundaries of the sinus may disappear. Purulent inflammatory processes appear as a horizontal fluid "level." Chronic conditions are seen as a more or less clear thickening of the borders as a result of reactive sclerosis of the surrounding bone; this is especially apparent in the area of the zygomatico-alveolar crest.

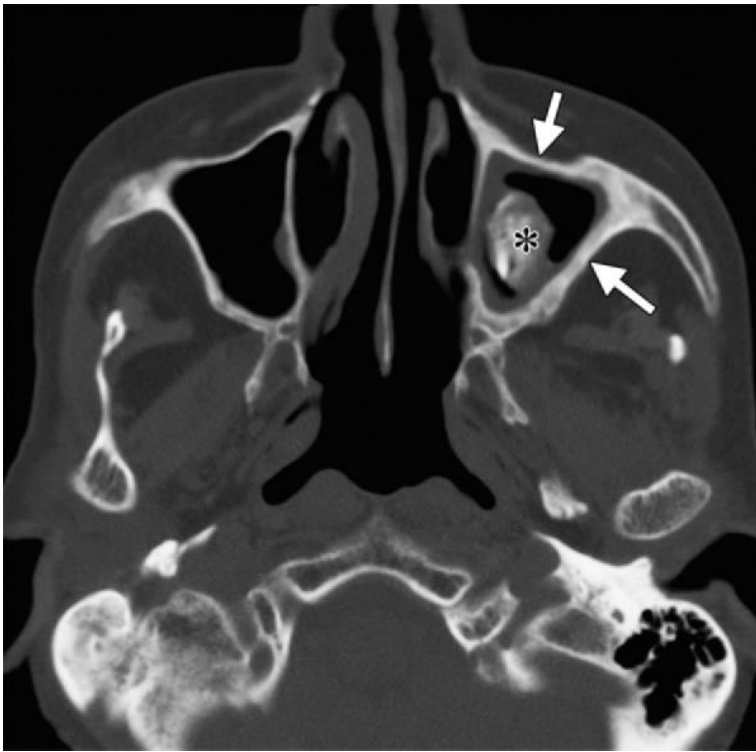


Fig. 6.12. Sinusitis from an ectopic tooth in an 81-year-old woman. Axial CT image shows an ectopic tooth in the maxillary sinus (*), with associated mucosal thickening and asymmetric cortical thickening (arrows), findings consistent with chronic sinusitis.

Studies have reported that 5% – 38% of cases of maxillary sinus mucosal disease are caused by apical periodontitis and periodontal disease. Differentiating between sinusitis caused by obstructed drainage pathways and odontogenic disease is important to direct patients to the most appropriate treatment.

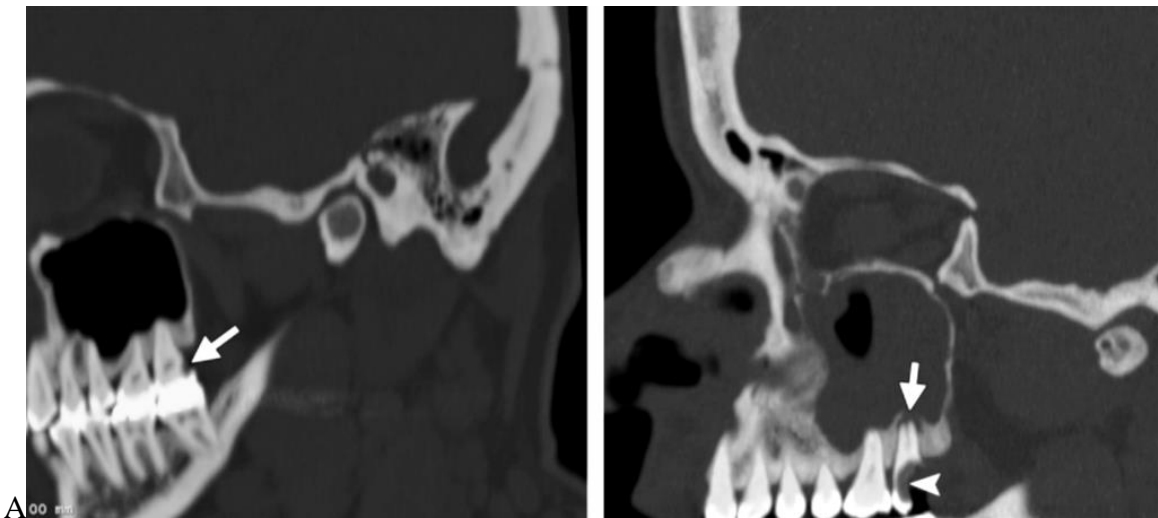


Fig. 6.13. Progression of a carious tooth to odontogenic sinusitis over a period of 3 years and 2 months. (A) CT image shows a carious lesion (arrow) in the second maxillary molar. (B) CT image obtained 3 years and 2 months later shows marked progression of the carious lesion (arrowhead) and a new periapical lucency (arrow), a finding consistent with apical periodontitis. Gross dehiscence of the periapical bone (arrow) is also seen, with near total opacification of the maxillary sinus, a finding indicative of odontogenic sinusitis.

07 Regress and Carious Lesions

Foreign Bodies, Root Fragments and Surgical Defects

Foreign bodies such as excess root canal filling materials often remain harmlessly in the sinus. Sometimes an aspergillosis ensues, however, which leads to the development of chronic sinusitis.

In general, root fragments are considerably easier to detect on a panoramic radiograph than in a periapical film, and this can obviate the necessity for additional films to localize the fragment. The oroantral fistula, which can be clinically diagnosed, can also be clearly documented in a panoramic radiograph due to the shadowing in the alveolar segment of the sinus and the frequent loss of clear sinus demarcation.

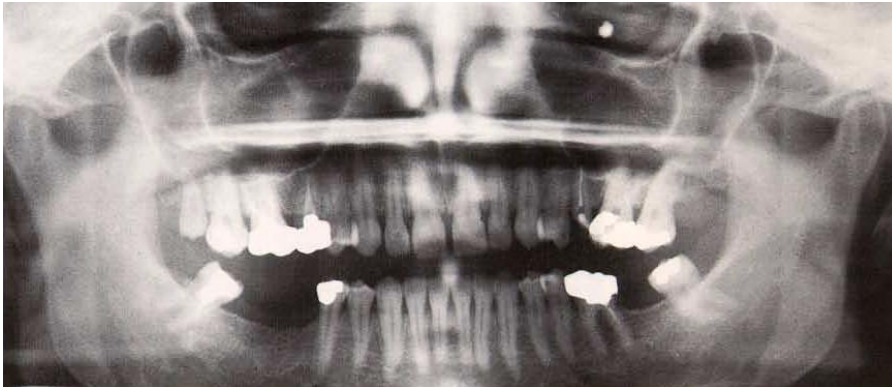


Fig. 7.1. Remnants of root canal filling from tooth 25 located dorsally and superiorly in the left maxillary sinus. Note that portions of the maxillary sinus and the orbit overlap in the panoramic radiograph.



Fig. 7.2. Renal osteodystrophy in a 75-year-old man. CT scan reveals diffuse sclerotic changes (arrows) throughout the entire mandible.

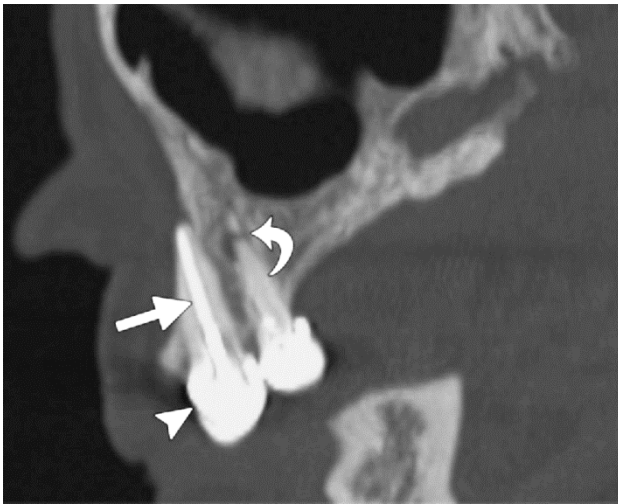


Fig. 7.3. Root canal therapy in a 58-year-old woman. Sagittal CT image shows the appearance of root canal therapy, in which the pulp canal is filled with radiocontrasting material (straight arrow), and the tooth is restored with a metallic crown (arrowhead). An area of radiolucency (curved arrow) indicative of apical periodontitis is also seen at the root apex of the adjacent first premolar.



Fig. 7.4. **Root fragment of tooth 26 in the maxillary sinus.** The fragment lies superior to the level of the root tips of other teeth and does not exhibit a periodontal ligament space. The surrounding sinus appears shadowed.

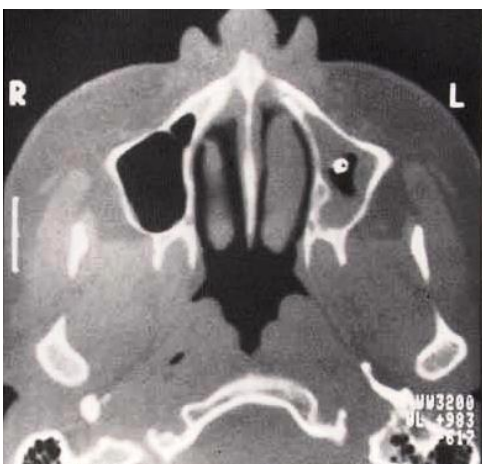


Fig. 7.5. **Axial CT with soft tissue window.** The computed tomogram of the same case reveals that the left maxillary sinus is almost completely filled with soft tissue structures. In the center of the sinus the opaque remains of the root canal filling can be seen. Reactive sclerosis is obvious in the medial sinus wall.

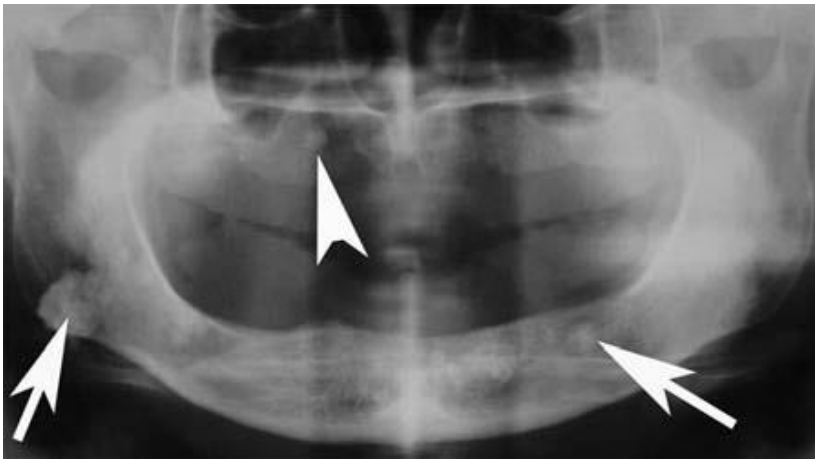


Fig. 7.6. Gardner syndrome in an 80-year old man. Panorex radiograph demonstrates multiple osteomas (arrows) throughout the mandible. Note the osteoma within the right maxilla (arrowhead).

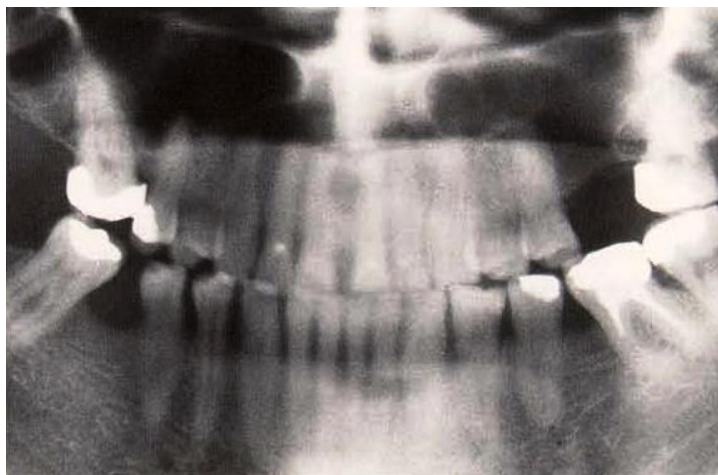


Fig. 7.7. **Oroantral fistula, left.** The slightly opaque left maxillary sinus does not exhibit the demarcation line of the alveolar sinus segment around tooth 26.

Carious Lesions

Carious lesions are foci of enamel and dentin demineralization caused by acid produced by bacterial fermentation of carbohydrates. Carious lesions may take years to penetrate through the enamel. Remineralization may cause them to regress, especially in the presence of fluoride. Once decay reaches the dentinoenamel junction, it spreads more easily and rapidly through the dentin, and the infection undermines the overlying enamel. Occlusal caries are on the chewing surface of the tooth, whereas approximal caries are between teeth. Saliva reduces the incidence of carious lesions, likely by neutralizing acid produced by cariogenic *Streptococcus mutans* and assisting in remineralization.

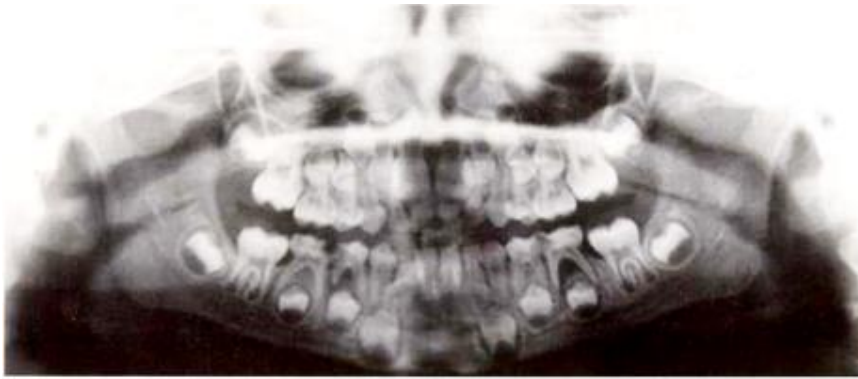


Fig. 7.8. Advanced caries on deciduous tooth 85. Pulpal necrosis was clinically evident on teeth 75 and 84, with interradicular osteolysis and a periapical abscess (84). Note the radiographic signs of local osteomyelitis in the region of teeth 85 – 83.

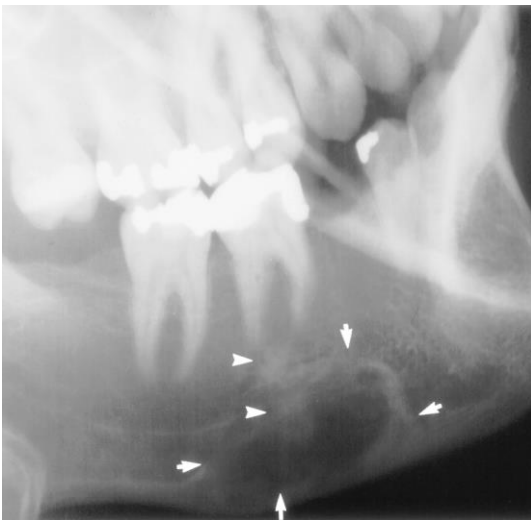


Fig. 7.9. Focal cemento-osseous dysplasia in an asymptomatic 25-year-old man. An abnormality was seen incidentally on a full-mouth radiographic series obtained for routine dental care; additional radiographic views were then obtained. There were no associated clinical abnormalities. Lateral oblique radiograph shows an ellipsoid, lucent lesion with hyperostotic borders (arrows). Amorphous mineralization is seen above and below the superior border of the lesion (arrowheads). There is depression of the inferior border of the mandible with erosion of the cortex. No tooth displacement is present. The patient underwent curettage of the lesion. The differential diagnosis includes focal cemento-osseous dysplasia, periapical cemento-osseous dysplasia, and ossifying fibroma.

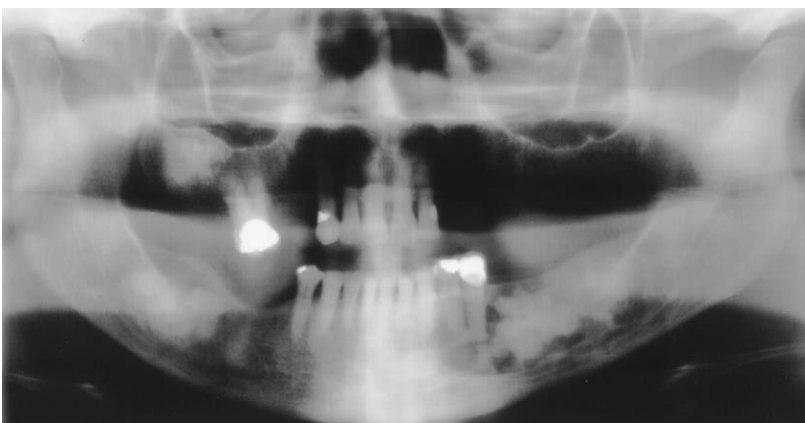


Fig. 7.10. Florid osseous dysplasia in a 65-year-old man. Panoramic radiograph shows primarily opaque masses in the right posterior aspects of the maxilla and mandible and a lesion of mixed opacity in the left aspect of the mandibular body.



Fig. 7.11. Fibrous dysplasia in a 28-year-old man. Contrast-enhanced CT scan demonstrates an expansile lesion containing numerous unorganized bone trabeculae (arrow) within the left mandibular body.

Exostoses and tori

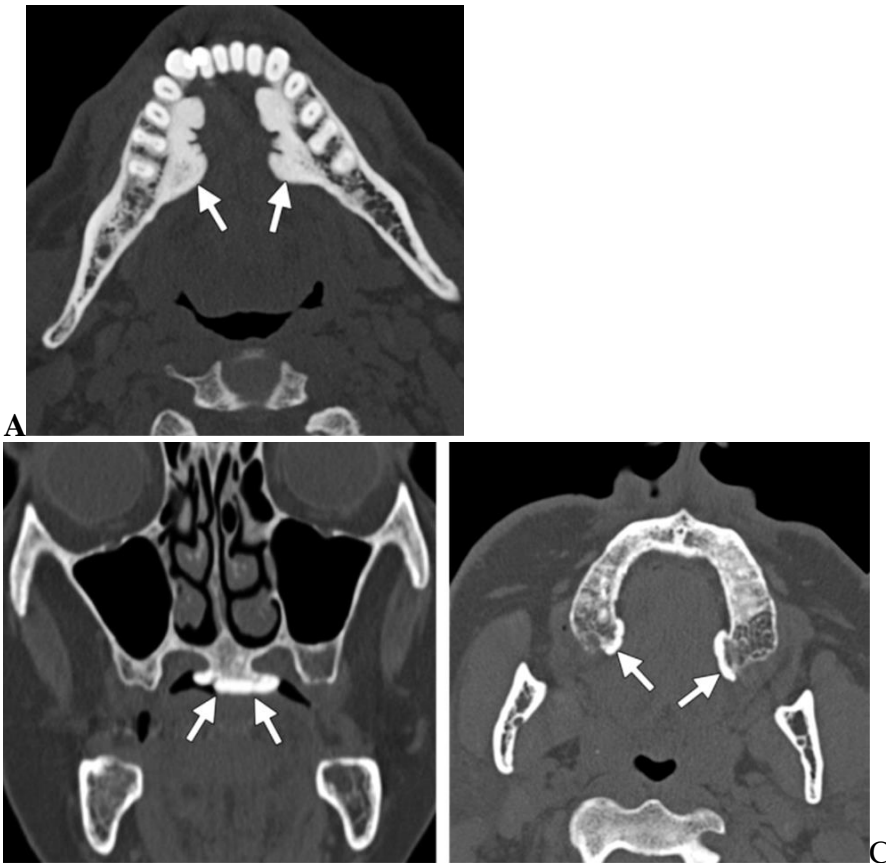


Fig. 7.12. Exostoses and tori. CT images obtained in three different patients show torus mandibularis (arrows in **A**), torus palatinus (arrows in **B**), and torus maxillaris (arrows in **C**).

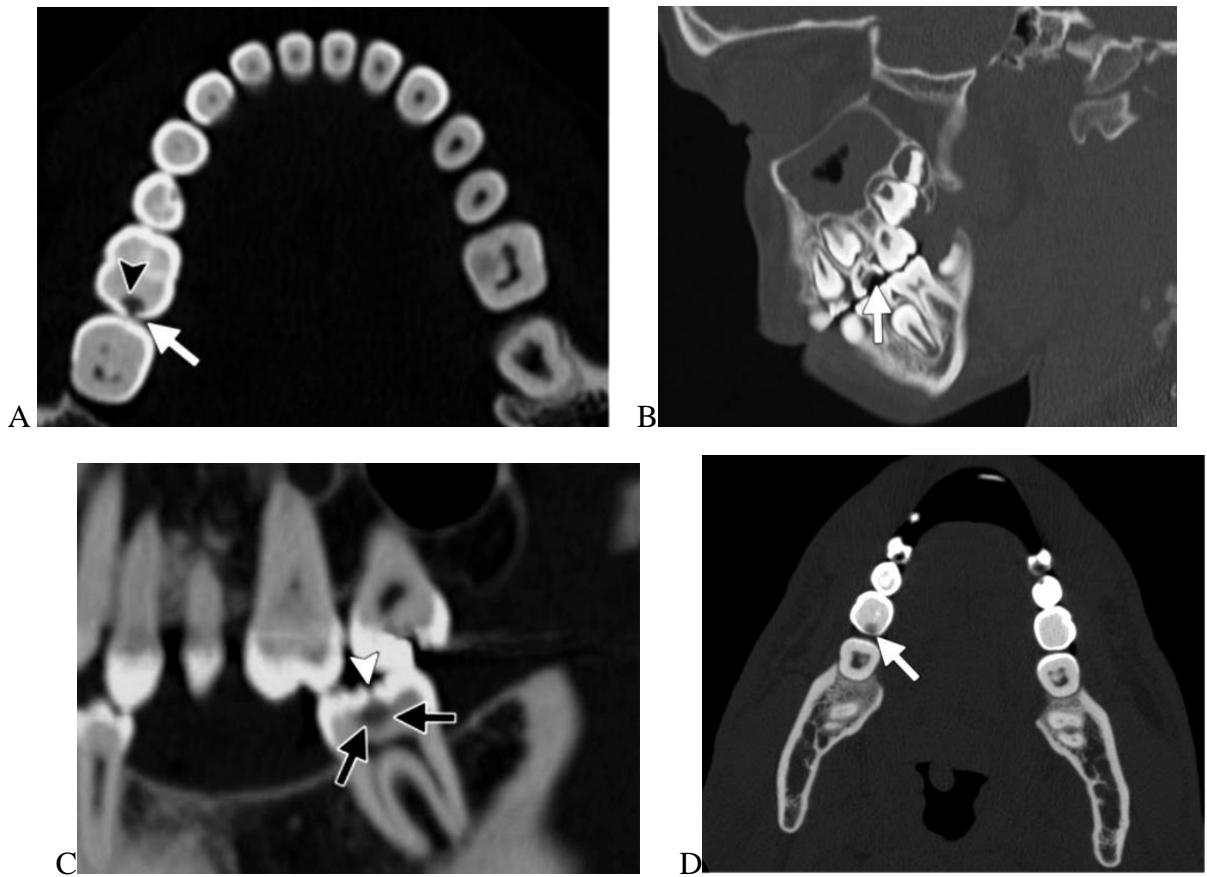


Fig. 7.13. Carious lesions in four patients. **(A)** Axial CT image obtained in a 27-year-old woman shows a carious lesion in the right first mandibular molar, with a typical narrow channel of demineralization through the enamel (arrow) and a broad area of demineralization in the underlying dentin (arrowhead). **(B)** Sagittal CT image obtained in an 11-year-old boy shows a markedly carious primary second molar (arrow). **(C)** Sagittal CT image obtained in a 30-year-old man shows a carious lesion on the occlusal surface of a tooth, with a typical small area of demineralization in the enamel of the crown (arrowhead) and a larger area of demineralization in the underlying dentin (arrows). **(D)** Axial CT images, obtained 1 year apart in a 33-year-old man at the level of the mandible, show progression of a carious lesion (white arrow) in the right mandibular first molar.

08 Temporomandibular Joint Disturbances

This broad term encompasses a wide range of radiologic findings in the temporomandibular joint that represent deviations from the normal. The possibilities for compromised function of the temporomandibular joints and for pathologic alterations are numerous, and may include:

Developmental disturbances	- Neoplasia
Early childhood trauma	- Accidents
Spreading inflammation	- Occlusal dysharmony
Systemic disorders	

Each of the etiologies listed above may lead to functional disturbance of the affected joint, which may in turn cause the development of degenerative changes in the temporomandibular complex.

In earlier times, the dentist seldom had the opportunity to examine radiographically both the jaws and the teeth at the same time. Today, however, the routine panoramic radiograph provides the opportunity to depict the masticatory organ as a functional entity, and to include all of its components in a comprehensive radiographic interpretation, accepting that the film is not a *precise* representation. The dentist should always examine and treat the masticatory organ as a complete yet complex functionally integrated entity consisting of the jaws, the temporomandibular joints, the occlusal system, and the masticatory muscles. For example, even minor occlusal dysharmony can adversely affect muscle tone and condylar position. Today, such facts may be taken for granted during clinical examinations, but even modern radiographic methods do not offer the opportunity to depict the masticatory system as a functional entity. Only the panoramic radiograph allows appropriate observation and inspection of the masticatory structures and the position of the condyles with sufficient quality, depending upon indication and proper selection of projection technique. It is important to point out, however, that in many cases it will be necessary to employ other radiographic methods of examination in order to accrue all the necessary diagnostic information.

The interpretation of any type of temporomandibular joint radiograph is not an easy matter, especially because clinical findings and the radiographic picture are seldom easy to bring into perfect correlation. Existing clinical symptoms become apparent radiographically only some time after the occurrence of destruction or neoplastic osseous changes; in addition, they are often incorrectly depicted because of the addition effect. It is therefore necessary to recommend that carefully executed tomography, arthrotomography or CT techniques with special positioning be employed to enhance the routine panoramic radiography if uncertainties persist.

Examination of the Masticatory Organ

To depict *occlusal relationships* simultaneously with the *position of the condyles*, it is necessary to take the radiograph with the patient in normal occlusion. The positioning of the patient demands particular attention: The position of the median sagittal plane at the back of the head must be checked precisely to avoid asymmetries of projection and resultant incorrect diagnosis.

For examination of *shape and structure of the condyles*, the patient is placed in the usual standard position and a bite plane is employed. A radiograph taken in this way generally depicts the condyles quite well in a zonographic layer of about 20 mm thickness. Perfect diagnosis of the condyles is only possible if the mandible is symmetrically positioned in a protruded position. It is well to remember that before proceeding to relatively more complicated radiographic examination, the possibilities provided by clinical examination, analysis of mounted study models, and panoramic radiographic analysis should be exhausted first. In many cases these will provide sufficient information to address any malocclusion.

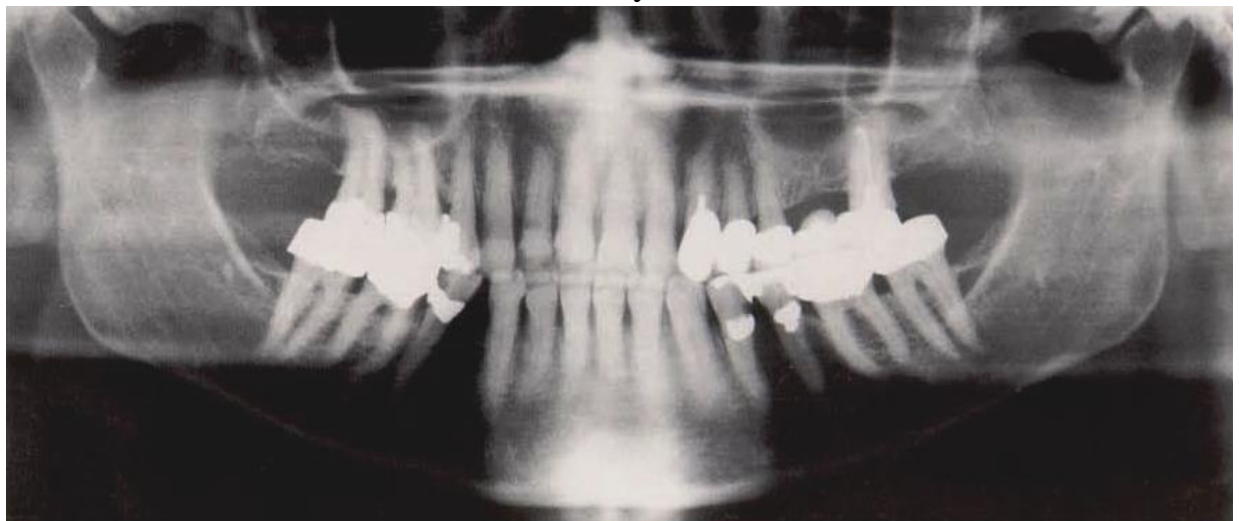


Fig. 8.1. Examination of occlusion with regard to condylar position in a fully dentulous patient. It is recommended to take the radiograph at high energy. This figure depicts a case of temporomandibular joint pathology on the right side accompanied by malocclusion. Note the differing positions of the condyles at the articular eminences.

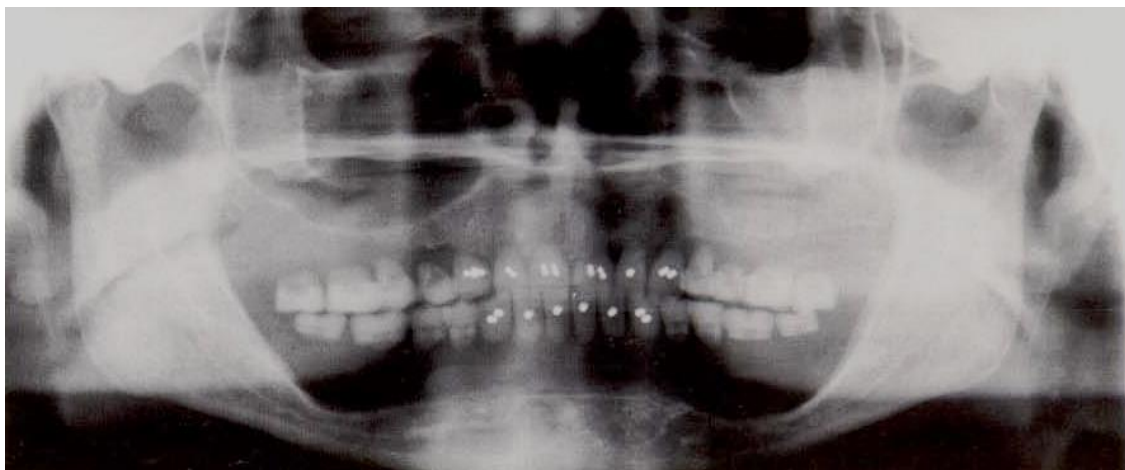


Fig. 8.2. Examination of occlusal relationships with regard to condyle position in an edentulous denture wearer. In this case it was necessary to leave the denture in place during exposure of the film. This panoramic film depicts a case with temporomandibular joint problems

on the right side, and with poor occlusal support on the left side. Note the differing positions of the condyles at the articular eminences.

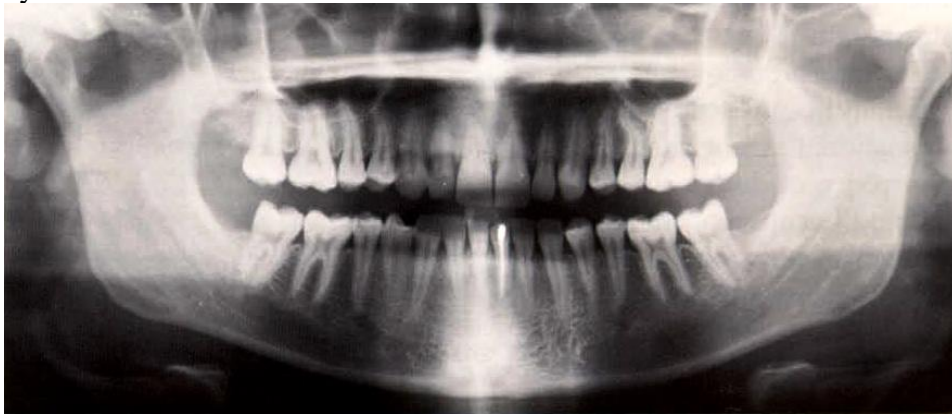


Fig. 8.3. Examination of the condyles in normal position with a bite plane in place. The slightly open mandible usually positions the condyles so that they can be observed without overlapping structures. In this 18-year-old female, the right condyle exhibits an osteochondral exostosis with a large cartilage component. Care must be taken to avoid asymmetric protrusive positioning of the mandible before taking the film.

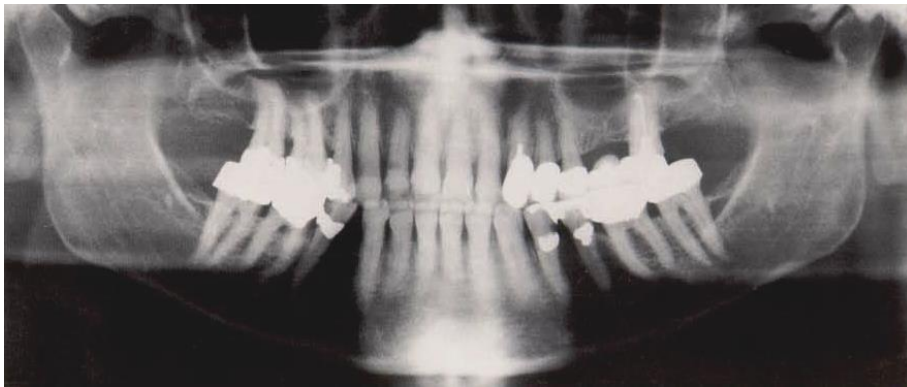


Fig. 8.4. Examination of occlusion with regard to condylar position in a fully dentulous patient. It is recommended to take the radiograph at high energy. This figure depicts a case of temporomandibular joint pathology on the right side accompanied by malocclusion. Note the differing positions of the condyles at the articular eminences.

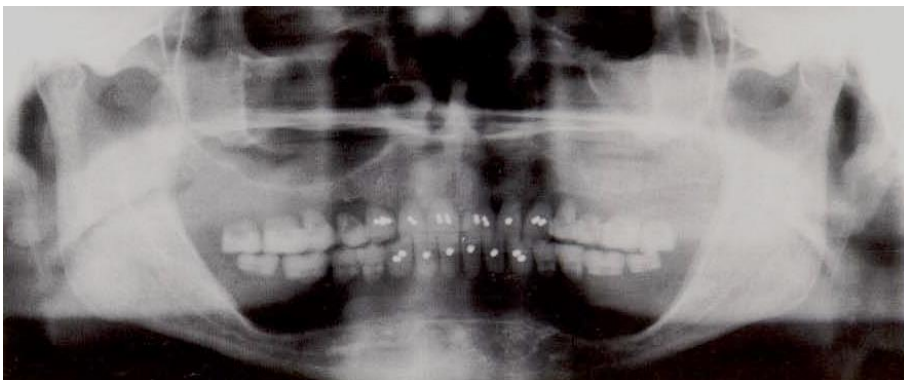


Fig. 8.5. Examination of occlusal relationships with regard to condyle position in an edentulous denture wearer. In this case it was necessary to leave the denture in place during exposure of the film. This panoramic film depicts a case with temporomandibular joint problems on the right side, and with poor occlusal support on the left side. Note the differing positions of the condyles at the articular eminences.

Tomography of the TMJ

Destructive parafunctions and unorthodox chewing habits as well as improperly contoured restorative work and occlusal wear can result in malocclusion. This can lead to functional disturbances, with ultimate trauma induced degenerative changes within the TMJ. In this condition, during closure the mandible usually rotates around one of the joints, resulting in anterior, posterior, lateral or medial malpositioning of the condyles; the result is often lesions in the articular disc, with subsequent joint pathology.

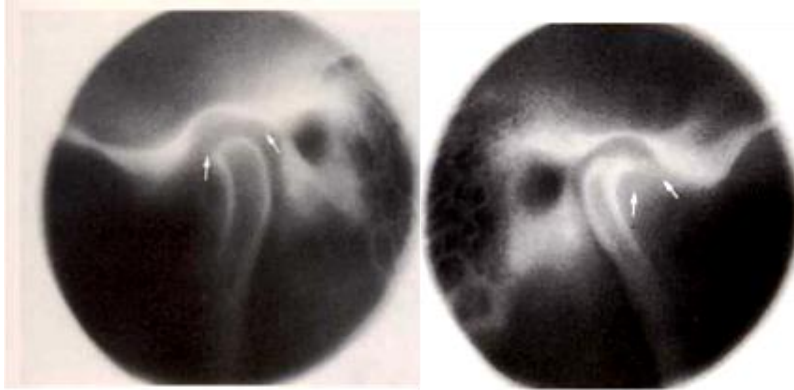


Fig. 8.6. **Spiral CT of left and right joints in normal occlusion.** The left disc resides anteriorly (arrows), and the condyle resides in a “compressed” position deep in the fossa; arthropathy is obvious. The right condyle is normally configured but displaced medially. The disc (arrow) is in its normal position.

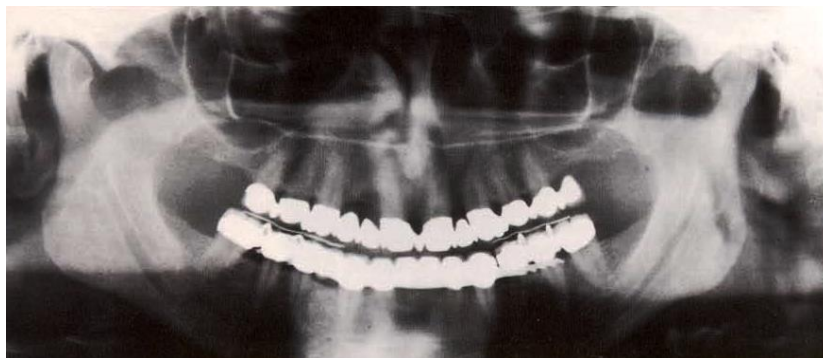


Fig. 8.7. **Confirming radiograph of the same case, taken with a bite plane in situ.** Note the positions of the condyles. After wearing the bite plane for 9 months, and after stabilization of the new occlusal position with temporary acrylic bridges, the patient could be dismissed without TMJ symptoms, despite irreversible joint pathology.

Hypoplasia and Exostosis of the Condyles

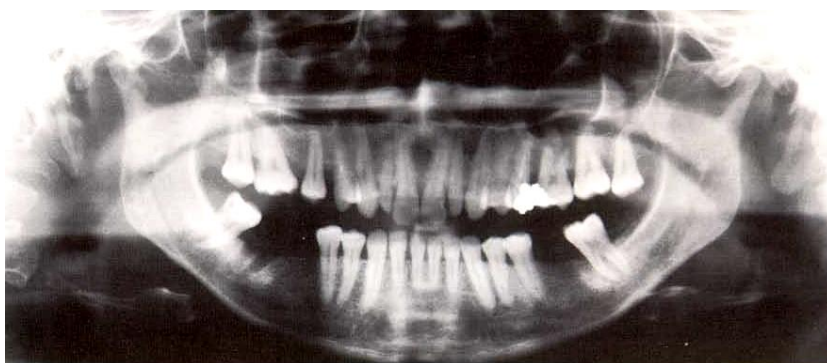


Fig. 8.8. **Bilateral hypoplasia of the condyles in a 34-year-old female with temporomandibular joint symptoms.** Note the effect of tooth loss on the occlusal plane.

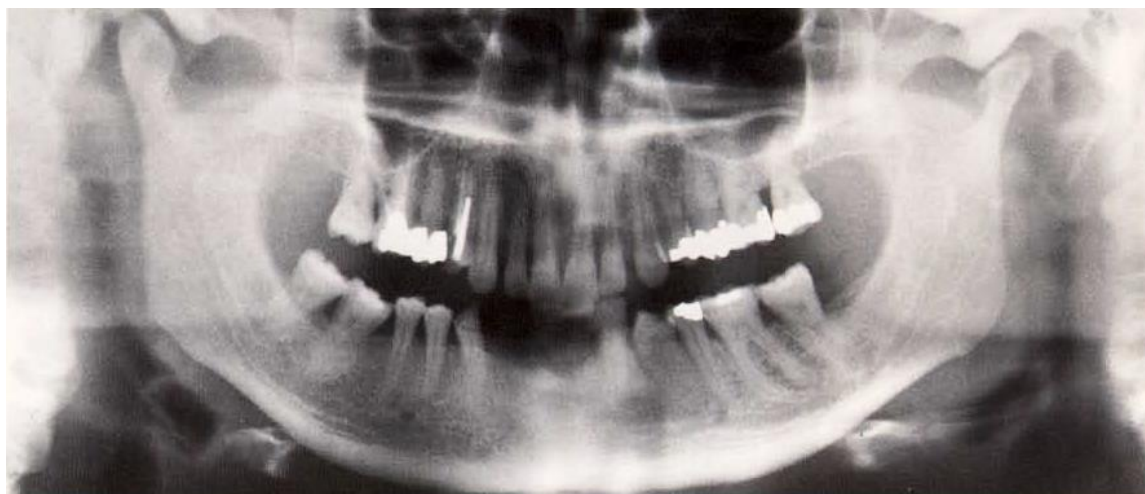


Fig. 8.9. Left-sided hypoplasia of the condyle in a 57-year-old female with temporomandibular joint symptoms. Hypoplasia of a condyle is often detected serendipitously; it does not always lead to temporomandibular joint pain. Sometimes, however, in cases offered orthodontic treatment, following tooth loss or during dental reconstruction, it may lead to clinically significant reactions in the temporomandibular joint area.

Hyperplasia and Osteochondral Exostoses

One of the causes of abnormal muscular hyperactivity and the often associated asymmetric jaw growth can be the early and unilateral closure of the cranial sutures. Other possible causes include osteochondral exostoses or osteochondromas that form not infrequently on the articular surfaces of the condyle in adolescents. These lesions can exert irritating and traumatizing effects on the joint and the masticatory musculature. Temporomandibular joint function is often seriously compromised after the initiation of degenerative changes.

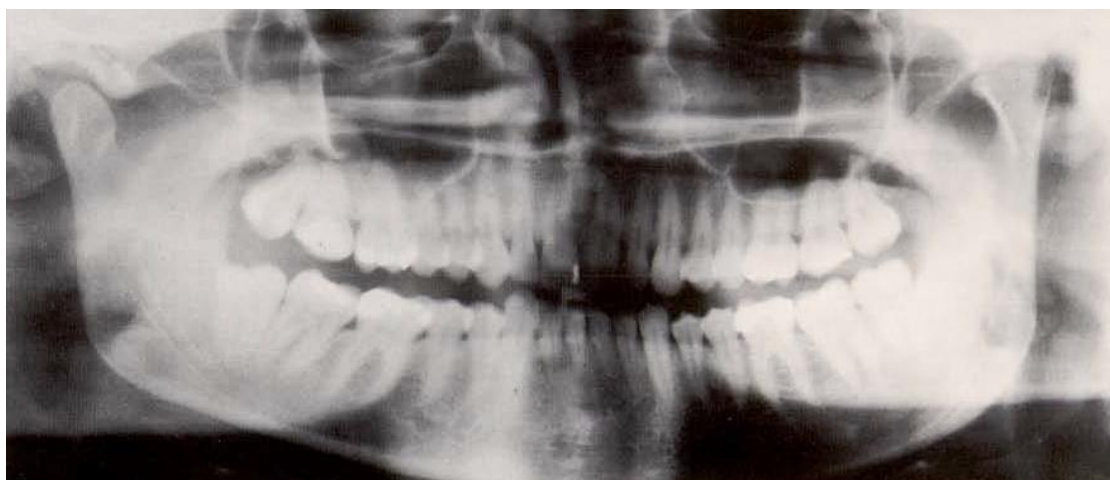


Fig. 8. 10. Unilateral condylar hypertrophy in a case of left-sided hemihypertrophy of the mandible. Observe on the left condyle in the anterior area of the joint surface a bone-like thickening, which appears not as arthrosis but rather as osteochondral exostosis.

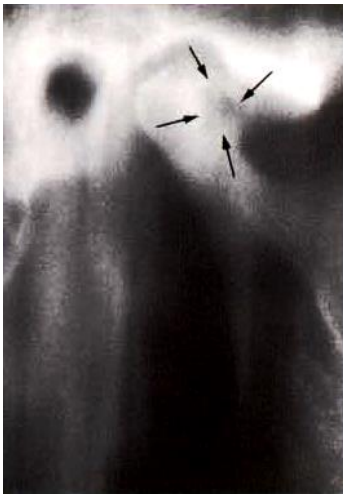
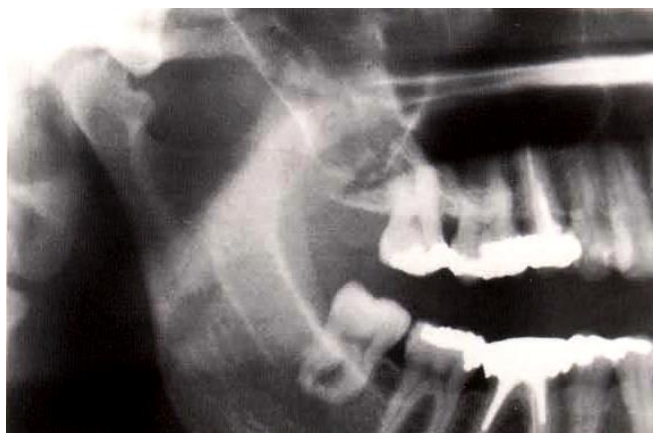


Fig. 8.11. **Osteochondroma of the left condyle in a 31-year-old female as seen in a reverse Towne projection.** The asymmetric opening movement of the mandible is clearly evident. Note that the left temporomandibular joint has remained in a protected position.



Fig. 8.12. **Identical case as seen in a linear tomograph of the left temporomandibular joint in centric occlusion.** The osteochondroma is surrounded by reactive sclerosis, which is a sign of existing arthritis (arrows). Particularly well depicted in this view are the arthritic changes in osseous structure that extend over the condylar fossa.



483

Fig. 8.13. **Osteochondroma on the right condyle of a 30-year-old female with temporomandibular joint disturbance.** Clearly visible are the "exostoses¹" on the anterior border of the joint surface. The obvious radiolucencies correspond to elements with a high percentage of chondral tissue, which tend to develop into bone debris. This may appear

radiographically as a cyst.

Inflammatory and Degenerative Changes

Arthritis, the inflammatory alteration of the temporomandibular joint, frequently occurs subsequent to inflammation of adjacent structures via hematogenic and traumatic pathways. The condyle is usually primarily affected, and exhibits structural degeneration and reactive sclerosis that resembles changes seen in osteomyelitis. These occur before actual osseous degeneration and replacement by bone of lesser quality and ultimately arthropathy. Under constant influence of functional loading, the radiographic demarcations of the joint become less distinct, and compensatory enlargements of the joint surfaces occur including formation of marginal bulges and spikes.

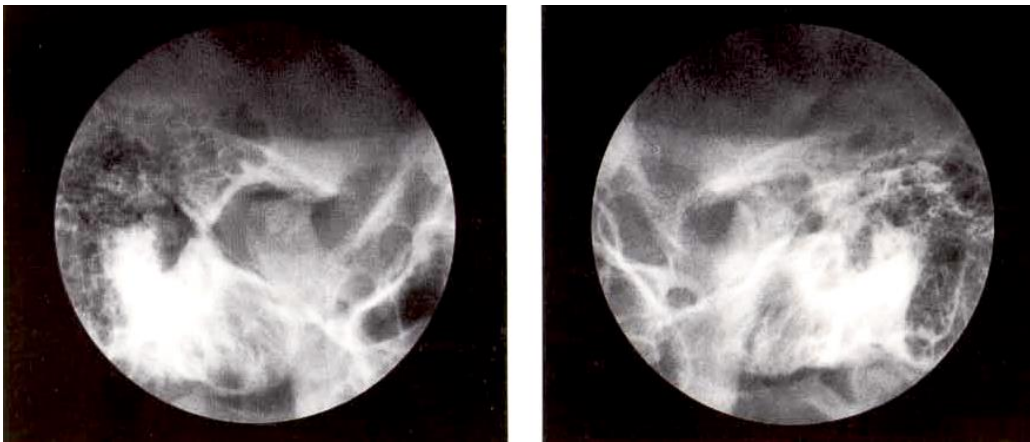


Fig. 8.14. Bilateral rheumatic polyarthritis. Both condyles exhibit an acute inflammatory exacerbation and a typical protected position. The condyles exhibit osteomyelitic changes including bone resorption, reactive sclerosis and loss of normal configuration.

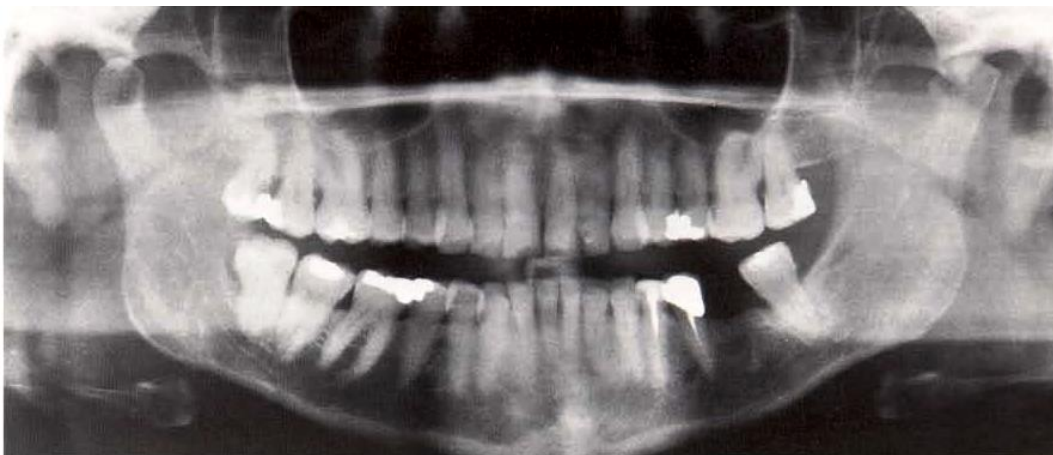


Fig. 8.15. Bilateral rheumatic polyarthritis. Both condyles exhibit an acute inflammatory exacerbation and Arthropathy (remodelling processes). The left condyle depicts pathologic alterations following intracapsular fracture of the condyle. The subsequent loss of vertical dimension and the widening of the articular surface can be seen.

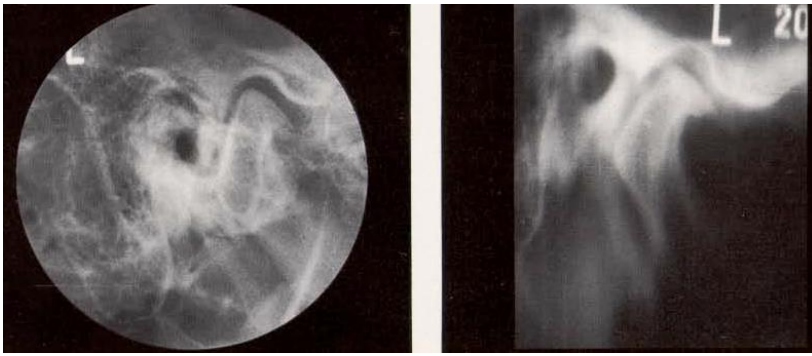


Fig. 8.16. Formation of marginal spikes due to arthroposis. The Schuller projection and the linear tomograph of the same patient reveal typical marginal spike formation and less clearly demarcated borders between the head of the condyle and the fossa: Typical signs of arthropathy.

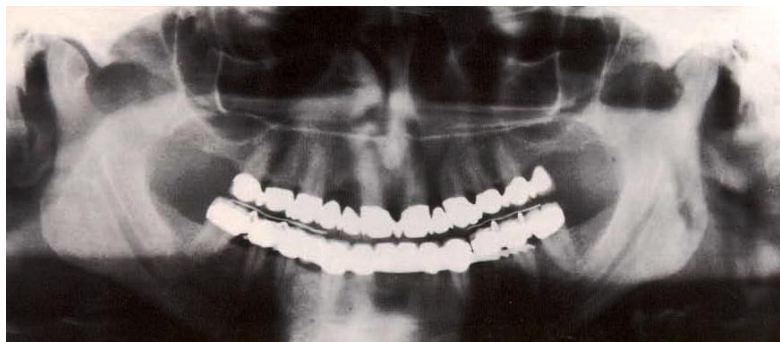


Fig. 8.17. Confirming radiograph of the same case, taken with a bite plane in situ. Note the positions of the condyles. After wearing the bite plane for 9 months, and after stabilization of the new occlusal position with temporary acrylic bridges, the patient could be dismissed without TMJ symptoms, despite irreversible joint pathology.

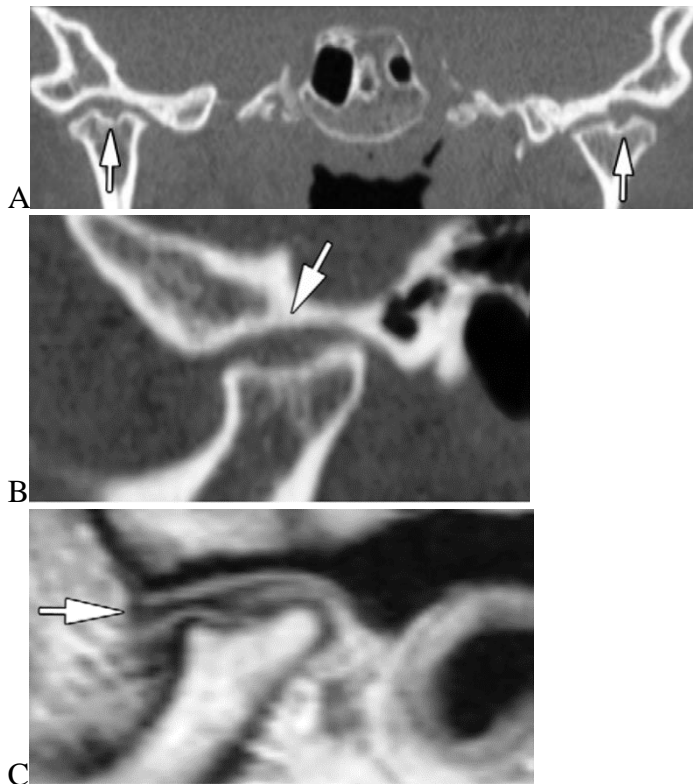
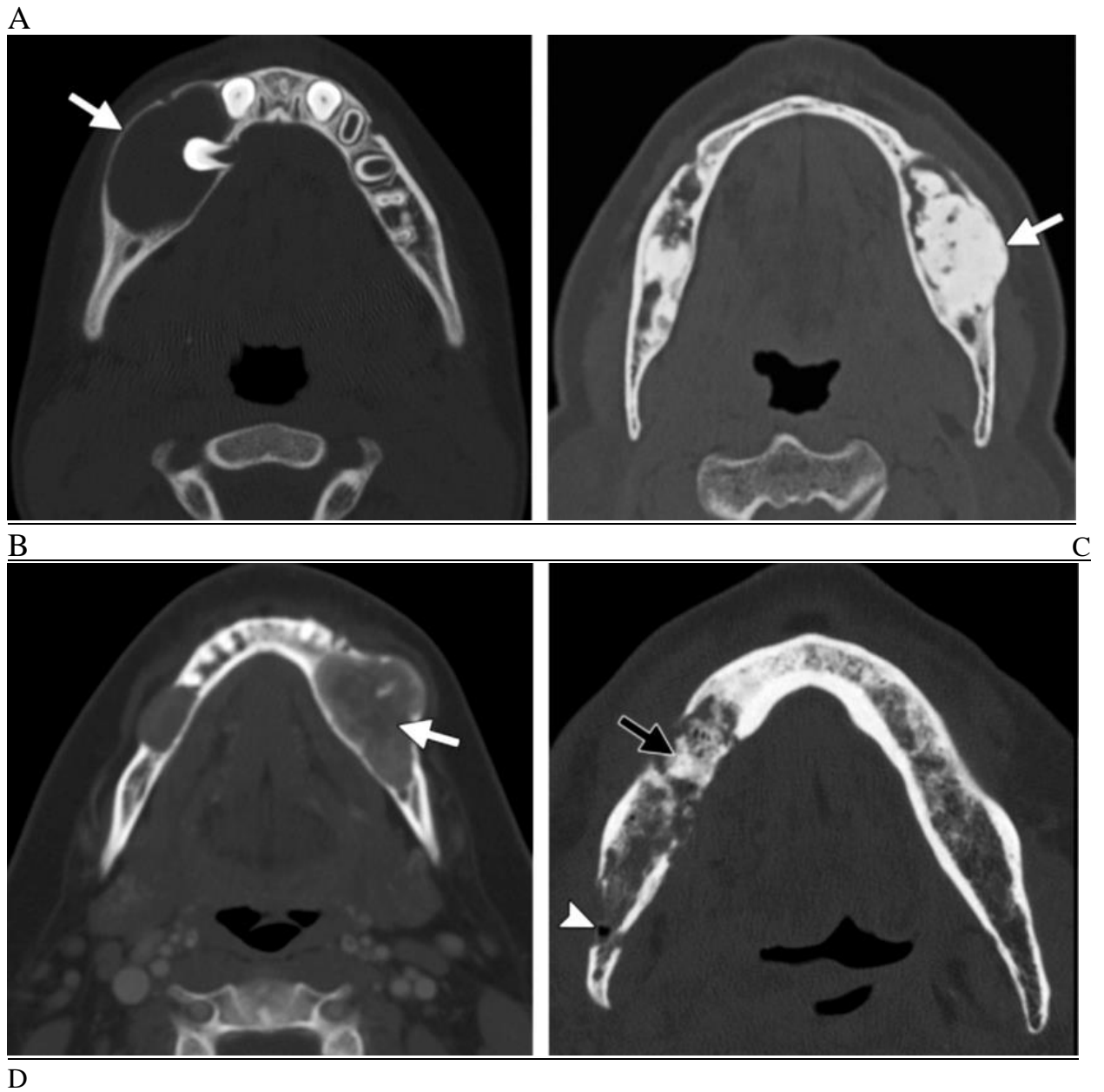


Fig. 8.18. Juvenile idiopathic arthritis (JIA) in TMJ of 34-year-old woman. (A) Coronal CT image shows condylar concavities in both TMJs (arrows). (B) Oblique-sagittal CT image

shows condylar concavity and flat wide fossa (arrow). (C) Oblique-sagittal intermediate-weighted MR image shows thin but intact disk (arrow), adapted to condylar deformity.



D Fig. 8.19. Various jaw lesions. (A–C) Axial computed tomographic (CT) images show jaw lesions (arrow) that demonstrate lysis (A), sclerosis (B), and ground-glass attenuation (C). (D) Axial CT image shows a mixed lytic (arrowhead) and sclerotic (arrow) lesion.

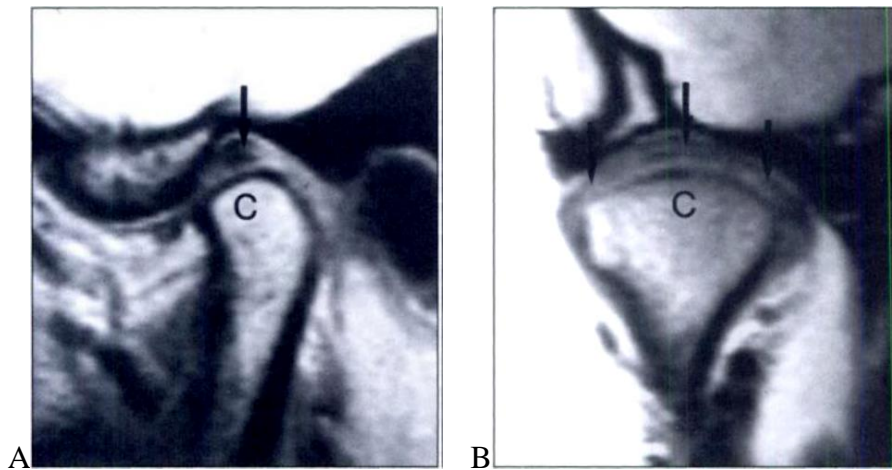


Fig. 8.20. Normal superior disk position. (A) Sagittal MR of 37-year-old female patient with no temporomandibular joint (TMJ) symptoms shows posterior band of disk (arrow) located in 12-o'clock position above condyle (C). (B) Coronal MR of 38-year-old healthy male volunteer shows disk (arrows) located on top of condyle.

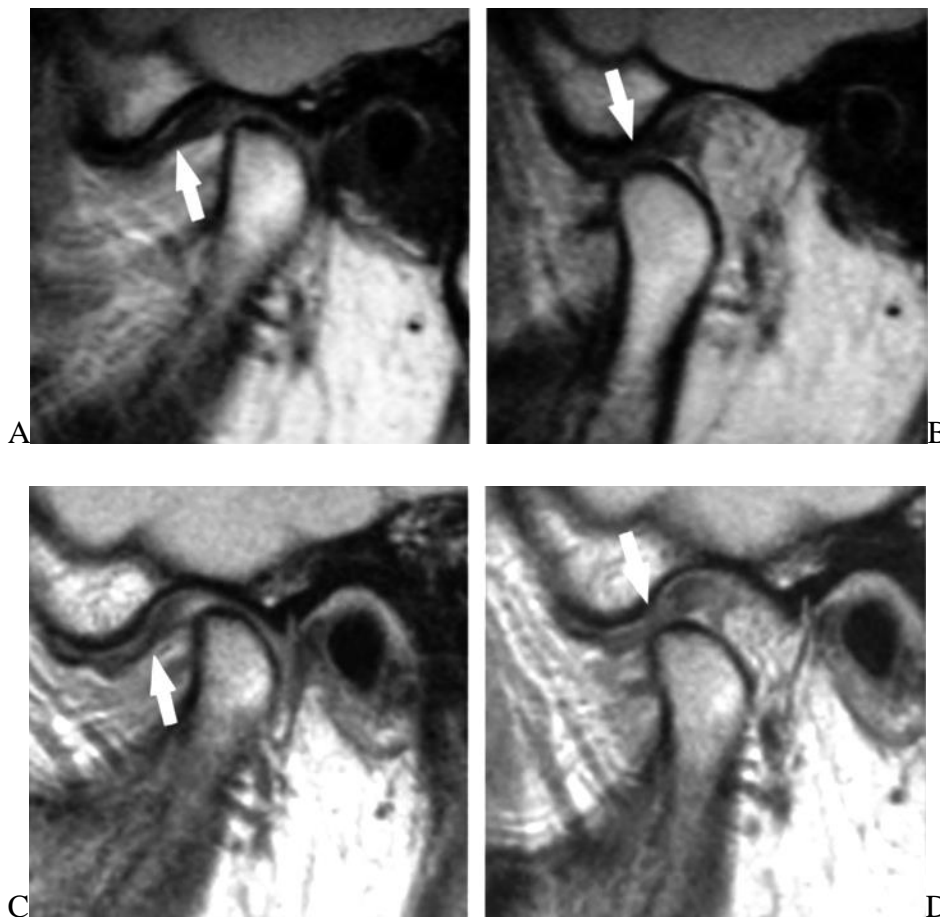


Fig. 8.21. MR images of anterior TMJ disk displacement with reduction (arrow) at inception and at 15-year follow-up in a 37-year-old woman (22 years old at study inception). Proton density-weighted sagittal images were obtained in (A) closed-mouth and (B) open-mouth position at inception and (C) closed-mouth and (D) open-mouth position at 15-year follow-up.

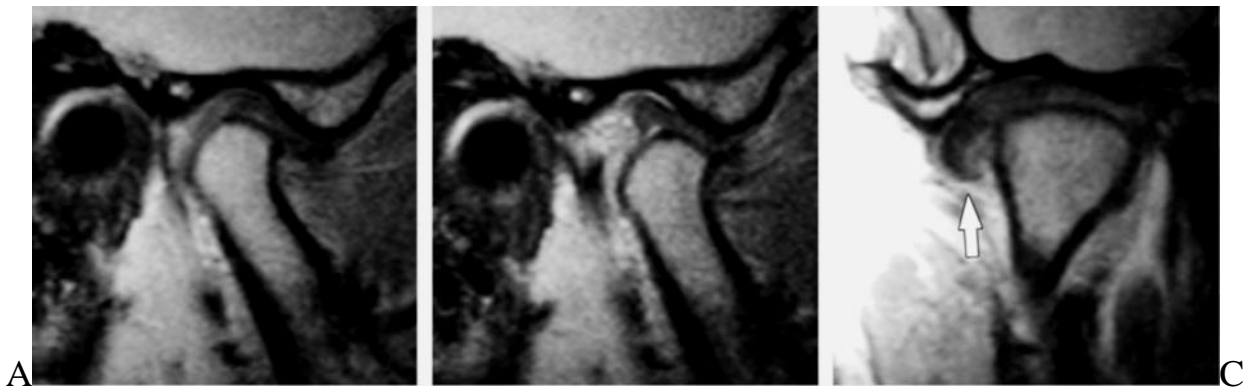


Fig. 8.22. MR images of lateral TMJ disk displacement with reduction (arrows, c) at inception and at 15-year follow-up in a 42-year-old man (27 years old at study inception). Sagittal images were obtained at inception in (A) closed-mouth and (B) open-mouth positions, and (c) coronal image was obtained in closed-mouth position.

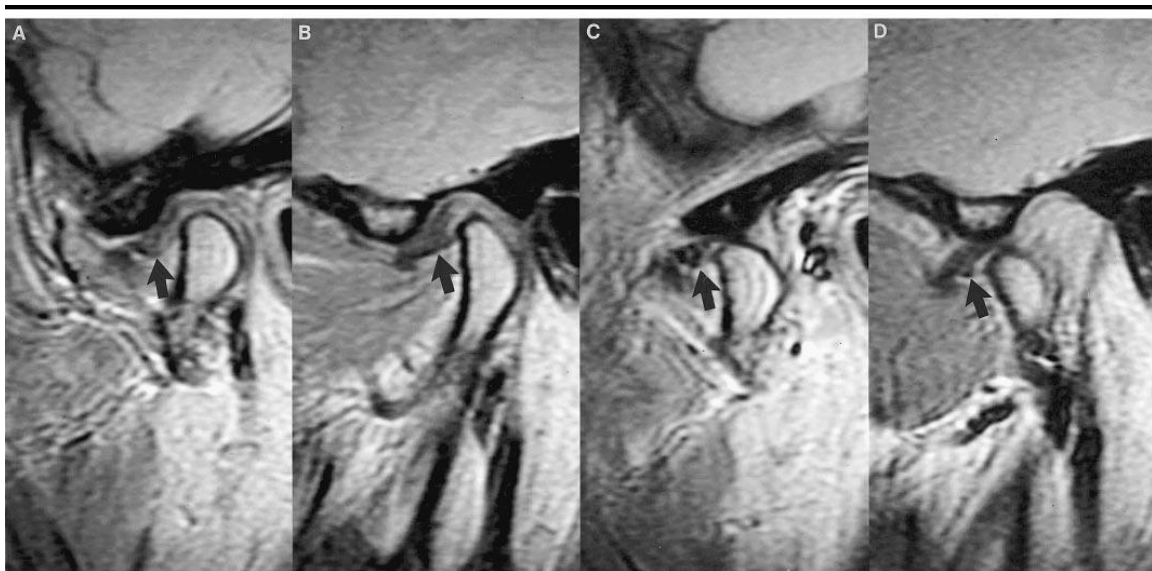


Fig. 8.23. Oblique sagittal MR images of the TMJ of a patient show complete anterior displacement of the disk with the mouth closed in A and B and open in C and D. Arrow indicates the posterior band of the disk.

09 Cysts and Pseudocysts

Pathologic cavities are classified as true cysts if they exhibit an epithelial lining when viewed histologically, whereas pseudocysts lack this histologic feature. Radiographically, in the noninflamed condition cysts and pseudocysts typically appear with a well-delineated border which, however, is lacking when inflammation is present. Their growth is slow and displaces the surrounding anatomic structures depending upon their resistance. One may distinguish between odontogenic and nonodontogenic cyst formation. Other epithelium-lined cysts that develop in the soft tissues, e.g., the nasoalveolar cyst, can only be rendered visible radiographically through use of contrast filling material. Such cysts will therefore not be discussed in this book. Other soft tissue cysts, however, for example the mucocele of the maxillary sinus, can be detected radiographically and will be presented. We will also discuss pseudocysts that are not lined by epithelium, including solitary and aneurysmatic bone cysts as well as other entities that are characterized radiographically by radiolucencies, such as the latent bone cavity of the mandible.

Radicular apical and radicular lateral cysts arise from epithelial remnants, the rests of Malassez, which derive from the Hertwig epithelial sheath. These cells proliferate as a result of inflammatory stimulation that always derives from nonvital teeth. Following nutritional disturbances and dissolution of epithelial layers in the center of the lesion, a cavity forms and typical cystic growth is initiated. *Periodontal cysts* develop similarly, but derive originally from a bony pocket; this is the reason why the involved tooth need not necessarily be nonvital.

Follicular cysts that develop before the formation of dental hard substances, e.g., primordial and keratocysts, arise from the dental lamina. They form near regular or supernumerary teeth, and may sometimes be encountered together with the basal cell nevus syndrome. The epithelium of keratocysts will become cornified.

Follicular cysts, which develop after the formation of dental hard substances, derive their epithelium from the inner and outer enamel epithelia of the tooth primordium. They appear to develop after traumatic stimulation, e.g., the eruption cysts, or as a result of numerous other (unknown) factors. Residual cysts of the odontogenic type may occur anywhere that teeth are extracted and a portion of the cyst is left behind.

Nonodontogenic epithelium-lined cysts develop, depending upon their localization, from epithelial remnants of the Hochstetter epithelial wall, the nasopalatine tract or the palatal suture. Less frequently they occur as odontogenic cysts and, because of the superimposition effect, may lead to diagnostic difficulty and subsequent therapeutic problems.

Pseudocysts are not lined with epithelium, and may result from trauma, marrow hemorrhage, resorptive disturbances, osmotic exclusion, circulatory disturbances and developmental disturbances. They have also been viewed as reparative processes after resolution of bone tumors.

Classification of the cysts

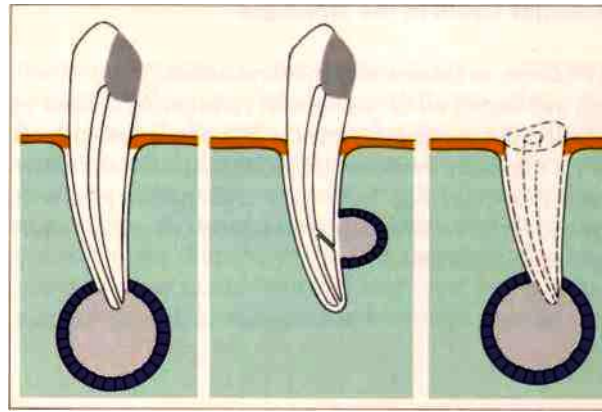
I. Odontogenic cysts (with epithelial lining)

1. Radicular cysts
 - apical cyst
 - lateral cyst
2. Periodontal cysts
3. Follicular cysts
 - a. before formation of hard tooth substance
 - primordial cyst
 - keratocyst
 - b. after formation of hard tooth substance
 - eruption cyst
 - coronal cyst
 - lateral cyst
 - cyst with rudimentary tooth
4. Residual cysts of all types

II. Nonodontogenic cysts

1. Nasopalatine cysts
2. Median (fissural) cysts
 - median alveolar cyst
 - median palatal cyst
3. Lateral (fissural) cysts
 - nasoalveolar cyst
 - globulomaxillary cyst
4. Median mandibular cysts
5. Residual cysts of all types

**III.Pseudocysts
lining)**



(without epithelial

1. Solitary bone cyst
 2. Aneurysmatic bone cyst
 3. Latent bone cavity (Stafne)
- Cysts**

**Odontogenic
Radicular Cysts**

Radicular cysts develop around the apex of a diseased tooth (apical radicular cyst) or around an accessory canal from the pulp (lateral radicular cyst) (Figure 9.1). The root is within the cystic cavity. The radiographic appearance of a clinically symptom-free cyst reveals a clear, opaque delineation border that displaces neighboring structures. An acutely inflamed cyst lacks the radiographic sign of opaque delineation.

Fig. 9.1. Schematic representatic of apical, lateral and residual Cysts.

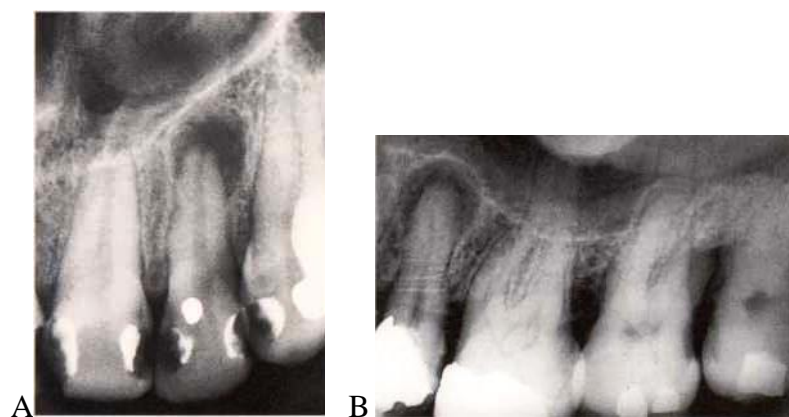


Fig. 9.2. (A) Small, symptom-free radicular cyst exhibits the typical opaque boundary. Cysts of this size are impossible distinguish radiographically from granuloma. (B) **Small, clinically symptom-free radicular cyst that is expanding towards the floor of the maxillary sinus. The periodontal ligament space no longer discernible.**

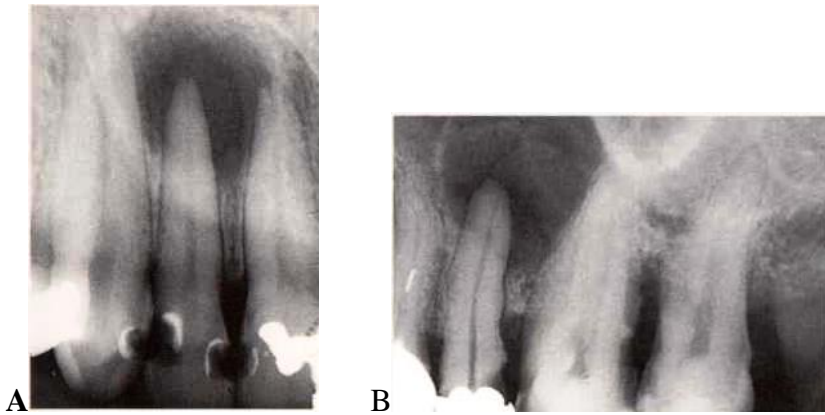


Fig. 9.3. (A) Infected radicular cyst. This cyst has lost its typical radiographic signs as a result of serous infiltration of the surround tissue. Such cysts present radiographically without the sharply demarcated borders are tunneling. (B) Infected radicular cyst emanates from tooth 25 and displaces the floor of the maxillary sinus. The widened periodontal ligamentum space indicates “elongation” of the tooth, and its mobility. The odontal ligamentum space is no lot discernible around the tip of root penetrating the cystic cavity.

Radiographic Signs of Radicular Cysts:

- round radiolucency with an opaque border,
- apex of the tooth is within the radiolucency,
- adjacent teeth and structures are displaced.

Infected cyst:

- cystic cavity exhibits poorly demarcated borders.
- background structures become invisible and the defect appears as tunneling.
- periodontal ligament space around the involved tooth becomes widened.

Radicular Cysts in the Mandible

In addition to those cases that are clinically symptomfree, yet depict all of the typical radiographic signs of radicular cysts, one sometimes encounters infected cysts with a clinically corroborated diagnosis. On the other hand, however, one may also encounter cysts with atypical features, which are reminiscent of other pathologic manifestations.

The sections from panoramic radiographs again show clearly the degree to which this technique has broadened our basis for information gathering from radiographic examination.



Fig. 9.4. **Typical manifestation of a radicular cyst.** The cyst extends from the residual root tip of tooth 34. The case was clinically symptom-free and was an incidental radiographic finding. Even the extraction of root tips should not be performed without previous radiographic.

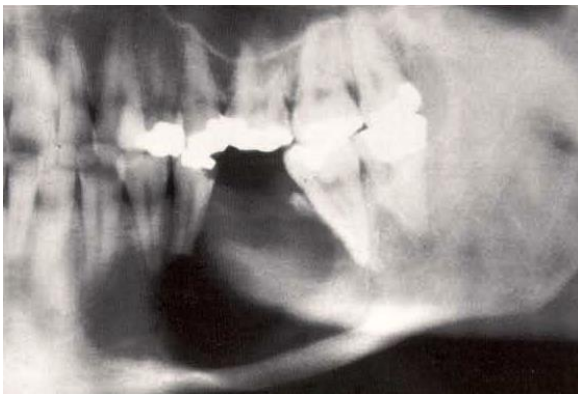


Fig. 9.5. **Infected radicular cyst.** This cyst emanates from tooth 35, which lacks a periodontal ligament space and resides within the cavity. The delineation of the cyst is not sharp, and without knowledge of the clinical findings the radiograph alone is insufficient for unequivocal diagnosis.



Fig. 9.6. **Atypical manifestation of a radicular cyst.** This cyst emanates from the residual root tip of tooth 32. The radiograph mimics a "multi-chambered" process. A radiographic picture with this localization could equally represent an ameloblastoma, a giant cell granuloma or keratocyst.

Radicular Residual Cysts in the Mandible

The nonvital tooth whose root tip appears within the sharply demarcated radiolucency is an unequivocal radiographic sign for the existence of a radicular cyst. Radicular residual cysts lack this sign, and it is for this reason that an edentulous space coronal to a radiolucency is the radiographic sign that may be used

for a suspected diagnosis. However, because residual cysts may also originate from atypically impacted teeth with follicular cysts, radiographic diagnosis cannot be based upon the localization of a round radiolucency in the jaw.

Noteworthy also is that radiolucencies interpreted radiographically as “residual cysts” may also result from other odontogenic or nonodontogenic lesions. The ameloblastoma deserves particular attention here since it can develop even years after tooth extraction and is responsible for most ameloblastomas that develop in patients older than 30 years. It is therefore absolutely necessary that tissue removed from cyst-like lesions at surgery should be subjected to histologic examination.

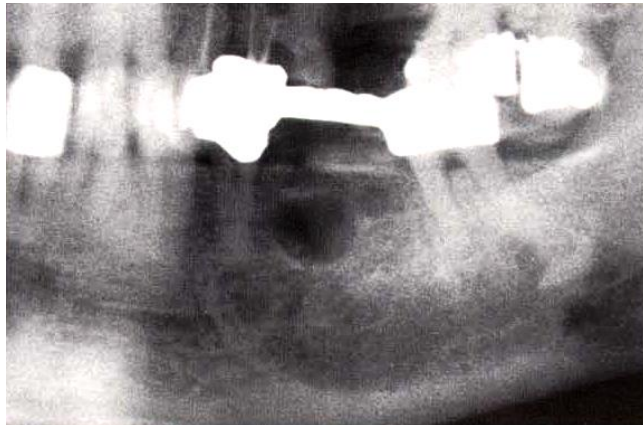


Fig.9.7. Radicular residual cyst emanating from missing tooth 35. With this type of localization, it is entirely possible that the lesion is an ameloblastoma. This case serves to point out vividly that the radiographic differential diagnosis can be extremely difficult in practice. For this reason it is highly recommended that tissue removed from cyst-like lesions be examined histologically.

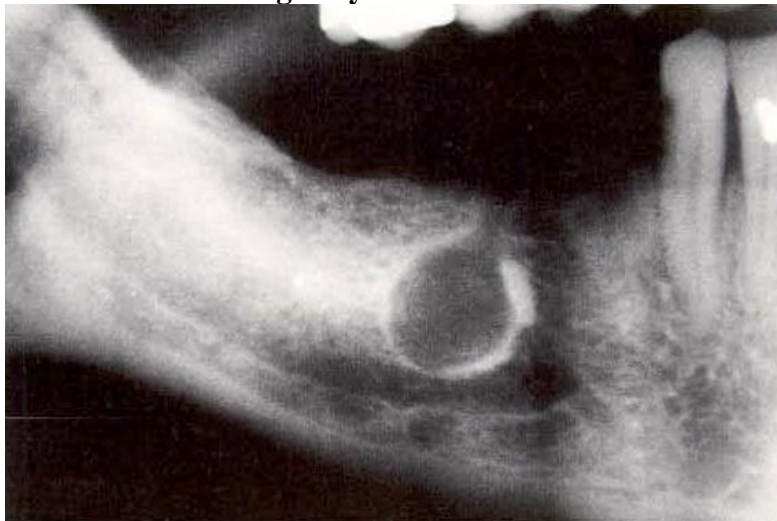


Fig. 9.8. Radicular residual cyst emanating from tooth 46. Note the root tip that has been displaced laterally as a result of growth of the cyst.

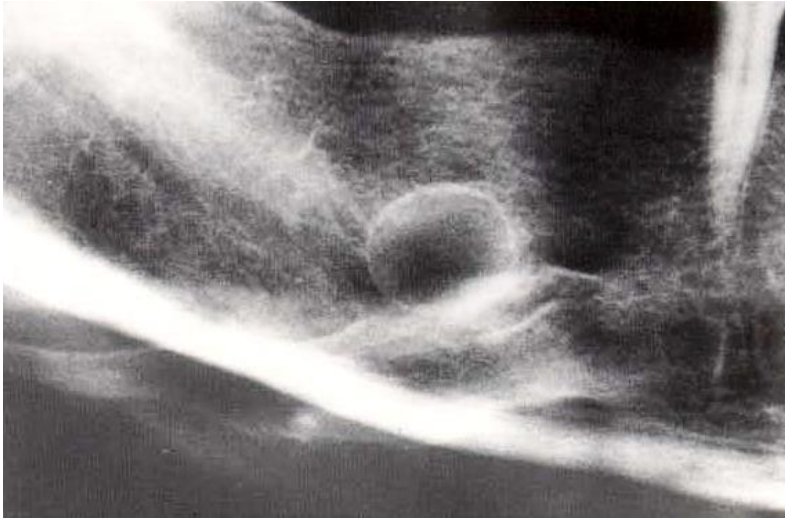


Fig. 9.9. Ossifying fibroma mimicking a radicular residual cyst in a 57-year-old male. Note that the mandibular canal is displaced. Note also the slight radiopacity within the opaque delineation, which may possibly indicate the presence of an ossifying fibroma.

Radicular Cysts in the Maxilla

Epidemiologic studies reveal that radicular cysts occur more often in the maxilla. They often expand toward the maxillary sinuses, achieving dramatic size because of the lack of resistance to their growth and the availability of space. The patient is usually unaware of the presence and growth of such cysts. The vertical expansion of these lesions will be clearly visible in the panoramic radiograph, but depiction of the third dimension will be enhanced by occlusal films. In the case of large maxillary cysts, the use of frontal film tomography or computed tomography is indicated.

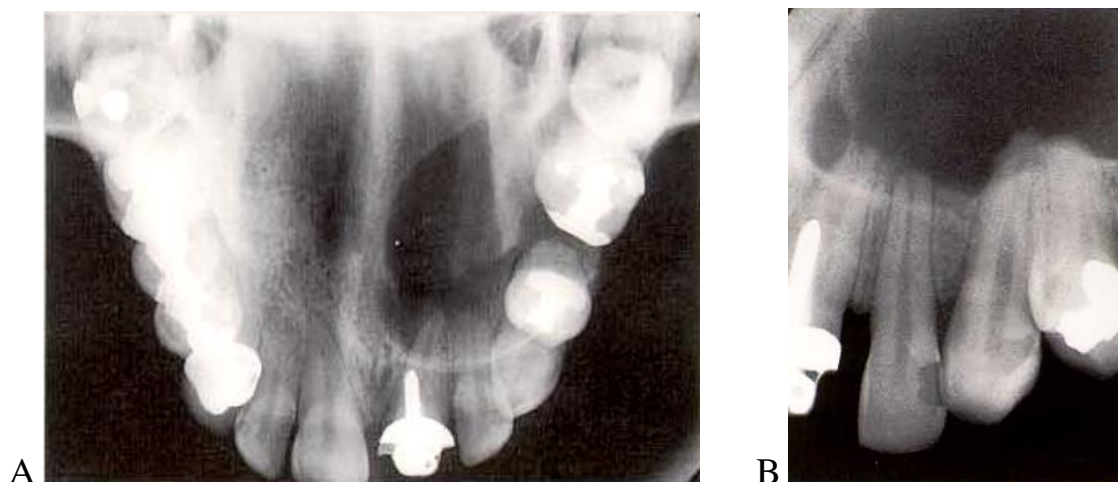


Fig. 9.10. (A) Radicular maxillary cyst extending from teeth 21 and 22 (occlusal radiograph). The expansion of the cyst in the horizontal plane is well depicted (with the exception of minor distortions). (B) Same case (periapical radiograph). The expansion of the cyst cannot be appropriately depicted on a periapical radiograph.

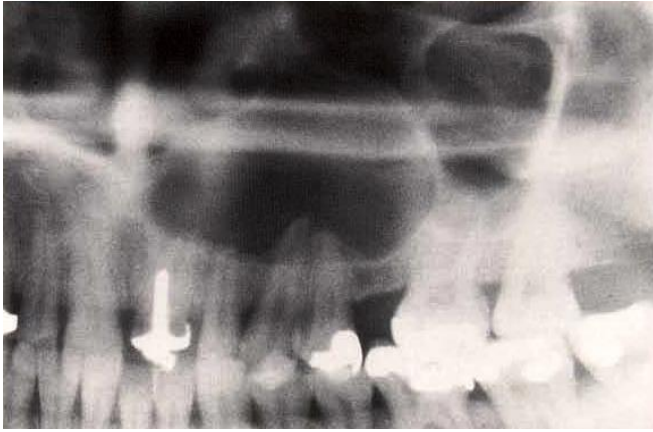


Fig. 9.11. Section from the panoramic radiograph of the same patient. The lateral projection shown in this section from a panoramic radiograph depicts perfectly the vertical expansion of the cyst, which almost completely fills the left maxillary sinus. Note the fine, opaque line of demarcation, which persists even in the sinus. An occlusal radiograph can serve to document the expansion of the cyst in the horizontal plane. Tomography or computed tomography may also be applied in such cases.



Fig. 9.12. Radicular residual maxillary cyst extending from the extraction site of tooth 16. Again the fine, opaque line of demarcation is visible. It is pushed forward by the growing cyst and may, over a long period of time, protect the maxillary sinus from infection and associated sinusitis.

Follicular Cysts

These cysts originate before tooth development due to malfunction of the dental primordium. The primordial cyst frequently occurs in place of permanent or supernumerary tooth buds and at the angle of the mandible. The active epithelium has the capacity to produce keratin and develop into a keratocyst. The latter may develop satellite lesions, which cannot be detected radiographically in their early stages). The keratocyst is often observed in conjunction with Gorlin-Goltz syndrome.

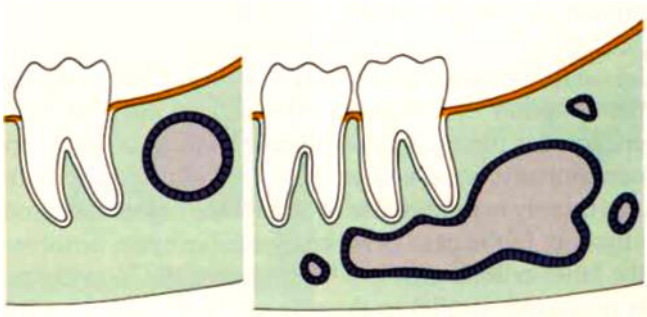


Fig. 9.13. Diagram of primordial cyst and keratocyst.

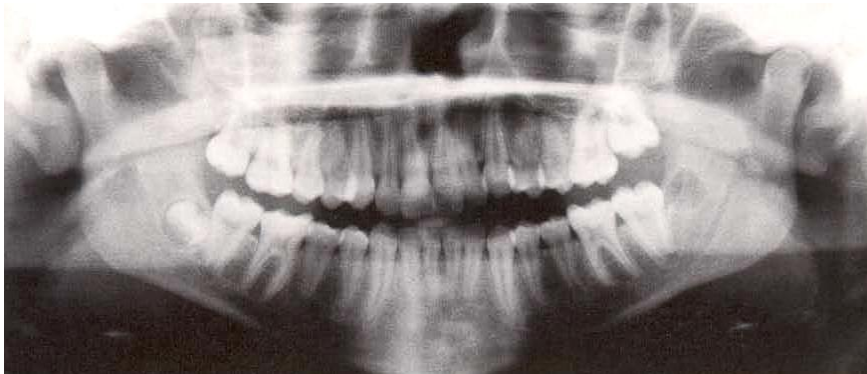


Fig. 9.14. Small primordial cyst. A cyst is visible where the primordium of tooth 38 would normally be seen in this 15-year-old male.

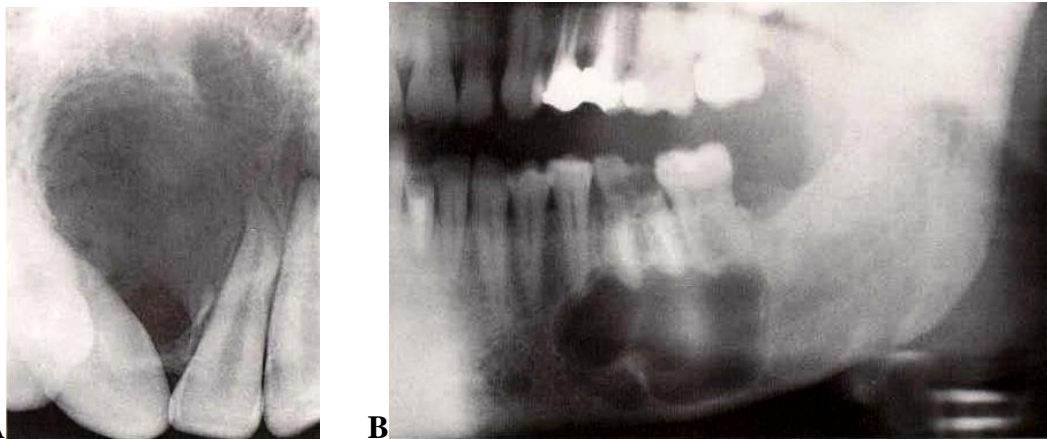


Fig. 9.15. (A) Typically formed keratocyst as seen in a panoramic radiograph. **This cyst appears to be multichambered.** (B) Multichambered keratocyst of the maxilla, mesial to tooth 13. The canine regions of maxilla and mandible are preferred sites for these cysts, as is the mandibular molar region.

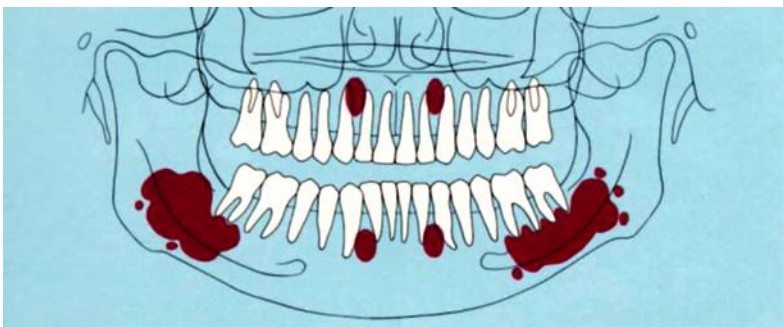


Fig. 9.16. The most important sites of keratocysts.

After the formation of dental hard tissues, cysts containing teeth (or parts of teeth) may develop from the enamel epithelium. Various types may be differentiated: Eruption cysts develop during the eruption of the third molars, and coronal cysts encompass the crowns of affected teeth. Such cysts are occasionally observed to enclose rudimentary teeth, and usually to be attached at or near the cemento enamel junction. In the case of more expansive cysts, however, the latter criteria may not be obvious if the X-ray beam is projected parallel to the axis of the impacted tooth.

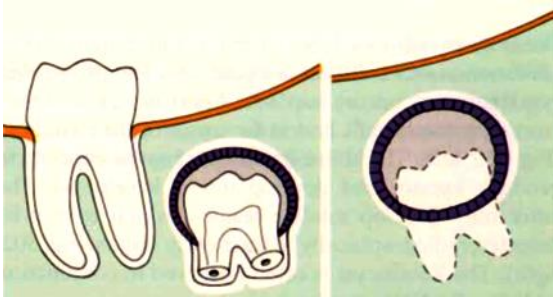


Fig. 9.17. Diagrams of tooth-containing cysts.

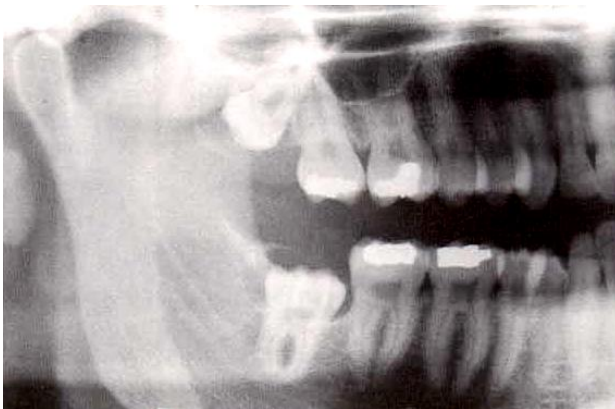


Fig. 9.18. Eruption cysts on erupting teeth 18 and 48. Note the typical attachment of the cyst at the cemento enamel junction.



Fig. 9.19. Eruption cyst on tooth 18 as seen in a periapical film.

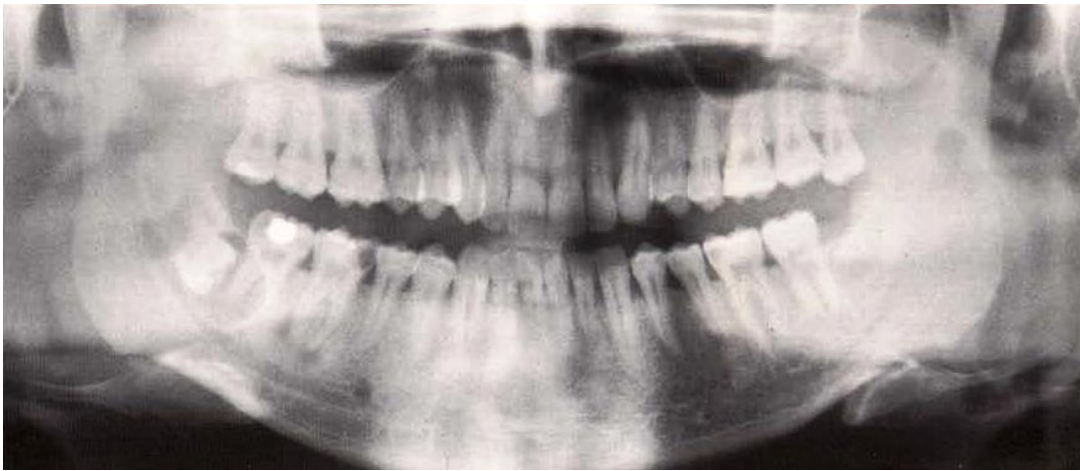


Fig. 9.20. Eruption cyst on tooth 18 as seen in a periapical film. Coronal follicular cyst on a completely impacted tooth 48. Note the chronic periapical periodontitis on tooth 46 and the elongation of tooth 28 with caries on the mesial surface. Lateral follicular cyst on completely impacted tooth 38.

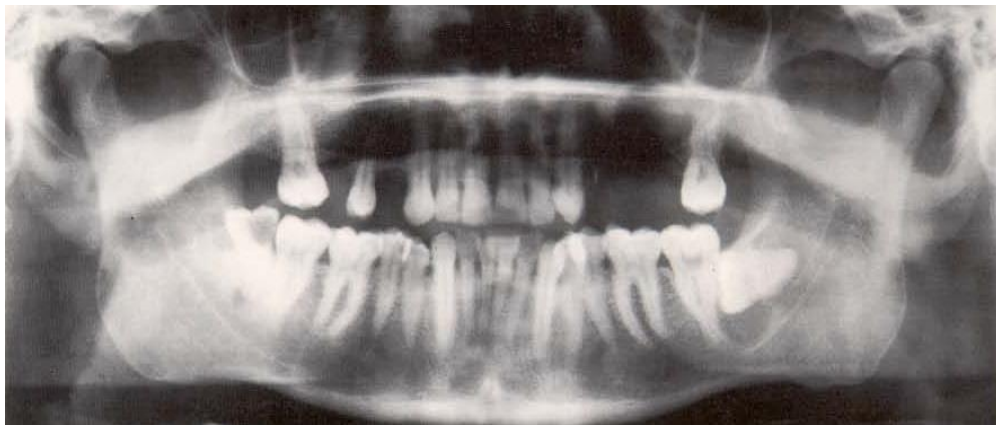


Fig. 9.21. Lateral follicular cysts may develop via a pocket around partially retained teeth and are therefore often clinically referred to as periodontal cysts. Note the pericoronal osteolysis, the deep caries and the apical periodontitis on tooth 48 that have led to primary chronic osteomyelitis at the angle of the mandible.

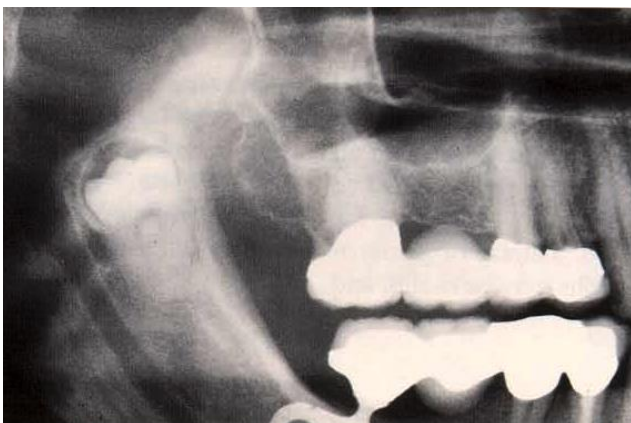


Fig. 9.22. Impacted tooth 48 in a 52-year-old male. This section from a panoramic radiograph shows the bony border surrounding the follicular sac. Discovery of this condition occurred during the course of placement of a Linkow implant and prosthetic reconstruction in both mandible and maxilla.

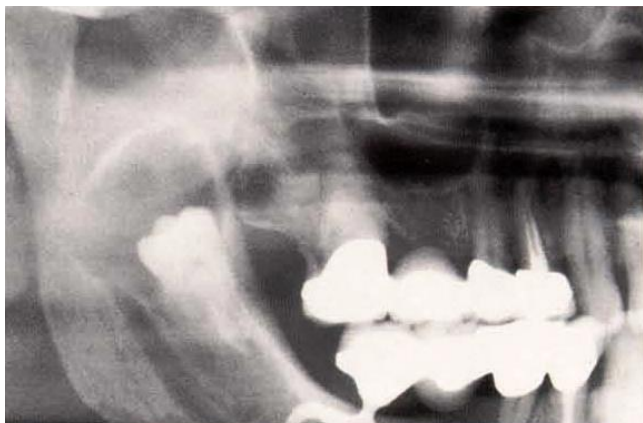


Fig. 9.23. Same case 5 years later. Clinical findings included parulis in the region of the right mandibular angle. The radiograph reveals the coronal follicular cyst within the ascending ramus. Note the typical attachment of the follicular cyst at the cemento-enamel junction and the border of the cyst that has become less sharply demarcated.



Fig. 9.24. **Same case in a section from a reverse Towne projection.** This follicular cyst has developed in the typical lingual direction. If a mandibular third molar is impacted in the ascending ramus, depiction of cystic expansion in frontal plane can usually be accomplished using the reverse Towne projection with maximum jaw opening. For localization of larger cysts in the body of the mandible or at the mandibular angle, it is extremely important to refer the patient for preparation of axial CT prior to any surgery.

Atypically Localized Follicular Cysts

Atypically localized follicular cysts that could only be diagnosed and localized using panoramic radiography and adjunctive special projections are demonstrated on the previous page and on this page. In the dental practice precisely prepared occlusal films can be helpful for diagnosis of the third dimension. Lateral or postero-anterior cephalometric radiographs may be useful, and the reverse Towne projection with maximum jaw opening can be recommended. Furthermore, in the case of large cysts in the maxilla it is absolutely necessary that the patient be referred

for film tomography or computed tomography in a hospital or radiology clinic.

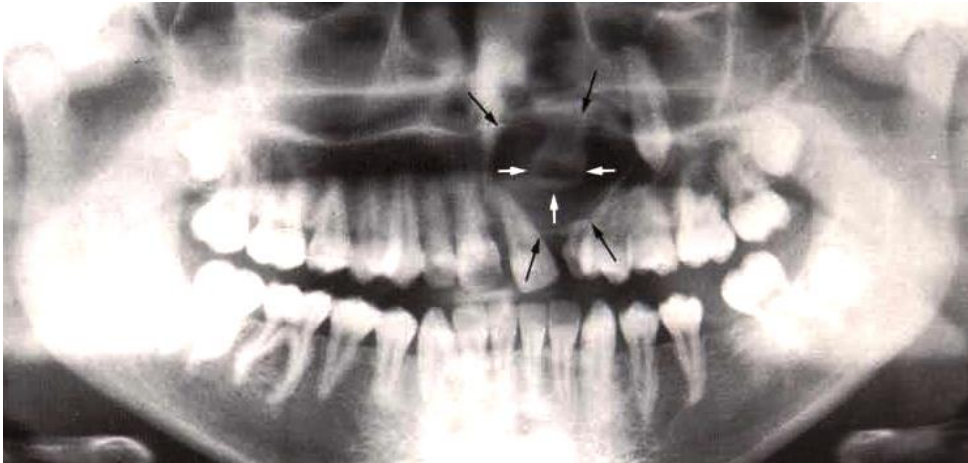


Fig. 9.25. Coronal follicular cyst on tooth 22 with displacement of 23 and retention of 63 in a 17-year-old female. Tooth 22 appears enlarged and overexposed, and it is displaced palatally, while tooth 23 is dramatically displaced in the vestibular direction (arrows).

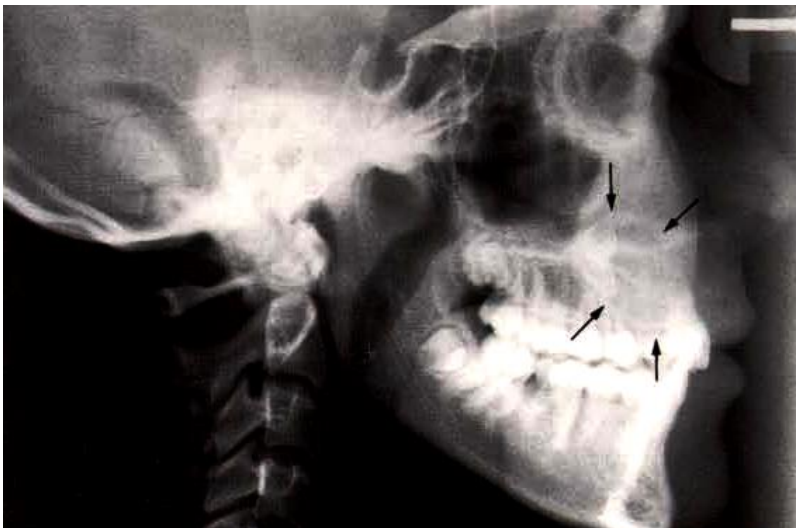


Fig. 9.26. Same case as seen in the lateral cephalometric radiograph. Positions of the cyst and teeth as seen from the lateral view (arrows).

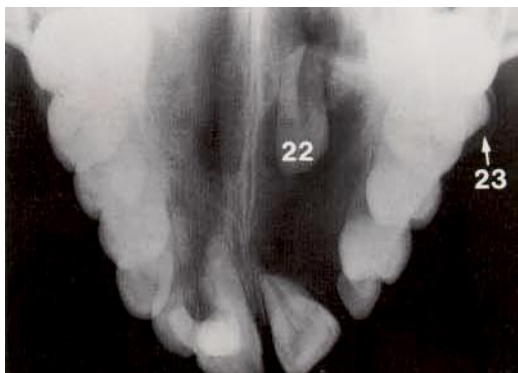


Fig. 9.27. Occlusal film of the same patient. Although teeth 22 and 23 (with arrow) appear in this projection to be positioned rather obliquely toward the dorsal, the occlusal

view provides a good overview of the third dimension.

Nonodontogenic Cysts

These cysts derive from epithelial remnants of the nasopalatine tract, the embryonic Hochstetter wall and the facial fissures. According to site and expanse, the so-called ductal cysts as well as nasopalatine cysts may develop in the incisive canal; these cysts may expand between the central incisors. The nasal septum and the nasal spine anteriorly force the formation of the typical heart shape. The median fissure palatal cyst may develop in the middle of the palate from remnants of the embryonic palatal processes.



Fig. 9.28. Diagram and schematic radiograph of nasopalatine (A) and the median fissural cysts (B).



Fig. 9.29. (A) “Ductal cyst” in the incisal canal. In this periapical radiograph, the cyst is superimposed upon the apex of tooth 21, giving the impression of a periapical lesion (vitality testing!). (B) Nasopalatine cyst in an early stage. The cyst develops between the roots of teeth 11 and 21, forcing them apart.



Fig. 9.30. Nasopalatine cyst. The cyst has developed palatally from the anterior teeth in the nasal portion of the duct. In this position, it does not displace the roots of teeth 11 and 21.

In addition to nasopalatine cysts which occur more frequently, nonodontogenic cysts of the incisive papilla have also been described; however, it is not possible to detect them radiographically because they occur within the soft tissues. The “midline (median) alveolar cyst” has been described between the maxillary central incisors; its origin likely derives from the epithelium of the dental lamina. The median fissure cyst, which can develop from displaced remnants of the palatal suture is rare, as are cysts from the palatal transverse sutures. A rare median mandibular cyst has also been described.

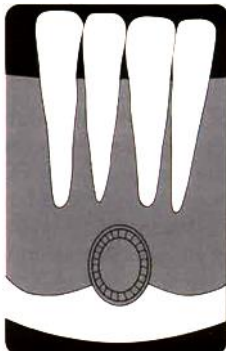


Fig. 9.31. Diagram of a median mandibular cyst.

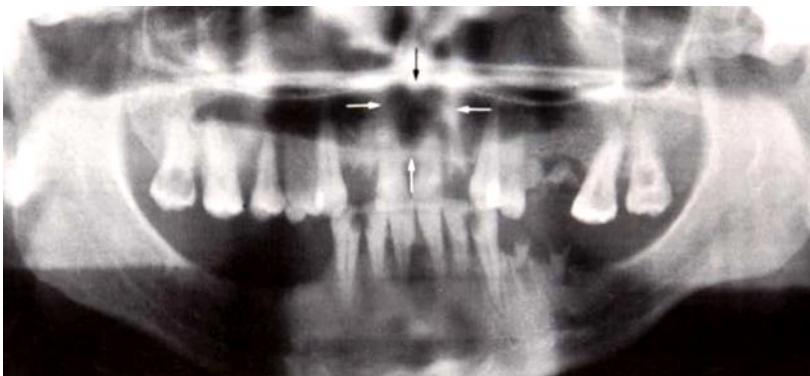


Fig. 9.32. Nasopalatine cyst as seen in a panoramic radiograph. Typical heart-shaped cyst, but without displacement of roots of teeth 11 and 21 (arrows). This appearance indicates the cyst has developed palatally from the anterior tooth roots.

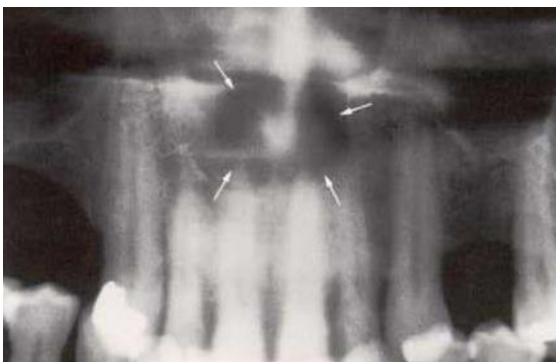


Fig. 9.33. Median (fissural) palatal cyst. The cyst distends the floor of the nasal sinus (arrows). The anterior nasal spine, portions of the nasal crest of the maxilla and the vomer (collectively referred to as the osseous nasal septum) remain intact.

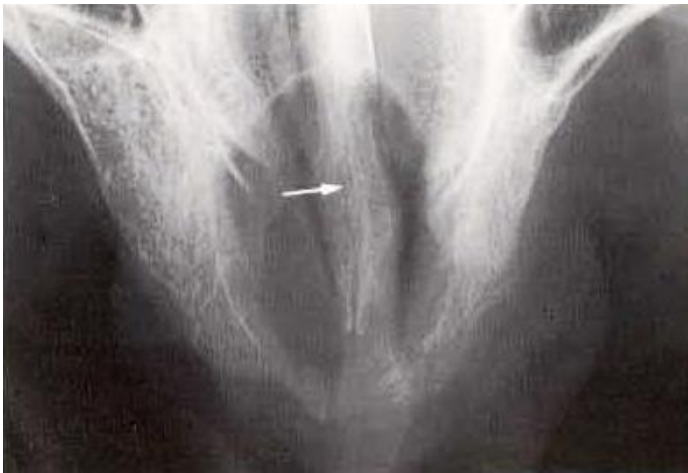


Fig. 9.34. Median (fissural) palatal cyst as seen in an occlusal projection. Because the caudal portion of the osseous nasal septum in the region of the nasal crest has already been resorbed by the growing cyst, the median suture is no longer visible in its entirety (arrow).

Two cysts may derive from the embryonic Hoch-stetter epithelial wall. The nasoalveolar cyst resides subperiosteally in the region of the nasolabial groove; it is possible to show this cyst radiographically only by using contrast media. The second type of cyst develops between the roots of vital lateral incisors and canines and presents as a globulomaxillary cyst, which appears radiographically as a lucent area in the shape of an inverted pear.

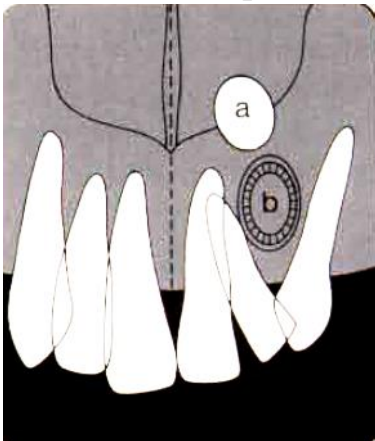


Fig. 9.35. Diagram of nasoalveolar and globulomaxillary cysts.



Fig. 9.36. Median palatal cyst. View of the maxilla taken with intraoral source radiography.



Fig. 9.37. Bilateral lobulomaxillary cysts. The arrows depict how the cysts displace the roots of lateral incisors and canines, resulting in a cystic cavity with the shape of an inverted pear. Cysts of this kind may also be regarded as an aberrant form of cleft palate.

Possible causes for radiolucencies in the canine region of the maxilla: Apical radicular cyst, Periodontal cyst, Globulomaxillary cyst, Keratocyst, Adenomatoid odontogenic tumor, Osteoblastoma, Ameloblastoma.

Pseudocysts

The term “pseudocyst” exists because these cavities that are free of epithelium often appear radiographically as cysts. Depending on patient history and contents, these “cystoid” structures may be categorized as solitary bone cysts and aneurysmal bone cysts. Many of the solitary bone cysts can be ascertained from the medical history (trauma); thus the term “traumatic bone cyst” has persisted. When opened surgically, such solitary bone cysts present as an empty cavity.

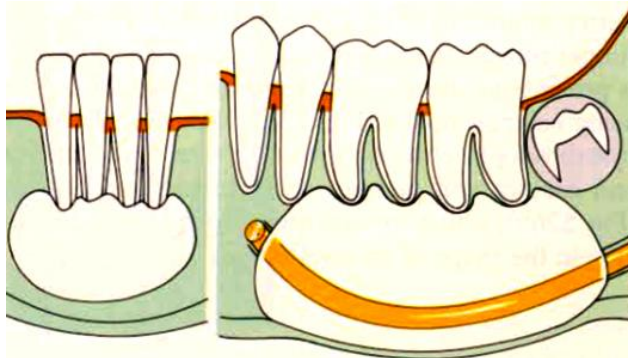


Fig. 9.38. Diagram of solitary bone cyst in the mandible. The typical localization of the traumatic bone cyst is displayed on the left.

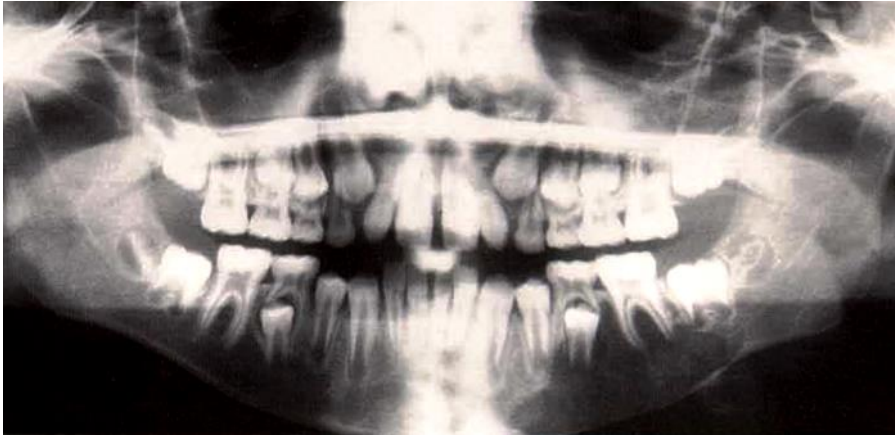


Fig. 9.39. **Solitary bone cyst in the left mandibular body in a 9-year-old female.** Noteworthy is the thinning and distension of the osseous cortical lamella. This radiographic sign is typical for pseudocysts in the horizontal ramus.



Fig. 9.40. **Section from a panoramic radiograph of the same patient.** Note the radiolucency that is not completely free of trabecular bone, and the distended but thinned cortical bone. The cavity is traversed in the molar area by the mandibular nerve.

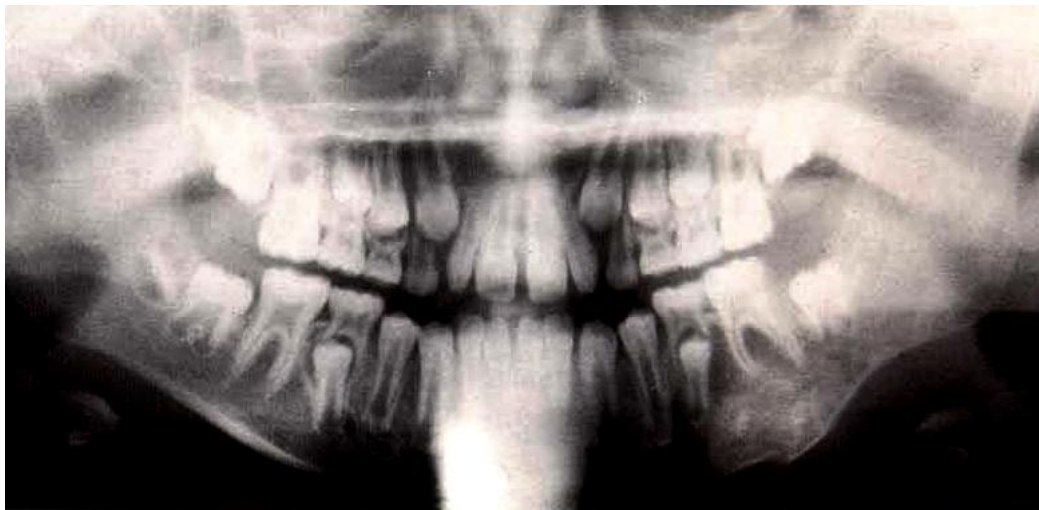


Fig. 9.41. **Solitary bone cyst.** This is a panoramic radiograph of the identical case, postoperatively. Note the *apparent fracture* in the surgical area; the patient moved during exposure.

Aneurysmal bone cysts histologically exhibit a fibrous network as well as a rapidly expanding “cystic” lesion filled with a central mass of calcifying osteoid, and endothelium-lined cavities. For this reason the “cyst” presents radiographically as a solitary bone cyst. Radiographic differential diagnosis is therefore impossible.

The preferred site for such lesions is the body of the mandible in 11- to 15-year-

old males. These lesions are extremely radiolucent and are therefore more clearly visible in radiographs taken with shorter exposure times.

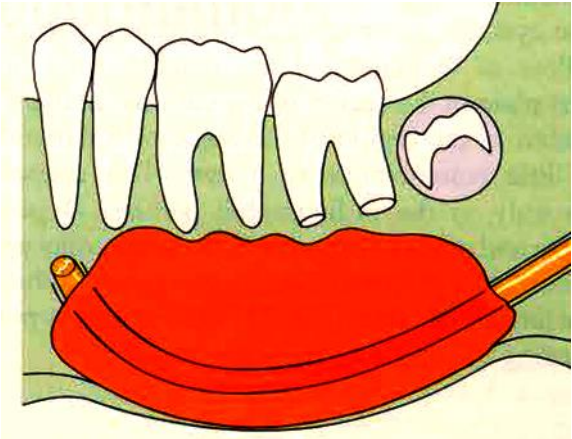


Fig. 9.42. Diagram of aneurysmal bone cyst.

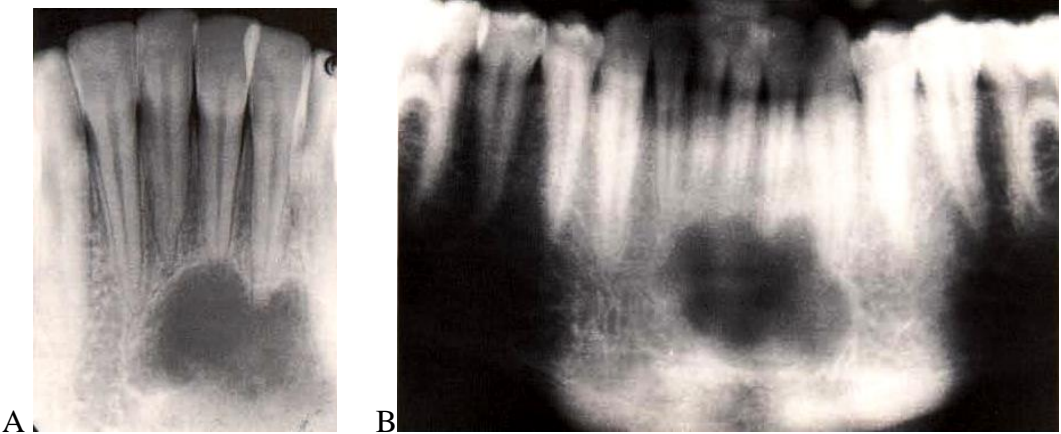


Fig. 9.43. Traumatic bone cyst in the mandibular anterior region of an 18-year-old male. Compare the periapical radiograph with the panoramic film. It is extremely difficult to differentiate this lesion from a central giant cell granuloma.



Fig. 9.44. Solitary bone cyst in an uncommon location in a 7-year-old female.

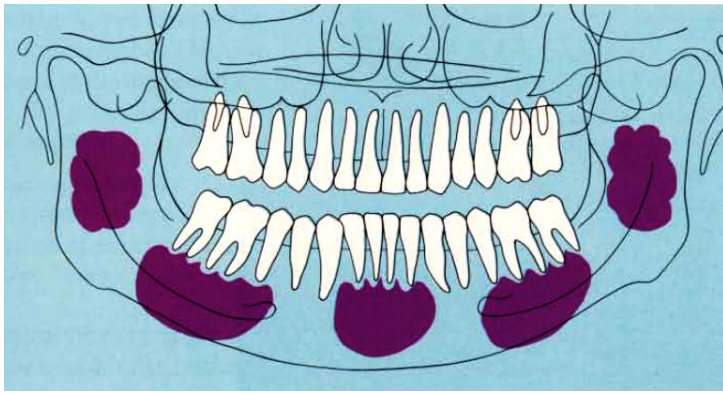


Fig. 9.45. Typical site of solitary bone cysts. These cysts are most often observed in the first and second decades of life. The aneurysmal bone cyst is usually seen in the horizontal ramus of the mandible in 10- to 15- year-old patients.

The latent bone cavity, which is also known as the “Stafne cyst,” is sometimes classified as a pseudocyst regardless of the fact that the defect of the lingual osseous plate in the region of the submandibular fovea (less often in the region of the angle of the mandible) bears little resemblance to a cyst. This association relates only to the radiographic picture. Depending upon site and angle of projection, the lesion may appear more cortically or open caudally as a result of the well- known tangential effect. Controversy persists concerning the origin of these lesions.

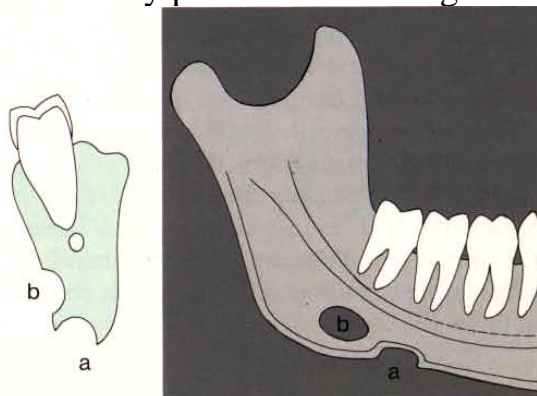


Fig. 9.46. Diagram of a latent bone cavity as it might appear in a periapical radiograph or in a panoramic film



Fig. 9.47. Latent bone cavity open caudally as viewed in a periapical radiograph. Note the corticalization of the deep defect, which appears open caudally also.



Fig. 9.48. Latent bone cavity of a similar type, viewed in a panoramic radiograph. Note the thickening of the surrounding cortical bone. It is interesting to note here that an ossifying fibroma, an “angular process” or a peripheral osteoma can develop at the same site.



Fig. 9.49. Latent bone cavity, closed type. Note the thickening of the compact bone around the defect, which typically is located below the mandibular canal and usually anterior to the mandibular angle.

Traumatic Bone Cyst

A traumatic (simple) bone cyst is not a true cyst because it lacks an epithelial lining. The cause of traumatic bone cyst is unknown, although some believe that it develops in response to trauma. These lesions are usually discovered in the 2nd decade of life. Their most common site of occurrence is the mandible. Traumatic bone cysts are usually asymptomatic and are incidental radiographic findings. The lesions are typically unilocular, lucent defects that often have a characteristic scalloped superior margin extending between the roots of teeth. There may be attendant thinning of the mandibular cortex with osseous expansion. Multiple lesions occur in some unusual cases. The differential diagnosis includes vascular lesions, central giant cell granuloma, and ossifying fibroma.

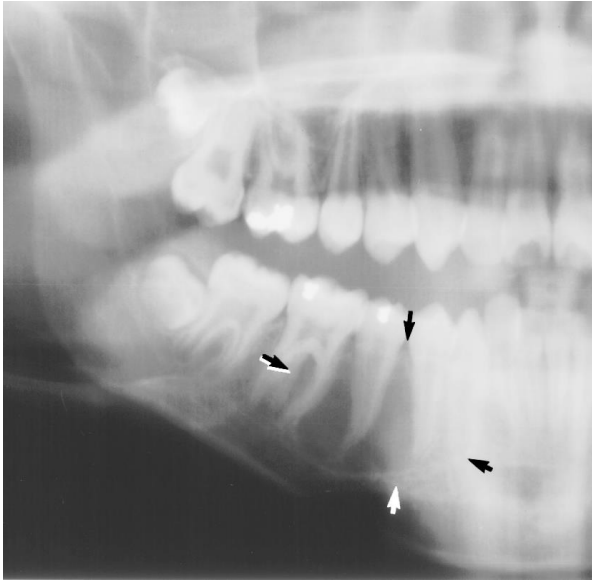


Fig. 9.50. Traumatic bone cyst in a 12-year-old boy. A lesion was discovered on a routine panoramic radiograph obtained for planning of orthodontic treatment. (a) Panoramic radiograph shows a large, ellipsoid, well-defined, corticated, lucent lesion undulating between the premolar and molar teeth on the right side of the mandible (arrows). Minimal tooth displacement is present along with loss of the lamina dura of roots within the lesion. All teeth were vital.



Fig. 9.51. Static bone cavity (Stafne cyst) in a 35-year-old man. CT scan reveals a cortical defect (arrow) in the lingual surface of the right mandibular angle, a finding that does not represent a true cyst.

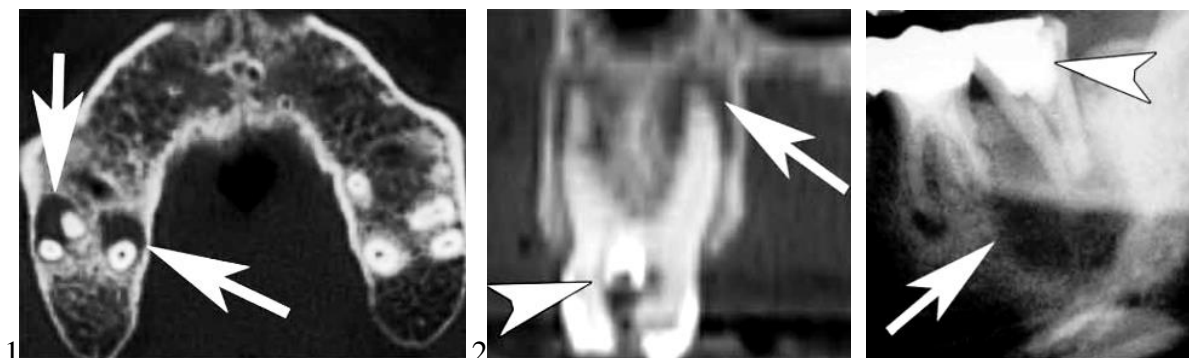


Fig. 9.52. Periapical cyst in a 60-year-old woman. Computed tomographic (CT) scan (1) and coronal reformatted CT image (2) demonstrate a radiolucent lesion (arrows) surrounding the apex of a molar. A defect with dental filling (arrowhead) is present within the crown of the tooth.

(3) Periapical cyst in a 40-year-old man. Panorex image demonstrates a circular radiolucent lesion (arrow) at the apex of a molar. Note the dental filling (arrowhead) from a prior procedure.

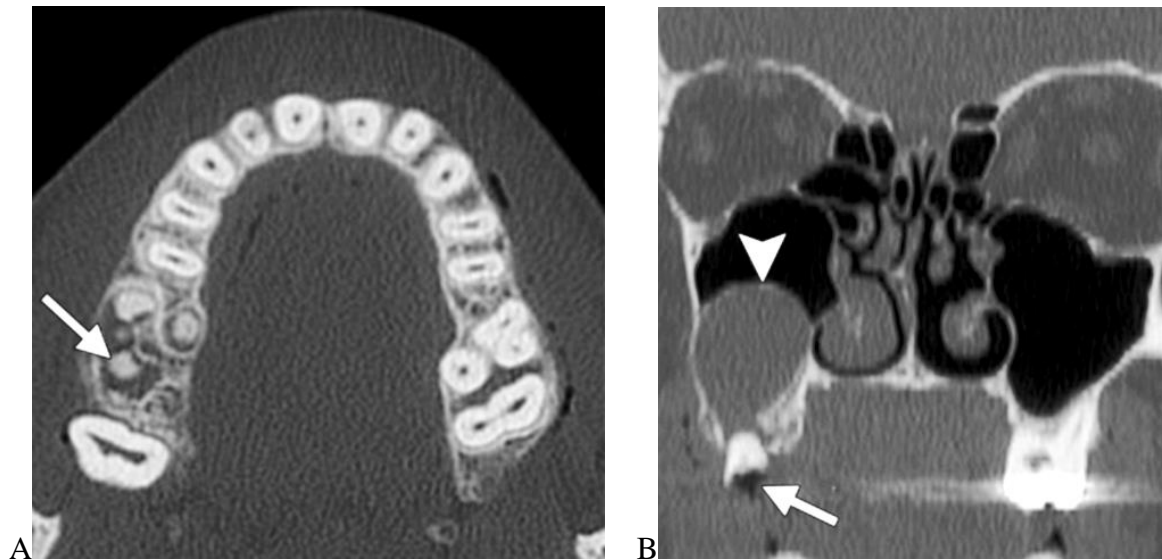


Fig. 9.53. Periapical cyst in a 48-year-old-man with left eye pain after an assault. **(A)** Axial CT image shows an incidental large cystic lesion involving the root of a carious right maxillary second molar (arrow) with adjacent sclerotic borders. **(B)** Coronal CT image shows the periapical lucency (arrow), with extension superiorly into the right maxillary sinus (arrowhead).



Fig. 9.54. Odontogenic keratocyst in a 13-year-old boy. An abnormality was seen incidentally on conventional radiographs obtained for planning of orthodontic treatment. Lateral oblique radiograph shows an ellipsoid, expansile, lucent lesion occupying the anterior two-thirds of the left ramus with an impacted third molar crown displaced inferiorly within the lesion. The mandibular canal appears to be displaced inferiorly as well.



Fig. 9.55. Solitary (hemorrhagic) bone cyst in a 25-year-old woman. Coronal reformatted CT image demonstrates a cystic lesion (arrows) within the mandibular body. The mandibular cortex is thinned. Note the normal tooth (arrowhead) within the lesion, a finding that helps distinguish the cyst from radicular or other odontogenic cysts.



Fig. 9.56. Follicular cyst in a 40-year-old man. Coronal reformatted CT image reveals a cystic lesion with an unerupted tooth in the right molar region (arrow). The crown of the tooth is contained within the lesion.



Fig. 9.57. Dentigerous cyst in a 42-year-old man with painful third molars. A full-mouth radiographic series showed an abnormality; additional radiographic views were then obtained. (a) Panoramic radiograph shows an ellipsoid, expansile, well-defined, corticated, lucent lesion with undulating margins in the right mandible. An associated tooth is seen within the lesion.

10 Benign and Malignant Lesions of the Jaws

Mandibular lesions develop from both odontogenic and nonodontogenic origins and have varying degrees of destructive potential. Common benign cystic lesions include periapical (radicular) cysts, follicular (dentigerous) cysts, and odontogenic keratocysts. Benign solid tumors represent a broad spectrum of lesions such as ameloblastomas, odontomas, ossifying fibromas, and periapical cemental dysplasia. Malignant tumors that often involve the mandible include squamous cell carcinomas, osteosarcomas, and metastatic tumors. In addition, vascular lesions such as hemangiomas and arteriovenous malformations may develop, further expanding the differential diagnosis. Because mandibular lesions have a wide range of pathologic features but similar imaging appearances, familiarity with embryologic characteristics and secondary findings is crucial. Patient age at manifestation, prevalence, location within the mandible, cystic or solid appearance, border contour, and effect of the lesion on adjacent structures are all considerations in making the diagnosis.

Odontogenic Tumors and Pseudotumors

Odontogenic tumors and tumor-like “pseudotumors” develop as neoplasias from the dental lamina. They are usually benign, but several of them have a tendency, albeit seldom, toward malignant transformation. Because growth occurs only slowly, asymptotically and without any change in mucosal appearance, the existence of such lesions in their early stages is usually detected only by chance, or after the development of some structural deformation or obvious asymmetry of the facial skeleton. The growth of such entities, for example the ameloblastoma, can occur invasively, which renders complete surgical excision difficult; it is for this reason that such lesions often recur postoperatively, while other lesions, e.g., the odontoma, are routinely removed surgically without subsequent recurrence. On the other hand, it is seldom necessary to treat surgically lesions characterized by excess cementum formation. With appropriate radiographic follow-up in the second and third decades of life, the potentially negative consequences of such lesions in later life can be obviated for most patients.

Ameloblastoma

Ameloblastoma which according to the literature is the most common tumor in the jaw region, occurs relatively late, mainly in the fourth decade of life. This is probably an incorrect picture, however, because the painless and slowly growing tumor does not elicit any mucosal changes nor any expansion of the jaw; it is for this reason that before the era of the panoramic radiographic technique such tumors were detected only years later in advanced stages. The tumor affects both sexes equally; it has a tendency to recur and may malignantly transform in approximately 2% of cases. The histologic picture is variable: Solid forms infiltrate, while cystic forms generally remain comparatively benign.

Ameloblastomas are benign epithelial neoplasms and represent about 10% of odontogenic tumors. These neoplasms develop from various sources of odontogenic epithelium, including dental follicular lining epithelium, and exhibit locally aggressive behavior. Ameloblastomas typically manifest in the 3rd to 5th decades of life but have

also been reported in younger or older individuals. Patients usually present with a slowgrowing, painless mass. Most ameloblastomas occur in the ramus and posterior body of the mandible (80% of cases). Large tumors may infiltrate adjacent soft tissues, usually secondary to perforation of the lingual cortex.

Localization. Approximately 80% of all ameloblastomas occur in the mandible. Of these, 70% occur in the molar regions and at the angle of the mandible, approximately 25% in the premolar area, and the remainder in the anterior segment.

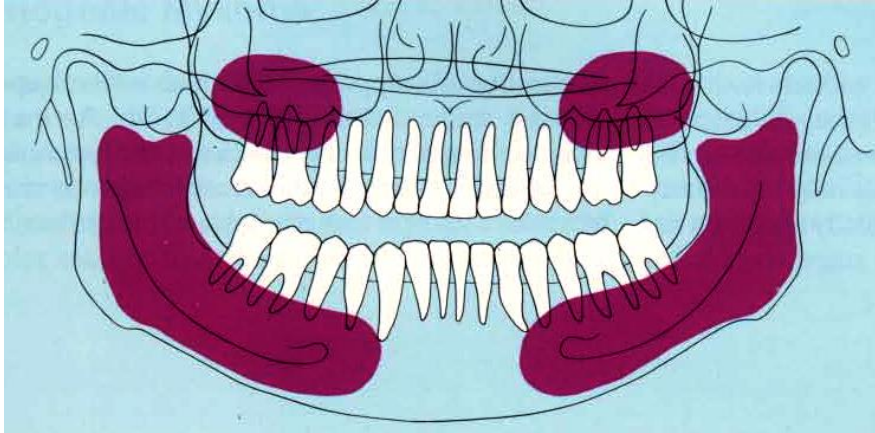


Fig. 10.1. Most common ameloblastoma sites. These lesions occur most often in the second and third decades of life, thus in caries-free young adults the exclusive use of bite-wing radiographs will not provide adequate overview of the jaw. The site of 80% of ameloblastomas is in the mandible and only 20% in the maxilla.

Examination technique:

- panoramic radiography, in later stages utilizing reduction of exposure time,
- reverse townes projection, using reduced exposure time,
- periapical films to target early lesions,
- lateral mandibular occlusal films, with reduced exposure time,
- CT, indicated for lesions in the maxilla and in later stages.

Radiographic signs. The ameloblastoma may present radiographically as “unilocular” (often even lobular in appearance) or “multilocular.” The multilocular forms exhibit either relatively large, round “soap bubbles” with slender septa and a thin cortical plate (in late stages), or numerous small bubbles resembling a honeycomb and with thick septa. The latter form may present a radiographic picture similar to a central hemangioma. Not infrequently, a tooth may be incorporated in the lesion.

Differential diagnosis:

- odontogenic myxoma, especially at the angle of the mandible,
- central giant cell granuloma, especially in the premolar area of the mandible,
- late stage follicular cysts,
- adenoid odontogenic tumor, unilocular, in the canine region of the maxilla,
- ameloblastic fibroma in late stage.

The **ameloblastic fibroma** is a mixed tumor that occurs during the first and second decades of life, especially in the molar areas of the mandible. In rare cases, the ameloblastic fibroma can undergo malignant transformation to a sarcoma. The **ameloblastic fibro-odontoma** is classified with the odontomas.

In all its forms, ameloblastoma radiographically exhibits sharp demarcation; this may erroneously lead to the suspicion that, histologically, infiltrative growth is occurring. The radiolucencies are generally described as honeycomb or soap bubble in appearance. Impacted or neighboring teeth are displaced, with roots often partially resorbed. The cortical bone is extremely thin but not penetrated. Recurrent lesions frequently reveal a picture that closely mimics the odontogenic myxoma. In younger persons the tissue of origin appears to be primordial and follicular cysts; in older individuals epithelial remnants resulting from tooth extraction, sometimes years earlier, may represent the etiology. It is for this reason that histologic examination should be performed after removal of any cyst-like lesion.

In the mandible and especially in the third molar region, incipient ameloblastomas can only be detected

radiographically after they have reached a certain size, due to the addition effect of remaining osseous structure in the background.



Fig. 10.2. Ameloblastoma at the angle of the mandible in a 48-year-old male. Expansive form with oval radiolucencies traversed by a few very thin septa. The osseous ceiling, which is normally shown, is not seen here despite use of a low energy projection. This is a late stage lesion, with clinical signs including distention and fluctuation.



Fig. 10.3. Soap bubble-like form of an ameloblastoma of the molar region in a 35-year-old female. Recurrent lesion. In addition to the multilocular soap bubble-like shape, note that the mandibular canal is no longer distinguishable, and a reactive sclerosis of the osseous structure is visible at the angle of the mandible.

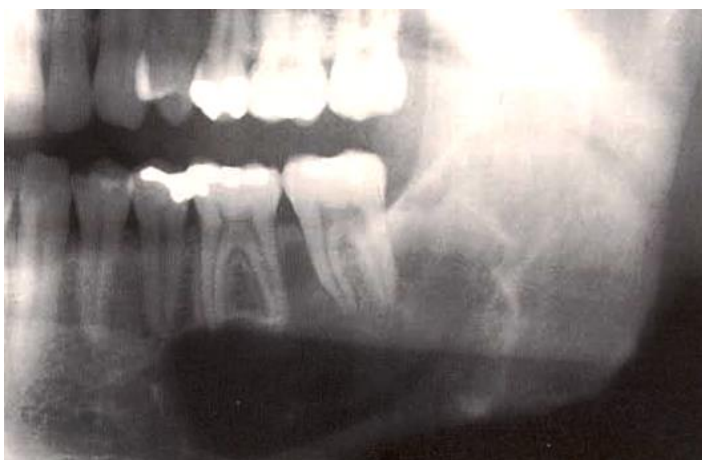


Fig. 10.4. Ameloblastoma, resembling a keratocyst, in a 28-year-old male. Relatively early stage with lobular distentions from unilocular radiolucency.



Fig. 10.5. Honeycomb-like small ameloblastoma in a 19-year-old female, as seen in a periapical radiograph. Early stage. The relatively thickly bordered "bubbles" elicit a radiographic subtraction effect giving the appearance of root resorption.

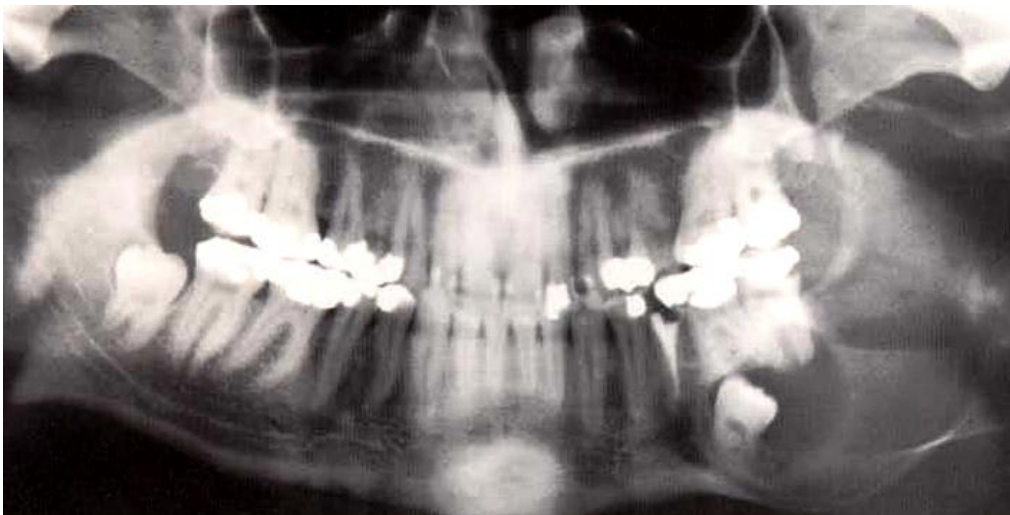


Fig. 10.6. Large soap bubble-shaped ameloblastoma typically located in the molar region, angle of the mandible and ascending ramus. Late stage. Often a third molar or a second molar is enclosed within the lesion. Note the distention and thinning of the cortical bone, which is only visible with low energy reverse Towne projection or even better in CT.

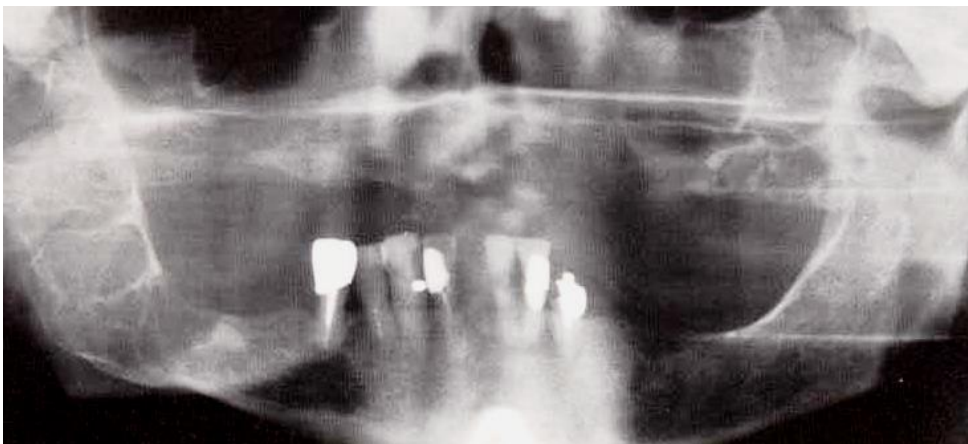


Fig. 10.7. Recurrent ameloblastoma in the right ascending ramus of the mandible. The radiographic picture is similar to a myxoma. The condyle is seldom involved even with such large lesions; however, spontaneous fractures are possible.

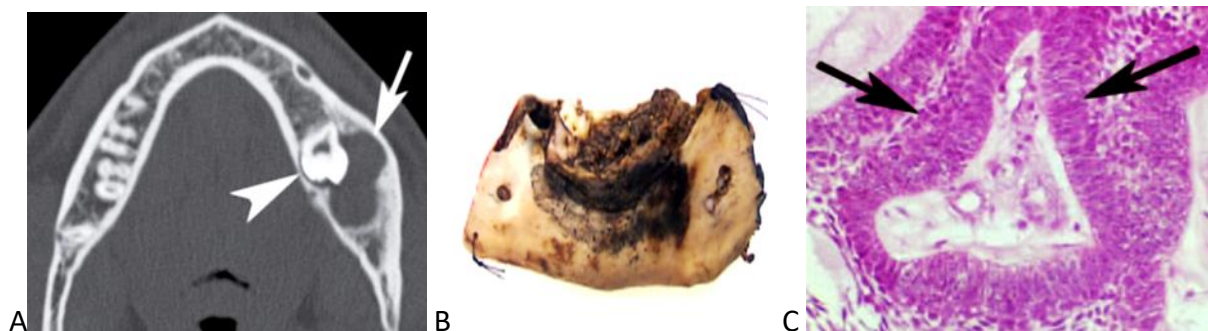


Fig. 10.8. Ameloblastoma in a 20-year-old man. (A) CT scan demonstrates a multiloculated cystic lesion (arrow) within the left mandible. The crown of an impacted tooth (arrowhead) identified within the lesion is a clue to the diagnosis. (B) Photograph shows a soft-tissue mass in the resected mandible. (C) High-power photomicrograph (hematoxylin-eosin [H-E] stain) reveals numerous well-defined islands of odontogenic epithelium with palisading and polarizing nuclei (arrows).

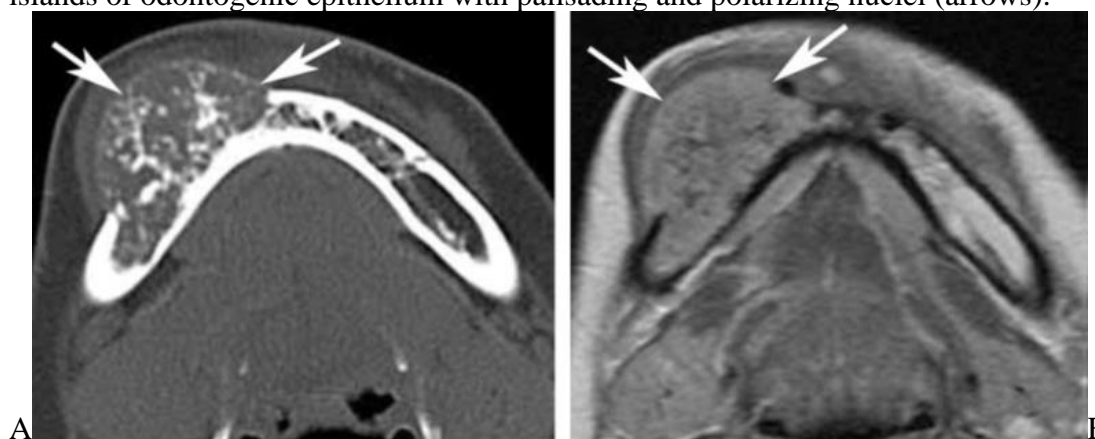


Fig. 10.9. Desmoplastic ameloblastoma in a 30-year-old woman. CT scan (A) and contrast-enhanced T1-weighted magnetic resonance (MR) image (B) demonstrate an expansile enhancing lesion within the right mandibular body (arrows) that causes significant buccal cortical destruction.

Ameloblastic Fibroma

The most common ameloblastic mixed tumor is probably the ameloblastic fibroma. It may be detected as early as the end of the first decade of life and can be definitively diagnosed radiographically only in this early stage. While the follicular cyst is classically located at the cemento-enamel junction, in its early stages the ameloblastic fibroma appears to sit like a “hat” upon the occlusal surface of the affected tooth. As the lesion increases in size, this characteristic is no longer discernible, and this can render differential diagnosis vis-a-vis a follicular cyst or a true ameloblastoma impossible.



Fig. 10.10. Ameloblastic fibroma in an 8-year-old male. One can see in (his and also in the following radiograph) how the ameloblastic fibroma “sits” upon the occlusal surface of the second molar. In contrast, follicular cysts appear to attach to the cemento-enamel junction.

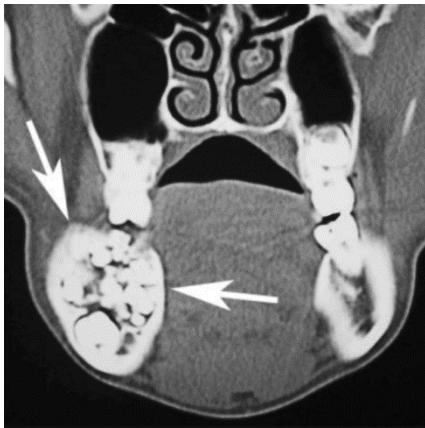


Fig. 10.11. Ameloblastic fibroma in a 15-year old boy. Coronal reformatted CT image reveals a slightly lobulated, well-defined expansile lesion (arrows) within the right mandibular body.



Fig. 10.12. Ameloblastic fibroma in an 8-year-old female. This somewhat more advanced case demonstrates how the follicular sac is now opening, and how this obscures the previously clear radiographic sign. Note also the displacement of the tooth bud of tooth 48 in the ascending ramus.

Cementoma

Today, the term cementoma includes a number of cement-forming changes in the jaws; however, only some of them may be classified as odontogenic tumors whereas others are of mesenchymal origin, or may even be reactive in etiology. This latter group includes the periapical cemental dysplasia that is often observed primarily in middle-aged females. The radiographic picture of this lesion will be discussed here in connection with those of the cementoblastoma and the cement-forming fibroma. Indistinct transition forms and combined forms render difficult any definitive and radiographically diagnostic or clinically practical classification of these entities. Only histopathologic observation of excised material can provide such information. Because fine tissue examination and appropriate therapy are usually only used in cases where differential diagnosis is doubtful, one is reconciled in practice to recognizing basic diagnostic/radiographic characteristics of such radiographically evident changes.

Periapical cemental dysplasia

This type of cementoma affects the mandibular anterior teeth in females usually in middle age. An initial “fibrous” stage may be confused with a granuloma (vitality testing!). The initial stage is followed by stages with accumulation of material having the density of calcified tissue. Multiple manifestations in the mandible may sometimes be combined with solitary lesions in the maxilla; cementoblastoma of the premolar and molar regions of the mandible may also occur concomitantly.

Cementomas in the family of periapical dysplasias occur most commonly in middle-aged females, particularly in the anterior region of the mandible. In such cases, especially in younger persons, individual anterior teeth in the maxilla may also be involved. Schematically, such changes can be divided into three stages of development. They usually occur in multiple form, and are most common in non-Caucasian races, sometimes combined with cementoblastomas of the premolar and molar regions of the mandible.

Localization. Mandibular anterior region, sometimes combined with lesions on individual teeth of the maxillary anterior segment or with cementoblastomas in the posterior mandibular regions.

Examination technique:

- panoramic radiography,
- concomitant use of targeted periapical radiographs.

Radiographic signs. Periapical radiolucencies and shadows where boundaries are not always sharply demarcated. Three stages of development may be observed:

- stage of fibrosing, with circumscribed periapical radiolucency,
- stage of initial calcification, with flake-like shadowing,
- terminal stage with evenly dense shadowing; the lesion depicts the typical root contact.

Differential diagnosis:

- chronic apical periodontitis (vitality testing!),
- hyperparathyroidism,
- with shadowing: infarct of bone,
- paget's disease of bone, depending upon age and gender.

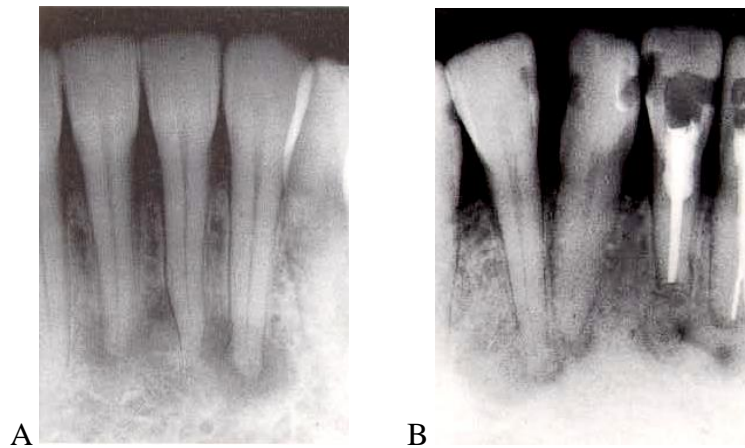


Fig. 10.13. (A) Periapical cemental dysplasia. This periapical radiograph depicts an early "fibrous" stage. It is imperative to test the vitality of the apparently affected teeth. (B) Periapical cemental dysplasia. Typical results of an incorrect radiographic interpretation (note root canal treatment on teeth 31 and 32). Teeth 42 and 41 exhibit the second stage described as deposition of material with the density of calcified tissue.



Fig. 10.14. Periapical cemental dysplasia. Second and third stages of cementum deposition in two films from the same patient. The affected teeth remained vital during the 4 to 6-year development

from the incipient stage.

Cementoblastoma

This tumor, which is particularly common in young females of non-Caucasian races, preferentially affects the premolar and molar segments of the mandible. It may occur as a solitary lesion or in multiple forms. Radiographically it often depicts only a weakly visible uniform opacity which, in comparison to the surrounding areas, appears as a radiolucency. It may be difficult to distinguish this lesion from an ossifying fibroma.

An additional form of the cementoblastoma usually occurs as a solitary lesion in the mandibular first molar area, and affects mostly young males. Early stages appear coarsely structured with radiolucencies due to connective tissue appearing as spots or strands. In more mature stages, the lesions may achieve remarkable size and a high degree of radiopacity. The roots of the affected tooth may initially be overlaid with radiolucencies, giving the appearance of resorptions.

Cementoma, in the general classification of cementoblastoma, occurs in the second and third decades of life, slightly more frequently in males.

Localization. Cementoblastomas are found almost exclusively in the premolar and molar regions of the mandible. They may be observed very rarely in the posterior segments of the maxilla.

Examination technique:

- panoramic radiography,
- concomitant use of targeted periapical films.

Radiographic signs. Often difficult to discern, but with well-demarcated shadows. The uniform or spotty shadowing of all grades suggests deposits of material with density similar to calcifying tissue.

Differential diagnosis:

- periapical lesions and bone scars,
- bone infarct,
- paget's disease of bone, depending upon age and gender,
- osteoblastoma, without root contact,
- ossifying fibroma, no root contact.

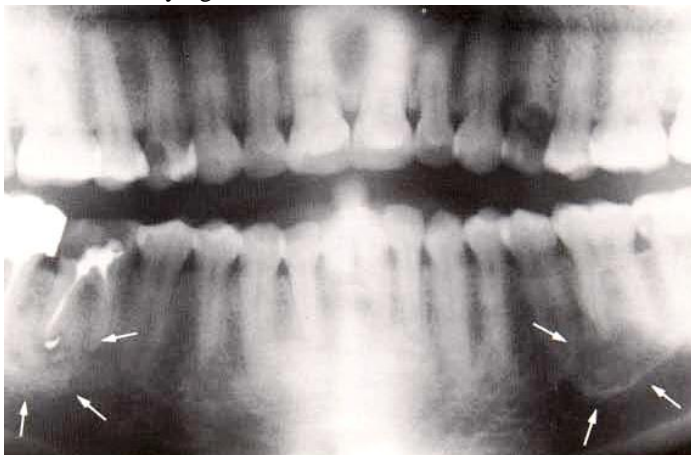


Fig. 10.15. Cementoblastoma around the root tips of the first permanent molars in the mandible. A slight, uniform opacity is visible (arrows), with opaque borders near tooth 36. The over-filled root canal of tooth 46 exhibits a reactive sclerosis of the surrounding bone.



Fig. 10.16. Cementoblastoma. The moderately dense opacity created by this lesion, in contact with the lamina dura and the root of tooth 45 is surrounded by an opaque boundary (arrows).



Fig. 10.17. Cementoblastoma. Tooth 37 exhibits a cementoblastoma that encompasses both roots. Following extraction of the tooth, such cementoblastomas remain in the jaw where they are frequently demarcated, resulting in sequestration.



565

Fig. 10.18. Cementoblastoma on tooth 36. This early stage is characterized by a spotty structure, deposition of material with cementum-like density, and a highly fibrous component.



566

Fig. 10.19. Cementoblastoma. The opaque structure of this fully developed lesion is surrounded by a wide radiolucent band and almost completely covers the root tips of tooth 36.



567

Fig. 10.20. Cementoblastoma. The obvious demarcation of the cementoblastoma that developed around the root of tooth 44 is most likely the result of chronic, apical periodontitis on tooth 46. Note the primary chronic osteomyelitis in this section of the mandible, which was probably induced by the lesion.

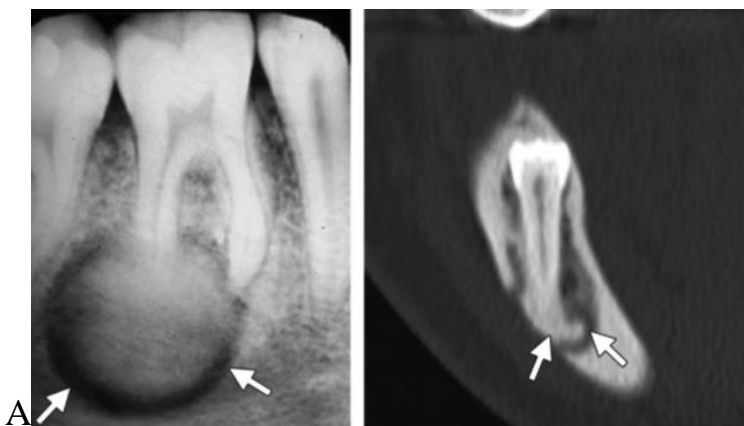


Fig. 10.21. Cementoblastoma. Bite-wing radiograph obtained in an adult patient (A) and coronal CT image obtained in a 34-year-old woman (B) show a periapical sclerotic lesion with sharp margins and a lucent or low-attenuation halo (arrows) that is fused to the root of the tooth. Cementoblastoma arises in the molar or premolar region in 90% of cases.

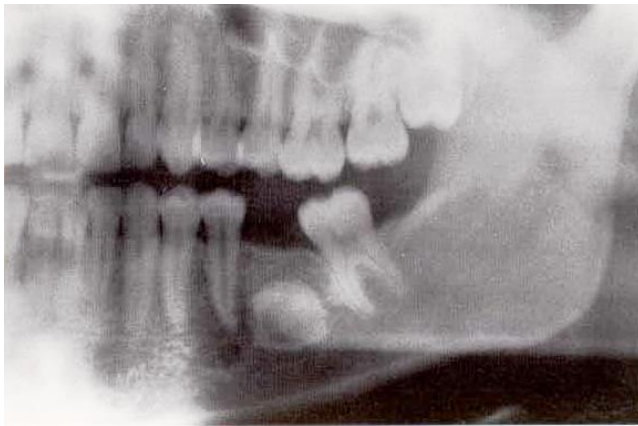


Fig. 10.22. Cementoblastoma. Following tooth extraction, cementoblastomas that are not removed, for example here in the region of tooth 36 in a 21-year-old female, may remain symptom-free or may sequester after inflammatory stimulation from apical or marginal periodontitis. The radiolucency around the root tips of tooth 35 and tooth 33 indicate that in this region more cementoblastomas exist in the stage of fibrosis.

Cement-forming fibroma

Cementomas in the general classification of cement-forming fibromas are radiographically similar to certain forms of cementoblastoma as well as ossifying fibroma; for this reason it is virtually impossible to differentiate them radiographically. Usually only in later stages do these lesions exhibit a detectable expansion with signs of distention and thinning of the cortical bone. These lesions develop frequently in middle-aged females, but also sometimes in young males; for this reason and because of their localization they may be confused with a solitary bone cyst.

Odontoma is a lesion that is viewed today more as a developmental abnormality than as a true tumor even though, for example, the ameloblastic fibro-odontoma could equally well be categorized as a mixed tumor. Depending upon the degree of development of the lesion, it is possible to differentiate two basic forms which may appear radiographically anywhere from amorphous masses to completely differentiated teeth. The first form always exhibits a poorly organized and very opaque conglomeration of dental elements such as enamel, dentin, cementum and connective tissue; such lesions are called **complex odontoma**. If the lesion consists of one or several rudimentary or hilly formed teeth, it is a **compound odontoma**.

Depending on their location, supernumerary tooth buds have the capacity to develop unimpeded, concurrent with certain stages of dental development. Therefore the classification **odontoma** is appropriate for all stages of abnormal dental development, from a scarcely detectable radiolucency caused by a non-calcified tooth primordium to a fully formed supernumerary tooth.

Many of the cementoblastomas that are diagnosed persist for years without causing any clinical manifestations. Others, however, may show demarcation and sequestration as a result of inadequate vascularization, trauma, or because of inflammation in the surrounding tissues. Even a pathologist may encounter difficulty differentiating between osteomyelitis, ossifying fibroma or cementoblastoma, depending on the site of the histologic section.

Localization. The several variations of complex odontoma are most commonly observed in the region of the mandibular third molars in males, and in the tuberosity region in females. The compound odontoma is detected almost exclusively in the anterior segment of both mandible and maxilla.

Examination technique:

- panoramic radiography,
- concomitant targeted periapical films,
- CT of the mandibular angle (mandibular nerve),
- CT of the tuberosity region (maxillary sinus).

Radiographic signs. The complex odontoma exhibits either a sharply demarcated, amorphous and uniform shadow surrounded by a narrow radiolucent border, or an exceptionally radiopaque shadow with irregular borders created by more highly differentiated enamel segments. Impacted adjacent teeth are a common finding. The compound odontoma exhibits rudimentary or completely formed teeth, which are usually surrounded by a radiolucent border.

Differential diagnosis: With a typical localization, none.

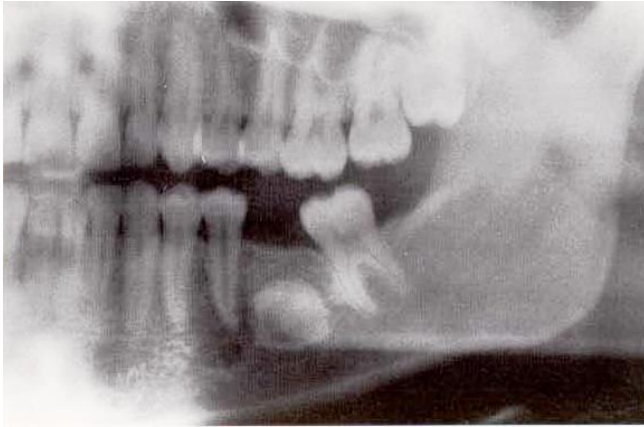


Fig. 10.23. Cementoblastoma. Following tooth extraction, cementoblastomas that are not removed, for example here in the region of tooth 36 in a 21-year-old female, may remain symptom-free or may sequester after inflammatory stimulation from apical or marginal periodontitis. The radiolucency around the root tips of tooth 35 and tooth 33 indicate that in this region more cementoblastomas exist in the stage of fibrosis.

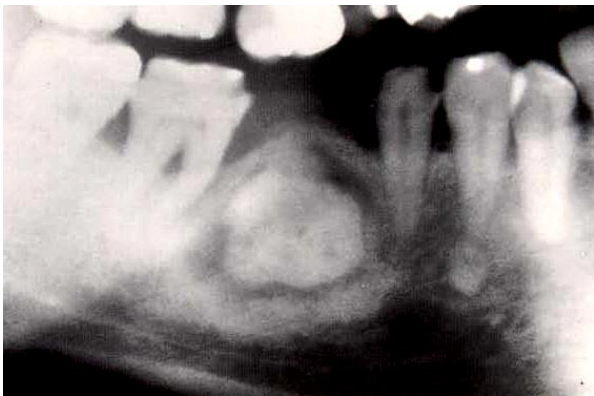


Fig. 10.24. Demarcated cementoblastoma. The expansive cementoblastoma in the extraction site of tooth 46 in a 40-year-old male is surrounded by radiographic signs of chronic inflammation and reactive sclerosis; this lesion is in the sequestration stage. The likely cause was chronic marginal periodontitis on tooth 47. Note the periapical cemental dysplasia on tooth 44.



Fig. 10.25. Cementum-forming fibroma. This unilateral occlusal radiograph of the mandible, which was intentionally taken with an occlusal projection, exhibits the structural details of a cementum-forming fibroma in a 19-year-old male. The well-demarcated lesion allows one to easily discern distention and thinning of the cortical bone. Also visible is the deposition of cementum with a radiographic density that is similar to calcified tissue.

Technical tip for correct projection of large, radiolucent cysts, tumors and tumor-like lesions:
 - by using reduced exposure data and appropriate standard projections the normally much thinned osseous

demarcation can be rendered visible. The clear depiction of demarcations and structural details is often of decisive importance for differential diagnosis, and above all in comparison with malignant lesions.

Odontogenic Myxoma

This benign, mucous-containing tumor that originates from the tooth bud affects both sexes equally. It grows slowly and, in later stages, leads to distention of the jaws and thinning of the distended cortical plate. The characteristic radiographic appearance in the mandible resembles soap bubble-like or wispy structures, often described as a “torn fishing net.” In the maxilla, on the other hand, structures are difficult to discern. The radiographic signs are reminiscent of those of an ameloblastoma or a follicular cyst. The odontogenic myxoma has a particular tendency to recur.

An uncommon benign neoplasm (3%–6% of odontogenic tumors), odontogenic myxoma originates from mesenchymal odontogenic tissue. This tumor can be locally aggressive and cause considerable destruction of adjacent bone and soft-tissue infiltration (1). Odontogenic myxomas develop only in the bones of the jaws (2) and have a slight predilection for the maxilla. They are typically found in 10–30-year-old patients, slightly more often in female patients (1). Congenitally missing or unerupted teeth may be associated with this neoplasm. Odontogenic myxomas are usually painless.

Both sexes are equally affected. As a fibromyxoma, this lesion occurs as a benign mesenchymal tumor with little tendency toward recurrence, also in nonoral skeletal components, where it may develop from dissipated mucous-forming connective tissue. As an odontogenic myxoma, it derives from odontogenic mesenchyme, affects young persons and young adults in the second and third decades of life, and commonly recurs in the jaws after surgical excision.

Localization. The odontogenic myxoma is generally observed in the mandible, and typically in the molar regions at the angle. It is seldom seen in the maxilla.

Examination technique:

- panoramic radiography, with reduction of exposure data in late stages,
- reverse townes projection with reduced exposure data,
- lateral mandibular occlusal films, and with reduced exposed time,
- CT, indicated for lesions in the maxilla, and in later stages.

Radiographic signs. Odontogenic myxomas bear a close resemblance to the soap bubble-like picture of ameloblastoma. If it is possible to depict fine structure, one can observe the thin, wispy and “disintegrated” trabecular pattern, with more straight lines. In advanced cases, the cortical bone is thinned and distended. Displacement of teeth with inclusions is possible.

Differential diagnosis:

- ameloblastoma in the region of the angle of the mandible,
- giant cell granuloma in the mandibular premolar region,
- aneurysmal bone cyst in the mandibular premolar region.



Fig. 10.26. Odontogenic myxoma in the left mandibular angle. The picture shows very well the infiltrative growth that has dissolved the structures of the mandibular canal. Tooth 38 appears displaced and enclosed.

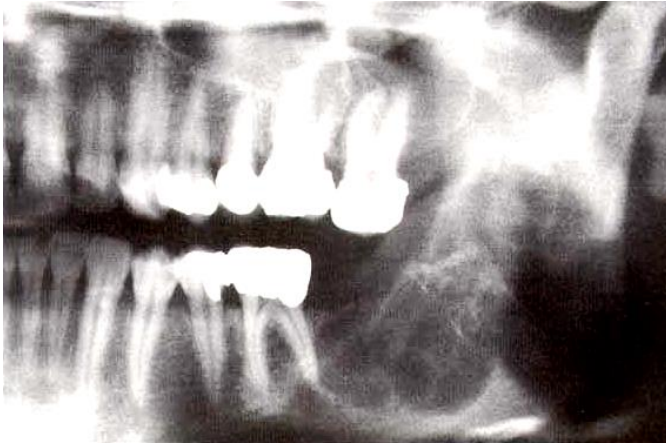


Fig. 10.27. Recurrent odontogenic myxoma. The structural picture is reminiscent of a multilocular ameloblastoma with soap bubble-like appearance.

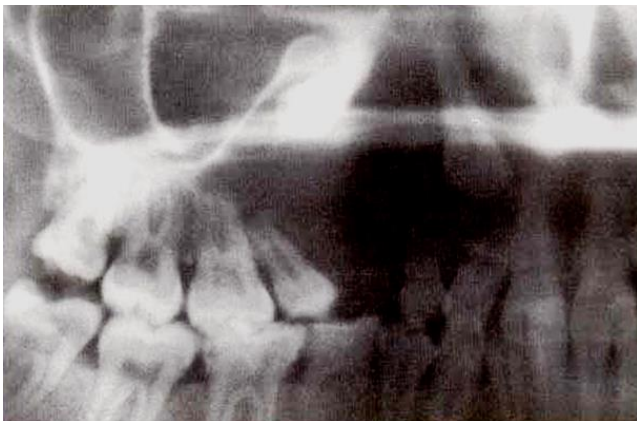


Fig. 10.28. Odontogenic myxoma of the maxilla. Only the lack of the demarcation line typical for follicular cysts provides a vague hint about the nature of this radiolucency. It is impossible to distinguish it radiographically from a follicular cyst or an ameloblastoma.



553

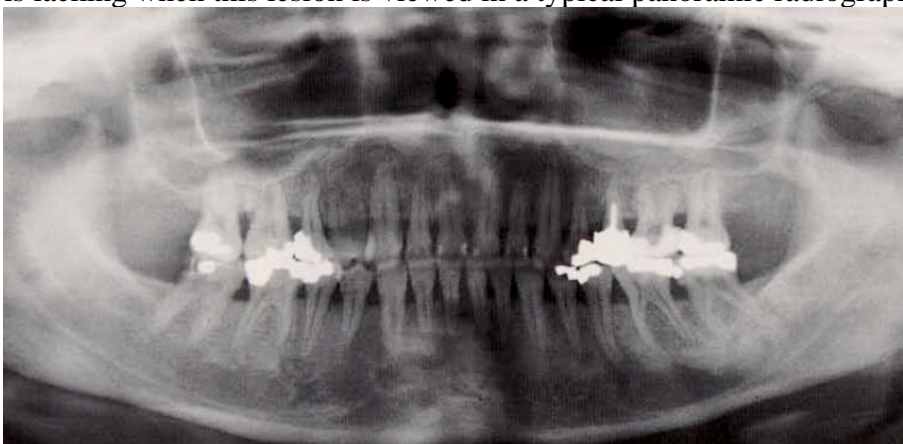
Fig. 10.29. Odontogenic myxoma of the mandible, viewed in an occlusal film. The radiographic differential diagnosis between myxoma and ameloblastoma localized in the mandibular molar area can possibly be clarified through use of a low energy, lateral occlusal projection. As seen in the figure, this projection is superior to other methods for showing the later stages of the odontogenic myxoma with its typical structure, and including distention, cortical thinning and wispy trabecular pattern.



Fig. 10.30. Myxoma in the articular process. Lateral tomography of the ascending ramus exhibits the compartmentalized structure of this nonodontogenic myxoma. This type of myxoma, which also occurs in other parts of the skeleton, tends to behave less aggressively than the odontogenic myxoma, and recurrence is rare.



Fig. 10.31. Identical case as seen in a reverse Towne projection. This film depicts the ascending ramus in a frontal plane, and reveals the expanse of the tumor in the third dimension, which is lacking when this lesion is viewed in a typical panoramic radiograph.



559

Fig. 10.32. *Periapical cemental dysplasia.* Multiple lesions in a 45-year-old female in the mandibular anterior area and in the premolar and molar regions of the mandible. All mandibular teeth reacted positively to the CO₂ vitality test.

In some cases the maxillary anterior teeth may also exhibit radiographic signs of lesion formation besides the classic site in the mandibular anterior segment. It must

be kept in mind, however, that osteoblastoma of the maxillary anterior region not infrequently leads to a similar form, and that the radiologist often makes clinical decisions only on the basis of radiographic characteristics of the root contact. Because the teeth in both cases remain vital, therapy need be instituted in most cases only when clinical manifestations occur.

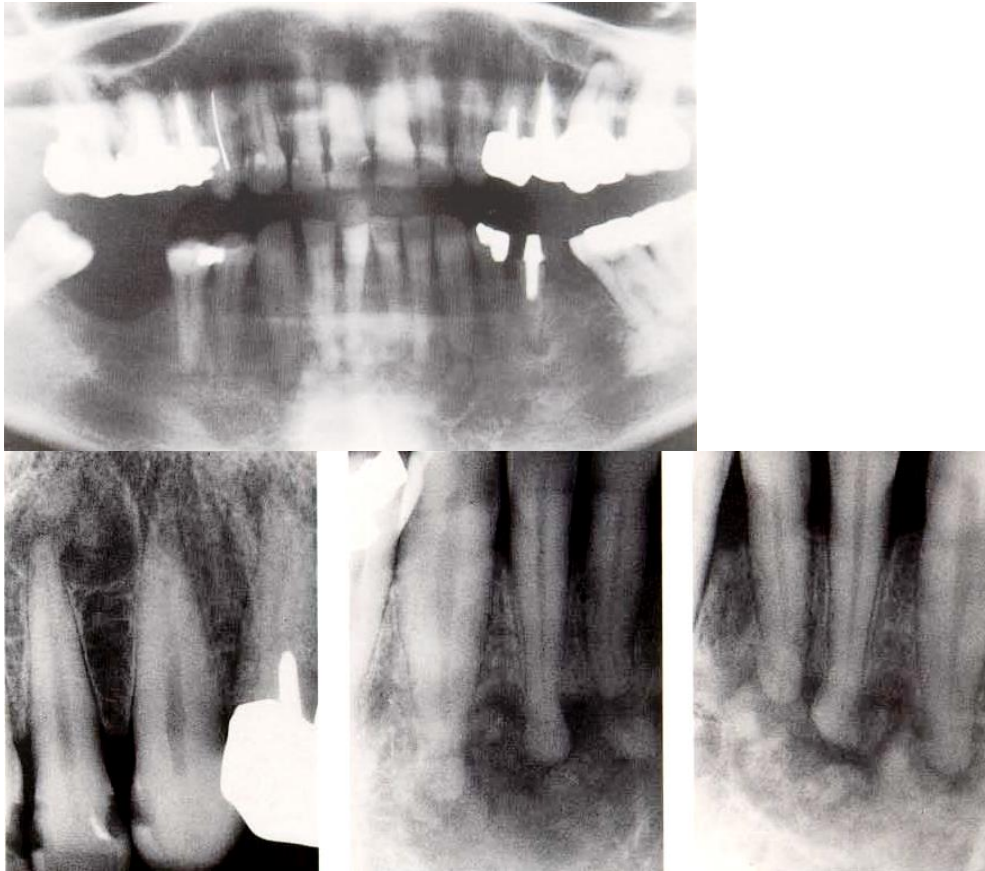


Fig. 10.33. Periapical cemental dysplasia in a 50-year-old female. The panoramic radiograph and the three following periapical films exhibit the second stage of cementum formation on teeth 33-43 and on teeth 21 and 22. In the mandibular anterior segment, the lesions appear to coalesce and the root tips of the affected teeth exhibit typical root contact with material having the density of calcified tissue.

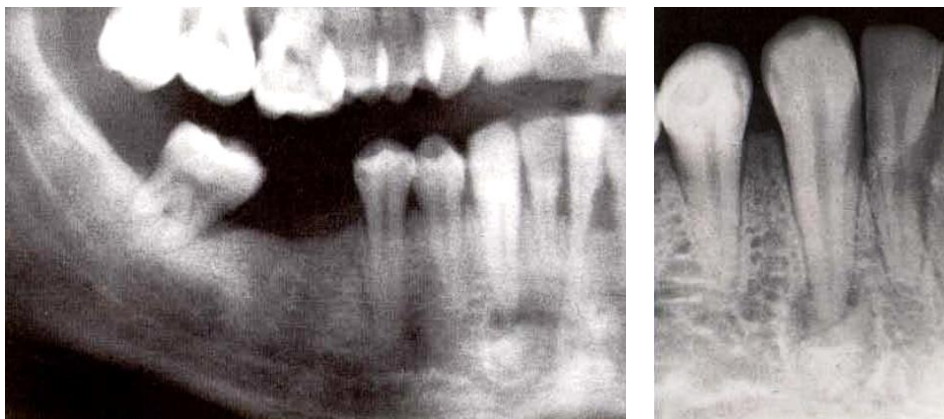


Fig. 10.34. Periapical cemental dysplasia. The panoramic radiograph and the periapical film depict the solitary involvement of tooth 43 with signs of complete shadowing in the third stage, as well as the formation of a radiolucent border.

Odontoma

The amorphous form of this odontoma occurs most frequently in young males, usually in the area of the mandibular third molars and has a tendency to erupt. These lesions are not particularly radiopaque and therefore must be visualized using low-energy radiographic exposures. Primarily in females, a more highly differentiated and extremely radiopaque form of odontoma develops that exhibits irregular borders in the radiograph. It may be located in either maxilla or mandible.

An odontoma is an odontogenic hamartomatous malformation, often referred to as a tumor, that is composed of any or all odontogenic tissues in various states of morpho- and histodifferentiation. It is the most common odontogenic “tumor” (67% of cases). There are two types of odontomas: complex and compound. Complex odontomas contain multiple masses of dental tissue and are seen as well-defined lesions with amorphous calcifications on radiographs. The more common compound odontoma contains multiple teeth or toothlike structures. Odontomas are typically discovered in the 2nd decade of life, often during the search for a nonerupted permanent tooth.

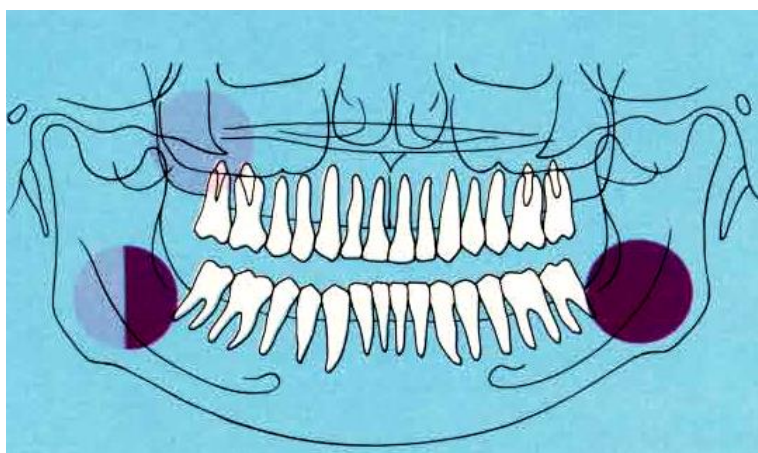


Fig. 10.35. Sites of odontomas. The most frequent sites are show for males (violet) and for female (pale violet).



Fig. 10.36. Complex odontoma. The low energy radiograph permits easy depiction of the layered masses of the odontoma. The lesion has displaced tooth 38, and is in the process of clinical eruption. In this 25-year-old male, the area surrounding the lesion exhibits reactive sclerosis due to chronic inflammatory irritation.

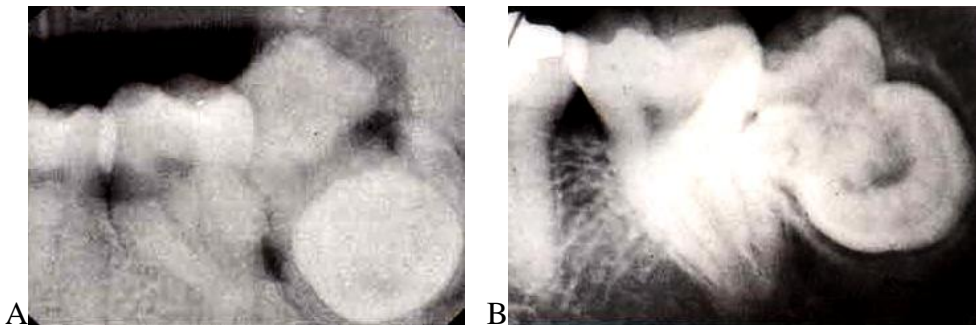


Fig. 10.37. (A) Complex odontoma. The periapical radiograph reveals an erupting complex odontoma in the same patient as above. (B) Intermediate type odontoma. For comparison, this periapical film exhibits a mixed odontoma.

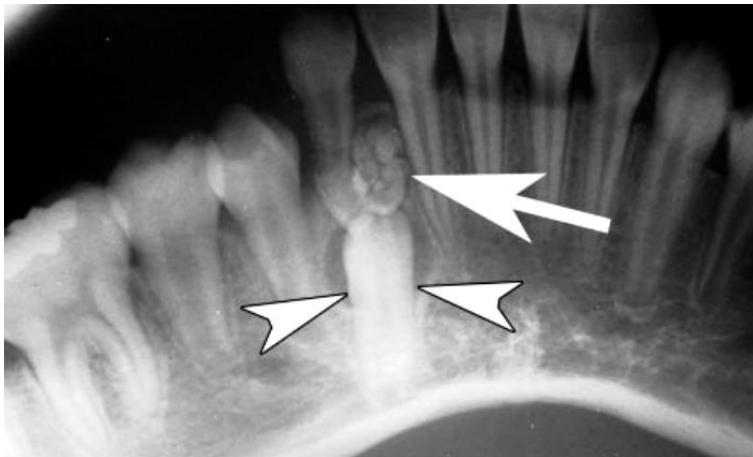


Fig. 10.38. Compound odontoma in a 28-year-old woman. Panorex image demonstrates a focus of radiopaque enamel surrounded by a thin radiolucent follicle (arrow). Note the impacted tooth (arrowheads) deep to the odontoma.



Fig. 10.39. Cystic odontoma in a 17-year-old boy with painful third molars. An abnormality was discovered incidentally on a panoramic radiograph obtained for planning of tooth extraction. Panoramic radiograph shows a large, focal area of heterogeneous calcification with displaced second and third molars. The opaque portions are surrounded by a lucent follicular space (arrowhead). There is marked cystic expansion of all bone margins (arrows).

Nonodontogenic Tumors and Pseudotumors

Benign Lesions

The title of this chapter is a simplified term chosen to describe a summary of the radiographic characteristics of the most often encountered benign and malignant tumors, granulomatous lesions and osteofibrous lesions of the jaws. As in the previous chapter, it must be clearly pointed out how important the experience of the person interpreting the radiograph is for the results of any radiographic examination because in most cases it is fundamentally impossible for the radiologist to provide a "histologic" diagnosis. The age and sex of the patient as well as the site of the lesion will provide important clues, as will the complete description of the clinical situation. Nevertheless, there will always be infrequent manifestations of rare diseases as well as misleading imitations of apparently clearly classifiable radiographic signs. Such radiographic signs may deceive even the experienced radiologist. For these reasons, we would warn against premature radiographic diagnoses.

The title of this chapter is a simplified term chosen to describe a summary of the radiographic characteristics of the most often encountered benign and malignant tumors, granulomatous lesions and osteofibrous lesions of the jaws. As in the previous chapter, it must be clearly pointed out how important the experience of the person interpreting the radiograph is for the results of any radiographic examination because in most cases it is fundamentally impossible for the radiologist to provide a "histologic" diagnosis. The age and sex of the patient as well as the site of the lesion will provide important clues, as will the complete description of the clinical situation. Nevertheless, there will always be infrequent manifestations of rare diseases as well as misleading imitations of apparently clearly classifiable radiographic signs. Such radiographic signs may deceive even the experienced radiologist. For these reasons, we would warn against premature radiographic diagnoses.

Central reparative giant cell granuloma

This type of granuloma grows expansively within bone and occurs more frequently in females under the age of 25 than in males. It is characterized by an asymptomatic swelling of the affected jaw that is manifested by facial asymmetry.

The central giant cell granuloma is most often observed in young females, usually in the mandible with a predilection for localization in the premolar region and sometimes also in the mandibular anterior area. Radiographically, the lesion exhibits a sharply demarcated, soap bubble-like radiolucency with thinning of the compact bone in advanced cases. For this reason it is hardly possible to differentiate it from the ameloblastoma, although the latter is more common in the molar regions and at the angle of the mandible. The lesion may also be mistaken for a solitary bone cyst.

Localization. The central reparative giant cell granuloma usually occurs in the mandible, and preferentially in the premolar region. It is less common (3:1) in the maxilla.

Examination technique:

- Panoramic radiography,
- Reverse Towne projection with maximum jaw opening,
- Lateral mandibular occlusal radiograph, with reduced exposure time,
- Computed tomography in late stages and if tumor is sited in the maxilla.

Radiographic signs. The isolated or multilocular radiolucencies are sharply demarcated and exhibit soap bubble-like structures with lobulated margin contours.

In late stages, the cortical plate of bone may be distended and thinned. The differential diagnosis from ameloblastoma is difficult.

Differential diagnosis:

- Ameloblastoma,
- Eosinophilic granuloma,

- Odontogenic cyst,
- Aneurysmatic and solitary bone cysts.

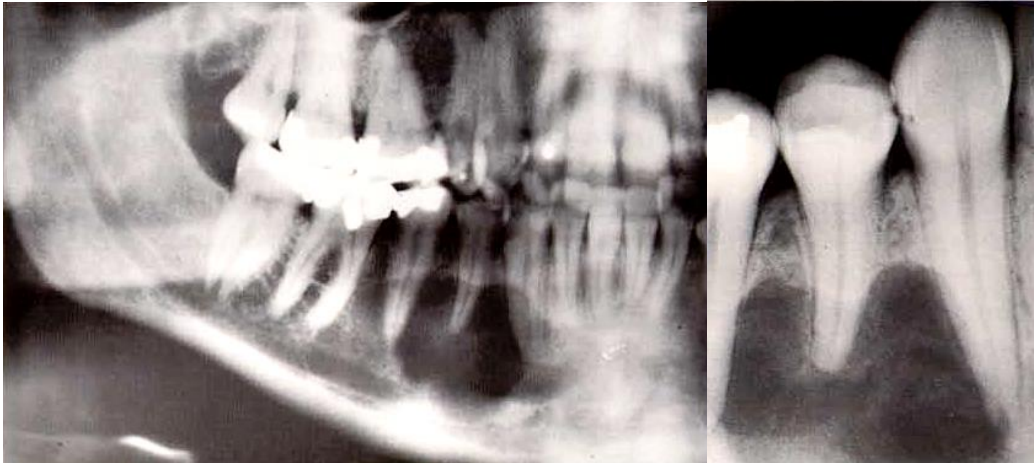


Fig. 10.40. Central giant cell granuloma. In the panoramic radiograph (left) the soap bubble-like structure is easily seen; this leads to easy confusion with an ameloblastoma. The periapical radiograph (right) cannot provide an overview of the extent of the lesion.

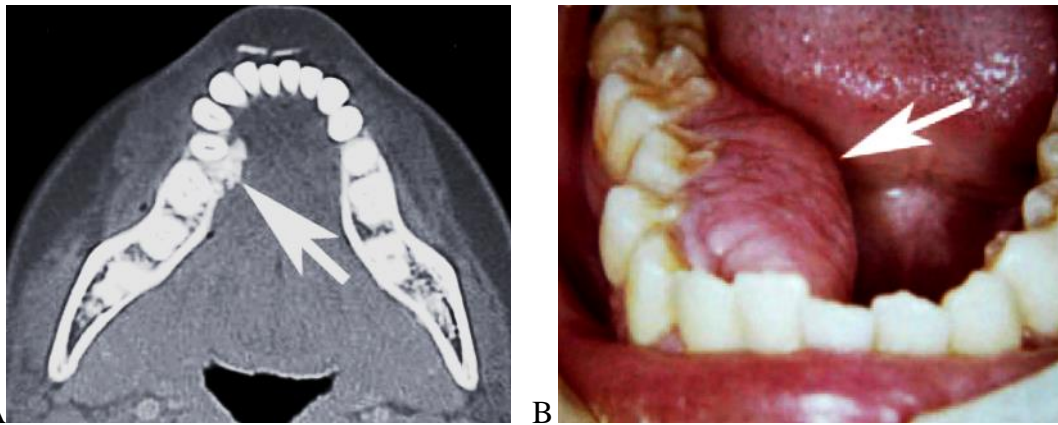
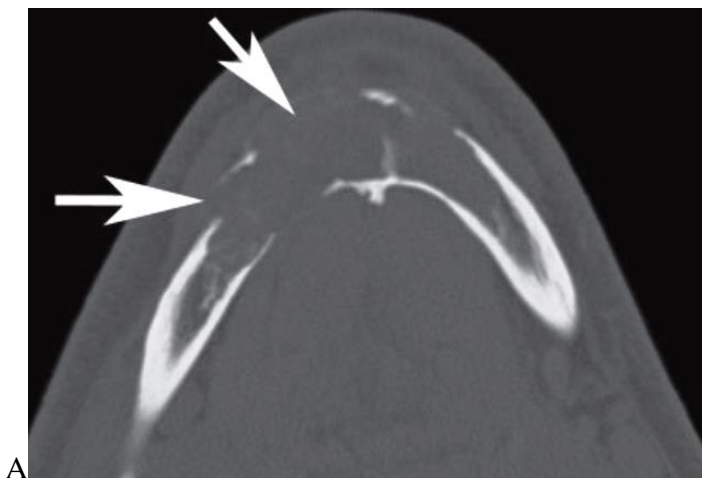
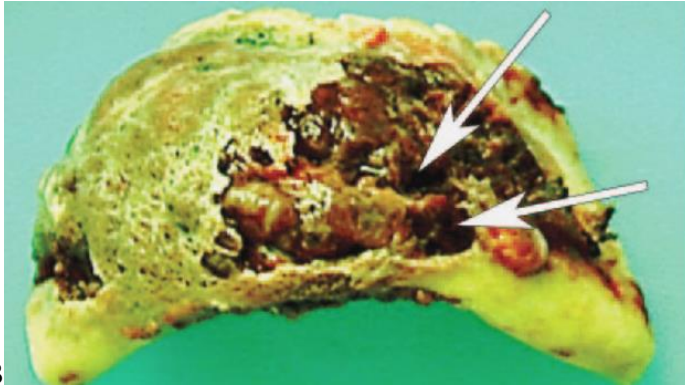


Fig. 10.41. Epulis fissuratum in a 22-year-old woman. (A) CT scan shows calcification and soft-tissue thickening (arrow) in the lingual aspect of the right mandible. (B) Intraoral photograph reveals a lump (arrow) in the gingiva.





B

Fig. 10.42. Central giant cell granuloma in a 34-year-old man. (A) CT scan (bone windowing) demonstrates a cystic lesion (arrows) within the mandible. Note the erosion of the mandibular cortex. (B) Photograph of the gross resected specimen shows multiple cystic cavities (arrows). Photomicrography with H-E stain revealed multinucleated giant cells within the lesion.

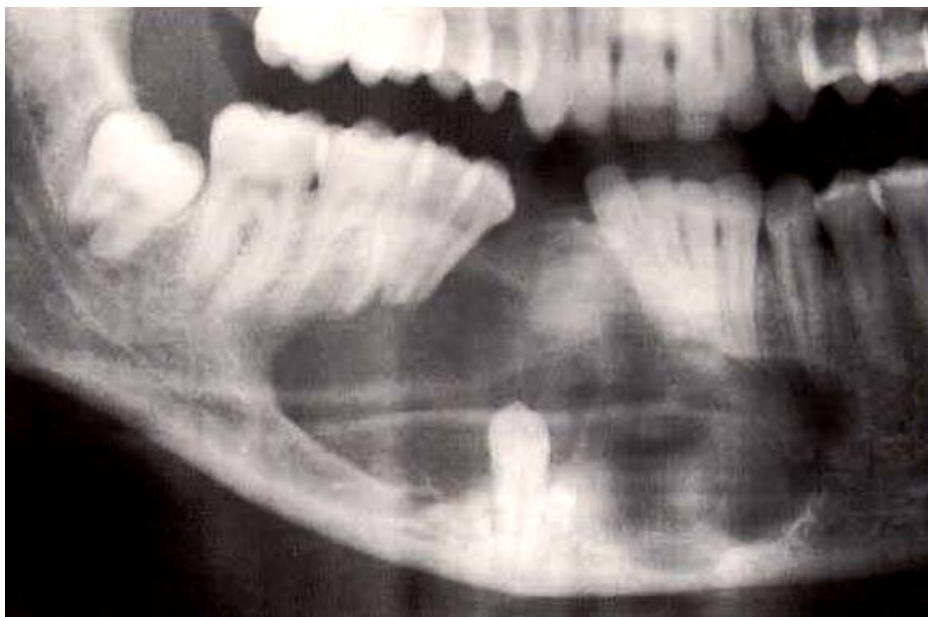


Fig. 10.43. Central giant cell granuloma. The impacted and ankylosed tooth 43 and the displacement of the teeth may also be signs of a follicular cyst; on the other hand, the fine septum and the soap bubble-like contour resemble an ameloblastoma.

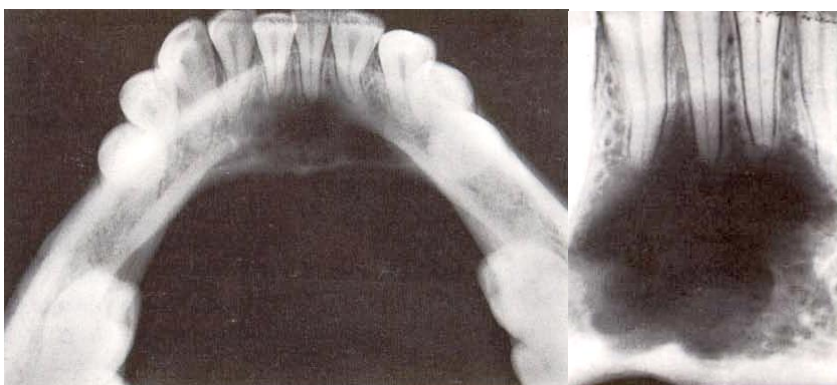


Fig. 10.44. Central giant cell granuloma. The occlusal radiograph (left) and especially the periapical film (right) depict the multilocular and soap bubble-like character of the lesion. Note the thinned and distended compact bone.

Peripheral reparative giant cell granuloma

The lesion is most frequently found on the gingiva of younger females. Clinically the lesions may resemble normal gingiva or may exhibit brownish to bluish exuberances of firm or soft consistency. They usually exhibit limited expanse (up to 2 cm in diameter), and may erode the alveolar bone.

- The peripheral reparative giant cell granuloma occurs primarily as a gingival tumor in young adult females and may achieve a diameter of up to 2 cm. The lesion may elicit radiographically demonstrable osseous defects in the anterior region of both mandible and maxilla. The lesion grows along the alveolar entrance into the periodontal ligament space, creating bowl-like defects of the alveolar ridge. The lesions tend to recur if incompletely removed. A cursory examination of the radiograph may lead the clinician to a diagnosis of a periodontal lesion.

Localization. These lesions are more often found in the anterior region of the mandible than in the maxilla. A typical characteristic is the proliferation of the lesion along the periodontal ligament space.

Examination technique:

- Panoramic radiography,
- Supplemental radiographs, including periapical films taken with reduced exposure time to display the cervical region of the tooth.

Radiographic signs. Wedge-shaped expansion of the periodontal ligament space at the entrance to the alveolus; in later stages, localized bowl-like defect.

Differential diagnosis:

- Marginal periodontitis.

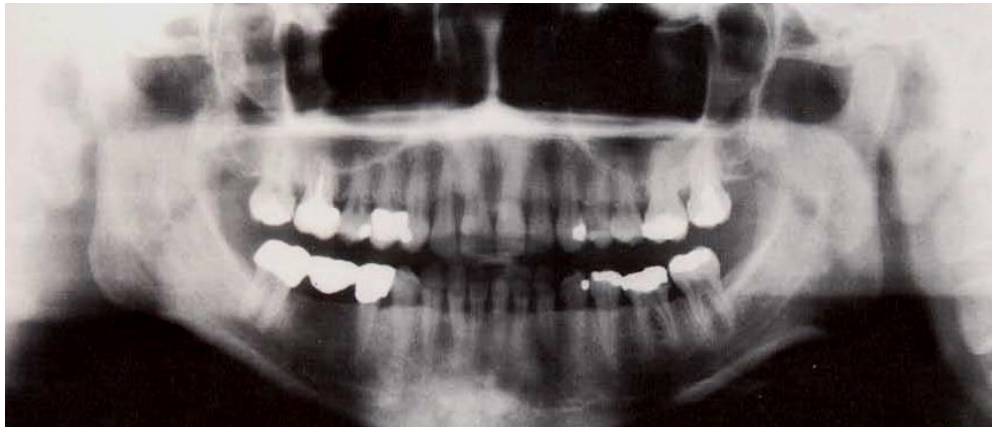


Fig. 10.45. Peripheral giant cell granuloma. The panoramic radiograph exhibits a peripheral reparative giant cell granuloma with bowl-like osseous defects in the region of tooth 12 in this 38-year-old female.

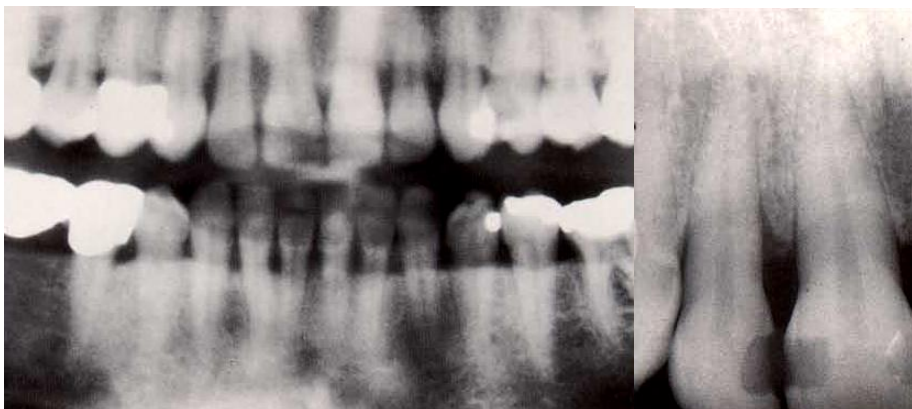


Fig. 10.46. Peripheral giant cell granuloma. This section from the above panoramic radiograph (right) and the periapical film (left) depict the situation in detail. Note the expansion of the lesion along the periodontal ligament space and the cuff-like expansion of the alveolar entrance.

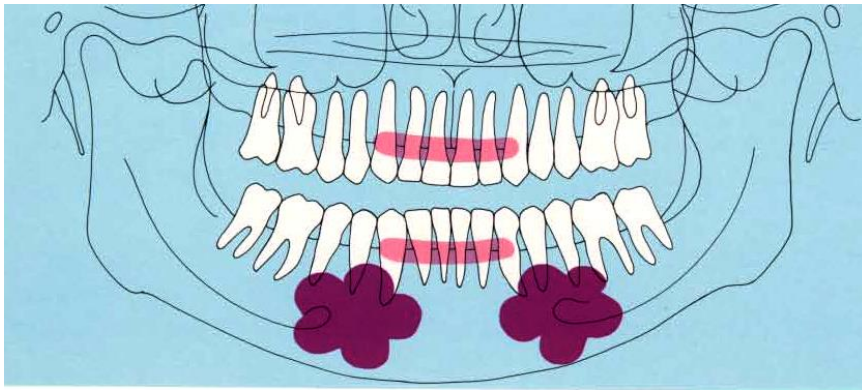


Fig. 10.47. The most common sites for central (dark) and peripheral (light) reparative giant cell granulomas.

Histiocytosis X

This term includes three different disease entities that are characterized histologically by the proliferation of histiocytes and by lipid storage. It is possible to differentiate a lethal form in small children (Letterer-Siwe disease), a chronic disseminated form that affects school children (Hand-Schiiller-Christian disease), and a relatively moderate localized form known as *eosinophilic granuloma* that is observed in adolescents but also in older patients. The latter disease often leads to tooth mobility and bone destruction, especially in the mandible. Extraction wounds heal particularly poorly.

- Under the rubric “histiocytosis X” are grouped a series of lesions characterized by histiocyte proliferation. To this group of diseases belongs the eosinophilic granuloma, which results from an increased infiltration of eosinophilic granulocytes into tissue exhibiting histiocyte proliferation, Hand-Schiiller-Christian disease and the Letterer-Siwe syndrome. The eosinophilic granuloma depicted here may affect all age groups beginning at 20 years, and it may occur as solitary or multiple lesions in the jaws. A pathognomonic radiographic sign are teeth which “hang in the air,” while the radiolucency often exhibits mildly sclerosed and arcuate bony boundaries. Periapical radiographs may give the appearance of advanced stages of marginal periodontitis, but clinically one observes that the pathologic tooth mobility in such cases occurs before any marginal periodontal changes and not afterwards. An additional important clinical sign is the poor healing tendency following tooth extraction.

Localization. In addition to lesions in the skull that appear as punched out areas, in the dental area lesions are observed primarily in the mandible.

Examination technique:

- Panoramic radiography,
- Supplemental periapical radiographs.

Radiographic signs. The pseudoperiodontal form begins with sharply demarcated radiolucencies in the depth of the interradicular septa. The structural damage, which usually occurs in the molar segment of the mandible leads to loss of the lamina dura, and progresses to confluent areas of osteolysis that often exhibit arcuate demarcations. In the final stages, the typical picture of the tooth “suspended within the radiolucency” may be observed.

Differential diagnosis:

- Marginal periodontitis,
- Central reparative giant cell granuloma,
- Cherubism.



Fig. 10.48. Eosinophilic granuloma. This section from a panoramic radiograph depicts the

right molar region in a 17-year-old male. Note the early expression of the lesion, with diffuse radiolucency. Some of the bony walls persist and therefore the classic picture of a “hanging tooth” is not yet so pronounced.



Fig. 10.49. **Same patient, two years later.** This is the classic radiographic picture. The roundish foci have become confluent, thus forming the arcuate boundary while leaving the tooth "hanging in the air." The extraction sites have not healed and the granuloma is likely expanding.



Fig. 10.50. **Eosinophilic granuloma.** Panoramic radiograph of a 66- year-old male. The few remaining teeth have tipped dramatically due to chewing forces. Note the arcuate boundary with opaque margins.

Chondroma

This benign, cartilage-forming tumor occurs relatively frequently in the skeleton but only seldom in the jaws or the temporomandibular joint. All age groups of both sexes are equally affected. However, the chondroma, the chondroblastoma and the osteochondroma appear to predominate especially in the temporomandibular joint region of adolescent patients.

Localization. Most often affected are the anterior segments of the maxilla, the premolar region of the mandible (including mandibular tori) and the region of the condylar joint surface.

Examination technique:

- Panoramic radiography,
- Lateral cephalometric radiograph,
- In the maxilla, lateral and frontal spiral tomography,
- CT if the lesions are expansive (density measurements).

Radiographic signs. Sharply demarcated radiolucencies at the condyle; in the jaw, often pinhead-sized calcification centers within sharply demarcated radiolucencies. The cortical bone may be perforated in late stages.

Differential diagnosis:

- Osteochondroma,
- Primary bone tumors.

Osteochondroma

This is usually a benign bone tumor. Some authors classify it under cartilaginous exostoses. Because it exhibits segments with pronounced trabeculation, however, it may appear radiographically as a trabecular osteoma. Growth of the lesions usually ceases in puberty. Continuously growing forms in older patients are suspected to undergo malignant transformation in certain sites (e.g., maxilla).

Localization. At the temporomandibular joint at the beginning of the second decade of life, near the condylar joint surface; less frequently in the region of the median suture and in the premolar region of the mandible.

Examination technique:

- Panoramic radiography in normal jaw position (depicting the condyles),
- Lateral cephalometric radiography of the maxilla,
- Maxillary occlusal radiograph,
- In the maxilla, lateral and frontal spiral tomography,
- CT.

Radiographic signs. Circumscribed, well-demarcated radiolucency with or without areas of radiopacity (sometimes predominant). If localization is in the maxilla, the panoramic radiograph will show overt thickening and higher density in the region of the anterior nasal spine.

Differential diagnosis:

- If lesions are small, degenerative arthritis of the head of the condyle,
- Palatal torus,
- Trabecular osteoma.

The osteochondroma is an osteochondral exostosis and is one of the most common benign tumors of the adolescent skeletal system. It is also one of the most common benign tumors of the condyle, together with the osteoma (a more heavily ossified form) and the chondroma (a more cartilaginous form). Therefore the osteochondroma may appear radiographically as a radiopacity with the density of bone, or as a radiolucency with some dense areas, and sharply demarcated condylar radiolucencies. Only the relatively recent introduction of panoramic radiography into routine dental screening has enabled the dentist to visualize such tumors. Mainly in females, an exceptionally large osteochondroma may form on the condyle, ventral to the actual articular surface. This tumor may lead to rather grotesque facial asymmetry. The articular eminence, with its usually flat dorsal articular surface appears to demonstrate that the tumor arises from about the beginning of the second decade of life. Small osteochondromas are frequently observed on the condyle, and may lead sooner or later to traumatic lesions of the disc and to temporomandibular joint disorders.

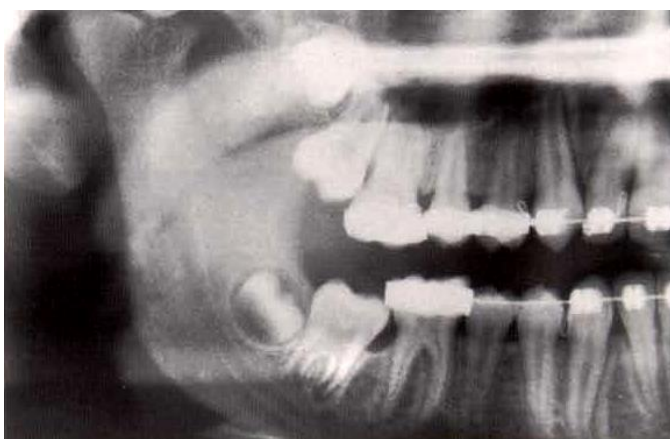
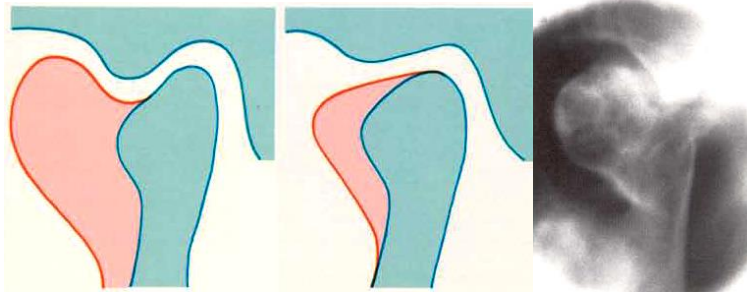
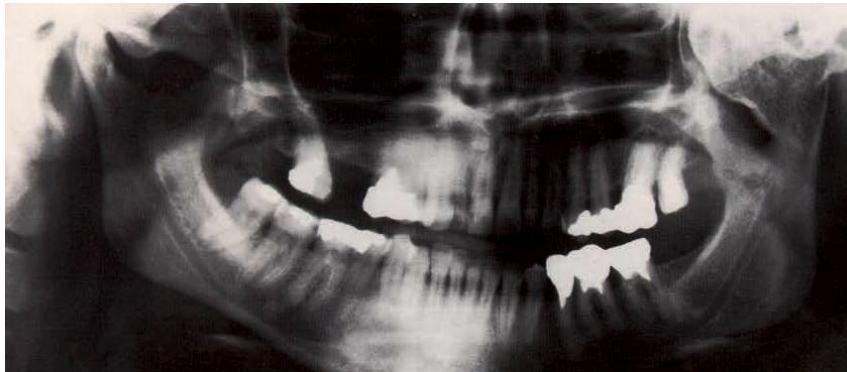


Fig. 10.51. Osteochondroma of the right condyle in a 12-year-old male. This section from a panoramic radiograph displays an osteoblastic tumor at the anterior border of the articular surface. Also apparent is a vague demarcation with a rather loose spongy bone structure.



598

- Fig. 10.52. Osteochondroma. The otherwise sharply demarcated tumor exhibits radiolucencies within its cartilaginous areas. The patient was a 34-year-old female with pronounced facial asymmetry. The diagram (left) depicts two typical shapes of the osteochondroma as they would appear from lateral view on a panoramic radiograph.



- Fig. 10.53. Osteochondroma of the left condyle. Extraordinarily large lesion, accompanied by pronounced development of asymmetry of the jaw. This reveals the exceptional compensatory mechanisms of the jaw musculature and the supportive apparatus. Compare to forms of the so-called facial hemihypertrophy.

Nonodontogenic (desmoplastic) fibroma

- Desmoplastic fibromas and other lesions that have not ossified contain connective tissue or not yet calcified osteoid; for these reasons, such lesions present diagnostic difficulty in radiology. They present as uni- or multilocular lesions with lobular projections of the normally sharply demarcated border contour; in later stages the thinned cortical plate may be perforated. The same radiographic appearance can occur with an ossifying fibroma where the bone is poorly calcified, and if high energy exposure was used. For this reason, specific diagnosis can only be made after histologic evaluation of a biopsy.

This is a benign, usually well-encapsulated connective tissue tumor of the skeleton with no signs of calcification. It occurs less often in the jawbones of younger patients of both sexes. It may also be observed in elderly adults.

Localization. The molar region of the mandible is more frequently involved than the maxilla.

Examination technique:

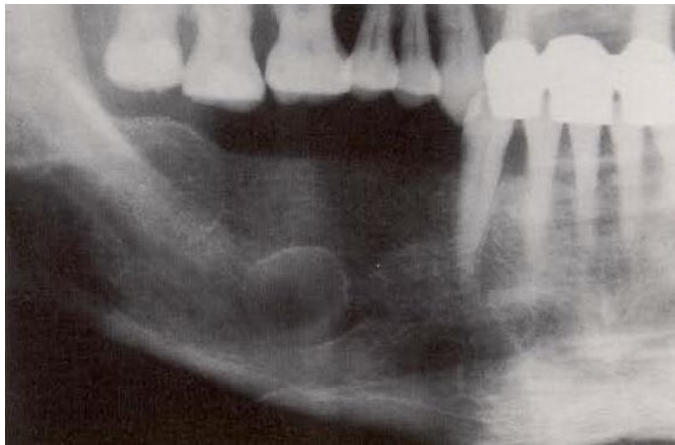
- Panoramic radiography
- Reverse Towne projection with maximum jaw opening
- Lateral spiral tomography
- In the maxilla, CT

Radiographic signs. Unilocular, sometimes multilocular, sharply demarcated and not particularly transparent (exposure data!) radiolucencies without calcification. In late stages, the cortical bone may be distended and thinned, sometimes perforated. Root resorptions may be observed.

Differential diagnosis:

- Central reparative giant cell granuloma,

- Keratocyst,
- Residual cysts in edentulous patients.



601

Fig. 10.54. Non-ossifying fibroma in a 52-year-old male. Note the sharp demarcation of this cystoid, round radiolucency, whose site and configuration could lead one to an incorrect diagnosis of apical residual cyst.

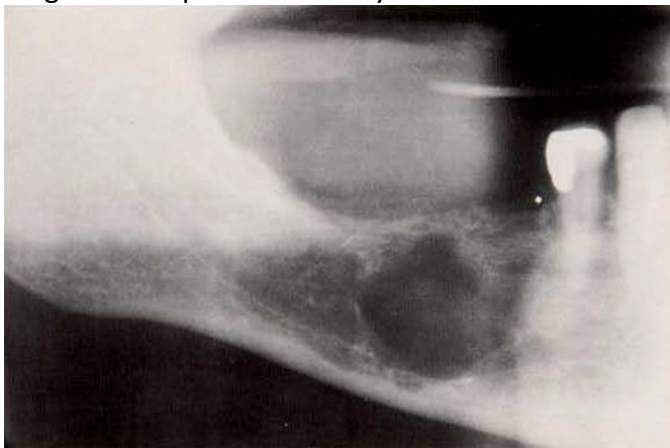


Fig. 10.55. Recurrent non-ossifying fibroma in a 46-year-old male. Note the loss of regular and sharp demarcation, which is reminiscent of a malignant osteolytic tumor. The multilobular form is still visible and is characteristic for desmoplastic fibroma.

Ossifying fibroma

The slowly growing ossifying fibroma may achieve considerable mass in edentulous patients without being detected, and from time to time may cause difficulties for patients who wear dentures. The ossifying fibroma of the maxilla, which affects young persons most often, may also enlarge considerably into the maxillary sinuses and nasal cavity without any external deformation of the face. It therefore remains unnoticed for a long time. Heavily calcified forms viewed in a Waters' projection may be mistaken for expansive osteoma in the maxillary sinus, and may lead secondarily to clinical difficulties.

Children and adolescents under the age of 15 may be affected by the juvenile ossifying fibroma. As one of the most common tumors of the jaw, the lesion is also observed in adults of all ages, especially in the third and fourth decades of life. The lesions are seen most frequently in females and present as well-demarcated areas with varying degrees of calcification and ossification.

Localization. The juvenile ossifying fibroma has a clear preference for the maxilla. The ossifying fibroma in adults is more often observed in the mandible.

Examination technique:

- Panoramic radiography,
- In the maxilla, CT.

Radiographic signs. The juvenile form is well demarcated and may displace the structures of the maxilla and the sinuses as a result of its growth. An ossifying fibroma should therefore always be suspected if the radiographs depict milk glass-like areas, calcifications, and ossifications.

Differential diagnosis:

- Fibrous dysplasia (lacks demarcation)
- Late stage osteoblastoma
- Osteoma.



Fig. 10.56. Ossifying fibroma in a 63-year-old female. Even the histopathologist encounters difficulties in diagnosis and classification of such cases. The spectrum of differential diagnostic possibilities includes tumors that are characterized by ossification or cementum formation.



Fig. 10.57. Ossifying fibroma of the mandible. The radiograph reveals a sharply demarcated radiolucency with spotty calcifications in its center.



Fig. 10.58. Ossifying fibroma of the maxilla in a 40-year-old female. The axial CT with soft tissue window reveals the size and the clear demarcation, with displacement of the sinus and the nasal cavity. Clearly visible are some heavily calcified foci. Recurrent lesions have a tendency toward malignant transformation into sarcoma.

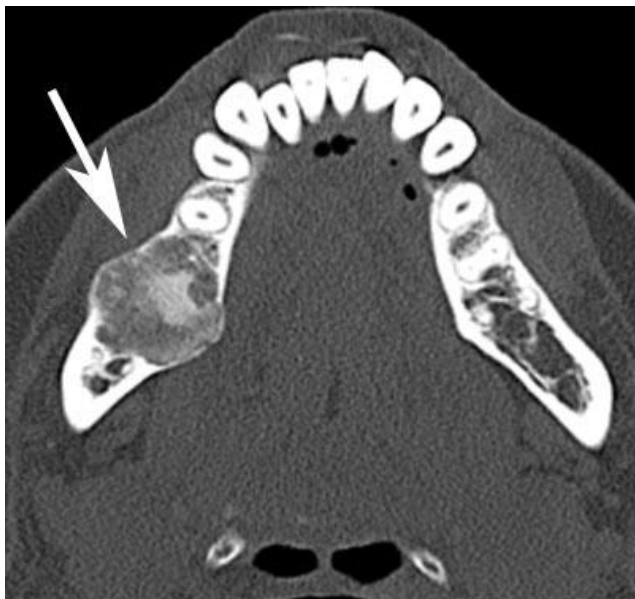


Fig. 10.59. Ossifying fibroma in a 33-year-old woman. CT scan reveals a circular, partially calcified lesion (arrow) within the mandible. Note the internal ground-glass calcifications.

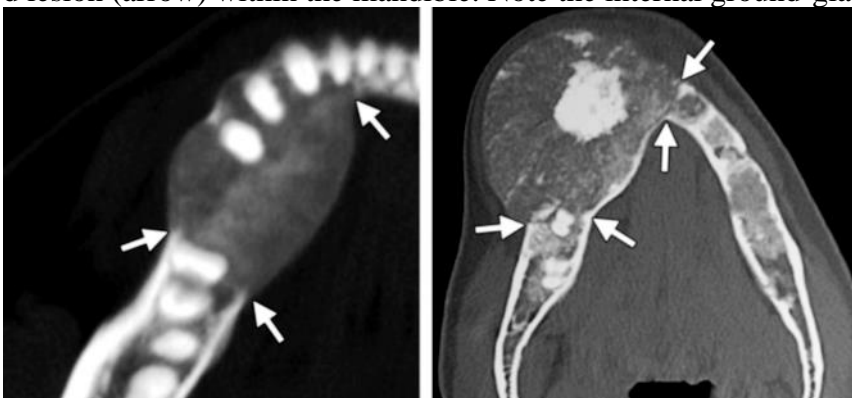


Fig. 10.60. Ossifying fibroma. Axial CT images obtained in two different patients show well-defined, focally expansile, sharply margined lesions with predominantly ground-glass attenuation. The presence of a narrow zone of transition (arrows) helps differentiate ossifying fibroma from fibrous dysplasia

Fibrous Dysplasia and Cherubism

This disease, also known as juvenile osteofibrosis deformans (Uehlinger), originates between 5 and 15 years of age, affects females approximately twice as often, and the clinical course may extend in bursts far beyond puberty. The disease derives from improper differentiation during bone formation. Initially, normal spongiosa and bone marrow are replaced with fibrous ground substance and fibrous bone is formed later. Spontaneous healing or stagnation of the disease process during puberty are possible. The course of this disease may be monostotic or polyostotic, the maxilla is more frequently affected than the mandible, and osseous sutures limit expansion. Distention and thinning of the cortical plate are often observed especially in the maxilla, and this can result in significant facial asymmetry. In the mandible the poorly demarcated “cystoid” radiolucencies and opacities of various degree are arranged one

against the other, reminiscent of chronic recurrent forms of osteomyelitis. The newly formed fibrous bone may develop pronounced opaque areas, in addition to spongy structures.

This condition is characterized by early pain and swelling of the bone, with connective tissue replacement of the spongiosa, fibrosis of the bone marrow and fibrous bone formation of varying degree.

This disease usually affects children and adolescents between 5 and 15 years old. It may occur either monostotic or polyostotic and therefore presents an extremely diverse radiographic picture. One extremely rare form is so-called cherubism.

Localization. In addition to ribs, femur and tibia, the skull and particularly the maxilla, the mandible or both jaws may be affected. The osseous sutures in the maxilla limit the growth of the lesion.

Examination technique:

- Panoramic radiography,
- Occlusal radiographs for structural analysis,
- CT.

Radiographic signs. Lesions originate with oval radiolucencies and structural disturbances in the maxilla, leading soon to a milk glass-like and orange peel-like spotty shadowing of the bone, with thinning and distention of the cortical plate. In the mandible, the usual presentation includes uniform shadowing with multiple cyst-like radiolucencies. After replacement by fibrous bone, extremely opaque or abnormally structured areas dominate. When distention and thinning of the compact bone of the mandible occurs, the demarcation of these lesions is usually unclear.

Differential diagnosis:

- Recurrent chronic osteomyelitis,
- Ossifying fibroma,
- Osteoma,
- Paget's disease of bone.

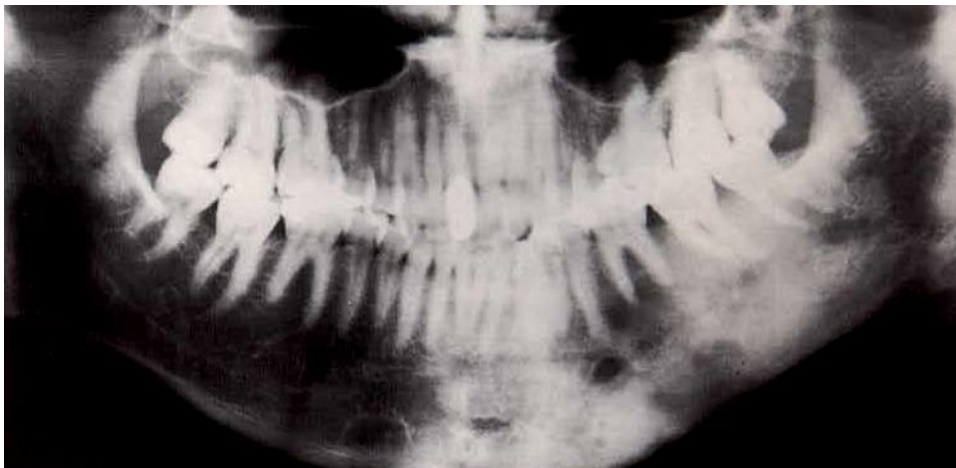


Fig. 10.61. Fibrous dysplasia in the mandible of a 28-year-old male. In addition to mild distention of the left mandible, note the milk-glass shadowing with honeycomb-like radiolucencies. The radiographic picture is often difficult to differentiate from the chronic form of osteomyelitis.

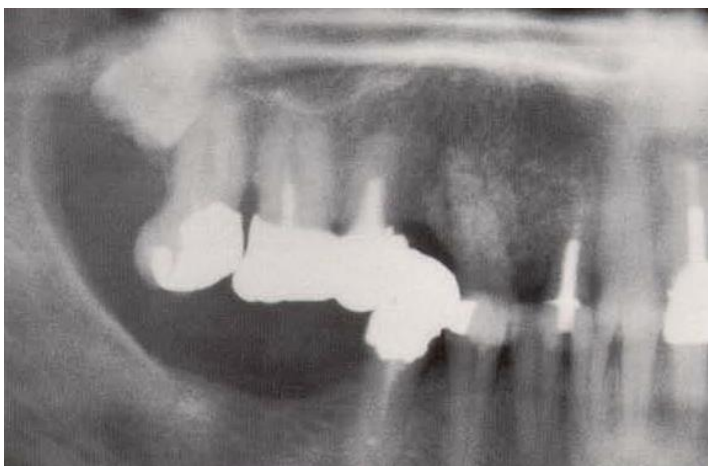


Fig. 10.62. Fibrous dysplasia in the maxilla of a 57-year-old female. Here also the demarcation between the lesion and healthy bone is vague. The distention is locally demarcated and shows a random spongy bone organization.

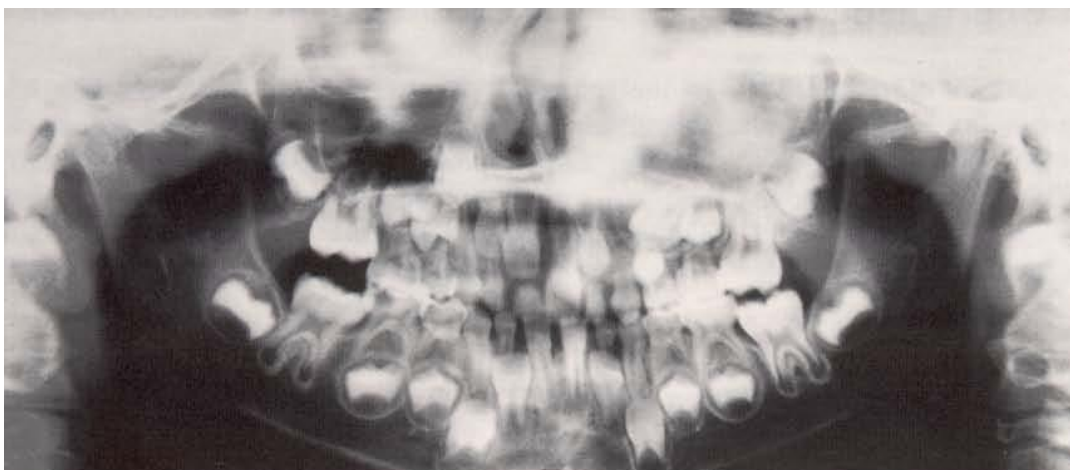
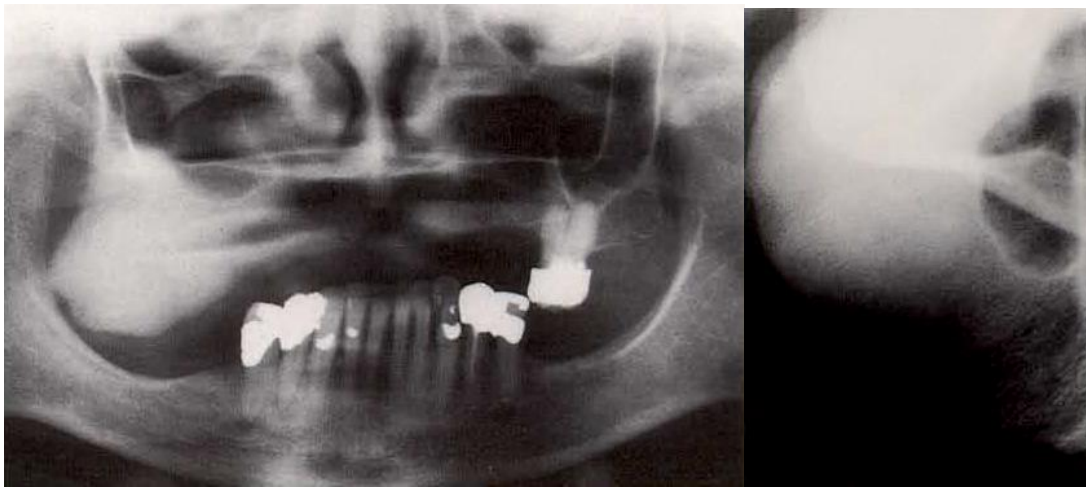


Fig. 10.63. Fibrous dysplasia as seen in the panoramic radiograph of a 6-year-old female. Despite the high-energy radiographic exposure, the entire left side of the maxilla exhibits radiopacities. The expansive process is made more apparent because of the displacement of the teeth and the tooth buds. The ossifying fibroma may exhibit similar radiopacities in the maxillary sinus when viewed in a panoramic radiograph. However, it usually occurs only later in life, during puberty.



Fig. 10.64. Same case, occlusal radiograph. Clearly visible is the massive expansion of the maxilla with displacement of tooth buds and the typical milk-glass-like structure, resembling an orange peel. Note that the median suture remains intact.

Fibrous dysplasia of the jaw may exhibit quite variable radiographic signs depending upon the age of the patient, thus making the differential diagnosis extremely difficult. Poorly demarcated radiolucencies localized to one side of the jaw may alternate with milk-glass, honeycomb or pumice-like radiopacities. A peculiar dysplasia is the bilateral involvement of both maxilla and mandible, and is characterized by polycystic, misshapen enlargements, especially at the angle of the mandible; and in the maxilla. This results in a clinical appearance called cherubism.



613

Fig. 10.65. Fibrous dysplasia in the right maxilla of a 56-year-old female. The panoramic radiograph (left) and the occlusal radiograph (right) both reveal extreme enlargement with displacement of the maxillary sinuses. Note the poorly demarcated borders and the radiopacity, which is typically uniform due to the accumulation of fibrous bone.



Fig. 10.66. Cherubism, lateral skull radiograph. In comparison to the previous examples of fibrous dysplasia, note here the polycystic structure that crosses anatomic boundaries; such lesions usually appear only in the skeleton, especially in the ribs. Particularly obvious is the thickening of the base of the skull. Malpositioning of the teeth and retention of the second and third molars are frequently observed. This condition usually begins during the first decade of life.

Osteoid osteoma and Osteoblastoma

These are benign tumors of the ground substance of bone; they are relatively rare, usually occurring in females under 25 years old (osteoid osteoma) or in adults over the age of 40 as a fully matured osteoblastoma. Early lesions are virtually impossible to detect radiographically because of addition effects; on the other hand, clinically the patient may complain of diffuse or localized pain (depending upon site).

The exceptionally rare osteoid osteoma most often affects the mandible, particularly in young women. Radiographically, it exhibits an opaque nucleus within an oval radiolucency, the "nidus." The lesion is always smaller than 1 cm, and the surrounding tissue frequently exhibits significant reactive sclerosis. The osteoblastoma is also relatively rare; it is an osteoid-forming tumor, which occurs in both maxilla and mandible during adulthood. In its initial stage the lesion exhibits radiographically a diffuse radiolucency, which later matures into a very dense radiopacity greater than 2 cm in expanse with an obvious border.

1. Osteoid osteoma

Localization. These lesions occur more frequently in the body of the mandible than in the maxilla.

Examination technique:

- Panoramic radiography,
- Spiral tomography,

Radiographic signs. Within the “nidus,” the ovoid and not always sharply demarcated radiolucency, one observes an unstructured opacity of calcified tissue-like density, up to 1 cm in expanse. A strong reactive sclerosis is sometimes observed in the surrounding area.

Differential diagnosis:

- Cementoma,
- Osteoma.

2. Osteoblastoma

Localization. This tumor occurs in both maxilla and mandible in adults of all ages.

Examination technique:

- Panoramic radiography,
- CT, especially in the maxilla for demarcation.

Radiographic signs. Initially diffuse, poorly demarcated radiolucency. Later stages are almost always larger than 2 cm, with increasing density, and sharp demarcation and a radiolucent border. The neighboring teeth may be displaced and root resorptions may be in evidence.

Differential diagnosis:

- Cementoblastoma,
- Complex odontoma,
- Ossifying fibroma.

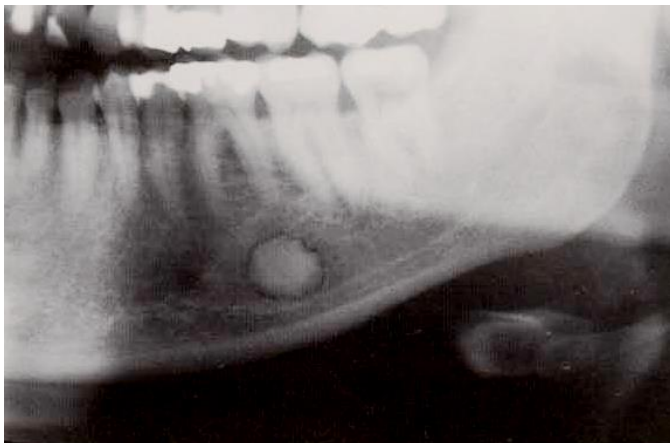


Fig. 10.67. Osteoid osteoma of the mandible. Note the “nidus” with its calcified core and the rather bright zone of uncalcified osteoid in this 29-year- old female.



Fig. 10.68. Osteoblastoma of the maxilla. Note the radiolucent lesion comprised of osteoid, approximately 1.5 cm in diameter in this 23-year-old female in the region of teeth 12,13 and 14 (arrows). Clinically, this lesion was painful.

Osteoma

As a pathologic entity, this lesion is difficult to differentiate radiographically from other lesions with pronounced ossification. Exostoses, osteosclerosis and similar alterations will therefore be discussed in connection with osteoma. Osteochondroma or certain forms of fibrous dysplasia may also be components of a differential diagnosis that are difficult to rule out radiographically. The osteoma can occur in all age groups, but has a preference for elderly adults. Clinically these lesions are associated only secondarily with manifestations due to displacement of surrounding tissues.

The osteoma may occur as a central or a peripheral lesion and is not always easy to differentiate radiographically from other heavily ossifying and calcifying lesions. The osteoma may occur in all age groups but exhibits a preference for elderly adults. Radiographically it exhibits either a well-demarcated and very dense radiopacity (compact osteoma) or a more loosely structured trabecular form (spongy osteoma). Osteomas of the peripheral type are frequently found in the frontal sinus and the maxillary sinus, and less often on the compact bone at the angle of the mandible.

Localization. Peripheral osteoma may occur as a solitary form in the frontal sinus, the maxillary sinus and on compact bone particularly in the mandible. Central osteoma may occur in the jaws as solitary or multiple lesions, for example in Gardner's syndrome, or as Paget's disease of bone.

Examination technique:

- Panoramic radiography,
- Lateral or frontal spiral tomography,
- CT in the maxilla and to demarcate the borders of larger lesions.

Radiographic signs. For the normally well demarcated and extremely opaque lesions, the term compact osteoma is often applied. Especially in the mandible, trabecular forms residing on compact bone have been described.

Differential diagnosis:

- Enostosis,
- Cementoma,
- Complex odontoma,
- Axially projected impacted tooth or root fragment,
- Fibrous dysplasia,
- Osteochondroma,
- Ossifying fibroma,
- Gardner's syndrome,
- Paget's disease of bone.

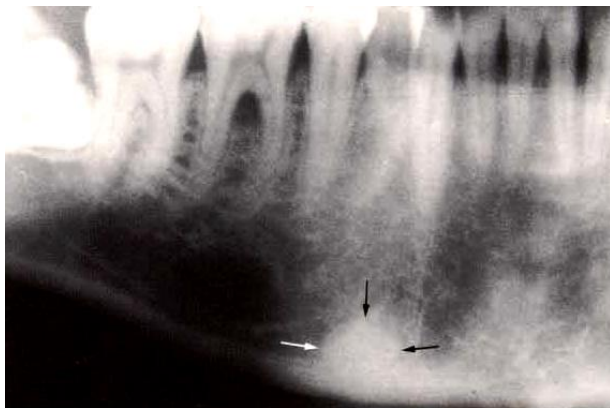


Fig. 10.69. Central osteoma. At the region of the mental protuberance such as in this 32-year-old male, one can often observe osteoid osteoma and osteoma (arrow).



Fig. 10.70. Central osteoma. Two osteomas of the compact type can be seen anterior to the root fragment of tooth 37.

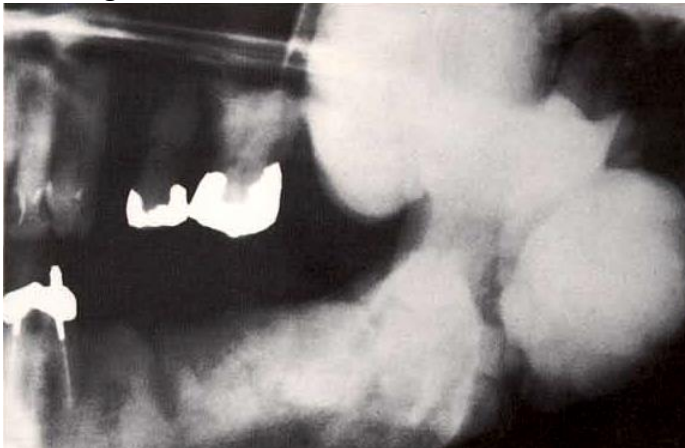


Fig. 10.71. Multiple osteoma. In male patients (especially among Blacks) the presence of multiple osteoma should lead one to consider the possibility of Gardner's syndrome, which is accompanied by intestinal polyps that often undergo malignant transformation. This disease is inherited as an autosomal dominant trait.

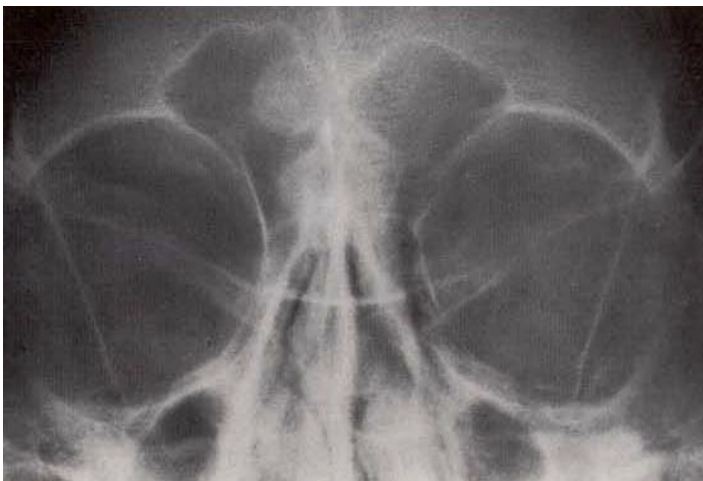


Fig. 10.72. Peripheral osteoma. This lesion is located on the medial wall of the right frontal sinus.



Fig. 10.73. Peripheral osteoma. Approximately 5% of all osteomas of the facial skeleton are observed in the maxillary sinus. In this patient the osteoma developed in the posterior lobe.⁶²⁴



Fig. 10.74. Peripheral osteoma at the right angle of the mandible. This peripheral osteoma has a cancellous structure and is located upon compact bone. Such lesions may be confused with calcified lymph nodes.



Fig. 10.75. Osteoma in two patients. (A) Axial CT image shows a well-circumscribed sclerotic mass with smooth margins in the mandibular ramus (arrows). The mass is associated with mild bone expansion. No low-attenuation halo is seen. In the absence of bone expansion, it may not be possible to differentiate osteoma and idiopathic osteosclerosis. (B) Sagittal volume-rendered CT image obtained in a different patient shows an osteoma (arrowheads) in the posterior mandibular body and ramus with associated simple bone cysts (arrows).

Exostosis and Enostosis

Depending upon its localization and shape, an exostosis is also termed osteoma, hyperplasia or torus. Enostoses may be observed radiographically as “compact islands” of unknown or inflammatory origin; such lesions may also be incorrectly diagnosed due to the addition effect. When examining a panoramic radiograph, one should always consider that *all* radiopacities even though they lie outside the jawbone will be projected in the radiograph. Typical in this regard is the possible existence of sialoliths, phleboliths or calcified lymph nodes. The occlusal radiograph can be of assistance

in arriving at the proper diagnosis.

Hyperostoses and Hypertrophies

Rarely, hyperostoses and hypertrophies may be observed in the jaws. Their etiology is for the most part unknown.

Osteoporosis

Characteristically the picture of osteoporosis is increased transparency resulting from reduction of bone density. This can be readily diagnosed in a panoramic radiograph (not overexposed) primarily in the mandible. On the other hand, the radiograph of the jaw provides a superficial hint only in extreme cases and can therefore not replace mandatory supplemental radiographic examination and laboratory findings.

Atrophy of aging

This usually occurs in combination with senile osteoporosis, and generally affects females about five years earlier than males. Endocrine, metabolic, and functional etiologies have been described. The residual, reduced bone mass of the mandible is at risk for fracture.

Bone marrow islands and addition effects of all kinds may occur particularly in panoramic radiographs, but also in periapical radiographs, and these carry the risk of incorrect interpretations.

In addition to its supportive functions, the bone also serves as a repository of minerals; as such, it participates in a system for regulating blood content of calcium, phosphates and magnesium, in conjunction with the kidneys and intestines. The normal homeostasis within this system often achieves a negative balance in elderly individuals, resulting in senile osteoporosis. In conjunction with senile inactivity atrophy of the jaws, this can lead to problems with masticatory function. Such conditions will demand all the skill and knowledge of the dentist in addition to the adaptability of the patient.



Fig. 10.76. Senile osteoporosis in a 93-year-old female. This panoramic radiograph clearly reveals enhanced radiolucency of the jaw, and thinning of the compact bone. The oblique line (represented here by the temporal crest) dominates the picture.

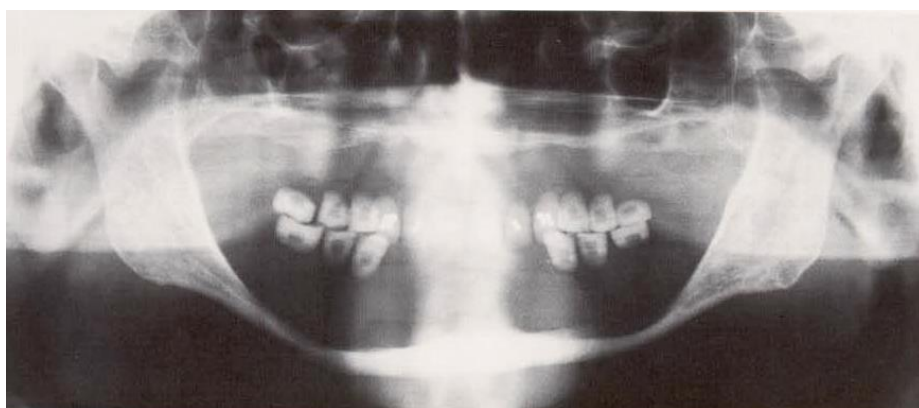


Fig. 10.77. Advanced senile osteoporosis and atrophy. This panoramic radiograph of a 79-year-old male reveals the thinned profile of mandibular bone. Both ascending rami exhibit spotty areas of osteoporosis as well as thinning of the compact bone, except for the oblique line, which remains clearly visible.

Osteogenesis imperfecta and Osteopetrosis

Osteogenesis imperfecta and osteopetrosis (also known as marble bone disease) result from disturbance of osteoblast function or from osteoclast insufficiency.

Osteogenesis imperfecta is frequently associated with a disturbance of osteoblast function and exhibits either a very early (*congenita*) or late (*tarda*) tendency toward spontaneous skeletal fractures. Since children with this condition die either before birth or in the first few months of life, the dentist may see only mild forms. The damaged jawbone can often respond to a dentogenic infection with a progressive form of osteomyelitis where the clinical course resembles that of osteoradionecrosis.

Osteopetrosis, also known as marble bone disease or Albers-Schonberg disease, and which is inherited as an autosomal recessive trait, exhibits on the other hand a structureless bone opacity with obliteration of the marrow spaces and delayed dental eruption. If affected children are born alive, they usually die within the first few months of life.

Osteitis deformans

Osteitis deformans, also called osteodystrophy deformans or Paget's disease of bone, is a rare bone disease of unknown etiology, which affects primarily males in the sixth or seventh decade of life. These monostotic or polyostotic lesions affect primarily the cranium, the petrous portion of the temporal bones and the zygoma, but also the jaws, especially the maxilla. In addition to hypercementosis, three developmental stages can be discerned, which are characterized by diffuse radiolucencies with spotty round opacities and confluent, cotton-wool condensation in the apical areas. The affected jaw may increase abnormally in size and dentogenic infection may induce a rapidly expanding osteomyelitis.

Localization. More frequently on the cranium, the petrous portion of the temporal bone and in the zygoma region; less frequently in the jaws. Sometimes the maxilla alone is affected: "macrocranium"; "leontiasis ossea."

Examination technique:

- Panoramic radiography,
- Supplemental periapical radiographs,
- Lateral cephalometric radiographs (cannot provide a complete overview),
- Posteroanterior skull projection (cephalometric view cannot provide a complete overview),
- CT.

Radiographic signs. Hypercementosis on the teeth, milk glass-like cloudiness, diffuse radiolucency in the apical areas. The lamina dura is no longer visible. Cotton-wool opacities, which may become confluent in later stages. Disproportionate increase in opacity and size of the affected bone with disturbed intermaxillary relations in centric occlusion.

Differential diagnosis:

- Recurrent chronic osteomyelitis,
- Multiple cementoma,
- Periapical cemental dysplasia,
- Osteosclerosis.

Hemangioma

The hemangioma is a blood vessel tumor that is associated with considerable diagnostic difficulties radiographically in its intraosseous form. The lesion is rare and is most often diagnosed only in adults. Females are preferentially affected. The appearance of these lesions in the jaw bones is extremely variable, and can mimic many other pathologic alterations.

Central hemangioma of the jaw is rare, but when it does occur it is more frequently observed in the mandible than in the maxilla, and females are more frequently affected. The radiographic picture of hemangioma can vary widely. One may observe soap bubble-like appearances, calcifications, osteolysis, radiating forms and abnormal bony structures with deformation of the cortical plate. These lesions are poorly demarcated. Sometimes phleboliths can be observed. The diagnosis of hemangioma can be verified using angiography.

Localization. More common in the mandible than in the maxilla.

Examination technique:

- Panoramic radiography,
- CT with a contrasting substance (medical history).

Radiographic signs. The lesions may vary in appearance from a vaguely demarcated osteolysis to a "soap bubblelike" or "radiating" lesion. Small lesions exhibit similarity to the honeycomb form of ameloblastoma, while large lesions may display distention and thinning of the cortical plate, which is, however, not perforated. Hemangioma that persist for long periods of time may exhibit phleboliths.

Differential diagnosis:

- Central giant cell granuloma Ameloblastoma,
- Aneurysmal or solitary bone cyst,
- Chondromatosis.

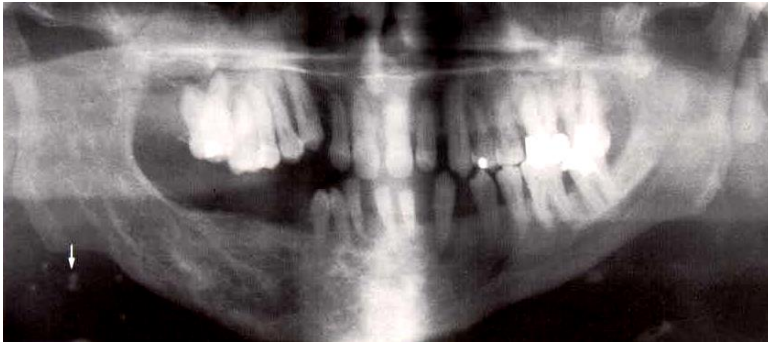


Fig. 10.78. Central hemangioma in the right mandible. This hemangioma extends from the semilunar notch to the region of tooth 43. Compare the stranded structure of the bone to that of the healthy side; note also the numerous phleboliths below the angle of the mandible (arrow).



Fig. 10.79. Small central hemangioma. This periapical radiograph shows quite well the soap bubble-like structure between teeth 24 and 25. The picture is reminiscent of the honeycomb appearance of ameloblastoma. The widening of the periodontal ligament space is evidence of the increased tooth mobility that is detected clinically in such cases. This radiograph is from a 21-year-old female.

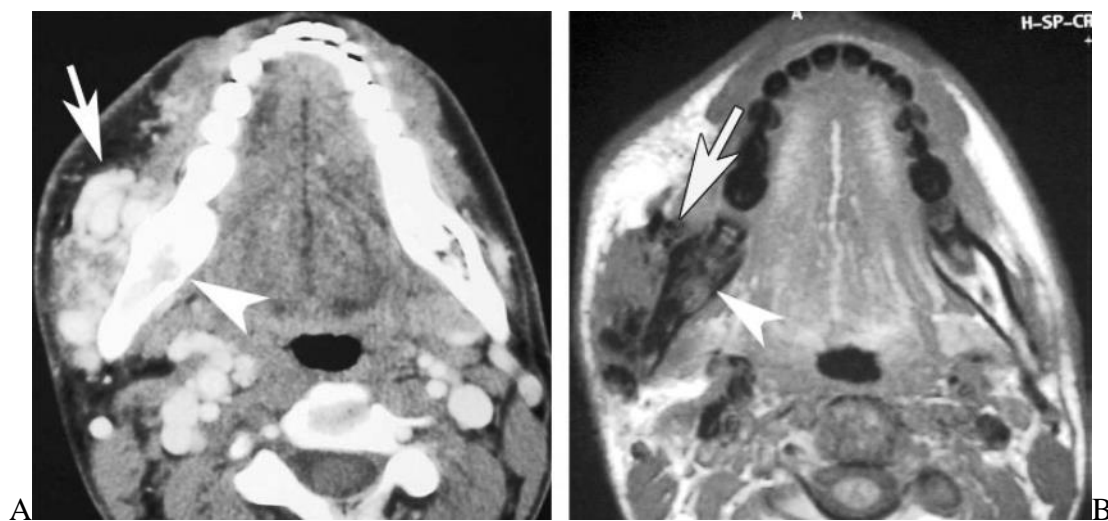


Fig. 10.80. AVM in a 28-year-old man. (A) Contrast-enhanced CT scan reveals multiple dilated and tortuous vessels (arrow) within the right masseter muscle. Note the abnormal enhancement (arrowhead) within the marrow of the mandible. (B) Axial T1-weighted MR image demonstrates a slightly expansile lesion (arrow) within the right mandibular angle and body. Multiple

flow voids are present within the right masseter muscle. Note the loss of normal fatty marrow (arrowhead) within the mandible.

Malignant Lesions

Sarcoma

This tumor, which affects males twice as frequently as females, exhibits a predilection for the mandible, where it frequently occurs in an osteoblastic-osteolytic mixed form of the osteogenic sarcoma. Sarcoma may destroy the mandibular canal, as does infiltrative carcinoma or osteomyelitis. Paresthesia is therefore a leading clinical symptom. Radiographically, bone destruction as well as new bone formation and osteolysis can be observed, along with perforation of the compact bone with spicules ("sunray effect") where the lesion borders on the soft tissues.

Depending upon their histology, a sarcoma may be classified as osteoblastic, fibroblastic, chondroblastic or some other form. The tumor cells of the extremely malignant *osteogenic sarcoma*, for example, produce osseous ground substance that can only be radiographically detected once it is calcified. On the other hand, it is not uncommon that, in addition to calcification (sclerosis), cartilage or connective tissue depositions contribute to the radiographic picture of the relatively common mixed form with osteolysis. The most common malignant tumor of the jaw occurs in men in the third and fourth decades of life, with a peak in the second decade. The sarcoma metastasizes via the blood system. It appears that in late adolescence the sarcoma may occur following trauma such as fracture or tooth extraction. Clinical cardinal symptoms include tooth mobility, hemorrhage from poorly healing wounds, soft tissue swelling and paresthesia.

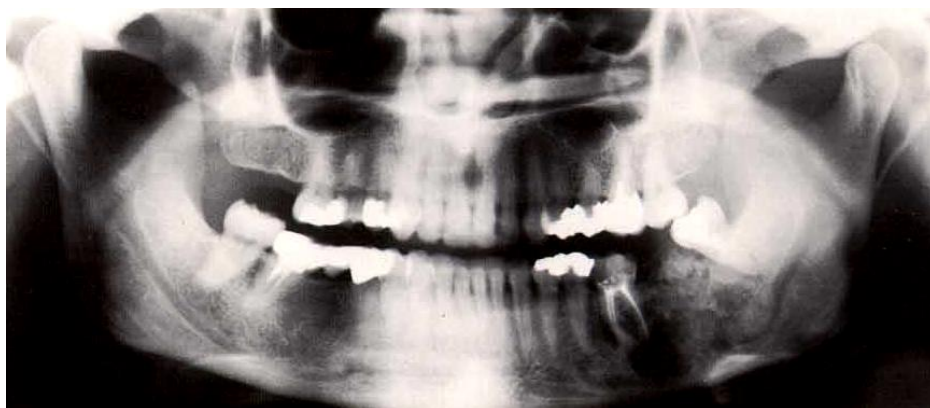


Fig. 10.81. Osteosarcoma. A mixed form of osteosarcoma has developed at the extraction site of tooth 37. In addition to osteolysis, this panoramic radiograph of a 38-year-old female also exhibits irregular and spotty ossifying new bone formation overgrowing the alveolar crest.

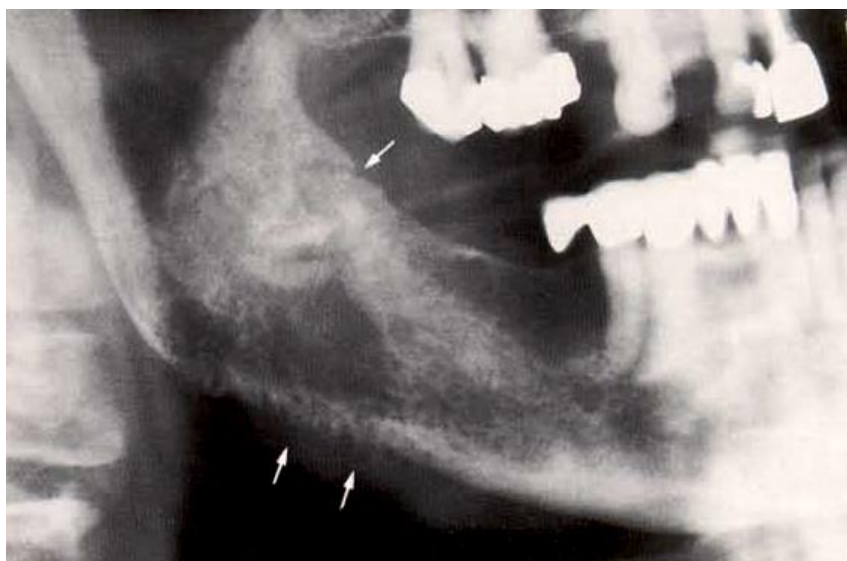


Fig. 10.82. Osteosarcoma. Mixed form. In addition to areas of new bone formation, osteolysis and destruction of the compact bone can be observed. Note the formation of spicules (arrows) and spontaneous fracture (arrow).

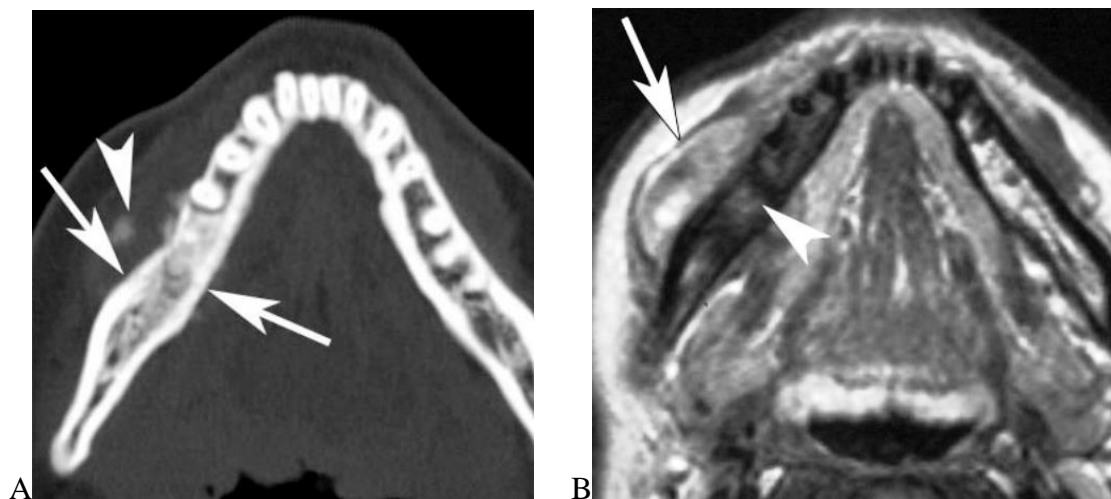


Fig. 10.83. Osteosarcoma in a 41-year-old man. (A) CT scan reveals osteoblastic changes (arrows) within the right mandibular body. Note the abnormal soft-tissue ossification (arrowhead). (B) MR image demonstrates an ill-defined lesion (arrow) arising from periosteum.

Localization. Most often in the premolar and molar regions of the mandible; less frequently in other regions of the jaws.

Examination technique:

- Panoramic radiography,
- Targeted periapical films, and tomography,
- CT for radiographic demarcation of the tumor; this technique can *never* depict the expanse within bone marrow.

Radiographic signs. In early stages, widening of the periodontal ligament space may be observed. Central forms exhibit relatively early the destruction of normal anatomic structures (e.g., mandibular canal), poorly demarcated boundaries, spotty sclerosis, and osteolysis. The lesions perforate the compact bone and are accompanied by new bone formation including spicules (“sunbeam effect”), which are only visible on low energy radiographs.

Differential diagnosis:

- Other primary bone tumors,
- Osteomyelitis (clinical diagnosis!),
- Noninfected odontogenic tumors and cysts with vague boundaries.

Ewing sarcoma

An extraordinarily malignant, though rare, tumor is the myelogenic Ewing sarcoma of the jaw in children. In contrast to other malignant tumors, the Ewing sarcoma is often accompanied by severe general symptoms such as pain, soft tissue swelling, high fever, elevated blood cell sedimentation rate, and leucocytosis. The lesion is most often observed in the first through third decades of life, with a peak in the second decade, and occurs more frequently in males.

Localization. Primarily in the mandible.

Examination technique:

- Panoramic radiography,
- CT (if technically possible).

Radiographic signs. Moth-eaten appearance of bone destruction with millimeter-size osteolysis and irregular contours. Periosteal reaction such as spicules and onion skin-like periosteal calcification provide typical signs, in addition to intraosseous spread.

Differential diagnosis:

- Acute forms of osteomyelitis,
- Osteogenic sarcoma.

Carcinoma of the oral mucosa

In addition to the extremely rare primary intraosseous epithelial cell carcinoma of the jaw, which may derive from remnants of the odontogenic epithelium, the radiographic depiction of bony infiltration of the oral mucosa by carcinoma is of significance for the planning of appropriate therapy. This is true even though it is well known that the

infiltration of, for example, the lingual portion of the alveolar process can be ascertained radiographically only in later stages.

Localization. Carcinoma of the oral mucosa can infiltrate not only into the hard palate but also into the alveolar process of the maxilla and the mandible.

Examination technique:

- Panoramic radiography. Alterations in the third dimension cannot be visualized in the early stages!
- Supplemental radiographs using periapical films (if the alveolar crest itself is eroded),
- Occlusal radiographs,
- CT.

Radiographic signs. Undermining destruction without sharp borders, which often leaves bony segments intact. The radiolucency may appear to contain “suspended” yet not displaced teeth.

Differential diagnosis:

- From the clinical point of view, none.

Mucoepidermoid tumor

The relatively benign mucoepidermoid tumor may also exhibit invasive and infiltrative growth into the jaw bones, and exhibit not only the radiographic signs of a benign tumor but also those of malignant expansion. Extending from a saliva gland tumor of the parotid, the palatal glands, the submandibular or the ducts of the floor of the mouth, this tumor may invade the maxilla or the mandible. The mucoepidermoid tumor is more often observed in females than in males and preferentially in the third and fourth decades. This tumor, which is radiographically extremely variable, may simulate odontogenic cysts or mesenchymal tumors; malignant forms can metastasize.

Based on these facts, it must be recognized that the radiograph cannot provide a histopathologic diagnosis.

Localization. More frequent in the mandible than in the maxilla.

Examination technique:

- Panoramic radiography,
- CT with measurement of density.

Radiographic signs. Soap bubble-like, arcuate border with multicystic radiolucencies may be observed in addition to the bone destruction.

Differential diagnosis:

- Odontogenic cysts and tumors,
- Benign and malignant mesenchymal tumors.

Metastasis

A metastasis is the satellite of a primary tumor which, despite a different anatomic localization exhibits histologic features identical to the primary tumor. If metastasis occurs via the blood system, the mandible is the preferential location with a ratio of 4:1 over the maxilla. This is because the angle of the mandible and the ascending ramus contain red marrow that becomes affected. In males, metastasis occurs most often from lung carcinoma and prostate carcinoma, while females exhibit jaw metastasis mainly from mammary carcinoma. Because they grow slowly and rarely cause clinical symptoms, such metastases were often discovered only after spontaneous jaw fracture before the era of panoramic radiography. Mild discomfort and paresthesia may, however, be initial symptoms.

Localization. *The mandible dominates in comparison to the maxilla.*

Examination technique:

- Panoramic radiography,
- Scintigraphy (in approximately 5% of cases, false positive),
- CT in unclear cases, especially in the maxilla.

Radiographic signs. *Usually vaguely demarcated osteolysis, sometimes with osteoblastic areas (mammary carcinoma) or sclerosis (prostate carcinoma). Moth-eaten appearance with millimeter size radiolucencies are sometimes also observed. The differential diagnosis is rendered difficult when lesions occur in the bone marrow islands of the mandibular premolar region.*

Differential diagnosis:

- Bone marrow island

- Primary bone tumor
- Osteomyelitis
- Meta hepatocellular ca



Fig. 10.84. Metastatic hepatocellular carcinoma in a 61-year-old man. Contrast-enhanced CT scan demonstrates an expansile, osteolytic mass (arrows) within the right mandibular body.



Fig. 10.85. Adenomatoid odontogenic tumor in a 14-year-old boy. CT scan demonstrates a unilocular radiolucent lesion with a linear calcification (arrow) centered between the lateral incisor tooth and canine tooth..

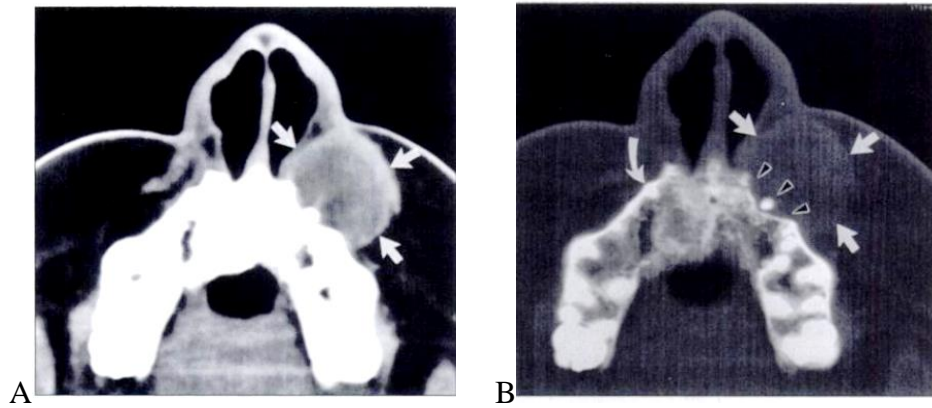


Fig. 10.86. 25 year-old woman with **periapical lesion causing soft-tissue mass** of face. **(A)** Soft-tissue window of axial CT scan shows soft-tissue mass (*arrows*). **(B)** Bone window of same axial CT scan as in A reveals that resorption of bone around root apex created penapical radiolucency (*arrowheads*). Compare with normal root apex on right side (*curved arrow*). Straight arrows show soft-tissue mass.

11 Traumatology

Radiography plays a particularly important role in traumatology. It must satisfy various demands because in such cases it is not only a mechanism for data collection, it also serves to provide documentation for the patient, the physician and other care providers. Forensic indications may also be of importance, as well as protection of the patient from excessive radiation exposure.

Dental radiology is important even for seemingly minor accidents, because such incidents are often followed by unexpected delayed consequences that must eventually be reported to insurance companies. It is worthy of note that fracture lines, regardless of their localization can only be diagnosed with certainty in the radiograph when the line of fracture is parallel to the central X-ray beam or when a dislocation is clearly revealed by the film.

Even if standard radiography does not provide clear evidence of a fracture, this is no guarantee that no fracture exists. The dentist is wise to remember that even in cases of apparently uncomplicated dental accidents in children, panoramic radiography should be employed in an attempt to identify fractures of the articular process of the mandible and greenstick fractures that are difficult to detect clinically, these must be recognized and documented for insurance purposes. Only in this way can incorrect interpretations that may lead later to tooth loss or growth disturbance be precluded. In general, to detect suspected fractures of teeth or condyles the panoramic radiograph is taken in the usual manner; however, in cases of dislocation radiographs taken with the patient in maximum intercuspation are recommended. Dislocations can be expected, especially in the mandible, not only due to the accident itself but also due to secondary muscular tension; such situations are not always readily apparent in panoramic radiographs due to the superimposition effects in the third dimension. Because such third dimension situations often provide unanswerable questions, additional radiographs with various projection angles are obligatory. Furthermore it is wise to note that appropriate soft tissue techniques should be used to search for splinters of glass (pp. 68 and 88). The vitality of traumatized teeth must be tested for at least a 6-month period to ascertain any delayed consequences.

The automobile accidents that are so frequent today often provoke multiple injuries. Polytraumatized or unconscious patients often cannot be effectively examined with conventional methods during initial examination because of problems of positioning. This often makes it necessary to refine and improve the data collection during a second examination. Computed tomography, which can be used successfully to portray injuries in the depth of the facial skeleton.

When it comes to diagnosis of facial fractures, only solid basic knowledge of anatomy and of the possibilities provided by modern imaging technology can lead to success in the diagnosis of fractures.

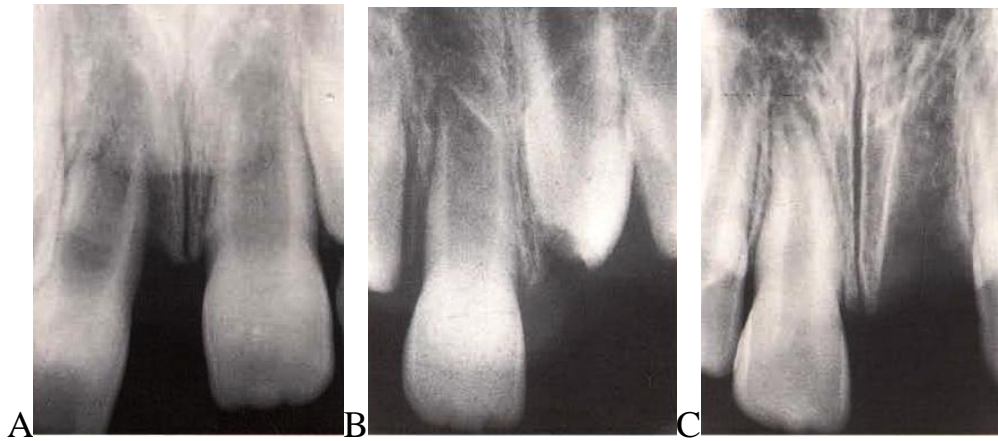


Fig. 11.1.(A) Subluxation of tooth 11, with root fracture, (B) central luxation of tooth 21, with crown fracture, (C) subluxation of tooth 11, and complete luxation of tooth 21.

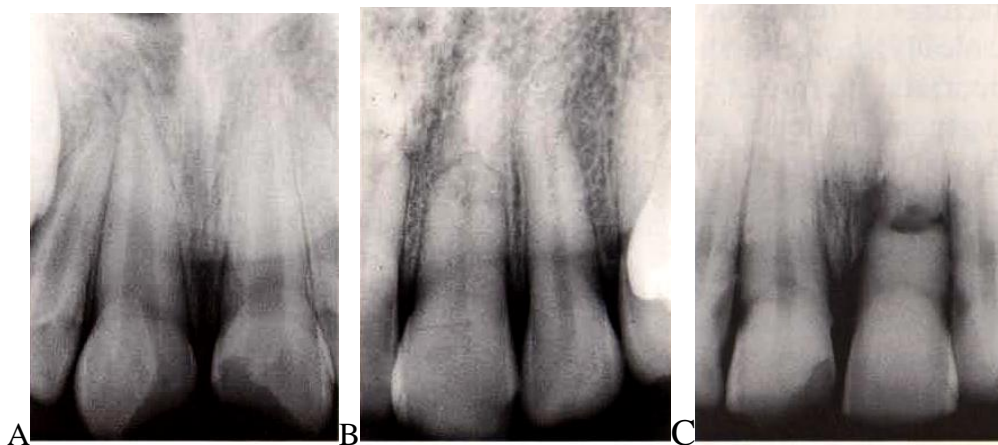


Fig. 11.2.(A) Crown fracture of teeth 11 and 21, with pulp exposure, (B) Healed transverse root fracture on tooth 21, which remained vital,(C)late result of a transverse fracture of tooth 21, with obliteration of the root canal.

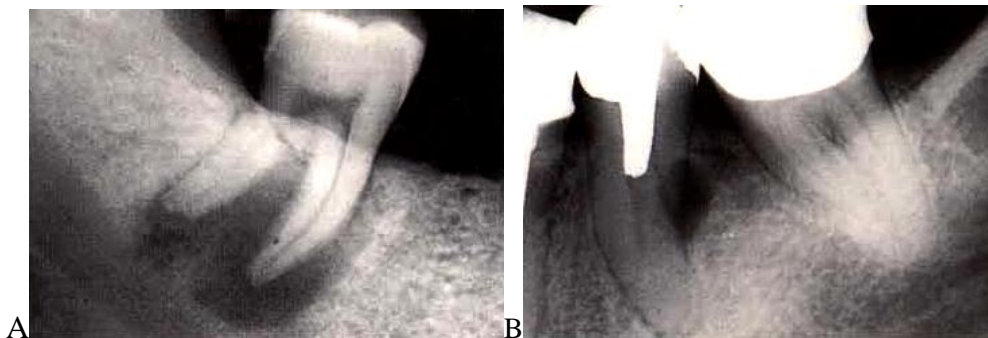


Fig. 11.3.(A)Late result with a transverse root fracture on tooth 47, which was not diagnosed initially, (B) axial tooth fracture that occurred subsequent to forceful insertion of a post reconstruction.

Radiographic Signs of Subluxation

Subluxation in the mandible must be approached with appropriate techniques.

- **Left:** If the tooth crown is displaced vestibularly due to trauma, the root will likely be displaced palatally. Using the normal central ray projection, any subluxation will hardly be detectable radiographically.

- **Center:** If an accident leads to a tooth crown being luxated palatally, the root will be displaced vestibularly. Using normal radiographic methods, the subluxation will be clearly shown.

- **Right:** If an accident causes a tooth to be intruded into its alveolus, the standard radiograph will show the apex of the affected tooth root to be located apical to adjacent teeth. In such cases, the lamina dura and periodontal ligament space are not visible.

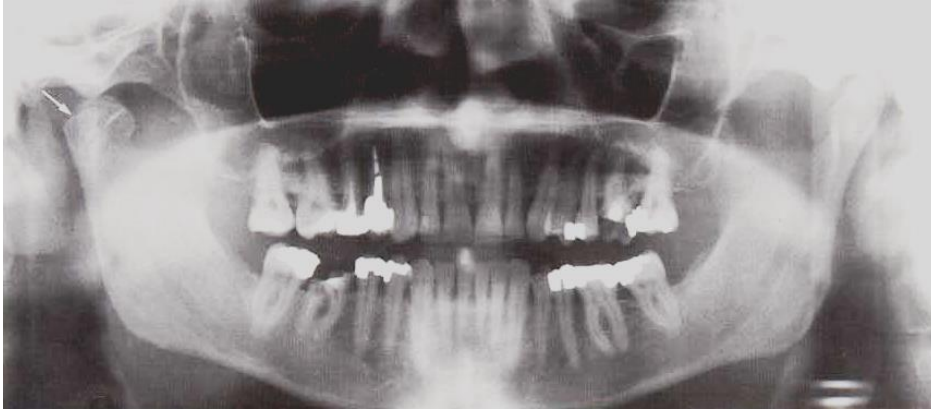


Fig. 11.4. Crown fracture of 15, 26, 34 and 46; high fracture of the right articular process. Even in a cases of simple tooth fractures one must consider the possibility that condylar fracture has occurred. The fossa on the right side is empty.

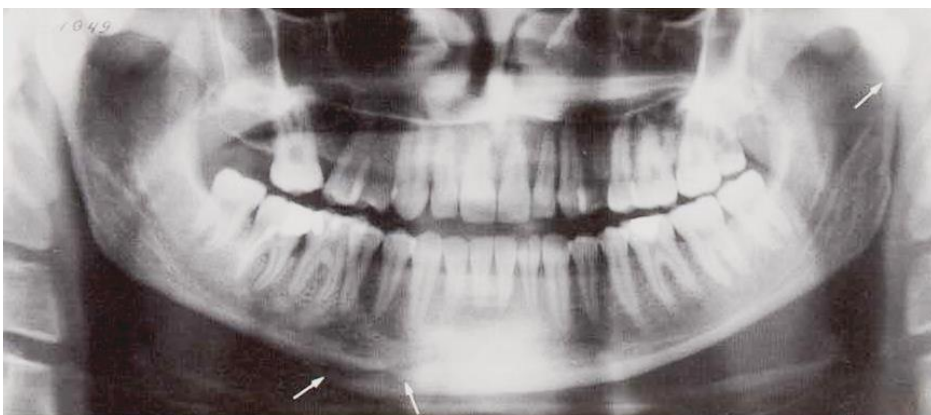


Fig. 11.5. Axial fracture of tooth 32, with transverse fracture of the mandible (arrows) and fracture of the left condyle. Note the vertical fracture of tooth 32, an oblique mandibular fracture extending from tooth 45 to tooth 46, and fracture of the left articular process.



Fig. 11.6. Deep fracture of the left articular process of the mandible. The condyle is not in its appropriate position, and it is easy to see the step on the dorsal border of the ascending ramus (arrows). Post-traumatic swelling of the soft tissues and the resulting radiographic shadowing can render detection of such fractures of the articular process much more difficult.

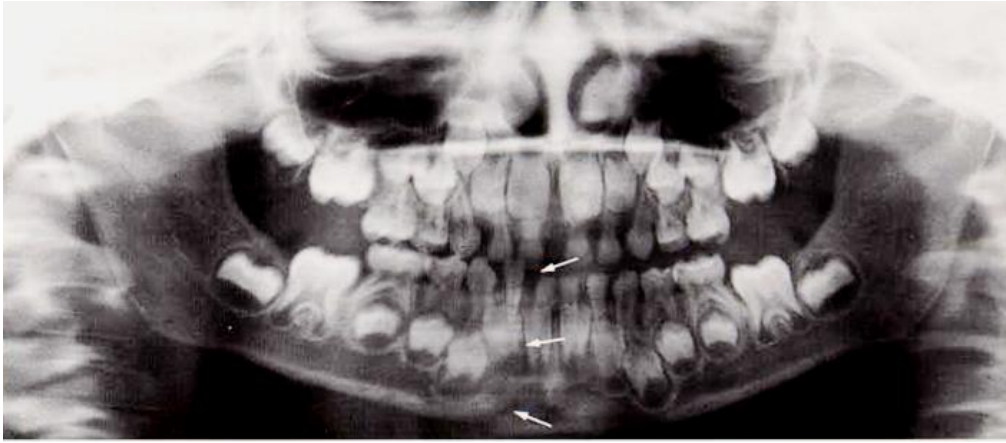


Fig. 11.7. Transverse fracture of the mandible. Step formation in the mandibular anterior area, with dislocation of the fragments (arrows) in a 5-year-old patient.

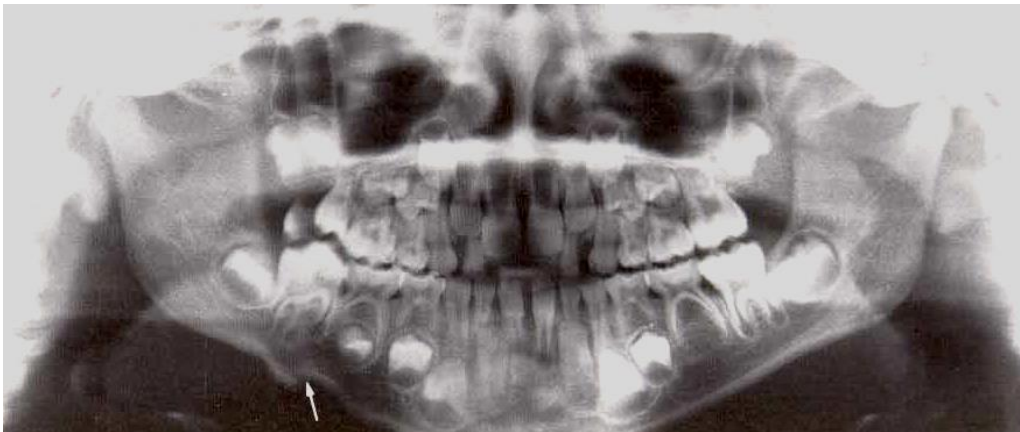


Fig. 11.8. Examination of a 6-year-old male following a minor accident. The double appearance of teeth 17, 16 and 46 indicates that the "step" formation of the compact bone is really an artefact caused by movement during the exposure and not a true transverse fracture of the mandible (arrow).

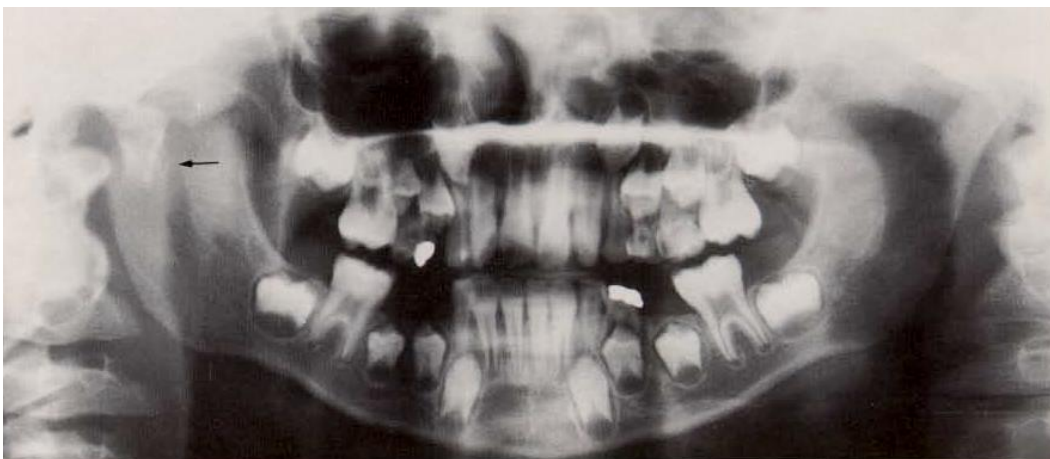


Fig. 11.9. Fracture of the neck of the condyle, right (arrow). Dislocation of a small fragment laterally and anteriorly. Note also that the condyle and the neck of the articular process are not visibly enlarged in this 7-year-old patient.

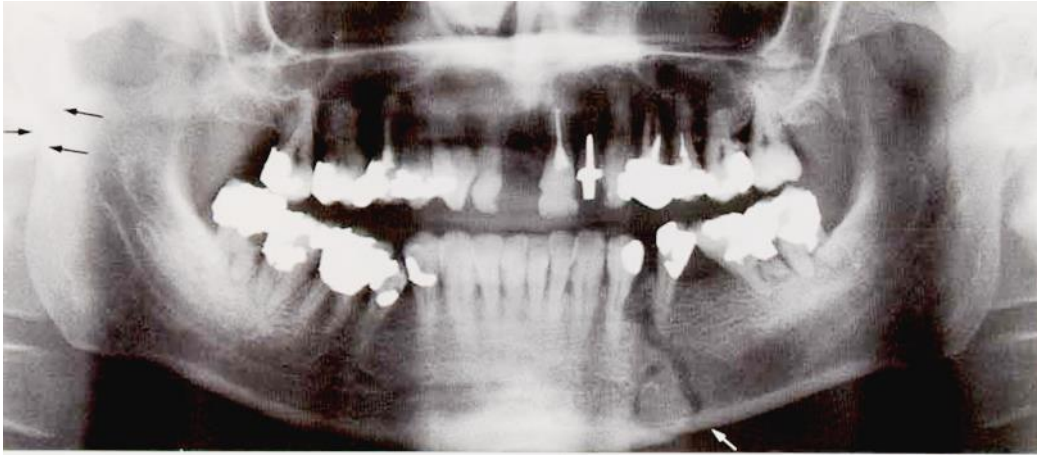


Fig. 11.10. Transverse fracture of the mandible with condylar neck fracture. Superimposed fracture cleft lines (apparent distention fracture) and fracture of the condylar neck of the right side (arrows, with superimposed fragments due to the addition effect).

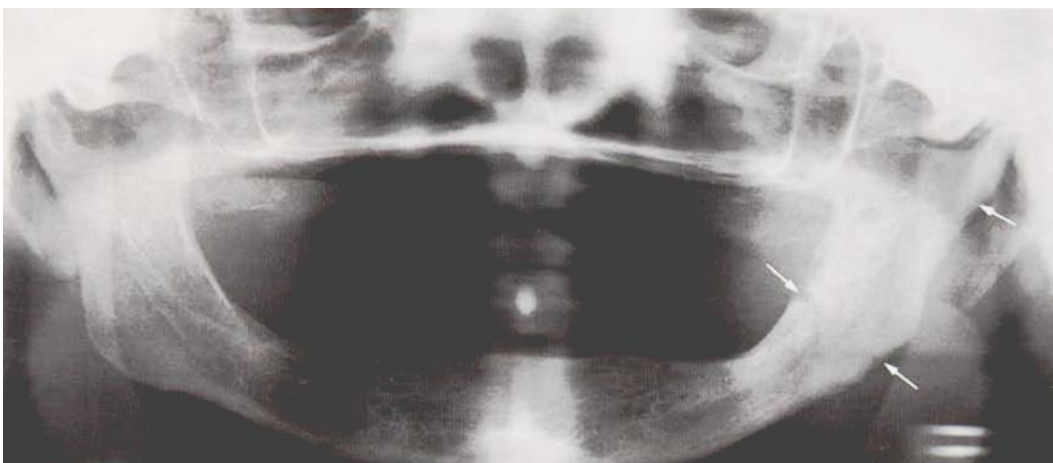


Fig. 11.11. Fracture at the angle of the mandible, with condylar neck fracture on the left side (arrows). Primary chronic osteomyelitis (so-called fracture cleft osteitis) in the ascending mandibular ramus on the left side. Compare this appearance with the healthy right side. Additional radiographs including the reverse Towne projection with maximum jaw opening are indicated to discern any possible dislocation in such cases.

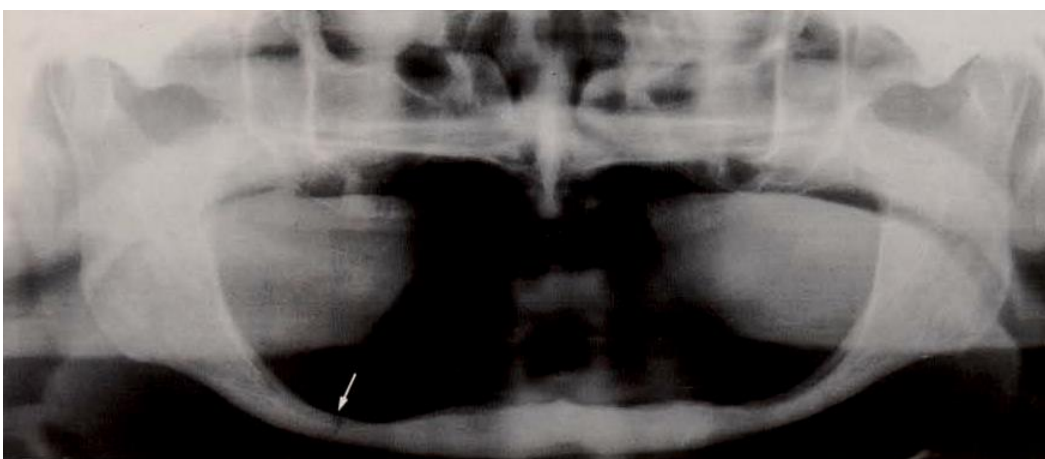


Fig. 11.12. Spontaneous fracture of the right mandible. This panoramic radiograph depicts advanced age-related atrophy in a 68-year-old male.

Mandibular Fractures During Mixed Dentition

The increasing number of traffic accidents has led to an increase in jaw and facial fractures in children. During the time of transition from the deciduous to the permanent teeth, the jaws are very fragile. The closely spaced and sometimes superimposed periodontal spaces of the deciduous teeth and the tooth buds of the permanent teeth weaken the jaw as development of the dentition progresses, resulting in typical fracture locations. Figure 11.13 illustrates the possible fracture locations.

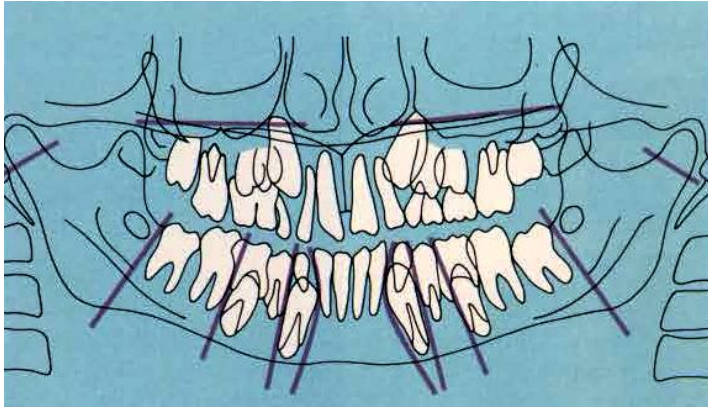


Fig. 11.13. Diagram of common fracture locations in the mandible during mixed dentition.

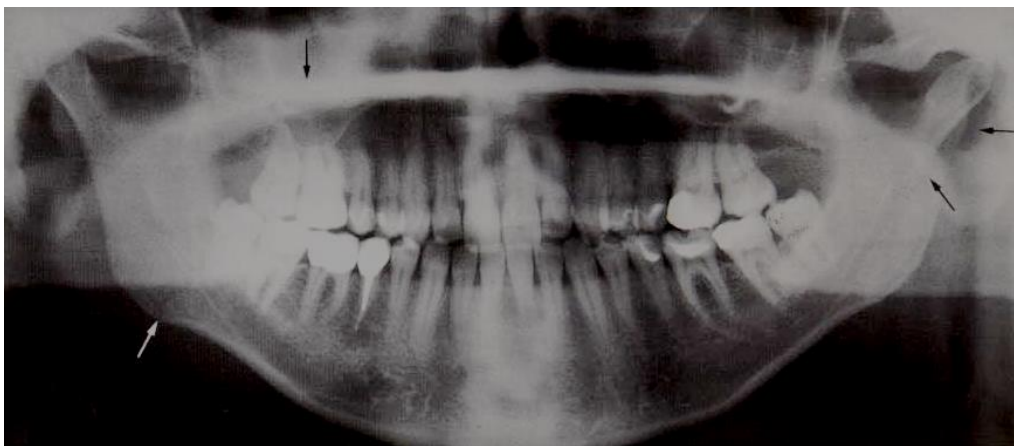


Fig. 11.14. Panoramic radiograph of the situation following trauma. Note the dislocation of the left condyle (arrows), a delicate fracture line at the angle of the mandible on the right side (arrow), and a massive radiopacity in the right sinus (arrow).

Foreign Bodies and Postoperative Conditions

Accidents and surgical procedures can introduce foreign bodies into the facial skeleton or into the soft tissues; in radiographs, such foreign bodies may appear to be located within the jaws because of superimposition. Included in this regard are also all foreign bodies that appear in radiographs of the head and neck region because of improper preparation of the patient. On the other hand, therapeutic measures may also result in late sequelae, leaving traces that persist in subsequent radiographs. All such situations must be interpreted during data collection, and many fall into the realm of forensic dentistry. In many cases, the patient is no longer available for clinical examination. For this reason, several typical examples are provided in this chapter.

Foreign bodies may be deposited in the jaws or in the soft tissues as a result of

all types of accidents, e.g., work-related, traffic, sport or hunting. Because facilities for xeroradiography are only very seldom available, glass particles often must be documented by means of tangential soft tissue radiographs using extremely low exposure. Even biocompatible filling materials such as those used in cosmetic surgery sometimes show up in panoramic radiographs and can lead to addition effects.

The spectrum of materials that may be deposited during therapy is broad: All kinds of filling materials often appear, e.g., in follow-up radiographs after extended procedures under local anesthesia, and occasionally fragments from dental hand instruments or drills are detected. In nuclear medicine, hollow needles filled with iridium or cesium are implanted during interstitial radiotherapy, and these needles are occasionally visible in panoramic radiographs. More and more frequently today, the radiograph is used to verify the position of implants or osteosynthesis materials. In this regard it should be noted that such therapeutically introduced foreign bodies may possibly elicit reaction in the neighboring tissues. This is usually in the form of chronic inflammation with tissue loss. It is beyond the scope of this atlas to provide a complete description of all the systems in use today for the detection of foreign bodies.

Radiographic examination is also indicated when the dentist is searching for root fragments in the jaws or in the sinus, and to determine the localization of bone fragments and sequestra that may occur after complicated tooth extraction. This chapter will portray the typical healing of defects created by root tip resection (apicoectomy) and other surgical procedures, in order to provide our colleagues outside the field of dentistry some directions to diagnostic criteria as seen by the radiologist.

Various Therapeutic Materials Seen in the Radiograph

Root canal filling materials sometimes extrude into the tissues surrounding a tooth through perforation of the floor of the pulp chamber or through the apex of the tooth. Attempts at root canal therapy in third molars frequently result in filling material being deposited in the mandibular canal. The panoramic radiograph may also depict filling materials used in cosmetic surgery, or the hollow needles implanted in nuclear medicine; these may raise diagnostic questions in the mind of the dentist.

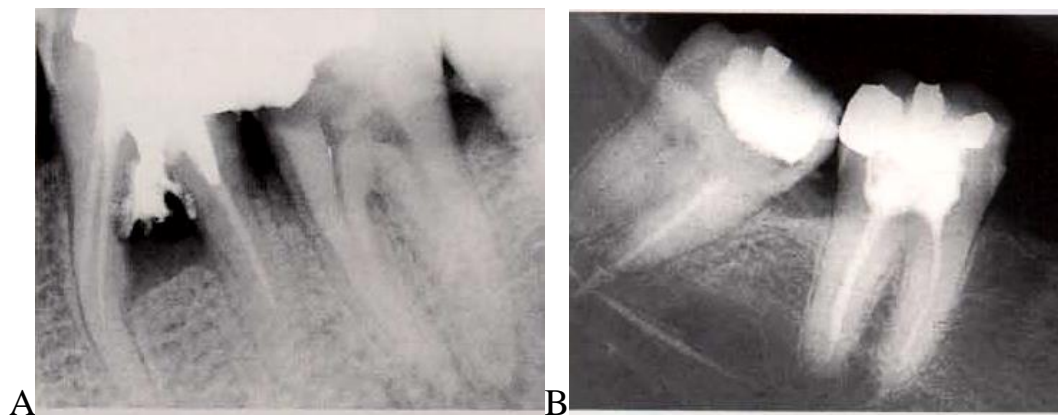


Fig. 11.15. (A) Perforation of the furcation and deposition of root canal filling material. (B) Overfilling of the mesial canal of tooth 48 with deposition of root canal filling material onto the roof of the mandibular canal.

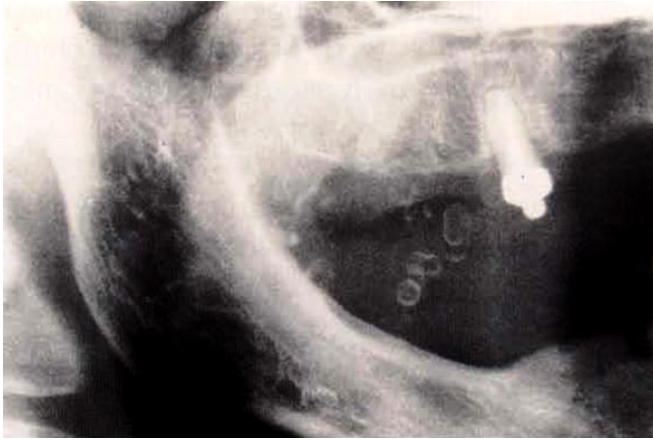


Fig. 11.16. Deposition of filling material after cosmetic surgery to improve cheek contour.

These spherical bodies are reminiscent of phleboliths, which are observed in similar sites.

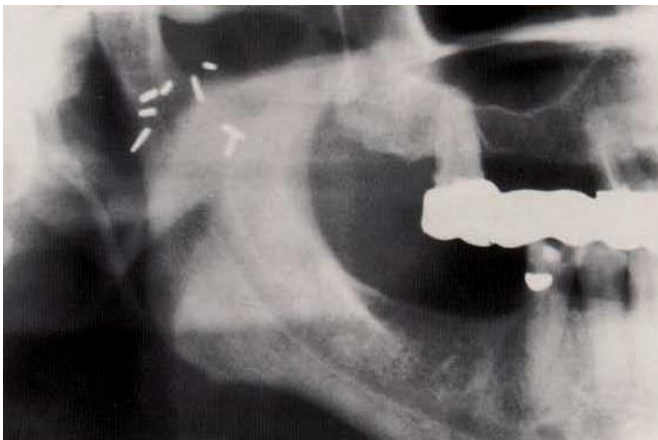


Fig. 11.17. Hollow needles for radiotherapy of cancer of the parotid gland. These small hollow needles are filled with cesium or iridium and are implanted for interstitial radiotherapy.

Accidents, Osteosynthesis Material and Implants

Metal fragments often become lodged in the jaws following accidents; such foreign bodies must be localized using radiography with various projection angles. Particles of glass may be disclosed using radiography or with short exposure soft tissue projection. Osteosynthesis materials and implants of all types may be projected onto the contralateral jaw and thus create radiopacities that prevent complete visualization of tissue structures. Under such conditions, artefacts may also occur in computed tomograms.

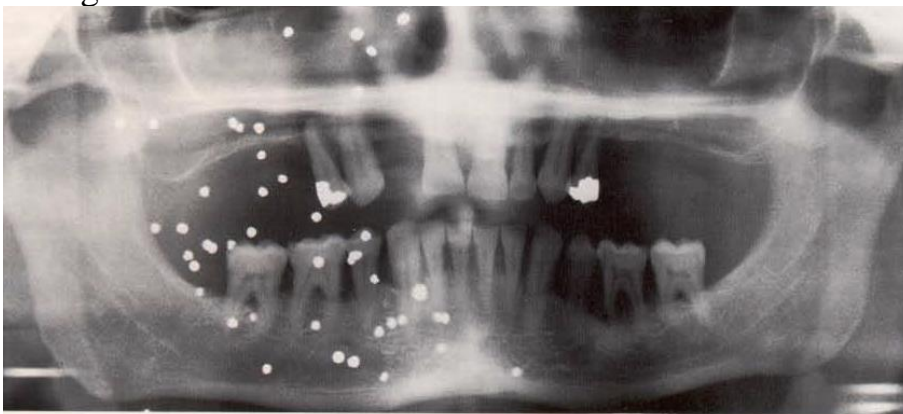


Fig. 11.18. Condition following a hunting accident. Depending upon the distance from the blast, the small shots usually become lodged in the soft tissues and projects into radiographs of the jaws. The eyes, of course, are at greatest risk.

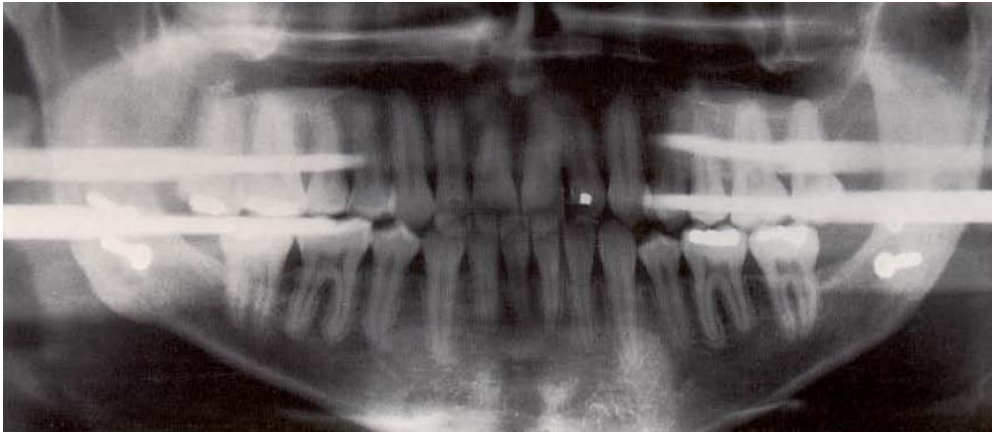


Fig. 11.19. Osteosynthesis material. Materials of all kinds may be observed radiographically at sites of surgical procedures. Often these materials project as interfering radiopacities on the contralateral jaw.

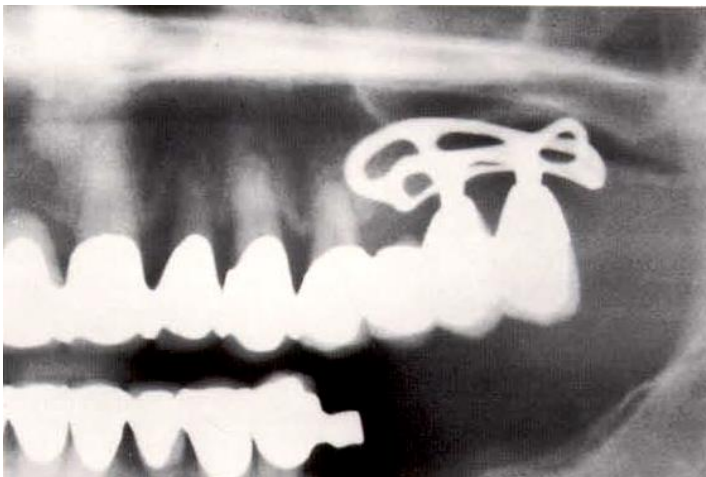


Fig. 11.20. Subperiosteal implant as seen in a follow-up radiograph. This implant had been in situ for 34 years and had been used on two separate occasions as a bridge abutment.

Radiography of Root Fragments

In the Alveolus

- The root fragment may be in its normal location at the “apex line” of adjacent teeth (an exception to this general rule would be root fragments from impacted or retained teeth)

- The periodontal ligament space and lamina dura are preserved (exception: chronic apical periodontitis)

- In most situations the pulp canal is visible radiographically (exception: root fragments from teeth with obliterated root canals).

Outside the Alveolus

- Root fragments that are *not* at their normal anatomic location at the “apex line” of adjacent teeth (exception: root fragments from impacted or retained teeth)

- The periodontal ligament space and the lamina dura are *not* visible

- In most situations the pulp canal is visible radiographically (exceptions: root

fragments from teeth with obliterated canals).

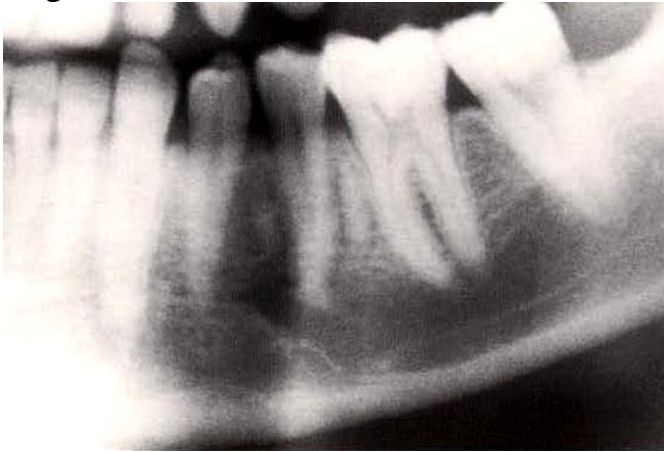


Fig. 11.21. Root fragments of tooth 75 reside on both sides of tooth 35 in this 26-year-old male.



Fig. 11.22. Root fragment of tooth 38. The surrounding tissues are chronically inflamed, and this is why the lamina dura cannot be discerned.

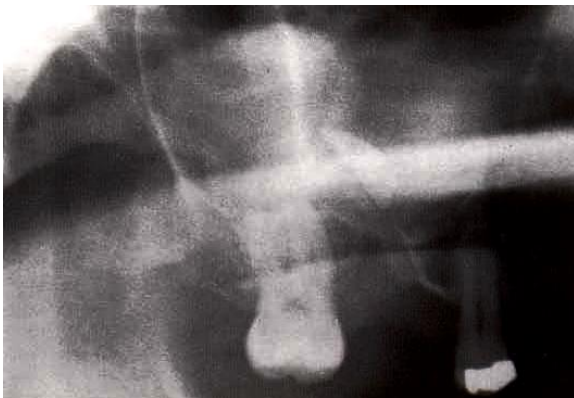


Fig. 11.23. Root fragment of tooth 16 in the maxillary sinus. The root fragment is located obliquely and apical to the apex line; no lamina dura is apparent. An oroantral fistula is present. The sinus has a radiopaque appearance because of mucosal swelling, and this probably also masks the pulp canal of the root fragment.

Fractured Bone and Sequestra

During complicated surgical removal of teeth, fracture of the surrounding bone sometimes occurs. The interradicular septum and the alveolar margin are often at risk if teeth are extracted using an elevator. Bony segments may be fractured and may remain in the tissue as sequestra, where they elicit delayed healing in the form of a dry socket. In the first few days after tooth extractions, such bony fragments are difficult to detect radiographically because of the superimposition effect; only when a

demarcation occurs are these fragments visible in the film.



Fig. 11.24. Fracture of the interradicular septum following extraction of tooth 4.

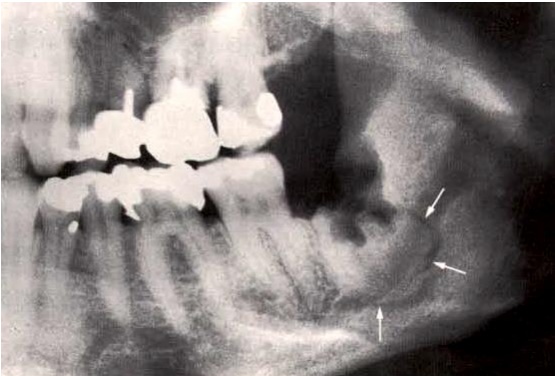


Fig. 11.25. This fracture occurred during an attempt to remove tooth 38 surgically (arrows). Note the position of the mandibular canal.

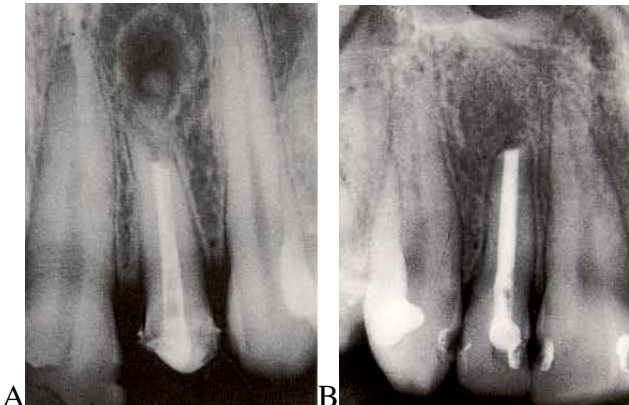


Fig. 11.26. (A) Failure of an apicoectomy. Incomplete removal of the root tip has left an area of radiolucency and reactive sclerosis as signs of a chronic inflammatory process. (B) Successful apicoectomy. Complete reossification and a small "connective tissue scar."



Fig. 11.27.Fracture of the maxillary alveolar process. Axial unenhanced CT image depicts a fracture of the maxillary alveolar process, with resultant avulsion of the medial and right lateral maxillary incisors.

Incidence of Temporomandibular Joint Changes After Whiplash Trauma

The term “whiplash” medical terminology is applied to a well-defined trauma to the cervical spine that includes extension followed by flexion without any direct trauma to the head. Apart from symptoms in the neck and adjacent structures after a whiplash trauma, other disorders that can be manifested include deafness, dizziness, tinnitus, headache, memory loss, dysphagia, and temporomandibular joint (TMJ) pain. Approximately two thirds of such associated disorders occur in women, and one third occur in men.

The impact of whiplash trauma on the TMJ is a matter of debate. A calculation of the mechanical and anatomic prerequisites for the development of TMJ disk displacement after whiplash trauma suggested that such displacement was not likely. This view was supported by the results of a low-velocity (8-km/hr) collision test performed on volunteers that indicated the force magnitudes generated at the TMJ would be insufficient to injure the joint.

Травми зубо-щелепної ділянки



Fig.11.28. Mandibular fractures. (A) Axial unenhanced CT image of the mandible depicts a nondisplaced left parasymphyseal fracture (blue arrow) and mildly displaced fracture of the right mandibular body (green arrow) with distraction of the mandibular canal. (B) Axial unenhanced CT image demonstrates a fracture of the right alveolar process (magenta arrow) with multiple missing teeth.

Tooth fracture

Radiographic Signs of Tooth Fractures

The diagram presented in Figure 11.10 shows the three most common root fractures of maxillary anterior teeth as well as the result that can be achieved with periapical radiographs using the standard techniques (from *left to right*).

- Only when the central X-ray beam is directed (fortuitously) onto the fracture cleft will it be clearly depicted on the film.
- If the central X-ray projection is directed oblique to the fracture cleft, the film may display several “fracture lines” and therefore simulate a complex fracture.
- Oblique fractures resulting from shearing forces often exhibit only vague radiographic signs. In many cases, only magnification will reveal tiny step formation

along the mesial or the distal root surfaces and/or a faintly visible addition effect caused by the superimposed root fragments. Axial root fractures adhere to the same rules: Fractures are only visible on radiographs if the fracture cleft is fortuitously parallel to the central X-ray beam.

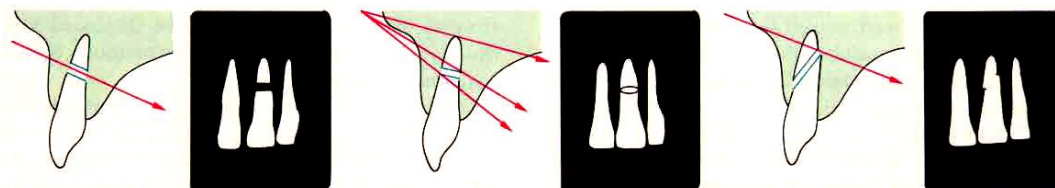


Fig. 11.29.Diagram of the radiographic signs of tooth fracture.



Fig.11.30. Tooth fracture in a 55-year-old man. Axial CT image of the maxilla shows a thin curvilinear area of low attenuation, a finding indicative of a vertical tooth fracture (arrow).

Tooth avulsion



Fig.11.31.Tooth avulsion in a 21-year-old woman. Sagittal CT image shows widening of the periodontal ligament space (arrow) and fracture of the buccal surface of the alveolar process (arrowhead).

12 REFERENCES

Abrahams JJ, Levine B. Expanded applications of DentaScan: multiplanar CT of the mandible and maxilla. *Int J Periodontics Restorative Dent*, 1990; 10:464–467.

Abrahams JJ, Olivario P. Odonotogenic cysts: improved imaging with a dental CT software program. *AJNR Am J Neuroradiol*, 1993; 14:367–374.

Abrahams JJ. Anatomy of the jaw revisited with a dental CT software program: pictorial essay. *AJNR Am J Neuroradiol*, 1993; 14:979–990.

Abrahams JJ, Berger SB. Oral-maxillary sinus fistula, oroantral fistula: clinical presentation and evaluation with multiplanar CT. *AJR Am J Roentgenol*, 1995; 165:1273–1276.

Abrahams JJ, Frisoli JK, Dembner J. Anatomy of the jaw, dentition, and related regions. *Semin Ultrasound, CT, MR*, 1995;16:453–467.

Abrahams JJ, Glassberg RM. Dental disease: a frequently unrecognized cause of maxillary sinus abnormalities? *AJR Am J Roentgenol*, 1996;166(5): 1219–1223.

Abrahams JJ, Berger S. Inflammatory disease of the jaw: appearance on reformatted CT images. *Am J Roentgenol*, 1998; 170:1085–1091.

Abrahams JJ, Hayt MW. Dental CT in pathologic changes of the maxillo-mandibular region. *Radiology*, 1999; 39:1035–1043. [German]

Abrahams JJ. Augmentation procedures of the jaw in patients with inadequate bone for dental implants: radiographic appearance. *J Comput Assist Tomogr*, 2000; 24:152–158.

Abrahams JJ. Dental CT imaging: a look at the jaw. *Radiology*, 2001;219(2):334–345.

Agerberg G . Maximal mandibular movements in young men and women. *Sven Tandlak Tidskr*, 1974 ; 67 (2): 81–100 .

Allareddy V, Allareddy V, Nalliah RP. Epidemiology of facial fracture injuries. *J Oral Maxillofac Surg* 2011;69(10):2613–2618.

Anthonappa RP, Lee CK, Yiu CK, King NM. Hypohyperdontia: literature review and report of seven cases. *Oral Surg Oral Med Oral Pathol Oral Radiol Endod* 2008;106(5):e24–e30.

Arabshahi B , Cron RQ . Temporomandibular joint arthritis in juvenile idiopathic arthritis: the forgotten joint. *Curr Opin Rheumatol*, 2006 ; 18 (5): 490 – 495 .

Armitage GC. Periodontal diagnoses and classification of periodontal diseases. *Periodontol* 2000,2004;34:9–21.

Arvidsson L.Z., Smith H.-J., Flatø B., Larheim T.A. **Temporomandibular Joint Findings in Adults with Long-standing Juvenile Idiopathic Arthritis: CT and MRI Imaging Assessment.** *Radiology*: V 256: Number 1—July 2010

Avery LL, Susarla SM, Novelline RA. Multidetector and three-dimensional CT evaluation of the patient with maxillofacial injury. *Radiol Clin North Am*, 2011;49(1):183–203.

Bras J, de Jonge HK, van Merkesteyn JP. Osteoradionecrosis of the mandible: pathogenesis. *Am J Otolaryngol*, 1990;11(4):244–250.

Brewer EJ Jr , Bass J , Baum J , et al . Current proposed revision of JRA criteria: JRA Criteria Subcommittee of the Diagnostic and Therapeutic Criteria Committee of the American Rheumatism Section of the Arthritis Foundation. *Arthritis Rheum*, 1977 ; 20 (2 suppl): 195–199 .

Brooks SL , Westesson PL , Eriksson L , et al. Prevalence of osseous changes in the temporomandibular joint of asymptomatic persons without internal derangement . *Oral Surg Oral Med Oral Pathol*, 1992; 73 (1): 118–122 .

Burt B. Epidemiology of periodontal diseases. *J Periodontol*, 2005;76:1406–1419.

Cassidy JT , Petty RE , Laxer RM , Lindsley CB . Textbook of pediatric rheumatology. 5th ed. Philadelphia, Pa: Elsevier Saunders, 2005; 206–260 .

Castillo M. Odontogenic cysts, tumors, and related jaw lesions. <http://www8.utsouthwestern.edu/utsw/cda/dept28151/files/445702.html>. Accessed December 15, 2009.

Chen L, Wei B, Li J, et al. Association of periodontal parameters with metabolic level and systemic inflammatory markers in patients with type 2 diabetes. *J Periodontol* 2010;81(3):364–371.

Ceylan Z. Cankurtaran, MD • et al. Ameloblastoma and Dentigerous Cyst Associated with Impacted Mandibular Third Molar Tooth. *RadioGraphics*, 2010;30:1415–1420 •

- Cohen MA, Hertzanu Y. Radiologic features, including those seen with computed tomography, of central giant cell granuloma of the jaws. *Oral Surg Oral Med Oral Pathol* 1988; 65:255–261.
- Cutright DE. The histopathologic findings in 583 cases of epulis fissuratum. *Oral Surg Oral Med Oral Pathol* 1974;37(3):401–411.
- Daffner RH. Imaging of facial trauma. *Curr Probl Diagn Radiol*, 1997;26(4):153–184.
- DelBalso AM. Lesions of the jaws. *Semin Ultrasound, CT, MR*, 1995;16(6):487–512.
- Drage NA, Whaites EJ, Hussain K. Hemangioma of the mandible. *Br J Oral Maxillofac Surg*, 2003;41(2):112–114.
- Dunfee BL, Sakai O, Pistey R, Gohel A. Radiologic and pathologic characteristics of benign and malignant lesions of the mandible. *RadioGraphics*, 2006; 26(6):1751–1768.
- El Nesr NM, Avery JK. Tooth eruption and shedding. In: Avery JK, Steele PF, Avery N, eds. *Oral development and histology*. 3rd ed. Stuttgart, Germany: Thieme, 2002; 123–140.
- Fragiskos FD. Odontogenic infections. In: Fragiskos FD, ed. *Oral surgery*. Berlin, Germany: Springer-Verlag, 2007; 205–241.
- Gahleitner A, Hofschneider U, et al. Lingual Vascular Canals of the Mandible: Evaluation with Dental CT. *Radiology*, 2001;220:186–189.
- Gentry LR, Manor WF, et al. High-resolution CT analysis of facial struts in trauma. II. Osseous and soft-tissue complications. *AJR Am J Roentgenol* 1983;140(3):533–541.
- Givol N, Buchner A, et al. Radiological features of osteogenic sarcoma of the jaws: a comparative study of different radiographic modalities. *Dentomaxillofac Radiol*, 1998;27(6):313–320.
- Goldman KE. Mandibular cysts and odontogenic tumors. *eMedicine* <http://emedicine.medscape.com/article/852734-print>. Updated May 20, 2009.
- Grimanis GA, Kyriakides AT, Spyropoulos ND. A survey on supernumerary molars. *Quintessence Int*, 1991;22(12):989–995.
- Grössner-Schreiber B, et al. Prevalence of dental caries and periodontal disease in patients with inflammatory bowel disease: a case-control study. *J Clin Periodontol* 2006;33(7):478–484.
- Güven O, Keskin A, Akal UK. The incidence of cysts and tumors around impacted third molars. *Int J Oral Maxillofac Surg*, 2000;29(2):131–135.
- Harris EF, Clark LL. An epidemiological study of hyperdontia in American blacks and whites. *Angle Orthod*, 2008;78(3):460–465.
- Hermans R, Fossion E, et al. CT findings in osteoradionecrosis of the mandible. *Skeletal Radiol*, 1996;25(1):31–36.
- Horner K. Central giant cell granuloma of the jaw: a clinico-radiological study. *Clin Radiol*, 1989; 40:622–626.
- Hopper RA, Salemy S, Sze RW. Diagnosis of midface fractures with CT: what the surgeon needs to know. *RadioGraphics*, 2006;26(3):783–793.
- Hudson JW. Osteomyelitis of the jaws: a 50-year perspective. *J Oral Maxillofac Surg*, 1993;51(12):1294–1301.
- Huomonen S, Ørstavik D. Radiological aspects of apical periodontitis. *Endod Top*, 2002;1(1):3–25.
- Kaneda T, Minami M, Kurabayashi T. Benign odontogenic tumors of the mandible and maxilla. *Neuroimaging Clin N Am*, 2003;13(3):495–507.
- Kellman RM. Maxillofacial trauma. In: Flint PW, Haughey BH, Lund, VJ, et al, eds. *Cummings otolaryngology: head and neck surgery*. 5th ed. Philadelphia, Pa: Mosby, 2010; 318–341.

- Klein HM, Fuhrmann R, et al, High-resolution CT of the dentate alveolar ridge in comparison with histological thin section preparations. *Rofortschr Geb Rontgenstr Neuen BildgebVerfahr*, 1993; 158:187–191.
- Kokich VG. Surgical and orthodontic management of impacted maxillary canines. *Am J Orthod Dentofacial Orthop*, 2004;126(3):278–283.
- Laine FJ, Conway WF, Laskin DM. Radiology of maxillofacial trauma. *Curr Probl Diagn Radiol*, 1993;22(4):145–188.
- Larheim TA, Haanaes HR, Dale K. Radiographic temporomandibular joint abnormality in adults with micrognathia and juvenile rheumatoid arthritis. *Acta Radiol Diagn (Stockh)*, 1981; 22 (4): 495 – 504 .
- Loesche WJ, Grossman NS. Periodontal disease as a specific, albeit chronic, infection: diagnosis and treatment. *Clin Microbiol Rev*, 2001;14:727–52.
- Longhini AB, Ferguson BJ. Clinical aspects of odontogenic maxillary sinusitis: a case series. *Int Forum Allergy Rhinol*, 2011;1(5):409–415.
- Meir H. Scheinfeld, Keivan Shifteh et al. Teeth: What Radiologists Should Know. *RadioGraphics*, 2012;32:1927–1944 •
- Mendenhall WM, Werning JW, et al. Ameloblastoma. *Am J Clin Oncol*, 2007;30(6):645–648.
- Miles DA, Kaugars GE, Van Dis M, Lovas JG. Oral and maxillofacial radiology. Philadelphia, Pa: Saunders, 1991.
- Minami M, Kaneda T, Yamamoto H, et al. Ameloblastoma in the maxillomandibular region: MR imaging. *Radiology*, 1992;184(2):389–393.
- Mourshed F. A roentgenographic study of dentigerous cysts. *Oral Surg Oral Med Oral Pathol*, 1967; 51:54–61.
- Müller L, Kellenberger CJ, et al. Early diagnosis of temporomandibular joint involvement in juvenile idiopathic arthritis: a pilot study comparing clinical examination and ultrasound to magnetic resonance imaging. *Rheumatology (Oxford)*, 2009; 48 (6): 680 – 685 .
- Nessi R., Minorati D., Dova S., Blanc M.. Digital panoramic radiography: a clinical survey. *Eur. Radiol.* 5, 391–394 (1995).
- Norman JE. Oroantral fistula. *Aust Dent J* 1977; 22:248–258.
- Oikarinen VJ. Keratocyst recurrences at intervals of more than 10 years: case reports. *Br J Oral Maxillofac Surg*, 1990; 28:47–49.
- Peltola J, Magnusson B, Happonen RP, Borrmann H. Odontogenic myxoma: a radiographic study of 21 tumours. *Br J Oral Maxillofac Surg*, 1994;32(5):298–302.
- Philipsen HP, Reichart PA, Zhang KH, et al. Adenomatoid odontogenic tumor: biologic profile based on 499 cases. *J Oral Pathol Med*, 1991;20(4):149–158.
- Rajab LD, Hamdan MA. Supernumerary teeth: review of the literature and a survey of 152 cases. *Int J Paediatr Dent*, 2002;12(4):244–254.
- Regezi JA, Kerr DA, Courtney RM. Odontogenic tumors: an analysis of 706 cases. *J Oral Surg*, 1978;36:771–778.
- Regezi JA. Odontogenic cysts, odontogenic tumors, fibrous, and giant cell lesions of the jaws. *Mod Pathol*, 2002;15(3):331–341.
- Reichart PA, Philipsen HP. Color atlas of oral pathology. Stuttgart, Germany: Thieme, 2000; 222–249/

- Rheumatology classification of juvenile idiopathic arthritis: second revision, Edmonton, 2001. *J Rheumatol* 2004 ; 31 (2): 390 – 392 .
- Rosenbloom L, Delman BN, Som PM. Facial fractures. In: Som PM, Curtin HD, eds. *Head and neck imaging*. 5th ed. St Louis, Mo: Elsevier, 2011; 491–524.
- Russell KA, Folwarczna MA. Mesiodens: diagnosis and management of a common supernumerary tooth. *J Can Dent Assoc*, 2003;69(6):362–366.
- Scholl RJ, Kellett HM, Neumann DP, Lurie AG. Cysts and cystic lesions of the mandible: clinical and radiologic-histopathologic review. *RadioGraphics* 1999;19(5):1107–1124.
- Schwarz MS, Rothman SLG, Rhodes ML, Chafetz N. Computed tomography. I. Preoperative assessment of the mandible forendosseous implant surgery. *Int J OralMaxillofac Implants*, 1987; 2:137–141.
- Schwarz MS, Rothman SLG, Rhodes ML, Chafetz N. Computed tomography. II. Preoperative assessment of the maxilla forendosseous implant surgery. *Int J OralMaxillofac Implants*. 1987; 2:143–148.
- Slootweg PJ. Lesions of the jaws. *Histopathology*, 2009;54(4):401–418.
- Steinbrocker O , Traeger CH , Batterman RC . Therapeutic criteria in rheumatoid arthritis . *J Am Med Assoc*, 1949 ; 140 (8) : 659 – 662 .
- Tang L, Zhou XD, Wang Y, et al Detection of vertical root fracture using cone beam computed tomography: report of two cases. *Dent Traumatol*, 2011;27(6):484–488.
- Torres-Lagares D, Infante-Cossío P, Hernández- Guisado JM, Gutiérrez-Pérez JL. Mandibular ameloblastoma: a review of the literature and presentation of six cases. *Med Oral Patol Oral Cir Bucal*, 2005;10(3):231–238.
- Trope M. Avulsion of permanent teeth: theory to practice. *Dent Traumatol* 2011;27(4):281–294.
- Tyndall DA, Rathore S. Cone-beam CT diagnostic applications: caries, periodontal bone assessment, and endodontic applications. *Dent Clin North Am*, 2008;52(4):825–841.
- Unger E, Moldofsky P, Gatenby R, et al. Diagnosis of osteomyelitis by MR imaging. *AJR Am J Roentgenol*. 1988;150(3):605–610.
- Van Merkesteyn JP, Groot RH, et al. Diffuse sclerosing osteomyelitis of the mandible: a new concept of its etiology. *OralSurg Oral Med Oral Pathol*, 1990;70(4):414–49.
- Waldron CA, Shafer WG. The central giant cell granuloma of the jaws: an analysis of 38 cases. *Am J ClinPathol*, 1966; 45:437–447.
- Weaver BD, Graves RW, Keyes GG, Lattanzi DA. Central neurofibroma of the mandible: report of a case. *J Oral Maxillofac Surg*, 1991;49(11):1243–1246.
- Weber AL. Imaging of cysts and odontogenic tumors of the jaw. *Radiol Clin North Am*, 1993; 31:101–120.
- Weber AL, Kaneda T, Scrivani SJ, et al. Cysts, tumors, and nontumorous lesions of the jaw. In: Som PM, Curtin HD, eds. *Head and neck imaging*. 4th ed. St Louis, Mo: Mosby, 2003; 930–994.
- Weiss PF , Arabshahi B , Johnson A , et al . High prevalence of temporomandibular joint arthritis at disease onset in children with juvenile idiopathic arthritis, as detected by magnetic resonance imaging but not by ultrasound . *Arthritis Rheum*, 2008 ; 58 (4) : 1189 – 1196.
- William M. Mendenhall, Mandibular Osteoradionecrosis. *J clin oncology*, Vol 22, No 24 (December 15), 2004: pp 4867-4868.

Winegar B.A., Murillo H., Tantiwongkosi B. Spectrum of Critical Imaging Findings in Complex Facial Skeletal Trauma. *RadioGraphics*, 2013;33:3–19. •

Worth HM, Stoneman DW. Radiology of vascular abnormalities in and about the jaws. *Dent Radiol Photogr* 1979; 52:1–23.

Wright JT. Normal formation and development defects of the human dentition. *Pediatr Clin North Am*, 2000;47(5):975–1000.

Yale SH , Allison BD , Hauptfuehrer JD. An epidemiological assessment of mandibular condyle morphology. *Oral Surg Oral Med Oral Pathol*, 1966 ; 21 (2): 169 – 177 .

Yanagisawa K, Friedman C, Abrahams JJ. DentaScan imaging of the mandible and maxilla. *Head Neck*, 1993; 14:979–990.

Yildirim G, Ataoğlu H, Mihmanli A, et al. Pathologic changes in soft tissues associated with asymptomatic impacted third molars. *Oral Surg Oral Med Oral Pathol Oral Radiol Endod*, 2008;106(1):14–18.

Yoshiura K, Weber AL, Scrivani SJ. Cystic lesions of the mandible and maxilla. *Neuroimaging Clin N Am*, 2003;13(3):485–494.

Zachariades N. Neoplasms metastatic to the mouth, jaws and surrounding tissues. *J Craniomaxillofac Surg*, 1989;17(6):283–290.

Zallen RD, Preskar MH, McClary SA. Ameloblastic fibroma. *J Oral Maxillofac Surg*, 1982;40(8):513–517.